AN ABSTRACT OF THE THESIS OF

Scott E. Allen for the degree of Doctor of Philosophy in Chemistry presented on September 03, 2002.

Title: Active Site Studies and Design of Ligands for Affinity Column Separation of 2,5-Dihydroxyacetanilide Epoxidase (DHAE) I and II.

Redacted for privacy

Abstract approved _____

Kevin P. Gable

A series of compounds, **7-8** and **20-25**, were tested as competitive inhibitors of 2,5-dihydroxyacetanilide epoxidase I (DHAE I) and DHAE II. A Hammett plot was constructed for each enzyme to determine the effect of electron density on inhibition. DHAE I gave a linear, highly correlated plot ($r^2 = 0.91$) that signifies the importance of the amide oxygen in **1** on substrate binding. The plot for DHAE II is curved showing the greatest degree of inhibition with **7** suggesting steric factors within the active site control substrate binding. From these data, we conclude that each enzyme binds substrate in an opposite fashion and that this alone controls the stereochemistry of epoxide formation in **2** and **3**.

Alternative substrates, **26-29** and **33**, were also synthesized and tested for product formation. All compounds, except **29**, were accepted as alternative substrates, although the rates varied significantly. Surprisingly, **33** was accepted as an alternative substrate of DHAE II suggesting that the conformation of the amide bond in **33** is similar to the conformation required for catalytic activity in this enzyme.

This information was then used to design ligands for affinity column separation of DHAE I and DHAE II from their protein mixtures. **35** and **36** were

synthesized and attached to carbonyl di-imidazole activated agarose. Column 1 was tested three times with DHAE I enzyme preparations. The first attempt did not result in active enzyme being eluted from the column. The second attempt maintained the resin in the oxidized state. Protein was found to elute very quickly; no protein was found after fraction 4. The third attempt resulted in active enzyme in fractions 4-23. Column 2 was used twice for the attempted isolation of DHAE II from its protein mixture. The second attempt for column 2 mirrored the results for the third attempt with column 1. Neither column resulted in homogeneous enzyme by SDS-PAGE.

Active Site Studies and Design of Ligands for Affinity Column Separation of 2,5-Dihydroxyacetanilide Epoxidase (DHAE) I and II

by

Scott E. Allen

A THESIS

submitted to

Oregon State University

in partial fulfillment of
the requirements for the
degree of

Doctor of Philosophy

Presented September 03, 2002

Commencement June 2003

Doctor of Philosophy thesis of Scott E. Allen presented on September 03, 2002.

APPROVED:

Redacted for privacy

Major Professor, representing Chemistry

Redacted for privacy

Head of the Department of Chemistry

Redacted for privacy

Dean of the Graduate School

I understand that my thesis will become part of the permanent collection of Oregon State University libraries. My signature below authorizes release of my thesis to any reader upon request.

Redacted for privacy

Scott E. Allen, Author

ACKNOWLEDGEMENTS

I am forever indebted to the people who have helped me along the way. To Professor Gable for his never ending dedication to the exploration of new and interesting scientific endeavors and for sharing that excitement with me. I know that your guidance will last far longer than just the time I have spent in your lab. To Professor Mathews for his thorough proofreading of my thesis and for his excellence in teaching the biochemistry course.

To Professor Deinzer, Professor Zabriskie, and Professor Penner for their help in pushing me along this arduous process and for allowing me the opportunity to make mistakes along the way.

A special thanks to undergraduates Kay Johnson and Veronica Chiu who have helped in data collection and synthesis. To all the friends that I have made along this journey; for their friendship and many lively conversations, I would like to thank: Sundaram Shanmugham, Eric Brown, Fedor Zhuravlev, Eric Korf, Ana Barrios, and Shannon Babb.

TABLE OF CONTENTS

TABLE OF CONTENTS (Continued)

TABLE OF CONTENTS (Continued)

TABLE OF CONTENTS (Continued)

LIST OF FIGURES

LIST OF FIGURES

LIST OF SCHEMES

LIST OF SCHEMES (Continued)

Scheme Page

LIST OF TABLES

dedicated to my parents, Wayne and Shirley Allen
for their constant support of all my dreams
and to Robert Patten who has taught me about life

Active Site Studies and Design of Ligands for Affinity Column Separation of 2,5-Dihydroxyacetanilide Epoxidase (DHAE) I and II

Chapter 1

Introduction to Molecular Recognition

Introduction

Simple recognition events control every aspect of chemical and biological processes.[13-17] These interactions can be as simple as two ions attracting or repelling each other by electrostatic forces or as complex as the interaction of an agonist or antagonist with a cell surface receptor. Binding of two components occurs often in biological systems: an antigen - antibody connection in an immune response, in the recognition of different parts of a protein during re-folding, the binding of a substrate with enzyme and the corresponding catalytic activity, and in the translation and transcription of genetic material. From the hydrogen bonding that holds the two DNA helices together, it is evident that molecular recognition is responsible for life itself.

Recognition events are present not only in biological systems, but are prevalent in many scientific fields: chemistry, biology, physics, and material science. Chemically, it is now possible to bind cations[9], anions[7], and other organic molecules selectively using an understanding of the factors responsible for molecular recognition.[4-6] At the interface of chemistry and materials science, we are capable of creating supramolecular assemblies[3] with molecular weights over 20 kDa. The possibility of building machines on the molecular level is becoming reality.[1] Enzyme mimetics,[2,12,41] systems that bind substrate and also bring about a desired chemical reaction, bridge the gap between chemistry and biology.

Molecular recognition involves the non-covalent interaction of two or more components present in solution.[13] This definition is so broad it may seem as though it includes all of chemistry. This discussion, however, will focus on the study of synthetic inclusion compounds before moving on to a discussion of biological molecular recognition. Inclusion compounds are formed by one of the two molecules acting as the host and the second component acting as a guest. Before discussing any particular system, an introduction will be given to the forces present in these systems that allow a recognition event to occur.

Fundamentals of Molecular Recognition

The driving force for the interaction of two molecules in solution is a lowering of the systems free energy. Non-covalent bond formation overcomes the entropy change required for these two components to form a complex. The strength of interaction between the host and the guest is determined by several factors. The most important is a geometrical match between the two interacting components, although there are cases where the guest can undergo a conformational change upon substrate binding (Figure 1).[21-23]

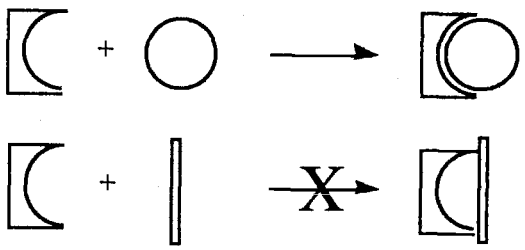

Figure 1: Shape complementarity is important in recognition events

Once the criterion of shape complementarity is met, several intermolecular forces can be present that will increase the binding energy and therefore the probability that a recognition event can occur. Ion pairing and hydrogen bonding represent common recognition elements, but ion-dipole, π – πstacking, and dispersion forces also play a role depending on the system. Although each interaction results in only a small energy change, when summed over the entire system the amount of bond energy obtained can reach or exceed that of a covalent bond. Many systems[4-11,18] have been designed based on an understanding and systematic manipulation of these interactions and energies. In fact, with the

increasing computing power available, these interactions can be modeled[35,36] and new systems can be designed before any experimentation begins.

Host-Guest Chemistry

The initial work on host-guest chemistry was discovered by Pedersen in the development of crown ethers.[42] Crown ethers are able to complex certain alkali metal cations selectively (Figure 2). Crystallographic studies show the potassium ion is the perfect size to fit within the 138 picometer cavity created by 18-crown-6. The positive charge of the potassium ion is attracted to the partial negative charge of the oxygen atoms by ion – dipole interactions. By varying the size of the internal cavity, changing the heteroatom, and/or expanding the complexity of the three-dimensional structure generated, both alkali and alkaline earth metal cations as well as alkyl ammonium ions could be bound.

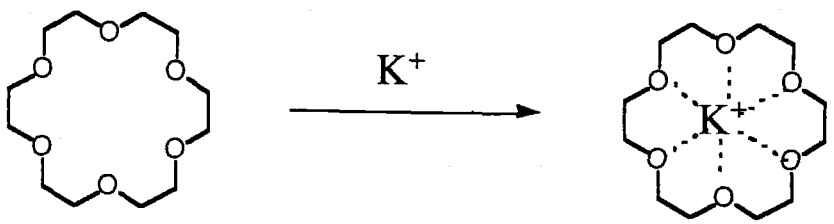

Figure 2 : The complexation of potassium ion in 18-crown-6.

Inclusion complexes of cyclodextrins were discovered about 15 years earlier by Cramer,[43] but didn't gain the popularity of the crown ethers despite their large application potential until after Pedersen and Cram were awarded the Nobel Prize for their work on crown ethers. Formed by the bacterial or enzymatic breakdown of starch, the cyclodextrins are circular polysaccharides with an open

cavity similar to the crown ethers. The most common of the cyclodextrins are six, seven, and eight membered complexes called α, β, and γ-cyclodextrin, respectively (Figure 3). A variety of applications have been discovered for the cyclodextrins, ranging from drug delivery to use as chiral stationary phases for the separation of racemic mixtures. The interior cavity is hydrophobic and will bind non-polar compounds of the correct size and shape as a result of van der Waals interactions.

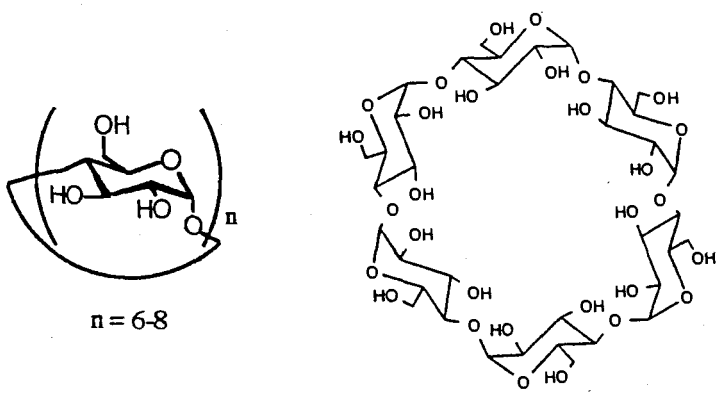

Figure 3: The repeating unit and 3-D structure of the cyclodextrins

The calixarenes[10,11] are a class of cyclic molecules formed from an aromatic phenol and formaldehyde in the presence of base. The rings vary in size, but generally have four to eight aromatic moieties within the ring (Figure 4). Due to intramolecular hydrogen bonding[11] by the four phenolic substituents they adopt a cone shaped structure with an internal cavity.

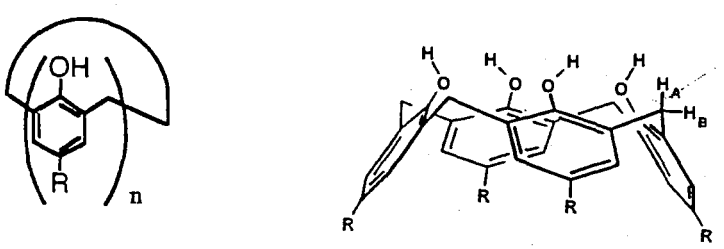

Figure 4 : The repeating unit and 3-D structure of calixarenes

Lithium and sodium ions are attracted by the negative charge on the oxygens of the phenol in calix-[4]-arene, whereas the tetrahedral ammonium ion has been shown to situate itself in the cavity created by the aromatic rings.

By selective choice of alkyl substituents on the aromatic ring, a variety of structures can be generated with customizable properties. Reinhoudt[44] placed two 2,4-diaminotriazine groups as substituents on aromatic rings opposite each other in the calix-[4]-arene. This resulted in a receptor selective for barbiturates. The structures of the barbiturates and the calixarene have an arrangement that allows hydrogen bond donors and acceptors to line up with each other creating a network of six hydrogen bonds (Figure 5).

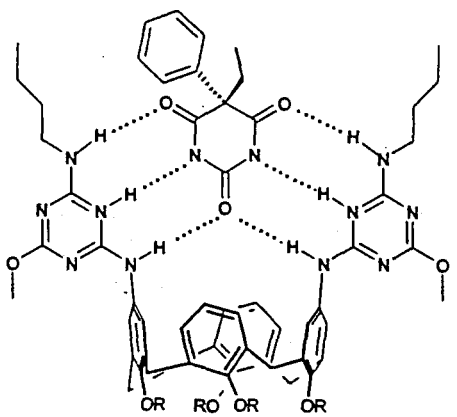

Figure 5: Selective receptor for barbiturates designed from calixarene

Another class of molecular recognition agents is derived from a branched central unit that bears a functional group at the end of each branch allowing for further functionalization or branching. These assemblies are called dendrimers because they resemble tree like structures.[8] Each branch leads to two more branches such that the number of outer groups expands dramatically as the number of branching operations is increased. Dendrimers can be divided into three main

parts: the main core, the outer shell, and an intermediate area lying between the core and the outer shell. Cavities are present in this intermediate region that allow dendrimers to bind a guest.

The dendrimer shown in Figure 6 is able to host both Rose Bengal and p-nitrobenzoic acid simultaneously, releasing each at unique times and conditions. Under slightly acidic conditions the outer shell t-Boc group is cleaved resulting in a shape change thus freeing the p-nitrobenzoic acid selectively.[45] Rose Bengal can be released only upon strongly acidic hydrolysis of the outer shell amide. No specific interactions between host and guest can be established. This interaction is assumed to be based on shape complementarity only.

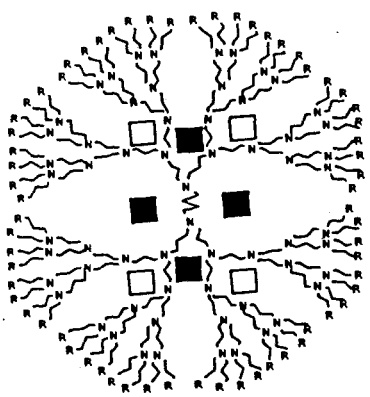

Figure 6: Structure of dendrimer showing cavity in intermediate region

Up to this point, we have seen chemical systems capable of recognizing a molecule either by shape resulting in an energy gain by van der Waals interactions or by proper alignment of donor and acceptor groups. In addition to the types of systems mentioned here there are many others (carcerands, resorcarenes, fullerenes and carbon nanotubes, porphyrin based hosts, spherands, and cyclophanes) that are slight variations on the general scheme presented above. Several monographs[16-18]

and reviews[4-9] are available that summarize each of these types of systems individually and as a whole.

Enzyme Mimics

Bridging the gap between host - guest chemistry and biological molecules such as enzymes and receptors are systems referred to as enzyme mimics.[2,12] Several distinct challenges need to be overcome in order to create synthetic versions of Nature's premier catalysts. The enzyme mimic must recognize the molecule of interest and properly align groups so a desired chemical reaction becomes favorable and is accelerated in the presence of the mimic. After a chemical reaction has taken place, the system must remain unchanged or be converted back to its original form. Lastly, product release should also be favored so that another molecule of starting material can react. Mattei and Diedrich[41] have modified a thiazoline containing cyclophane, which binds aromatic aldehydes, by attaching a hydride reducing agent directly to the cyclophane core. This system mimics the action of pyruvate oxidase (Figure 7).

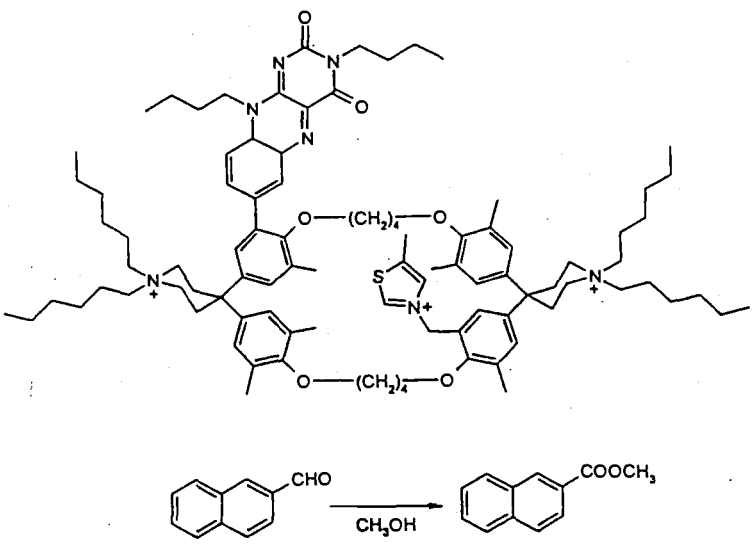

Figure 7: Diedrich's model for pyruvate oxidase

This system has been shown to produce 100 molecules of product for each enzyme mimic. The mimic is able to bind starting material by formation of a covalent bond with an aromatic aldehyde. This system is now activated for hydride transfer and subsequent reaction to form the aromatic ester. The flavin residue is electrochemically oxidized back to the active form. Analysis of factors responsible for binding of the aldehyde and placement of reactive centers within the same area allows the construction of the most active enzyme mimic developed so far.

Molecular Recognition in Enzymes

There are two theories of substrate binding in biological molecules. The first theory, proposed over 100 years ago by Emil Fischer, is based on shape complementarity discussed above. Called the lock and key hypothesis,[38] Fischer assumed that the enzyme acts like a lock and the substrate like a key. Substrate binding can only occur if the key fits into the lock. Fischer's hypothesis was an important advancement towards understanding molecular recognition in biological systems.

Koshland introduced an alternative theory in 1958 called induced fit.[37] The main idea of the induced fit theory is that substrate binding causes a conformational change, sometimes subtle and sometimes very large, in the enzyme that allows for tight binding between substrate and enzyme. There is evidence that these subtle conformational changes are responsible for the catalytic activity of enzymes.[21-23]

Regardless of the theory, there are several difficulties in understanding biological molecular recognition. First, most enzymes and receptors are large molecules; structural characterization requires the use of techniques other than standard physicochemical techniques (IR, UV, NMR). The molecular size also makes individual contributions to substrate binding difficult to distinguish. Although substrate recognition is the first step in the catalytic cycle we must also

concern ourselves with transition state stabilization and recognition as well as product destabilization since these are also important to the catalytic mechanism.

There are several ways to study enzymatic molecular recognition. The most powerful technique is X-ray diffraction.[32-36] With the advent of X-ray diffraction and the accumulation of X-ray crystal structure data[46] for a variety of enzymes both with and without bound substrate, the understanding of recognition events has increased dramatically in the last thirty years. X-ray diffraction allows for Ångstrom level resolution of individual atoms of the enzyme and bound substrate or inhibitor. When coupled to molecular modeling, the ability to understand the basis of molecular recognition between substrate and enzyme and to predict alternative substrates or potential inhibitors is expanded dramatically. However, this technique requires the ability to grow a diffraction quality crystal.

Site directed mutagenesis is another powerful technique.[15] Site directed mutagenesis involves isolating mutant versions of the natural enzyme that have substitutions of one amino acid for another. For example, an aspartate residue is replaced with alanine and the effect on the catalytic turnover and the substrate binding of the enzyme is determined. If there is no effect, the aspartate residue is not important in binding or catalytic turnover. This technique, however, is ideally suited to a situation where the three dimensional structure is known.

Another common method is to perform a structure - activity analysis. In this method, the goal is to analyze functional groups that may interact in the active site of the enzyme. The analysis begins with small modifications to or removal of hydrogen bond donors and hydrogen bond acceptors of the natural substrate. The effect on k_{cat} and K_m of these alternative substrates / potential inhibitors can allow the determination of importance of certain functional groups upon binding. In a lot of ways, site directed mutagenesis and structure – activity analysis are related. Site directed mutagenesis makes modifications to the enzyme and structure – activity method makes modifications to the functional groups of the substrate. Both are powerful methods to determine factors important for recognition.

Although X-ray diffraction and site directed mutagenesis represent definitive sources of information about substrate binding and the catalytic cycle, the first step in any study starts with a study of the rates of the individual reactions occurring in the enzyme. The simplest system assumes the substrate and enzyme bind to each other to form a Michaelis complex (Scheme 1).

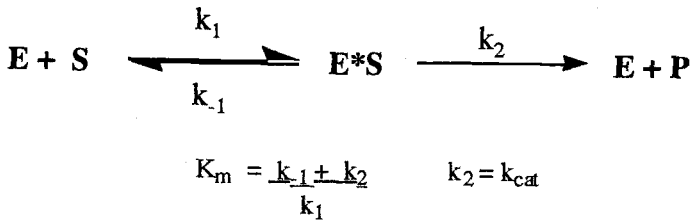

Scheme 1: Formation and fate of Michaelis complex

This complex can either dissociate to starting material and enzyme or can react to form product. The product is released and the active form of the enzyme can continue in the catalytic cycle. Once individual rate constants are determined, primarily k_{cat} and K_m, contributions to the binding energy can be established through the use of a linear free energy relationship.

Due to the amount of material available on each of these techniques, the following discussion can provide only a representative example of each technique. We will begin with the most powerful technique: X-ray diffraction.

X-ray Crystal Structures

The literature is expanding with three - dimensional structures of proteins, enzymes, and receptors with and without bound substrates, inhibitors, and co-

factors, allowing a first hand account of factors responsible for recognition as well as conformations responsible for catalytic activity.

Chang's group at Merck Pharmaceuticals recently solved the crystal structure of human immunodeficiency virus protease (HIV PR) with six different inhibitors bound.[33] Several groups have already used this information to design of inhibitors specific for HIV PR, while leaving the human proteases, pepsin and renin, unaffected.

HIV PR is a homodimer with each monomer contributing equally to the active site. Cyclic urea (CU) inhibitors have been discovered that displace a critical bridging water molecule in the active site of HIV PR. A generic form of the CU inhibitors is shown in Figure 8. The crystal structure data has allowed the authors to determine the following information about binding. The seven-membered ring adopts a twist chair conformation, the urea group remains planar, and the oxygen of the urea group is responsible for displacement of the water in the protein flap discussed earlier. The two alcohols of the diol hydrogen bond are then allowed to bind with the catalytic aspartates present at position 29 and 30 in the active site. They were also able to determine that the two - fold axis of the inhibitors mirrors that of the homodimer and upon binding a significant conformational change occurs resulting in a seven Ångstrom shift of the protein flap that completely covers the active site of HIV PR.

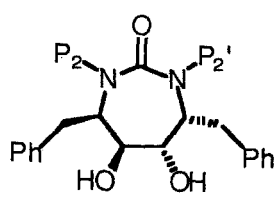

Figure 8: Cyclic urea (CU) inhibitors of HIV protease

Site Directed Mutagenesis

By replacing one amino acid in a peptide chain with another amino acid the functional groups responsible for binding can be elucidated. Determination of differences in the catalytic rate, k_{cat}, or the Michaelis - Menten constant, K_m, allows one to establish the importance of different amino acids for binding and catalytic activity.

Sierks and Svensson[29] have studied the effect of various substitutions on the binding and catalytic activity of glucoamylase (GA). GA is an enzyme that hydrolyzes the non-reducing ends of starch releasing D-glucose. GA is capable of recognizing both α-1,4- and α-1,6-glycosidic linkages, but has a preference for the former. GA is believed to contain seven subsites each of which binds a glucosyl residue of the substrate. The seven subsites are created by six $\alpha - \alpha$ helical contacts of the enzyme.

The choice of amino acid substitutions was based on X-ray crystal structure data previously reported in the literature.[46] Ten mutants were created and are summarized in Table 1 below. A comparison of the catalytic rate constants of each mutant versus the wild-type enzyme allows the determination of the groups responsible for transition state stabilization. K_m values are compared between mutant and wild type enzymes to determine the groups responsible for formation of the enzyme-substrate complex.

Substitution of glycine for aspartate-55 caused a 200-fold decrease in k_{cat} with no change in K_m. This indicates the importance of the aspartate residue in stabilizing the transition state during the hydrolysis reaction. Aspartate, though, has no effect on substrate binding. By including data from deoxygenated maltose derivatives, which are substrates, they found that when the 4' or 6'-OH groups of maltose were removed, an increase in free energy was observed indicating the significance of these hydroxyl groups in transition state stabilization. In a similar

fashion, the other factors responsible for both substrate binding and transition state stabilization were determined.

Table 1. Point mutations in glucoamylase and their effect on recognition

α – α Helical Contact Segment	Mutation	Effect on binding	
		k_{cat}	K_m
First	Asp55 → Gly	decreases	no change
Second	Tyr 116 → Ala	decreases	no change
	Ser119 → Tyr	no change	no change
	Trp120 → Phe	decreases	no change
Third	Asp176 → Asn	decreases	increases
	Trp178 → Arg	decreases	no change
	Glu180 → Gln	no change	increases
	Asn182 → Ala	no change	no change
Fifth	Tyr306 → Phe	no change	increases
	Asp309 → Asn	decreases	increases

Structure – Activity Relationships

This method of analysis requires small changes in substrate structure. By analyzing potential interaction sites of the substrate with the enzyme based on general intermolecular forces, slight modifications can be made that will allow an

estimation of the significance of the different parts of the substrate structure important for recognition. The advantage of using a structure-activity relationship is the ability to perform these studies using impure enzyme solutions. An example of this was seen above in the use of deoxygenated maltose derivatives to determine the interaction of specific hydroxyl groups with amino acids in the active site.

Gordon has taken this approach when studying ways to identify better fungal inhibitors.[28] *Candida albicans (C. albicans)* is an asexual yeast that infects 90% of AIDS patients at some point in the course of their disease. N-Myristoyltransferase (Nmt) has been determined to be important for the viability of the organism and therefore inhibition of this enzyme could result in new drugs to treat infections caused by this fungus. An octapeptide, GLYASKLS-NH_2, is a substrate for purified *C. albicans* Nmt in vitro (Figure 9). Gordon studied the effect of alanine substitutions in each position of this octapeptide to identify the functional groups responsible for binding.

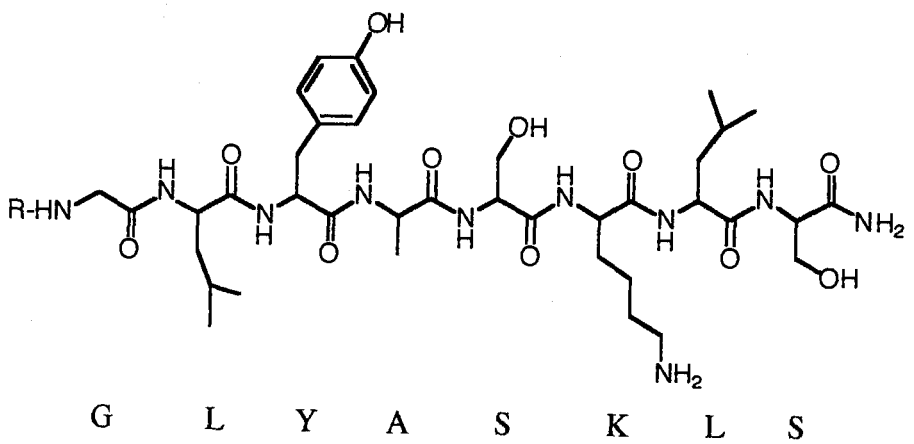

Figure 9: Octapeptide inhibitor of Nmt of *Candida albicans*

Substitutions of alanine at positions one, five, and six caused the largest increase in K_m, an indication that amino acids at each of these positions contain a

functional group or shape recognized by the enzyme active site. Further substitutions were carried out to determine the exact group responsible for the binding interaction. Replacement of the serine residue, at position 5, caused a 10,000-fold increase in K_m, suggesting that the hydroxyl group was important for binding. To test this, Gordon methylated the hydroxyl group of serine and saw an increase in the IC_{50} value from 29 ± 4 μM to 920 ± 110 μM. Change of the lysine group in residue 6 to a norleucine, ornithine, or arginine derivative causes a decrease in the kinetic parameters, K_m and V_{max}. This signifies the importance of a hydrogen bond donor as well as chain length in recognition at position 6 of the octapeptide.

The stereochemistry of the alkyl chain in position 1 is the major factor in binding. When D-glycine was replaced with L-glycine, a significant reduction in K_m was observed, although longer alkyl chains with D-stereochemistry were competitive inhibitors. The binding pocket at position 1 seems to be defined by hydrophobic interactions.

The authors tested further derivatives trying to ascertain the importance of the remaining five peptides. Replacing the first two amino acids with a six-carbon backbone, 5-aminopentanoyl, while maintaining the important terminal amino group resulted in an inhibitor 180-fold more active as an inhibitor than the initial octapeptide. Subsequent modifications to the original structure resulted in an inhibitor containing only two amino acids in the peptide chain. The complexity of the inhibitor had been decreased significantly, going from the original octapeptide with eight stereocenters to the final inhibitor that has only two stereocenters. Gordon's ultimate goal was to find an inhibitor containing no peptide bonds.

Linear Free Energy Relationships

Another common method is to determine the dependence of free energy changes on various physical or chemical properties of the substrate or system under study. In this method, a property of the system is systematically modified, the effect on the various kinetic parameters is determined, and these data related to the free energy of the system.

Quinn recently used a linear free energy relationship to elucidate factors responsible for binding of aryl-substituted carbamates in the two binding sites of porcine and rat cholesterol esterase (CEase).[30] CEase's catalyze the hydrolysis of a wide range of ester substrates; unfortunately little is known about the nature of the interactions between substrate and the CEase active site that leads to effective catalysis.

A series of aryl carbamates were synthesized that varied both the alkyl substituent of the carbamate nitrogen and the aryl substituent. Quinn determined that the energy of binding is a linear function of the partial molecular volume of either the N-alkyl chain or the aryl fused ring fragment. He used the following equation to describe this free energy relationship

$$-\ln K_C = (\Delta G_o - f\Delta\Delta G_f) / RT \qquad \text{Eqn (1)}$$

where ΔG_o is the extrapolated binding energy at zero fragment volume, f is the fragment volume, and $\Delta\Delta G_f$ is the fragment volume-dependent change in the binding energy. The magnitude of $\Delta\Delta G_f$ establishes the importance of hydrophobic interactions on ligand binding in the steroid and fatty acid binding sites in CEase. Values were obtained for the free energy terms in equation 1 by plotting $-\ln K_C$ versus fragment volume. The large and negative value obtained (Table 2) for $\Delta\Delta G_f$ indicate a stronger dependence on hydrophobic interactions in the fatty acid binding site for rat CEase.

Table 2: Binding free energy correlations for carbamate inhibitors of CEase

varied fragment	enzyme	ΔG_o (kJ/mol)	$\Delta\Delta G_f$ (J/mol*Å^3)
N-alkyl chain	rat CEase	14 ± 2	-190 ± 20
	porcine CEase	31 ± 5	20 ± 50
aryl fused ring system	rat CEase	28 ± 2	-40 ± 10
	porcine CEase	-27 ± 4	10 ± 30

As can be seen from the above discussion, the number of techniques and the information that can be obtained from these techniques can be extremely useful in learning more about substrate binding and the active site of enzymes. Several of these techniques have been used in research on DHAE I and DHAE II. Before discussing the results of the current research, let's talk about the previous research undertaken on these two enzymes.

Previous Work on DHAE-I and DHAE-II

Dihydroxyacetanilide Epoxidase I (DHAE-I) and DHAE-II are enzymes isolated from fermentation broths[19,20] of *Streptomyces* LL-C10037 and *Streptomyces* MMP3051, respectively. Both are unique enzymes requiring only substrates (2,5-dihydroxyacetanilide and molecular oxygen) for activity. There were reported to be no co-factors or metal ion requirements, although activity is enhanced in the presence of Co^{2+}.

DHAE I is a dioxygenase having either five or six equally sized subunits with an overall molecular weight of ~110 kDa. DHAE II, assumed to be a dioxygenase based on the similarity of the catalytic reaction, is a dimer whose

molecular weight is ~30 kDa. Both enzymes catalyze the conversion of 2,5-dihydroxyacetanilide to the corresponding epoxyquinone (Scheme 2).

The bulk of previous work related to DHAE I and DHAE II involves the purification of each enzyme and attempted N-terminal and internal amino acid sequencing. Shen and Gould[40] devised a purification procedure that took over five weeks to process. This procedure resulted in 112 μg of near homogeneous DHAE I from 180 grams of wet cells. There were eight bands present in silver stained SDS PAGE, but the band corresponding to DHAE I was never identified.

Kirchmeier and Gould[39] made some improvements in the purification scheme that resulted in a shorter processing time and homogeneous DHAE I. A single band was obtained from a procedure involving six chromatographic and two electrophoretic steps. A portion of the N-terminal and internal sequence was obtained, but the total amount of enzyme isolated did not allow for a complete sequence to be determined.

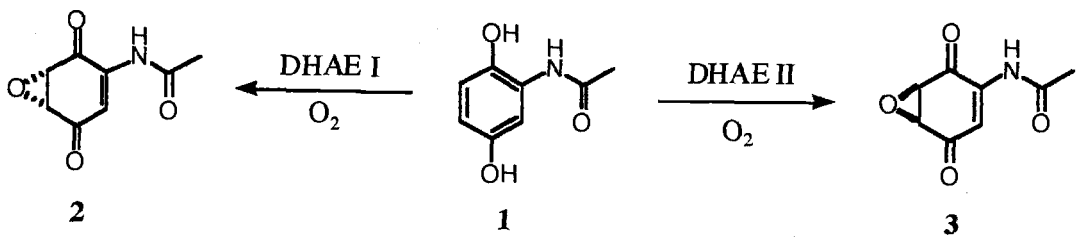

Scheme 2: Enzymatic reaction of DHAE I and DHAE II

Kirchmeier also prepared compounds **4-6** (Figure 10) as a means of determining the groups required for recognition between enzyme and substrate. Focusing first on the obvious hydrogen bond donors, Kirchmeier manipulated the position of the hydroxyl groups on the ring. Compounds **4** and **5** were determined to be poor competitive inhibitors for DHAE I. Compounds **4**, **5** and **6** were also

poor competitive inhibitors for DHAE II. From this information, it was concluded that both hydroxyl groups are required for binding and catalytic activity.

The inhibition constant, K_i, can be used to make observations about the importance of individual hydroxyl group contributions to the binding. The K_i value for **4** was much lower for DHAE I than for DHAE II, potentially indicating a more important catalytic role for the hydroxyl group at C-2 for DHAE I. On the other hand, the hydroxyl group at C-3 of **5** is more important for binding to DHAE II than for DHAE I (K_i values of 505 μM vs 1348 μM, respectively).

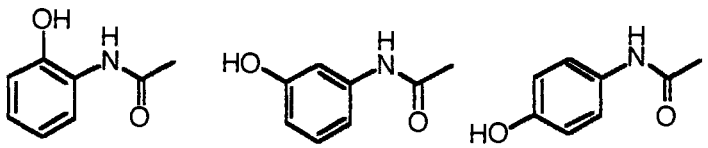

4 **5** **6**

Figure 10: Competitive inhibitors used to test function of hydroxyl groups

Kirchmeier modified the side chain by replacing the methyl group with a phenyl ring. The substituted benzanilides, **7** and **8** (Figure 11), were designed to test the active site flexibility and the effect of the amide carbonyl on binding of substrate. **7** and **8** were both strong competitive inhibitors for both enzymes having K_i values on the same order of magnitude as K_m.

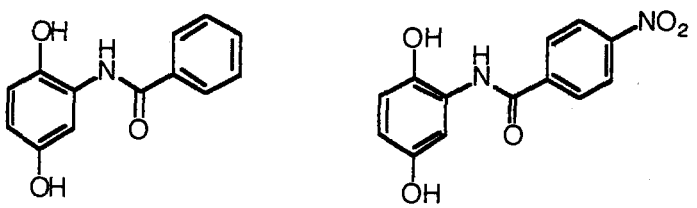

7 **8**

Figure 11: Competitive inhibitors designed by Kirchmeier

Purpose of the Present Study

Each part of this project deals with an aspect of molecular recognition[24-27]. The overall goal was to discover the aspects that control binding between 2,5-dihydroxyacetanilide and DHAE I or DHAE II.

To determine the role of the amide upon binding, a Hammett study has been performed. Taking advantage of the benzanilide series of inhibitors discovered by Kirchemeier, the aromatic ring of the phenyl substituent gave the opportunity to vary the electron density at the amide oxygen. By evaluating the effect that a decrease or an increase in electron density has on the inhibition constant, the importance of the amide bond can be established.

The second area uses information from the Hammett study mentioned above to identify a potential ligand for an affinity column. The affinity column would afford a better and faster separation of the enzymes from the complex cell-free extract mixture. The main obstacle that Kirchmeier and Shen had to overcome was the quantity of enzyme isolated. With milligram quantities of enzyme, the procedures and techniques available to study the enzyme mechanism as well as explore recognition events through site directed mutagenesis and X-ray crystal data will be possible.

As a last goal, alternative substrates were designed to test flexibility of the active site and to recognize the potential for using these enzymes as reagents in organic synthesis. The potential for using these enzymes in combination with traditional synthetic techniques could expand the ability to create complex enantiomerically pure synthetic targets efficiently. A major synthetic target based on structural similarity is the manumycin[47] class of antibiotics / anti-cancer compounds (Figure 12). A metabolite of manumycin retains biological activity and is shown below for comparison.

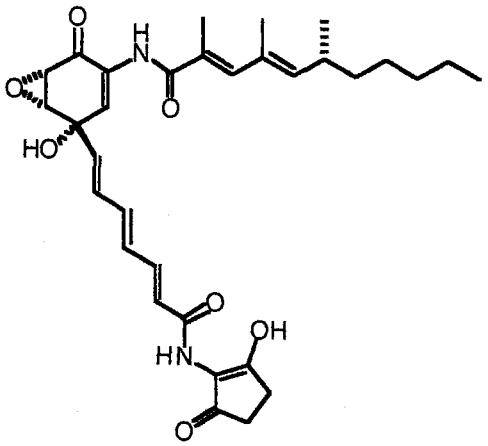

Manumycin

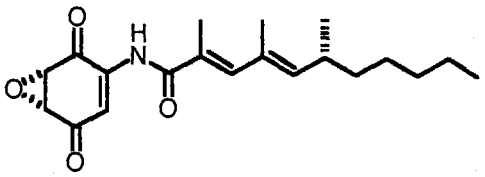

metabolite of Manumycin that retains biological activity

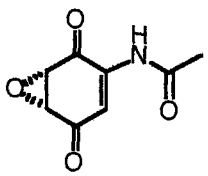

epoxyquinone from DHAE I shown to show structural similarity

Figure 12: Structure of manumycin and similarity to DHAE I epoxyquinone

References

1. Balzani, V.; Credi, A.; Raymo, F.M.; Stoddart, J.F. *Angew. Chem. Int. Ed.* **2000**, 39, 3348-3391

2. Feiters, M. C.; Rowan, A. E.; Nolte, R. J. M. *Chem. Soc. Rev.*, **2000**, 29, 375-384

3. Matile, S., *Chem. Soc. Rev.* **2001**, 30, 158-167

4. Konig, B.; Reichenbach-Klinke, R. *J. Chem. Soc., Dalton Trans.* **2002**, 121-130

5. Rebek, J.; Renslo, A.R. *Angew. Chem. Int. Ed.* **2000**, 39 (18), 3281-3283

6. Ogoshi, H.; Hayashi, T.; Asai, T.; Borgmeier, F. M.; Hokazono, H. *Chem. Eur. J.* **1998**, 4(7), 1266-1274

7. Beer, P.D.; Gale, P.A. *Angew. Chem. Int. Ed.* **2001**, 40, 486-516

8. Meijer, E.W.; Baars, M. W. P. L. *Topics in Current Chemistry*, **2000**, 210, 131-182.

9. Kaifer, A. E.; *Acc. Chem. Res.* **1999**, 32 (1), 62-71

10. Nolan, K.; Diamond, D. *Anal. Chem.* **2001**, 23A – 29A

11. Rudkevich, D.M. *Chem. Eur. J.* **2000**, 6(15), 2679-2685

12. Kimura, E. *Acc. Chem. Res.* **2001**, 34, 171-179

13. Roberts, S.M.; Legon, A.C.; Buckingham, A. D. *Principles of Molecular Recognition* Blackie Academic and Professional **1993** 1-17

14. Delaage, M. *Molecular Recognition Mechanisms* VCH Publishers **1991** 1-14

15. Delaage, M. *Molecular Recognition Mechanisms* VCH Publishers **1991** 219-238

16. Behr, J-P *The Lock and Key Principle Perspectives in Supramolecular Chemistry Vol. 1* Wiley and Sons **1994** 1-24

17. Roberts, S.M. *Molecular Recognition: Chemical and Biochemical Problems II* Royal Society of Chemistry **1992** 1-20

18. Dodziuk, H. *Introduction to Supramolecular Chemistry* Kluwer Academic Publishers **2002** 1-58

19. Lee, M.D.; Fantini, A. A.; Morton, G. O.; James, J. C.; Borders, D. B.; Testa, R. T. *J. Antibiot.* **1984**, 37, 1149

20. Box, S. J.; Gilpin, M. L.; Gwynn, M.; Hanscomb, G.; Spear, S. R.; Brown, A. G. *J. Antibiot.* **1983** 36 1631

21. Teague, S. J.; Davis, A. M. *Angew. Chem. Int. Ed.* **1999**, 38, 736-749

22. Tsou, C-L *Annals of N.Y. Acad. Sci.* **1998**, 864, 1-8

23. Blundell, T.; White, H. E.; Emsley, J.; Wood, S. P.; Dhanaraj, V.; Rufino, S.; Guruprasad, K.; Srinivasan, N.; Sowdhamini, R. *Pharm. Acta. Helv.* **1995**, 69, 185-192.

24. Khosla, C.; Cane, D. E.; Kudo, F.; Wu, N. *J. Am. Chem. Soc.* **2000**, 122 (20), 4847-4852

25. Johnson, W. W.; Clement, R. P.; Casciano, C. N.; Barecki, M.; Lew, K.; Wang, E. *Chem. Res. Toxicol.* **2001**, 14, 1596-1603

26. Eliseev, A. V.; Rudra, S. *J. Am. Chem. Soc.* **1998**, 120 (45), 11543-11547

27. Peters, T.; Biet, T. *Angew. Chem. Int. Ed.* **2001**, 40 (22), 4189-4192

28. Gordon, J. I.; Sikorski, J. A.; Getman, D. P.; Devadas, B.; Brown, D. L.; Freeman, S. K.; Zupec, M. E.; Rocque, W. J.; McWherter, C. A. *J. Biol. Chem.* **1997**, 272 (1), 11874 – 11880

29. Sierks, M. R.; Svensson, B. *Biochemistry* **2000**, 39, 8585-8592

30. Quinn, D. M.; Hui, D. Y.; Baker, N.; Lee, K.; Feaster, S. R. *Biochemistry*, **1996**, 35, 16723-16734

31. Wong, C-H. *Pure Appl. Chem.* **1997**, 69 (3), 419-422

32. Penning, T. M. *J. Ster. Biochem. and Molec. Biol.* **1999**, 69, 211-225

33. Chang, C-H.; Duke, J. L.; McCabe, D. D.; Weber, P. C.; Lewandowski, F. A.; Schadt, M. C.; Hodge, C. N.; Eyermann, C. J.; Lam, P. Y. S.; Jadhav, P. K.; Huston, E. E.; Deloskey, R. J.; Ala, P. J. *J. Biol. Chem.* **1998**, 273 (20), 12325 – 12331

34. Kim, J-J. P.; Dahms, N. M.; Weix, D. J.; Roberts, D. L. *Cell* **1998**, 93, 639-648

35. Massey, V.; Ballou, D. P.; Entsch, B.; Moran, G. R.; Palfey, B. A. *Biochemistry* **1999**, 38 (4), 1153-1158.

36. Kuramitsu, S.; Hirotsu, K.; Kawaguchi, S.; Nakai, T.; Ishijima, *J. Biol. Chem.* **2000**, 275 (25), 18939-18945

37. a.) Koshland, D. E. Jr.; *Proc. Natl. Acad. Sci.* USA **1958**, 44, 98
b .) Koshland, D. E. Jr.; *Angew. Chem.* **1994**, 106, 2468

38. Fischer, E. *Chem. Ber.* **1894** 27 2985

39. Kirchmeier, M. *Purification of 2,5-dihydroxyacetanilide Epoxidase and Mechanism of Hydroquinone Epoxidases.* Thesis, Oregon State Univ. **1997**

40. Shen, B. LL-C10037a and MM14201: *Structure, Biosynthesis, and Enzymology of two Epoxyquinone Antibiotics.* Thesis, Oregon State University, **1990**.

41. Mattei, P.; Diedrich, F. *Helv. Chim. Acta* **1997**, 80, 1555

42. Pedersen, C. J. *J. Am. Chem. Soc.* **1967**, 89, 7017

43. Cramer, F. *Angew. Chem.* **1952**, 64, 437

44. Reinhoudt, D. N.; Verboom, W.; Heida, J. F.; van Loon, J.-D. *Rec. Trav. Chim. Pays-Bas* **1992**, 111, 353

45. Jansen, J. F. G. A.; Meijer, E. W. *J. Am. Chem. Soc.* **1995**, 117, 4417

46. Harris, E. M. S.; Aleshin, A. E.; Firsov, L. M.; Honzatko, R. B. *J. Biol. Chem.* **1994**, 269, 15631-15639

47. Han, M.; Hara, M. *Proc. Natl. Acad. Sci. USA* **1995**, 92, 3333-3337

Chapter 2

Exploration of the Active Site of DHAE I and DHAE II: Use of a Hammett Study and Alternative Substrates to Determine Elements Responsible for Molecular Recognition

As discussed in Chapter 1, structure-activity relationships can be useful in determining the basis for substrate binding in enzymatic systems. A structure activity relationship has been applied to the study of substrate binding in the two enzymes, DHAE I and DHAE II. By systematic variation of functional groups present in the natural substrate, several questions can be addressed. First, what represents the third recognition element for substrate binding between **1** and DHAE I / DHAE II? Second, can we design alternative substrates based on an understanding of the recognition elements in the natural substrate? Finally, is there a conformational dependence of the amide bond upon binding to the enzyme? The main avenue by which these questions were explored was by designing potential competitive inhibitors coupled with a linear free energy relationship. Therefore, our discussion starts with brief introductions to enzyme inhibition, linear free energy relationships, and how they can be combined to generate useful mechanistic and molecular recognition information.

Inhibition in Enzymology

Several types of inhibition are commonly encountered when studying enzymes. Many enzymes follow Michaelis-Menten kinetics[20] and all formulas mentioned below will use this model as a starting point. Modifications to the Michaelis – Menten equation are necessary in the presence of each type of inhibitor. All forms of inhibition assume the inhibitor does not also act as an alternative substrate.

When an inhibitor and the natural substrate compete for the active site, the inhibition is referred to as competitive. A good competitive inhibitor therefore will require more substrate to overcome the effect of inhibitor resulting in an increase in the apparent K_m. The kinetics of the reaction in the presence of a competitive inhibitor will follow the equation shown below.

$$v = \frac{V_{max}[S]}{K_m(1 + [I]/K_i) + [S]}$$

The second type of inhibition, called uncompetitive inhibition, results when the inhibitor binds only to the enzyme – substrate complex. The inhibitor does not affect binding of substrate to the enzyme and therefore will not change the K_m value. However, because the catalytic reaction is slowed or prevented completely the maximum velocity will be reduced in the presence of an uncompetitive inhibitor. When uncompetitive inhibition is observed, the kinetics will fit the equation below.

$$v = \frac{V_{max}(1 + [I]/K_i)[S]}{K_m + [S]}$$

Mixed inhibition occurs when a mixture of competitive and non-competitive inhibition is present. The inhibitor is able to bind to the enzyme or the enzyme – substrate complex changing both kinetic parameters, K_m and $V_{max.}$

Linear Free Energy Relationships

A Linear Free Energy Relationships (LFER)[30] is frequently used in organic chemistry to study how perturbations in a physical or chemical property of the system can affect the thermodynamics or kinetics of a reaction. Both qualitative and quantitative data can be obtained from a LFER. For example, a study may show electron withdrawing groups retard the reaction rate or shift the equilibrium toward reactants, but it does not tell us the importance of the change. Qualitative

information is useful for predicting trends, but quantitative information tells us how significant the trend.

The Hammett Equation

The Hammett Equation is one of the most important LFER in organic chemistry.[30-33] By examining the effect of different functional groups on the equilibrium of benzoic acid dissociation (Scheme 3), Hammett was able to assign numerical values, called the substituent constant (σ), to different functional groups based on their electronic character relative to hydrogen.

Using the benzoic acid dissociation as a reference reaction, the shift in equilibrium of substituted benzoic acids was compared to the unsubstituted reference reaction. Electron withdrawing groups shifted the equilibrium towards product, resulting in a positive value for σ (Equation 2).

$$\sigma_X = \log (K_X / K_H) \quad \text{definition of substituent constant} \quad \text{Eqn (2)}$$

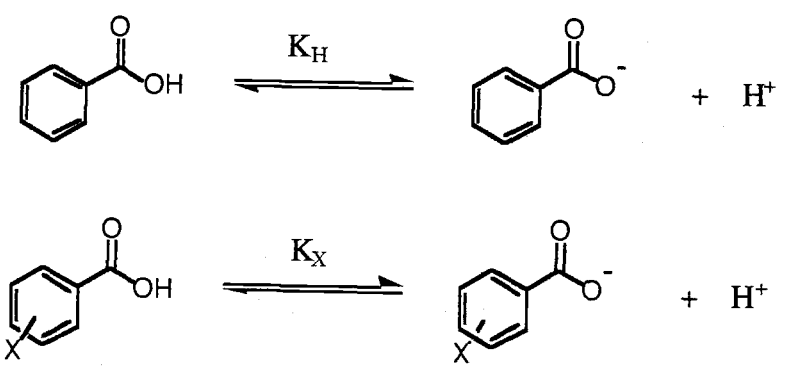

Scheme 3: Benzoic acid dissociation and effect of perturbations on the eq. const.

If this information were applicable only to benzoic acid dissociations, it would merely be a minor advancement. However, the wide applicability of the Hammett equation is based on the assumption that substituents will have the same effect on similar reactions and can be applied in those cases. The Hammett study can be used to probe equilibrium reactions as shown above, but information can also be gained about the transition state by looking at reaction rates (Equation 3). In the Hammett equation, the slope of the plot, given by the symbol ρ, is an indication of the sensitivity of the reaction to substituent effects. A large ρ value indicates significant charge build up at the transition state.

$\log (K_{X'} / K_{H'}) = \sigma_X * \rho$ Hammett equation for change in eq. const. Eqn (3)

$\log (k_{X'} / k_{H'}) = \sigma_X * \rho$ Hammett equation for change in rate const. Eqn (3)

Since the Hammett equation is an example of a linear free energy relationship, we can also express these equations in terms of free energy changes instead of equilibrium or rate constants (Equation 4).

$$\Delta G_X^{o'} - \Delta G_H^{o'} = \rho \, (\Delta G_X^{o} - \Delta G_H^{o}) \qquad \text{Eqn (4)}$$

$$\Delta G_X^{\ddagger,} - \Delta G_H^{\ddagger,} = \rho \, (\Delta G_X^{o} - \Delta G_H^{o}) \qquad \text{Eqn (4)}$$

Given that we are interested only in the electronic effect of the different substituents, there are several limitations to using a Hammett study. The substituent must be able to interact electronically with the reaction center. Also, ortho substituents cannot be used since they introduce an additional steric factor preventing isolation of the electronic effect. Before moving on to a discussion of the research undertaken, several issues of concern must be considered which are specific to the biological application of the Hammett equation.

The Hammett Equation in Enzymology

Because of the nature of substrate binding and the close geometrical fit between enzyme and substrate required to initiate catalysis, steric factors are an issue when evaluating enzyme kinetic or thermodynamic data. Difficulties also arise because two phenomena can be affected by the introduction of different substituents.[24-26] The typical enzymatic reaction can be divided into kinetic and thermodynamic processes (Figure 13). The first process is the equilibrium between enzyme and substrate. In order to use K_m to evaluate equilibrium changes, the catalytic rate constant must be assumed to be rate limiting. If we assume the catalytic rate constant, k_{cat}, is rate limiting, the K_m value approximates the equilibrium dissociation constant, K_s, between enzyme and substrate. The chemical reaction itself may also be affected. In order to gain valuable mechanistic information, isolation of the individual rate constants for each mechanistic step must be achieved. With the rate constants calculated, the mechanistic step affected by the perturbation in the system can be determined.

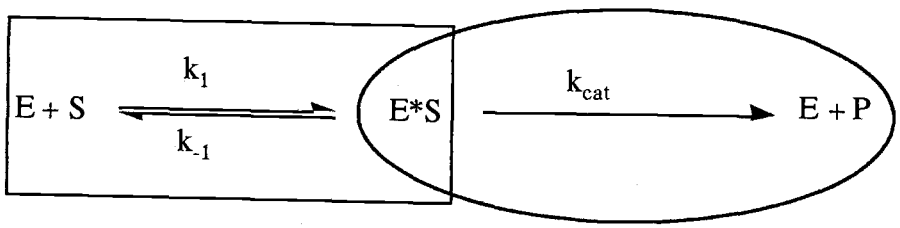

Thermodynamic Process — Kinetic Process

$K_m = (k_{-1} + k_{cat}) / k_1$ — if $k_{-1} \gg k_{cat}$, then $K_m \sim K_s$

Figure 13: Two different phenomena affected by variation in substrate structure

A Hammett study can be used to explore each of the processes discussed above. First, it can identify the functional groups required for recognition between substrate and enzyme by creating a series of competitive inhibitors containing all recognition elements present in the natural substrate. The inhibitor must be competitive, not be accepted as an alternate substrate, and have an aromatic system able to communicate electronically with a potential recognition site. The presence of the aromatic system will allow for systematic changes in electron density at the recognition site by proper choice and variation of substituents. The effect of a particular functional group on binding can be determined by evaluating the logarithmic relationship between the ratio of the two equilibrium constants, K_i and K_s, and σ (Equation 3).[12] To obtain information about the reaction mechanism, alternative substrates have to be created such that electron density can be modified at the reaction site and the logarithmic relationship between the ratio of the rate constants and σ determined. This is best shown with a few representative examples.

Representative Examples of Hammett Studies in Enzymology

GGT, γ – glutamyl transpeptidase, catalyzes acyl transfer of the γ – glutamyl residue of glutathione (GSH) to a variety of acceptor molecules. The ping pong mechanism is believed to start when an amino acid binds to the active site.[11] The acyl group is transferred and a product is released leaving the enzyme acylated. An acceptor molecule then binds and reacts with the acylated enzyme to form a new peptide bond. The product is then released. L-γ-glutamyl-p-nitroanilide, **16**, has been shown to be an excellent substrate for this enzyme. This information was used to construct a series of compounds that differed only in the identity of the para substituent (Figure 14). Kinetic parameters, k_{cat} and K_m, were determined for each substrate and a variety of Hammett plots were created. The only significant

relationship was obtained between log (k_{cat}^{X} / k_{cat}^{H}) vs. σ^{-}. An upward curvature in the plot starting at the fluorinated substrate, **13**, indicated either a potential change in mechanism or a substituent-induced change of geometry in the transition state.

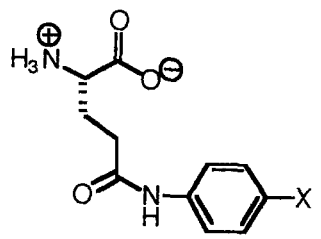

09 X = OMe
10 X = Me
11 X = Et
12 X = H
13 X = F
14 X = CF_3
15 X = CO_2Et
16 X = NO_2

Figure 14: Substrate analogues used to explore mechanism in GGT

The results indicate that both electron donating and electron withdrawing substituents accelerate the reaction rate. To explain this phenomenon, the authors proposed two slightly different mechanisms. In the presence of an electron donor, the amide bond is cleaved and before collapse of the tetrahedral intermediate, the nitrogen of the amide is protonated. Protonation generates a formal positive charge on the nitrogen atom that would be stabilized by electron donating substituents. In the presence of electron withdrawing groups, the tetrahedral intermediate collapses to release a negatively charged p-nitroanilide. Electron withdrawing substituents stabilize the negative charge on the nitrogen atom and therefore accelerate the decomposition of the tetrahedral intermediate (Scheme 4).

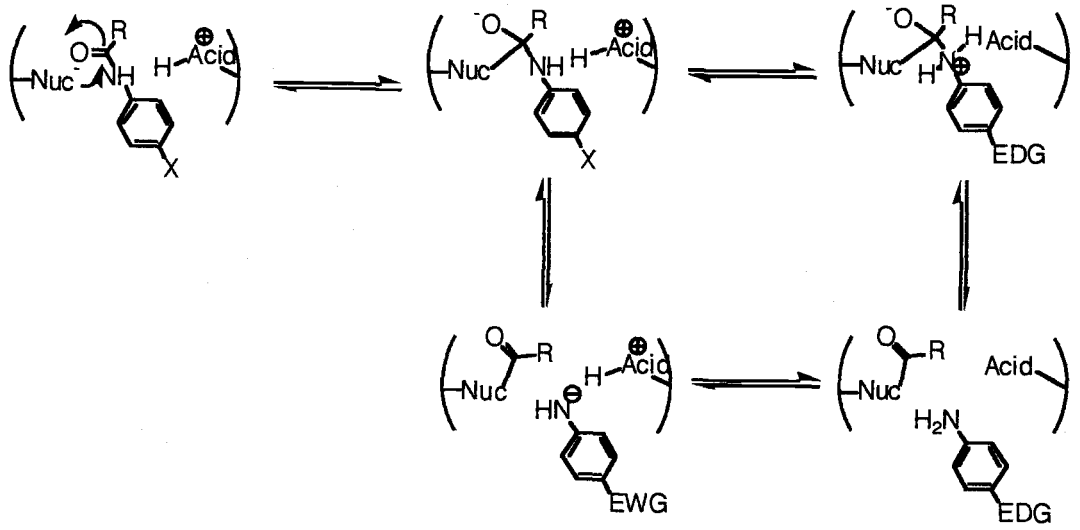

Scheme 4: Mechanistic rationale for observed behavior in Hammett plot

In a similar fashion, Whittaker and Whittaker investigated the effect of substrate variation on the proposed mechanism of galactose oxidase.[14] Galactose oxidase has an oxy radical bound to a copper (II) metal center that binds and oxidizes a variety of alcohols to the corresponding aldehyde. Upon release of the aldehyde, molecular oxygen binds and is converted to hydrogen peroxide. A series of substituted benzyl alcohols (Figure 15) were used as galactose oxidase substrates and the rate of the reactions were measured for both protio and deuterio derivatives.

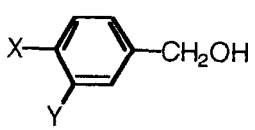

X = F, Cl, Br, I, SCH_3, H, CH_3, CF_3, NO_2, OMe
Y = F, Cl, Br, OMe, NO_2

Figure 15: Substrates used to determine mechanism in galactose oxidase

By plotting the logarithm of the individual rate constants for both the meta and para series of benzyl alcohols and [α,α]-dideuterio benzyl alcohols versus the

substituent constant, the authors were able to determine a ρ value for all four reactions. The ρ value for the para (hydrogen) series of substrates was ~0, indicating either a free radical or atom abstraction mechanism or a cyclic transition state that minimizes charge build up (Figure 16). The slope of the plot, however, is more negative for the deuterated derivatives. This dependence of the kinetic isotope effect on substitution is an indication of a change in the nature of the transition state for this reaction series.

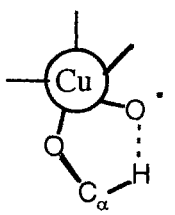

Figure 16: Proposed cyclic transition state for hydrogen atom transfer

In order to determine the meaning of this dependence of KIE on substitution, the individual steps of the mechanism must be determined. The oxidation of benzyl alcohol to benzaldehyde requires the transfer of two electrons and two hydrogens. Therefore, there are three elementary steps envisioned for this proton-coupled electron transfer. The first requires proton transfer from the alcohol to the solvent or to a basic site within the binding pocket. No significant solvent KIE was observed, ruling out this as the rate-determining step. The remaining two steps, single electron transfer and hydrogen atom transfer, were distinguished by the large KIE effect observed in the reactions. Only hydrogen atom transfer would be affected by replacement with deuterium. Additional support was provided by the logarithmic relationship between the rate and oxidation potential of the alcohol.

The Hammett relationship is not restricted to just enzymes in the biological realm; they are also being used to determine details about the phospholipid bilayer.

Recent research by Gokel has used the Hammett relationship to provide support for sodium ion flux through a phospholipid bilayer.[13] Using compounds **17 - 19** as a model for sodium ion channels (Figure 17), Gokel has shown that sodium ion flux was dependent upon the electron density at the nitrogen atom. This was the first application of a Hammett relationship to a functional cation channel model.

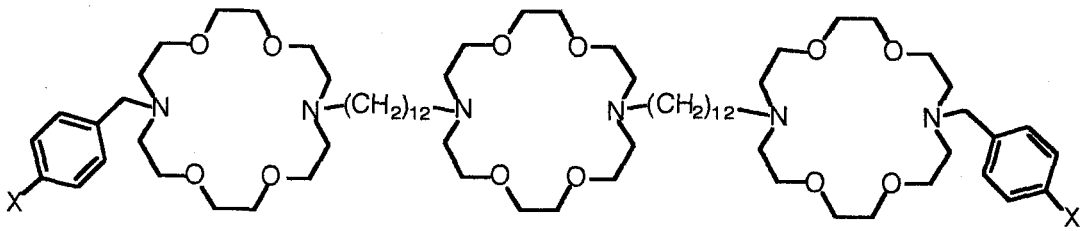

17 X = NO_2, **18** X = H, **19** X = OCH_3

Figure 17: Cation channel model developed by Gokel

Goals of the Present Research

There are four questions about each of the two DHAE enzymes: 1) What is the mechanism of the enzymatic reaction? 2) Is the conformation of the amide important in substrate binding? 3) What is the third recognition element responsible for substrate binding? and 4) What other methods can be used to purify each enzyme?

As discussed in Chapter 1, Kirchmeier provided support for the necessity of both phenolic hydroxyl groups in the two and five position for binding to the active site. However, the third point of attachment still needed to be determined.[16] With the knowledge of all three points of attachment, not only could better inhibitors be developed but potential alternative substrates could be envisioned to increase the

utility of these enzymes as chemical reagents in organic synthesis. As mentioned in Chapter 1, it is believed that DHAE I could be used to create the epoxyquinone core of the manumycin antibiotics

The most obvious third functional group is the amide that has two potential interaction sites; both the amide N-H and the amide C=O could participate in hydrogen bonding within the active site. Less likely is the possibility that the aromatic ring provides the third attachment necessary for binding. *p*-Hydroquinone showed no significant inhibition, implying the necessity of the amide group.[15] To probe the necessity of the amide C=O for substrate binding, a Hammett study was performed with the benzanilide series of competitive inhibitors developed by Kirchmeier. By varying the electronic nature of the substituent attached to the benzene ring, the effect of increasing or decreasing electron density at the carbonyl oxygen could potentially be correlated to the degree of inhibition. The variation in inhibitor size may also give a crude idea of the importance of steric, hydrogen bonding, electrostatic or hydrophobic interactions in the active site.

Recognition between a competitive inhibitor and enzyme could also be used to purify the enzyme. An alternative method for purification of these two enzymes needs to be determined. A variety of typical purification methods have been attempted, but to no avail. The difficulty with the chosen purification methods is a lack of specificity. Based on previous purification results, it can be assumed that a variety of enzymes or proteins with similar chemical and physical properties are present in the protein mixture. Affinity chromatography represents the most efficient method of enzyme purification because of its specificity (Chapter 3).[27-29] By using the knowledge gained from the Hammett study, it was hoped that a compound specific to each inhibitor would be developed to facilitate purification.

To test the dependence of conformation on binding and catalytic activity, a series of alternative substrates were synthesized and tested with DHAE I. Molecular modeling of the substrates as well as the competitive inhibitors used in the Hammett study may shed further light on features of the active site.

Synthesis of Substituted Benzanilide Inhibitors

Inhibitors were chosen to give the maximum range of σ values. Except for **22**, all inhibitors were prepared in three steps. Overall yields of the inhibitors varied, but the average overall yield for the three steps was approximately 50%. Preparation of an acid chloride from the corresponding carboxylic acid using oxalyl chloride or thionyl chloride began the synthesis. The crude acid chloride solution was added to a mixture of 2,5-dimethoxyaniline and triethylamine. All dimethoxy benzanilides were obtained as crystalline solids after purification. With the amide in hand, the methyl ether was cleaved in the presence of boron tribromide to yield the desired hydroquinone. A general synthetic scheme (Scheme 5) is shown below.

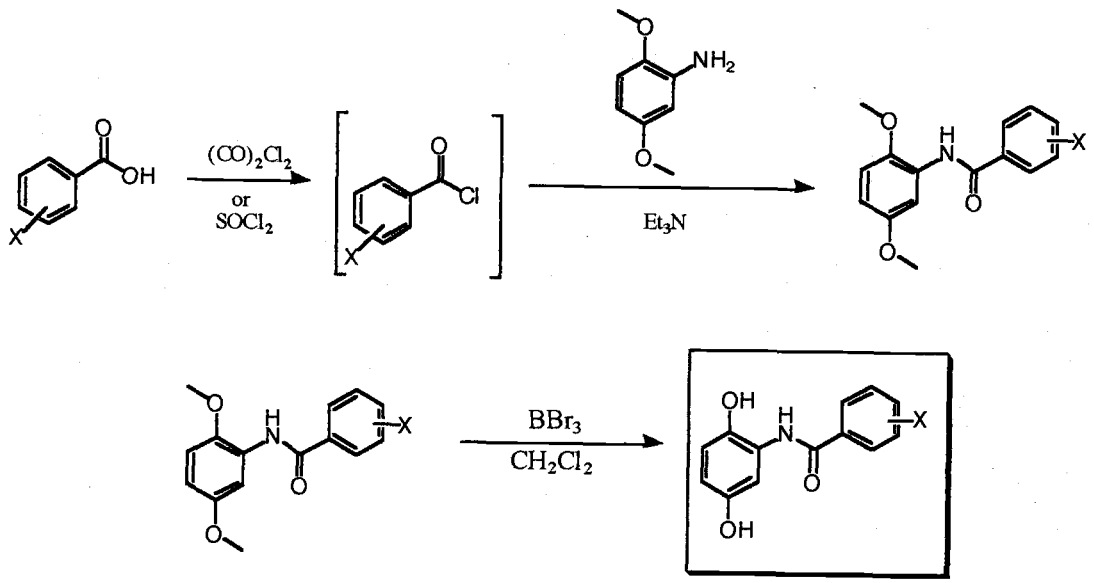

Scheme 5: Synthesis of potential competitive inhibitors

An extra step was required for the synthesis of 4-aminobenzanilide, **22**. Hydrogenation of **8** under transfer hydrogenation conditions using Pd / C and

ammonium formate (Scheme 6) was carried out and after aqueous workup, **22** was isolated in good yield.

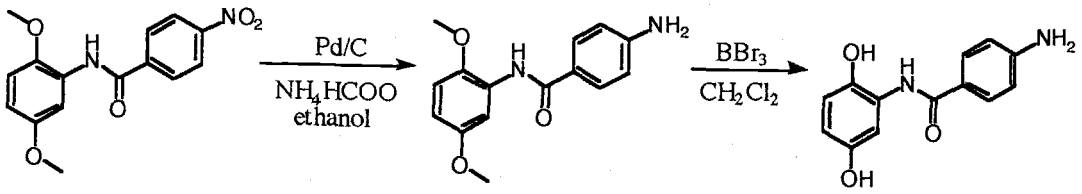

Scheme 6: Extra step in synthesis of **22**

Presentation of Results

The reaction of DHAE I or DHAE II requires two substrates, 2,5-dihydroxyacetanilide and molecular oxygen. The oxygen concentration (O_2) in solution and the reaction rate in the presence of excess substrate were measured by using an oxygen electrode. The oxygen concentration is large enough (100 μM) to justify the assumption it does not limit the rate of the reaction. However, since the oxygen concentration was not measured for every assay, the K_m values are reported as apparent values. Each enzyme, using velocity versus substrate curves (Figure 18), was shown to follow typical Michaelis – Menten kinetics.

Use of a Lineweaver – Burke double – reciprocal plot (Figure 19) allowed calculation of the apparent K_m and V_{max} values from overall velocity vs. average substrate concentration data. Velocity versus substrate curves and double reciprocal plots for each inhibitor trial are given in Appendix I.

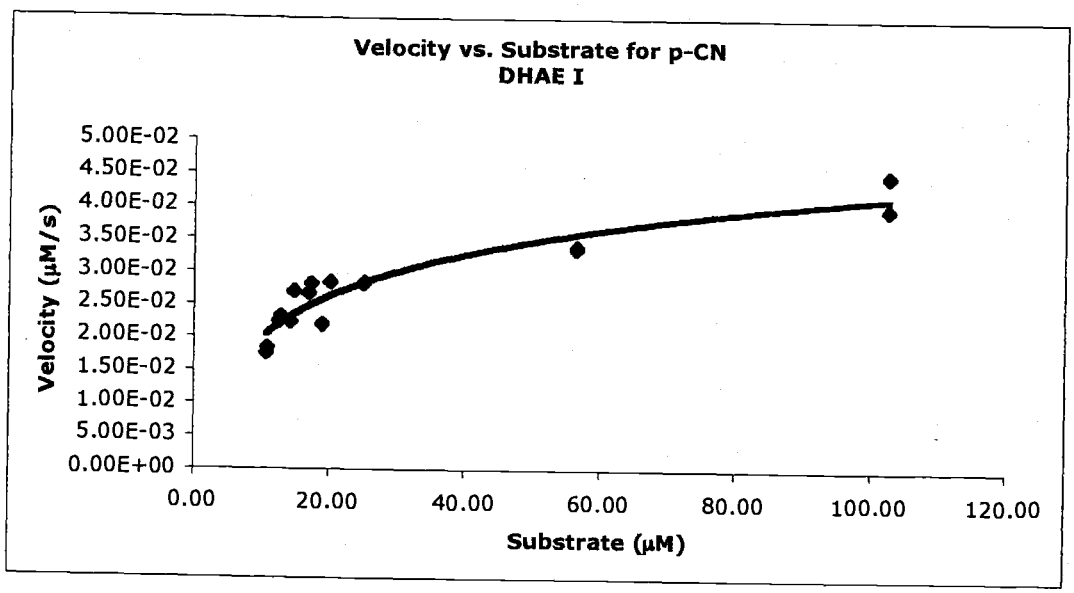

Figure 18: Velocity vs. substrate curve for p-CN inhibitor

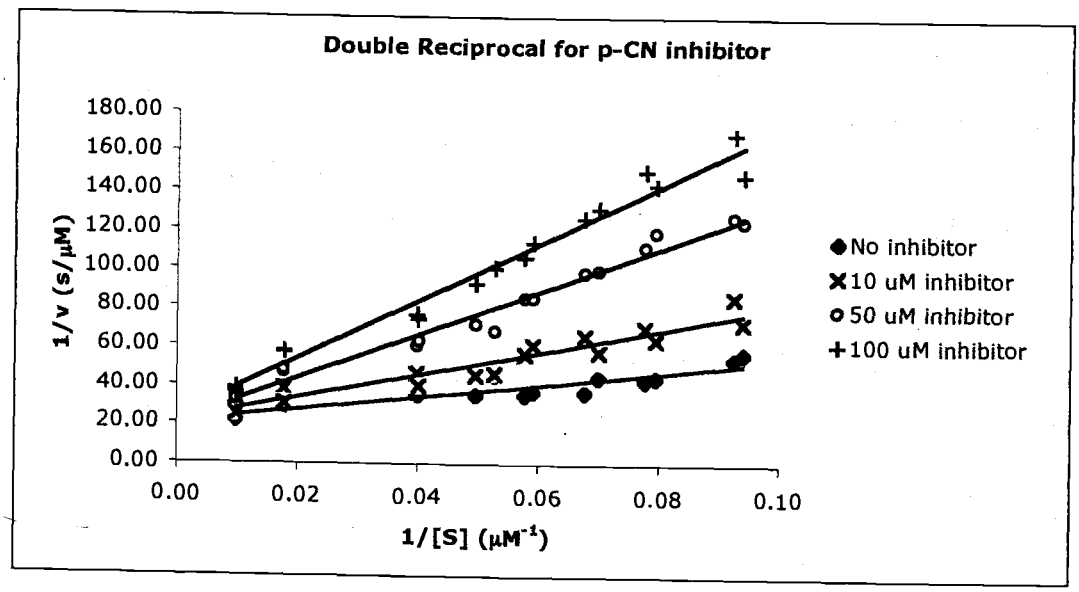

Figure 19: Double reciprocal plot for p-CN inhibitor

Typically, every effort is made to keep conversion of substrate to product under five percent. By keeping the conversion low, the substrate concentration

remains essentially constant, and the velocity remains constant over the assay. UV spectroscopy, 254 nm, was used to determine the relative concentration of components in solution and due to significant differences in molar absorptivities for substrate (4141 M^{-1}), product (1797 M^{-1}), and byproduct (10,419 M^{-1}) for the enzymatic reactions, the conversion was difficult to control. Conversions were generally over ten percent and sometimes as high as fifty percent.

Several alternative methods can be used in instances where the conversion is difficult to control. The first requires integrating the Michaelis – Menten equation and recording velocity and substrate concentration data at at least two different times. The second is to use an average substrate concentration (Eq 5); however, this method introduces a small percentage of uncertainty in the kinetic constants calculated. Higher conversions lead to a larger error (see Experimentals for details) in calculated values. The experimental method did not allow calculation of concentrations at two different times; therefore, average substrate concentrations were used for all calculations.

$$[S]_{avg} = 0.5 * ([S]_f + [S]_o) \qquad \text{Eqn (5)}$$

Values for the inhibition constants, K_i, were obtained by plotting the slopes of each double reciprocal line (K_m (app) / V_{max}) vs. inhibitor concentration. Using this plot for the determination of inhibition constants is preferred since a curvature in the line indicates mixed inhibition. A typical graph is shown in Figure 20.

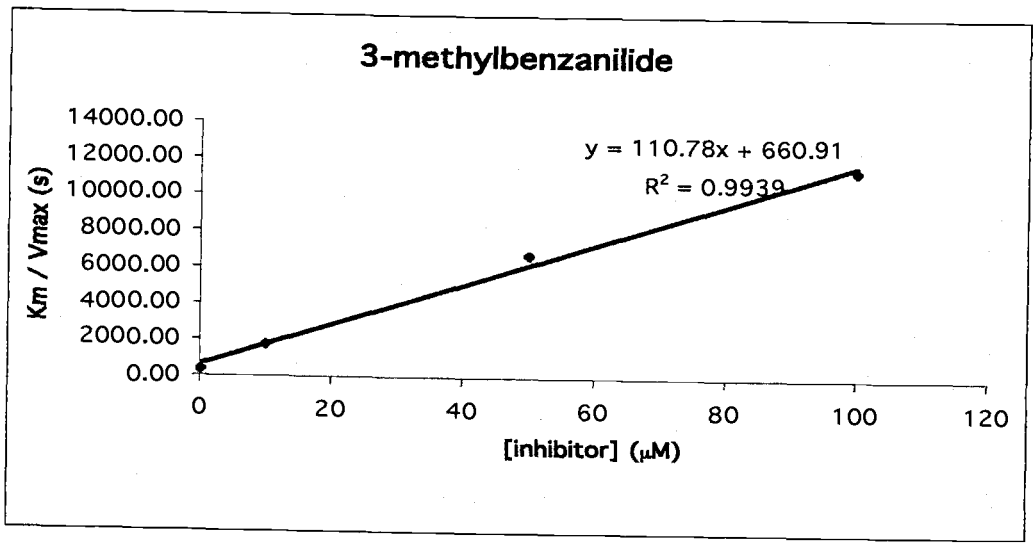

Figure 20: Plot used to determine inhibition constant

Multiple runs with enzyme isolated from a single growth of *Streptomyces* LL-C10037 gave values of K_m (app) that varied from 14 to 24 μM; values of V_{max} varied from 0.035 to 0.061 μM * s^{-1}. For S. MPP-3051, isolated enzyme exhibited K_m (app) values between 14 to 26 μM, and V_{max} values that ranged from 0.032 to 0.051 μM * s^{-1}. Comparison of kinetic assays for enzyme solutions isolated from different growths showed comparable variation. Values for all kinetic parameters for DHAE I and DHAE II are shown Tables 3 and 4, respectively.

Table 3: DHAE I kinetic parameters

Inhibitor	K_m (app) (μM)	V_{max} (μM/min)	K_i (μM)	K_i / K_m
p-nitro	18.4 ± 1.1	0.037 ± 0.001	44.1 ± 13.2	2.40 ± 0.73
p-nitro (2)	20.2 ± 1.9	0.061 ± 0.002	33.4 ± 9.7	1.65 ± 0.50
m-nitro	15.7 ± 4.8	0.036 ± 0.004	37.5 ± 7.2	2.38 ± 0.86
p-cyano	18.0 ± 3.4	0.046 ± 0.003	34.0 ± 5.2	1.89 ± 0.46
p-cyano (2)	14.2 ± 2.0	0.046 ± 0.002	26.2 ± 4.9	1.85 ± 0.44
m-cyano	18.9 ± 4.0	0.046 ± 0.004	41.5 ± 13.9	2.20 ± 0.87
hydrogen	16.6 ± 2.4	0.042 ± 0.003	5.7 ± 0.9	0.55 ± 0.07
hydrogen (2)	16.5 ± 2.2	0.047 ± 0.002	9.1 ± 2.9	0.35 ± 0.19
m-methyl	15.8 ± 3.8	0.043 ± 0.004	2.8 ± 0.2	0.18 ± 0.04
p-methyl	23.9 ± 8.2	0.035 ± 0.005	3.9 ± 0.0	0.16 ± 0.06
p-methyl (2)	17.8 ± 2.5	0.051 ± 0.003	2.3 ± 1.1	0.13 ± 0.04
p-amino	19.8 ± 1.8	0.049 ± 0.002	29.6 ± 0.3	1.50 ± 0.14
p-acetamido	41.4 ± 5.2	0.102 ± 0.007	17.2 ± 2.3	0.42 ± 0.08

Table 4: DHAE II kinetic parameters

Inhibitor	K_m (app) (μM)	V_{max} (μM/min)	K_i (μM)	K_i / K_m
p-nitro	21.7 ± 4.9	0.036 ± 0.005	49.5 ± 23.7	2.28 ± 1.21
p-nitro (2)	16.7 ± 4.3	0.041 ± 0.005	21.5 ± 4.9	1.29 ± 0.44
p-cyano	14.9 ± 3.3	0.032 ± 0.003	48.3 ± 2.8	3.24 ± 0.74
hydrogen	21.7 ± 5.9	0.046 ± 0.007	20.5 ± 2.1	0.94 ± 0.27
m-methyl	13.6 ± 2.0	0.034 ± 0.002	17.0 ± 0.4	1.25 ± 0.18
p-methyl	25.3 ± 9.3	0.048 ± 0.010	45.6 ± 8.2	1.80 ± 0.74
p-methyl (2)	17.4 ± 4.3	0.049 ± 0.004	33.4 ± 8.9	1.92 ± 0.62
p-acetamido	25.9 ± 5.9	0.052 ± 0.006	47.8 ± 5.9	1.85 ± 0.48

In all experiments, initial substrate concentrations were varied from 15 to 100 μM, and inhibitor concentrations ranged from 10 to 100 μM (DHAE I) or from 5 to 50 μM (DHAE II). K_i values were divided by the K_m values to allow for variations that may have occurred from assay to assay and to allow for evaluation of the change in equilibrium constants between substrate and inhibitors (K_m values were assumed to approximate the dissociation constant between enzyme and substrate).

A variety of compounds were prepared and evaluated for inhibition (Figure 21). As stated above, the relative importance of the amide side chain could be determined by varying the electronic nature of the side chain. For each potential inhibitor, enzyme activity for conversion of substrate to product was assayed in the presence of inhibitor and a K_i value calculated.

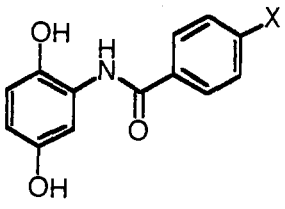

7: X = H
8: X = NO_2
20: X = CN
21: X = CH_3
22: X = NH_2

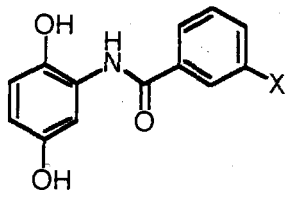

23: X = NO_2
24: X = CN
25: X = CH_3

Figure 21: Inhibitors chosen for Hammett study

To obtain the desired information about the correlation of electron density at the carbonyl oxygen of the amide versus inhibition, a Hammett plot was created for each enzyme by plotting log (K_i / K_m) vs. σ (Figures 22 and 23). It should be pointed out that by definition the lower the inhibition constant the greater the degree of inhibition and the magnitude of the slope reflects the significance of electron density on inhibition.

DHAE I shows a highly correlated ($r^2 = 0.92$) relationship providing support for the importance of the amide C=O. Compound **22** was not included in determination of the ρ value nor in assessment of linearity. DHAE II, however, shows significant scatter ($r^2 = 0.13$) suggesting a complex interplay of steric and electronic effects. The line obtained shows a slight dip at hydrogen although more

precision for the two trials with p-nitro inhibitor (**8**) would have to be obtained before making this statement with more confidence. Linear regression lines are shown on each graph.

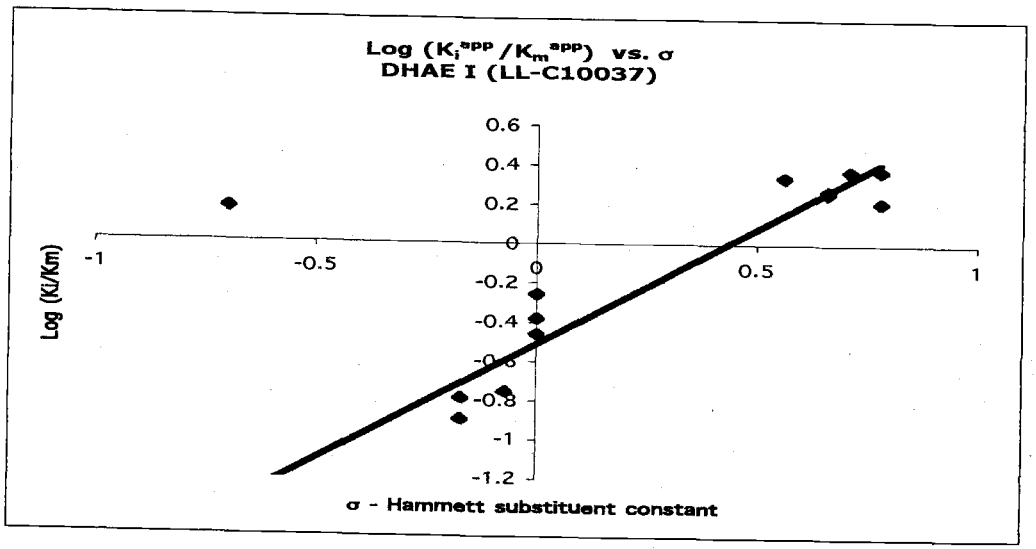

Figure 22: Hammett plot for competitive inhibitors of DHAE I

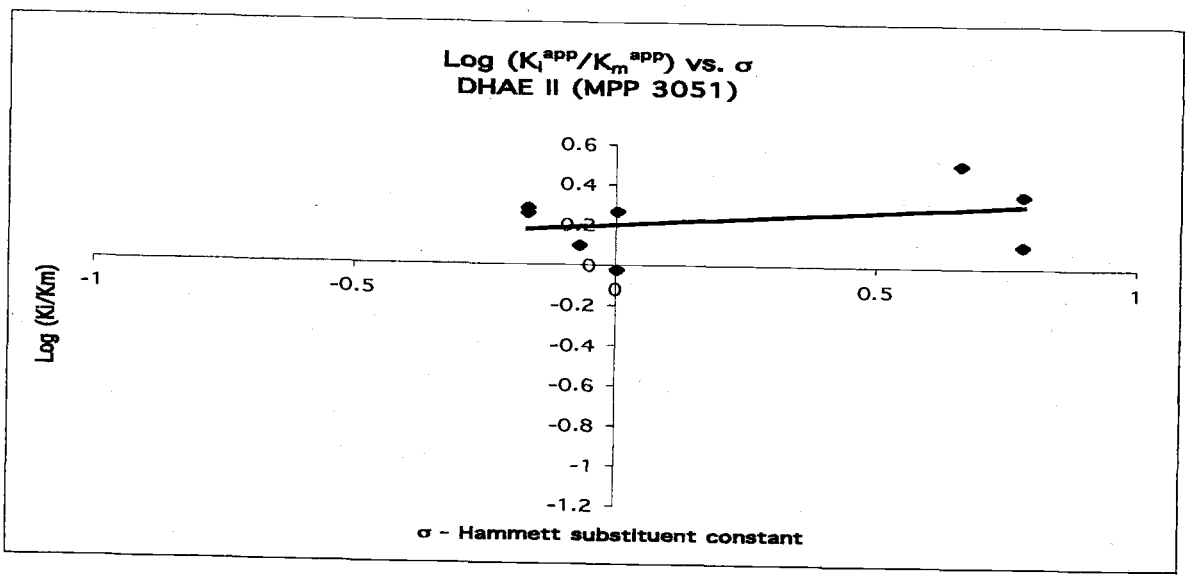

Figure 23: Hammett plot for competitive inhibitors of DHAE II

Discussion of Experimental Results

How does the information gained from the Hammett study help us understand the recognition events between DHAE I and DHAE II and 2,5-dimethoxyacetanilide? The implications for substrate binding, enzyme mechanism, and enzyme purification will be discussed below.

The Hammett Study

When discussing results from a Hammett study, one must be careful since steric factors may play unknown roles, particularly for an enzyme with a rigid active site.[30] The differences in the correlation in the two graphs point to differences in the active site environment of each enzyme. DHAE II shows a lot of scatter indicative of dominating steric factors. All inhibitors are significantly less potent binders when compared to DHAE I. Uninfluenced by steric factors, DHAE I shows a good correlation between substitution and inhibition. The large negative value of ρ (−2.1) indicates the importance of electron density at the carbonyl oxygen on the strength of inhibition (Figure 24). In fact, the data obtained suggest that the amide side chain in the substrate represents the functional group controlling the facial selectivity of oxygen addition and therefore the stereochemistry of the epoxide.

One exception to the observed trend was compound **22**. Expected to be the strongest inhibitor tested based on early results with other inhibitors, **22** deviates significantly from the line. There are several possible explanations for this result. Under the slightly acidic conditions of the kinetic assay the amino group could be protonated to form an ammonium ion. This is significant since the σ values for the amino substituent and the ammonium ion are essentially equal and opposite in magnitude (Figure 25). A ^{13}C NMR (D_2O, pH 6.5) was used to test the acid – base

behavior of the amino compound and the ammonium ion was not detected. Calculations based on relative K_a values also support the absence of protonation under the conditions of the kinetic assay. There is a possibility that upon binding to the enzyme, the amino group is protonated within the active site. Often the pK_a values change significantly when removed from an aqueous environment and placed in close proximity to an acidic residue within the binding pocket. However, based on our understanding of the conformation of inhibitor binding for DHAE I this seems unlikely (vide infra).

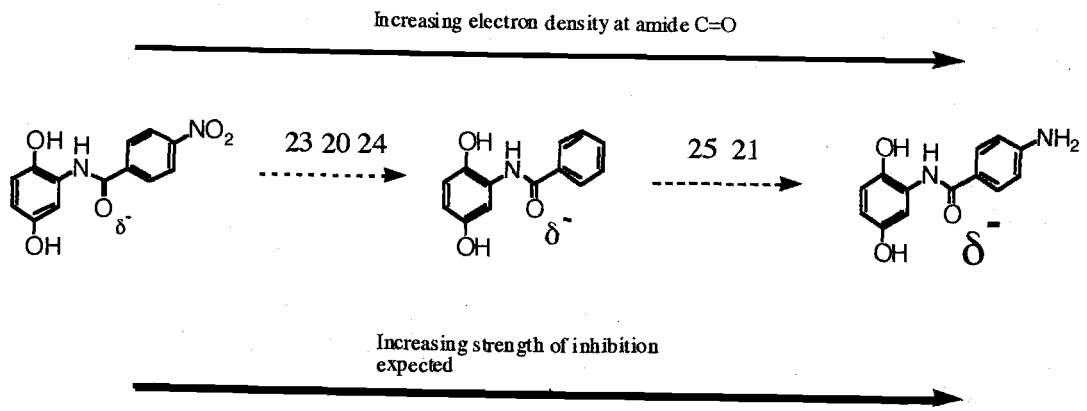

Figure 24: Correlation of electron density on amide oxygen to extent of inhibition

An alternative explanation lies in the reactivity of the amino group. This substituent is the only distinctly nucleophilic group used and could react with species present in the kinetic assay or at other positions of the enzyme. This would adversely affect its ability to act as a competitive inhibitor and explain the observed deviation. Another likely explanation is the presence of hydrogen bonding between the amino group and water that prevents binding in the active site. The energy required to disrupt the hydrogen bond would shift the equilibrium of binding towards enzyme and inhibitor reducing the value of the inhibition constant.

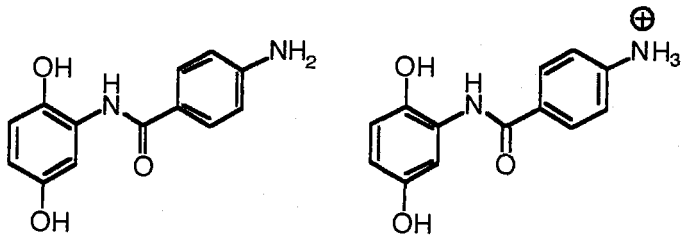

Figure 25: Difference in electron nature of substituent upon protonation

Implications for Substrate Binding

Within each enzyme's active site there are two possibilities for substrate binding. The amide side chain can point towards the protein exterior or be contained within the active site (Figure 26).

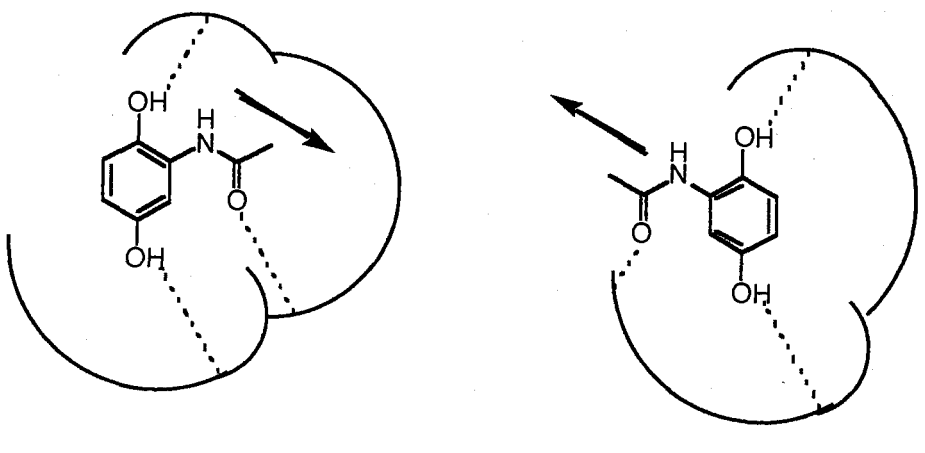

Figure 26: Enzyme pocket showing possible orientations of amide side chain

Due to the differences in the Hammett plot, we conclude that the substrate binds to each enzyme in an opposite fashion. As mentioned above, DHAE I seems uninfluenced by steric factors and because of this most likely has the amide side chain pointing towards the protein exterior. The alternative orientation is unlikely

due to the size of the inhibitors tested, but the possibility cannot be ruled out completely.

DHAE II's Hammett plot shows tremendous scatter ($r^2 = 0.13$) indicating that steric factors dominate the interaction between inhibitor and enzyme. The unsubstituted benzanilide was the strongest inhibitor, but as is evident from the slope of the graph the differences among inhibitors are small. Therefore, we assume that the amide side chain points toward the protein interior where steric clashes are more likely to occur with the amino acid side chains. Again, the possibility still exists for the alternative orientation but it is unlikely that steric factors would control binding on the exterior of the enzyme (Figure 27).

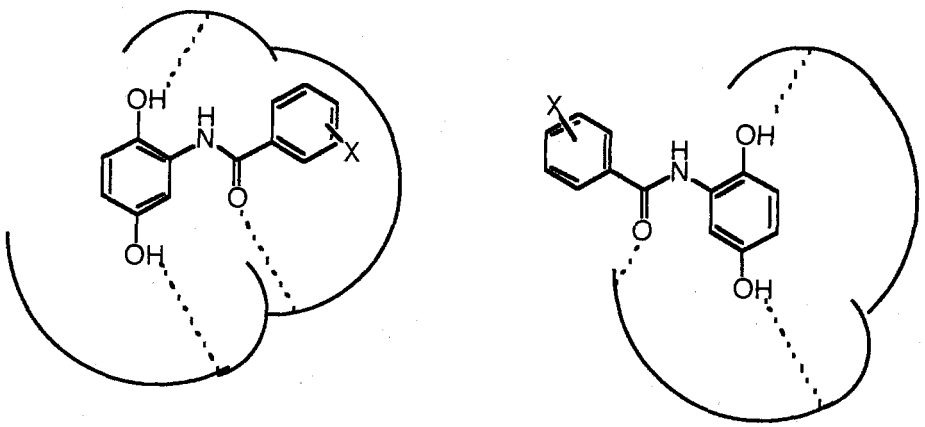

Unlikely that all inhibitors would bind without steric interactions.

Steric factors are prevented or at least minimized when in this orientation

Figure 27: Rationale for inhibitor binding to active site of DHAE I and DHAE II

Implications for Enzyme Mechanism

Considering the similarities between the products of the DHAE enzymatic reactions and dihydrovitamin K oxidase, both enzymes have been proposed to be operating under the same mechanism (Scheme 7).[21,22]

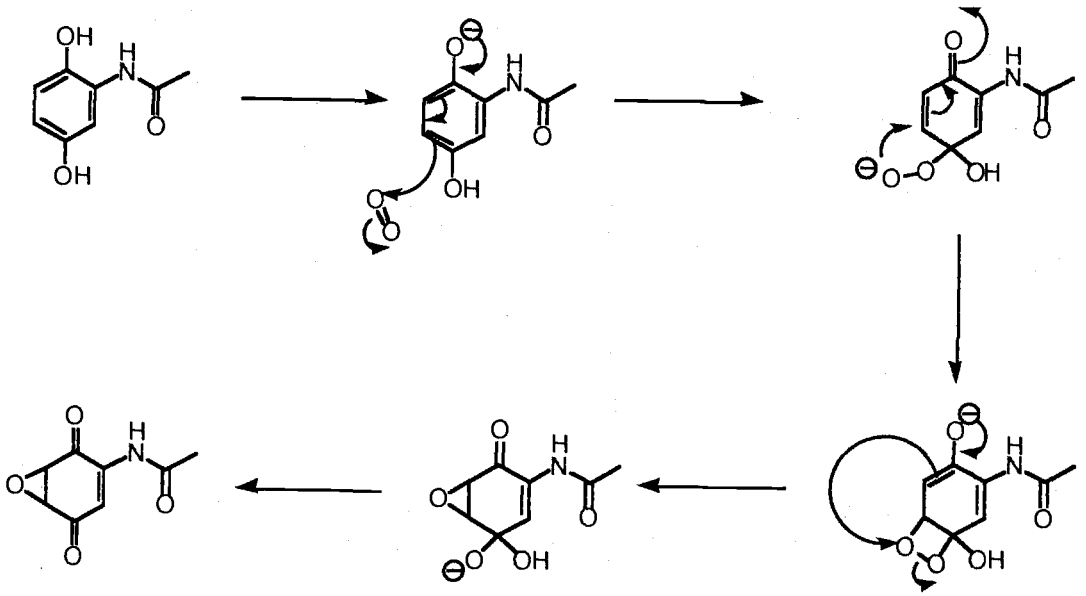

Scheme 7: Dowd mechanism for dihydrovitamin K oxidase applied to DHAE I / II

As discussed in Chapter 1, Kirchmeier provided support for the hydroxyl groups in substrate binding. Deprotonation of the phenol is most likely initiated by a basic residue within the active site. The most important mechanistic information is obtained from Kirchmeier's result with the monohydroxyacetanilides. **5**, having the hydroxy group in the 3-position, is the best of the three inhibitors indicating the importance of this hydrogen bond on substrate binding. Most likely the removal of this hydrogen by a basic residue within the active site initiates the reaction. The opposite is true in the active site of DHAE I. **4**, having the hydroxy group in position 2, is the strongest of the three monohydroxy inhibitors. This points to opposing positions of the basic residue in the two enzymes. The inhibition constants for **4** and **5** are higher than expected because of the weakening of one hydrogen bond in the absence of another group also important for recognition.[2]

The orientation of the amide side chain in substrate binding also controls the facial selectivity of oxygen addition. Based on a previous discussion, in both enzymes molecular oxygen would be in similar positions (Figure 28).

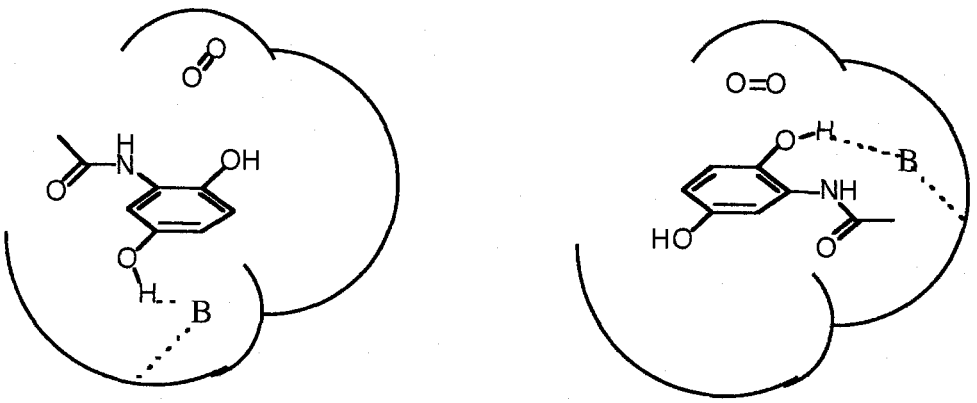

Figure 28: Relative position of basic residue (B) and molecular oxygen

Implications for Enzyme Purification

One of the main goals of the Hammett study was to identify an inhibitor capable of binding to each enzyme in the micromolar range. Creation of an affinity column by attaching this inhibitor to an affinity resin would allow for purification of each enzyme. Based on the differences in substrate binding, it will be necessary to create a different ligand for each enzyme. The amide bond points to the protein exterior when substrate binds to DHAE I therefore a slight modification to the benzanilide structure should be sufficient to allow for purification (Figure 29).

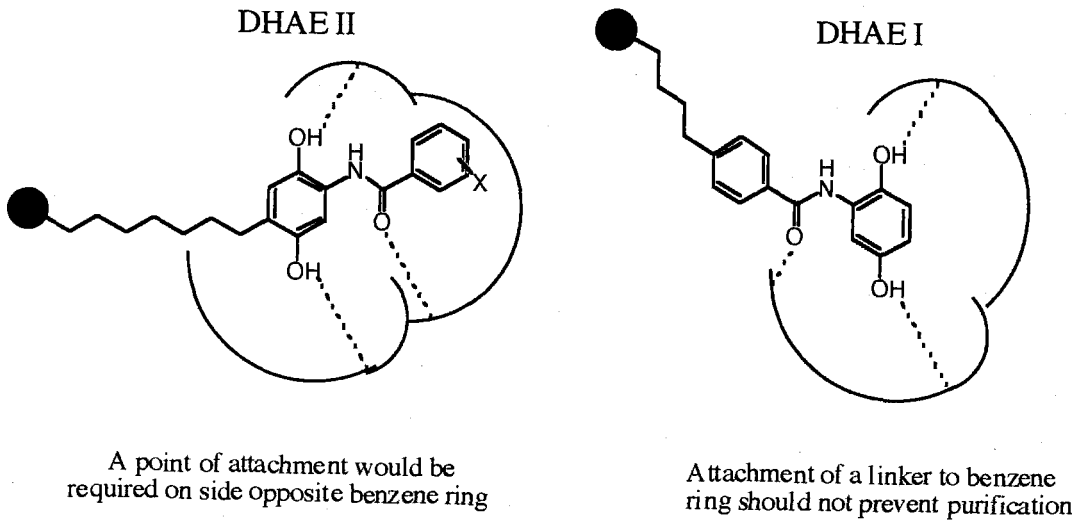

Figure 29: Different placement of linkers required depending upon binding

The opposite situation occurs in DHAE II. Upon substrate binding, the amide bond is enclosed within the active site and therefore the ligand used in DHAE I's affinity column would not be expected to purify DHAE II. An alternative ligand has to be synthesized (Figure 29). Enzyme purification is the scope of Chapter 3 and more about the methodology used will be discussed there.

Rationale for Exploring Alternative Substrates

Numerous natural products contain an epoxyquinone core similar to **2** and **3** and there has been intense effort directed towards the synthesis of these types of natural products.[3-10] The manumycins[10], a family of compounds containing an epoxyquinol core, represent the most sought after structures due to their anti – cancer properties. Taylor's group completed the first total synthesis of (+)-manumycin A in 1999.[6] The synthesis consists of 14 steps with an overall yield of

0.8%. However, Uchida et al.[34] has shown that the epoxyquinone, an oxidized form of manumycin, retains biological activity (Figure 12).

Using this result, Wipf and Taylor have each devised methods for the synthesis of the epoxyquinone core lacking the lower side chain.[5,6] The key compound in their syntheses is the protected amido quinone epoxide, **34**, that allows for the synthesis of derivatives having different amide side chains. Each synthesis begins with protection of the amine in 2,5-dimethoxyaniline. After protection, the aromatic ring is oxidized using a hypervalent iodine species generating a protected quinone derivative. Epoxidation followed by removal of the Boc group with boron trifluoride etherate generates **34**. Four additional steps were required to remove the protecting group and add the acyl side chain (Scheme 8). Both of these syntheses generated racemic mixtures of the final product.

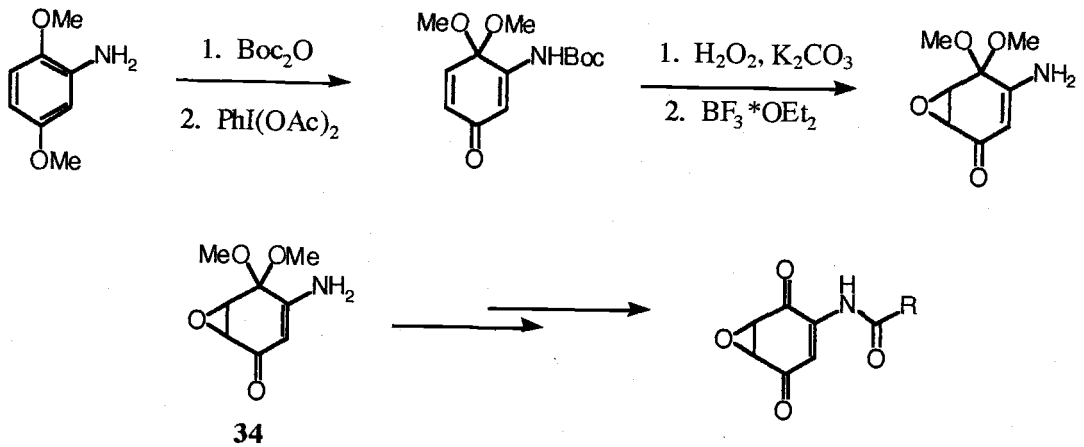

Scheme 8: Taylor's synthesis of epoxyquinones

DHAE I is well suited to create these same epoxyquinones in several steps enantiospecifically if alternative substrates can be accepted. To test DHAE I's capacity to accept alternative substrates and therefore to be used as a reagent in

organic synthesis, several compounds were synthesized that are slight variations on the natural substrate.[17]

Synthesis of Alternative Substrates

The choice of alternative substrates was based on similarity to the natural substrate. Eight compounds (**26-33**) were envisioned; however, only five were tested with DHAE I for product formation. Small variations in the amide side chain were believed to have the best potential for binding to the active site. For this reason, **26 - 29** were synthesized starting from 2,5-dimethoxyaniline and the corresponding anhydrides. Using boron tribromide to remove the methyl ethers again generated the hydroquinones (Scheme 9).

Another small modification would be necessary to test the necessity of having an amide linkage. Replacing the N-H bond with a methylene or an oxygen, one could potentially generate novel epoxyquinone structures. The dimethoxy compounds were easily prepared (Scheme 10); however, the corresponding hydroquinones were never prepared and therefore not tested as alternative substrates.[17,18]

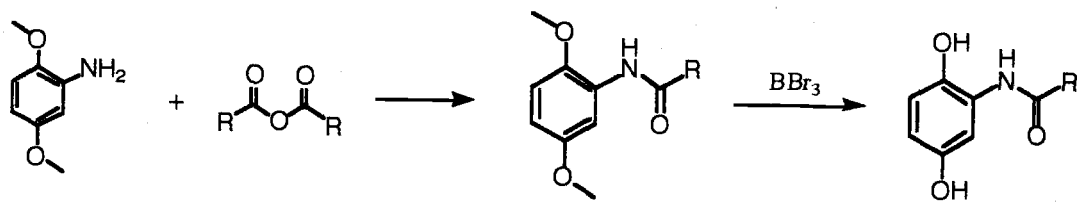

26 R = Et
27 R = Pr
28 R = t-Bu
29 R = CF_3

Scheme 9: Synthesis of alternative substrates

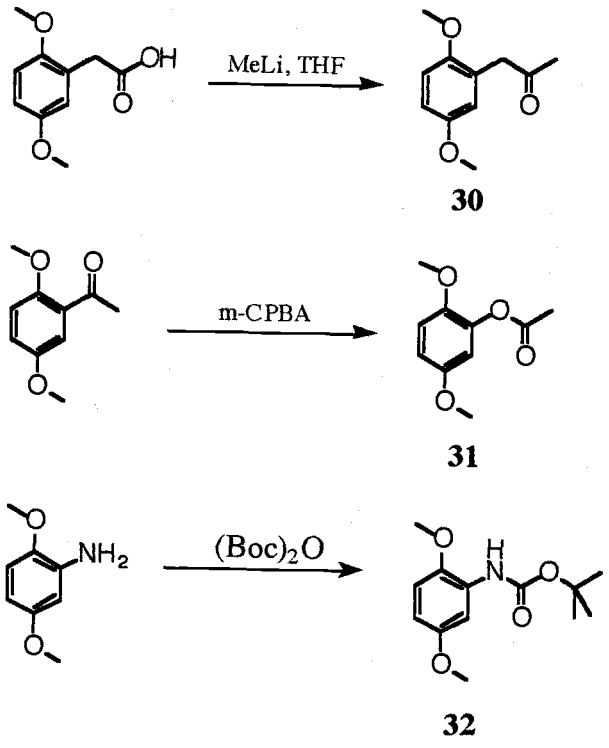

Scheme 10: First step in synthesis of other alternative substrates

One last idea was to test the dependence of the amide bond conformation on substrate binding. Up to this point, all of the amides have been drawn in the same conformation. Is this the actual conformation or are there other conformers preferred by the enzyme? Placing the amide within a ring and therefore limiting the number of possible conformations can easily test this. For this reason, 5,8-dihydroxy-3,4-dihydrocarbostyril, **33**, was prepared from literature procedures (Scheme 11).[19]

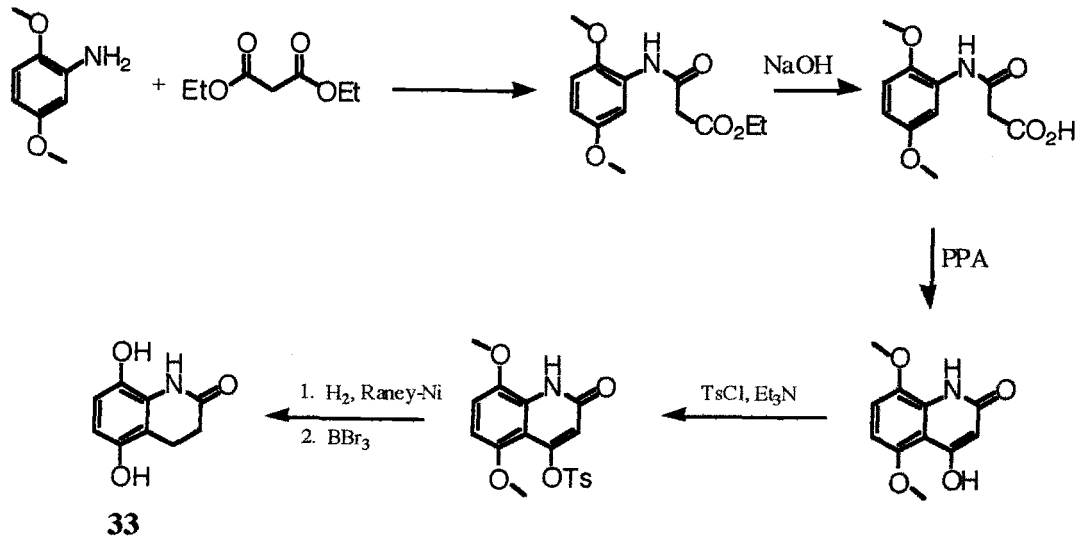

33

Scheme 11: Literature synthesis of **33**

Results with Alternative Substrates

26 - 29 and **33** were tested as alternative substrates by placing substrate in cell free extracts or DE-52 purified fractions of S. LL-C10037 cells. Product formation was monitored at increments of twenty minutes for one hour under the same conditions as the natural substrate. Product was detected for all substrates except **29**, although the percent conversion varied from approximately ten percent to less than 0.1%. An HPLC assay was used to quantify the extent of conversion as well as product identification. The products were identified by comparison of their UV spectra to that of compound **2** or **3**. It was assumed that the molar absorptivities of the starting material, product and oxidized starting material were similar to each other; therefore, no modification was made to the data. At this point in the search for alternative substrates, it was only necessary to identify which compounds could be converted to product. The results are summarized in Table 5.

Table 5: Results from alternative substrate studies

Alternative Substrate	Retention Time (min)			Percent Conversion
	Substrate	Product	Quinone	
26 (Ethyl)	6.97	11.38	14.43	10.2%
27 (Propyl)	10.67	21.30	27.27	trace
33 (Cyclic)	5.02	6.07	6.87	7.8
28 (t-Butyl)	19.27	6.79	17.32	2.1
29 (CF_3)	9.66	----------	----------	nd

nd – not detected

Discussion of the Alternative Substrate Studies

How does the information gained from the alternative substrate study help us understand the recognition event between DHAE I and DHAE II and 2,5-dimethoxyacetanilide? Also, can we use either enzyme as a reagent in organic synthesis. The implications for substrate binding in terms of amide conformation and the potential for using DHAE I or DHAE II as a reagent in organic synthesis are discussed below.[21]

It is not surprising that **26-29** were accepted as alternative substrates. All recognition elements are present and the size of the side chain does not vary dramatically. However, there are some surprises from this study. First, **29** is not

accepted as an alternative substrate, but product formation was observed in the reaction between DHAE I and **33**. Based on results from the Hammett study, the trifluoromethyl group may reduce the electron density on the amide carbonyl to the point that binding is not favored and therefore the reaction is slowed significantly so that no product is observed. Turnover of **33** is significant because it sheds light on the conformation of the amide bond in the natural substrate. **1** must adopt a similar conformation since **33** is readily accepted as substrate. The conformation of **33** changes the previous discussion about the active site of DHAE I only slightly. If the competitive inhibitors used in the Hammett study also adopt this conformation, a steric clash will occur between the C-6 hydrogen of the hydroquinone ring and the ortho hydrogen in the benzene ring. To alleviate the steric repulsion, the benzene ring must twist out of the plane or a rotation of the amide carbonyl bond must occur. The two possibilities are shown in Figure 30.

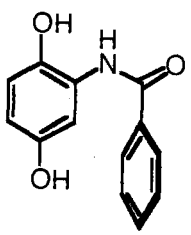

aromatic ring rotates away from hydroquinone ring

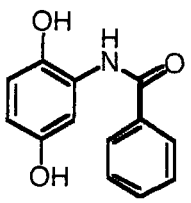

amide bond rotates to place aromatic ring above the hydroquinone ring

Figure 30: Possible orientations of phenyl ring in inhibitors of DHAE II

Amide Conformation

In order to explore the conformation of the amide bond further, molecular modeling was performed on the competitive inhibitors, alternative substrates, and the natural substrate. Ab-initio (3-21G and 6-31G*) and semi-empirical (PM3)

methods generate the same conformation for all modeled compounds except **29**. The amide carbonyl rotates so that hydrogen bonding can occur with the phenolic hydrogen in the two position. The distance between the two atoms is 2.41 Ångstroms and a seven-membered ring is formed (Figure 31).

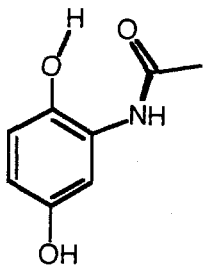

Figure 31: Ground state conformation of **1** (ab-initio)

29 deviates from this trend and could possibly explain the lack of activity seen as an alternative substrate. Hydrogen bonding is still present, though now it is between the oxygen of the phenol and the hydrogen of the amide bond (Figure 32).

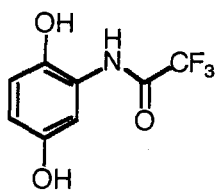

Figure 32: Ground state conformation of **29**

If the conformation of the amide bond in **33** does represent the true conformation required in the active site, the hydrogen bond in the ground state conformation of the natural substrate must be broken before binding. Since this

bond would be expected to fairly strong, the binding to the active site must overcome the energy required for separation. This is consistent with having a charged hydrogen bond present in the active site, but it does contradict the position of the basic residue discussed earlier for DHAE I.

In addition to the conformation of the amide bond, the van der Waals (vdW) volume of the different substituents can be calculated from the molecular modeling results. Because of the proposed influence of steric effects on binding in DHAE II, the logarithmic relationship between the ratio of the inhibitor constants and the vdW volume was explored (Figure 33).[1] Tremendous scatter was obtained, indicating that steric factors were not the only factor responsible for the variation in strength of inhibition.[18]

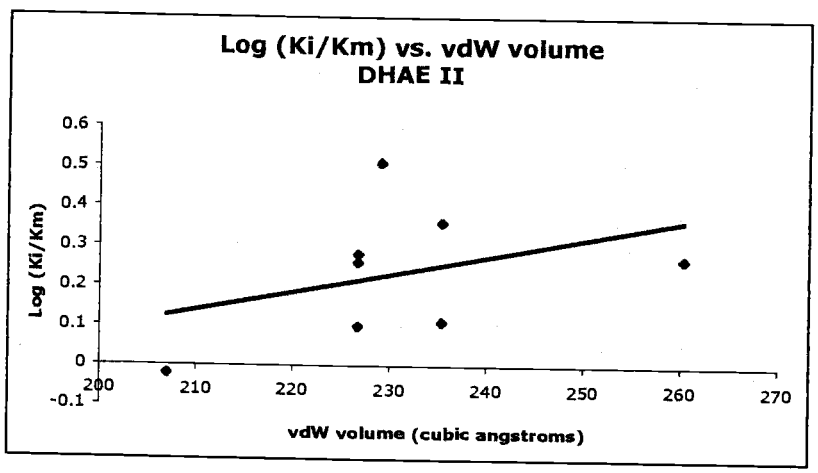

Figure 33: Relationship of volume to inhibition for DHAE II

Summary and Conclusions

All three elements of molecular recognition have been identified for DHAE I and DHAE II. It is not surprising that hydrogen bonding controls binding as well as the facial selectivity of epoxide formation. With the information extracted from

the Hammett study and the alternative substrate study, it will now be possible to devise more effective purification methods, stronger competitive inhibitors, and alternative substrates with activities that rival the natural substrate.

With the acceptance of an appropriately substituted derivative, the possibility of producing oxidized manumycin derivatives is feasible. Generally, the cost of the co-factors is a limiting factor to using enzymes in organic synthesis.[21] DHAE I and DHAE II avoid this cost and are well suited for use as inexpensive reagents for either total or semi-synthetic methods in organic chemistry. However, this idea will not be realized until larger quantities of pure enzyme are available.

Experimental

General Conditions

NMR Spectra were recorded by using either a Bruker 300 MHz or 400 MHz NMR. Low – resolution mass spectra were taken on a Varian MAT CH-7 spectrometer. High-resolution mass spectra were taken on a Kratos MS 50 TC spectrometer. Water was purified with a MilliQ system, Millipore Corp. Activity assays were analyzed by HPLC performed on a Waters 600E HPLC instrument (UK-6 injector) with a Waters 996 photodiode array detector and a Dell Pentium computer housing Waters Millenium software. Reverse phase C_{18} (Econosphere, 5 mm, 250 x 4.6 mm, Alltech Assoc.) columns were used for activity assay analyses. Bacterial fermentations were carried out in a gyrotary incubator (Lab Line incubator shaker). Cell disruption was performed with a sonicator (Model W-225 R, Heat Systems – Ultrasonic, Inc.). Eppendorf tubes were centrifuged in a Biofuge (Baxter Inc.). Refrigerated centrifugations were done in an IEC B-20a centrifuge. All purification steps were performed at 4 °C. All buffers were prepared from molecular biology grade reagents. Epoxidase activity was

monitored by following the consumption of **1** and the production of **2** or **3** simultaneously by HPLC. Fractions from each step were stored at –80 °C.

Standard Culture Conditions

S. LL-C10037 was maintained at 4 °C as spores on sterile soil. A loopful of this material was used to inoculate 50 mL of seed medium containing 1.0% glucose, 2.0% soluble potato starch, 0.5% yeast, 0.5% N-Z Amine A 59027, and 0.1% $CaCO_3$ in MilliQ water, the whole adjusted to pH 7.2 with 2% KOH. The culture, contained in a 250 mL Erlenmeyer flask, was incubated for 3 days at 28 °C, 240 rpm in a rotary incubator. Production broths (200 mL in 1 L Erlenmeyer flasks), containing 1.0% glucose, 0.5% bacto-peptone, 2.0% molasses (Grandma's famous light unsulfured), and 0.1% $CaCO_3$ in MilliQ water and adjusted to pH 7.2 with 10% HCl prior to sterilization, were subsequently inoculated to 5% (v/v) with vegetative inoculum from seed broths. The production broths were incubated for 96 hours.

S. MPP3051 was maintained at room temperature (20 – 25 °C) as spores on sterile soil. A loopful of this material was used to inoculate 50 mL of Lederle seed medium and the seed inoculum, contained in a 250 mL Erlenmeyer flask, was incubated for 48 hours at 28 °C, 250 rpm. Production broths (200 mL in 1 L Erlenmeyer flasks), consisting of either the Beecham medium[36] or the Lederle medium,[35] were subsequently inoculated 5% (v/v) with vegetative inoculum from seed broths. The production broths were incubated for 24 hours.

Collection of Cells

Cells were collected by filtering through 100 μm nylon mesh (Small Parts, Inc.). for DHAE I and through 10 μm nylon mesh for DHAE II. After filtering, the

cells were washed with the following solutions (enough to completely re-suspend the cells ---usually about one liter per wash): a) 100 mM KH_2PO_4, pH 7.0 (twice) b) 1.0 M KCl c) 0.8 M NaCl. After the last buffer solution, the cells were squeezed dry and placed in a -80 °C freezer until needed (generally no longer than two months).

DE-52 (Diethylaminoethyl) column

For a list of the buffers used in the following purification steps, please refer to Reference 16. The DE-52 anion exchange resin was prepared the night before running the column. To prepare the resin wash with the following solutions: 1) MilliQ water (twice) 2) Buffer I 3) Buffer II. The resin remained in buffer II until the column was prepared the following day.

The cell paste was removed from the -80 °C freezer and thawed at 4 °C using sonication buffer which contained XAD-4 resin (3 x amount of cells (in mg)) and polyvinylpolypyrrolidone (PVPP-10) resin (3 x amount of cells (in mg)). Upon re-suspending the majority of the cell paste, the solution was transferred to 100 mL beakers. The suspensions were sonicated (3 x 20 sec, full power, 90% duty), placed in centrifuge tubes (250 mL) and centrifuged at 10,000 rpm for 15 minutes at 4 °C. Sonication was performed using a Model W-225R sonicator (Heat-Systems Ultrasonic, Inc.) Refrigerated centrifugations were done in an IEC B-20a centrifuge.

The supernatants were combined to give the cell-free extract (CFE). The cell-free extract was added to the top of the DE-52 anion exchange column. The column was run under the following conditions:

Flow rate : 0.65 mL / min at 4 °C

A KCl step gradient (100 mL of each concentration---50 mM, 100 mM, 150 mM, and 200 mM) was performed after washing the loaded column with Buffer II (100 mL). All four fractions (32 mL each) showed activity in the 200 mM KCl

eluate. Only the most active fractions (highest specific activity) were taken on to the IMAC column. Active fractions were stored at -80 °C until needed.

Immobilized Metal Affinity Chromatography (IMAC) column

Active fractions from the DE-52 column were concentrated by using Amicon Centriprep 30 filter units (from ~130 mL to ~30 mL). The IMAC resin was poured directly from the container into a 2.5 x 20 cm column (Bio-Rad). The resin was allowed to gravity pack (~10 cm) before the addition of 100 mL of 100 μM $CuSO_4$. The resin turned brilliant blue upon binding of the Cu^{2+} ion. As soon as the $CuSO_4$ solution had just entered the resin bed, the column was washed with 500 mL Buffer IV to remove any excess (unbound) Cu^{2+} ion. A lot of this portion was visual, I ran enough buffer through the column to eliminate even the slightest hint of blue in the eluate. The column was then allowed to come to equilibrium with Buffer III before the addition of the enzyme preparation. At that point, the enzyme preparation (~30 mL) was added manually very carefully to the top of the resin bed. Once the last of the enzyme preparation had entered the resin bed, the following conditions were used:

Flow rate : 2.5 mL / min
0-50 min. buffer III
50-80 min. buffer III - 15% buffer IV
80-260 min. 15% buffer IV
260-290 min 15% buffer IV - 100 % buffer IV

12.5 mL fractions were collected throughout the run. 300 uL aliquots were taken every third fraction to assay for activity and to determine protein concentration.

Hydrophobic Interaction Chromatography (HIC) column

A preparative column was packed (C-5 agarose from Sigma, column BioRad econo, 2.5 x 20 cm). The column was wet packed in buffer V and stored in cold room at 4 °C. The column was first washed (gravity fed) with MilliQ water (200 mL), 0.1 N NaOH (100 mL) and a second time with 200 mL MilliQ water. After washing it was equilibrated with buffer V (200 mL) and allowed to drain until the top of the resin was visible. While the column was equilibrating, the IMAC fractions were prepared. The fractions were thawed at room temperature, but the temperature was never allowed to exceed 4 °C. The fractions were combined and brought to 1.2 M ammonium sulfate. This salted solution was slowly and carefully added to the top of the column. Upon the addition of all of the enzyme solution, the top of the column was washed by adding 2 mL of buffer V. The column again was allowed to drain until the top of the bed was visible. The column was topped off with buffer V and connected to the FPLC. The following linear gradient was started at 1.5 mL / min: 0 – 30 min. buffer V – 50 % buffer VI; 30 – 70 min 50% buffer VI; 70 – 150 min. 50% buffer VI – 60% buffer VI; 150 – 190 min. 60% buffer VI; 190 – 230 min. 60% buffer VI – 70% buffer VI; 230 – 270 min. 70% buffer VI; 270 – 310 min. 70% buffer VI – 100% buffer VI. Fractions were collected every 3 minutes (4.5 mL) and 300 µL of every other fraction where DHAE I elutes (~200 min) was taken for activity assays and protein quantitation. The fractions were stored at –80 °C.

Enzyme Activity Assay

Individual samples were assayed for activity by adding the following to a 1.5 mL Eppendorf tube:

25 µL 2 mM DHA (containing $Na_2S_2O_4$ - as a deterrent to oxidation)
50 µL 1 M KH_2PO_4, pH 6.5
100 µL $CoCl_2$
100 µL MilliQ H_2O

125 μL enzyme preparation
\+ 100 μL terminating solution (66:30:7;CH_3CN:H_2O:CF_3COOH)

The trials were run 3-15 minutes depending on the activity of the sample.

Determination of Protein Concentration

The concentration of protein in the samples was determined using the Bradford assay.[37] To a known volume of enzyme solution was added 200 μL of Bio-Rad Reagent (Bio-Rad) and enough water to obtain a total volume of 1400 μL. The absorbance was determined at 595 nm and compared to a standard curve previously prepared using the same procedure with known concentrations of bovine serum albumin (BSA).

Kinetic Assay in the Presence of Inhibitors

DHAE I (LL-C10037)

In order to dissolve the inhibitors in the reaction medium it was necessary to include 30% ethanol in the inhibitor solutions. This results in 7.5% total ethanol in solution during experiment. The added ethanol does inhibit the enzyme and therefore a small increase in K_m is observed. The kinetic trials for a given inhibitor were performed within a three-hour span and were run from the most concentrated (100 μM) inhibitor samples to the least concentrated (0 μM).

The substrate concentrations were chosen so they would be evenly spaced along the 1/[S] axis in the double reciprocal plot. The K_m for the substrate was known to be around 15 μM; therefore, the range of substrate concentrations was chosen so as to be below the K_m and to reach as high as 3 x K_m.

Assay Ingredients:

Without inhibitor	With Inhibitor
100 µL KH_2PO_4 (1M, pH 6.6)	100 µL KH_2PO_4 (1M, pH 6.6)
100 µL 30% EtOH/H_2O sol'n	100 µL appropriate [I]
x µL MilliQ H_2O	x µL MilliQ H_2O
y µL DHA (400 µM)	y µL DHA (400 µM)
100 µL enzyme (diluted)	100 µL enzyme (diluted)
100 µL terminating solution with $Na_2S_2O_4$	100 µL terminating sol'n with $Na_2S_2O_4$

x + y = 100 µL total

Dilute enzyme was prepared by adding 600 µL enzyme preparation to 2400 µL MilliQ water. Total volume 3000 µL (3 mL) → works out to be 16.6 µL enzyme preparation in reaction.

DHAE II (S. MPP3051)

Assay Ingredients:

Without inhibitor	With Inhibitor
100 µL KH_2PO_4 (1M, pH 6.6)	100 µL KH_2PO_4 (1M, pH 6.6)
100 µL $CoCl_2$ (10 mg/mL)	100 µL $CoCl_2$ (10 mg/mL)
50 µL 30% EtOH/H_2O sol'n	50 µL appropriate [I]
x µL MilliQ H_2O	x µL MilliQ H_2O
y µL DHA (200 µM)	y µL DHA (200 µM)
35 µL enzyme prep	35 µL enzyme prep
100 µL terminating solution with $Na_2S_2O_4$	100 µL terminating so'n with $Na_2S_2O_4$

x + y = 115 µL total

Kinetic Work Up for Both Enzymes

The samples were centrifuged in a microcentrifuge (Biofuge) at 13,000 rpm for 3 minutes. At this point, the samples were frozen (-80 °C) until needed. To determine the extent of conversion, the samples were separated by HPLC (Econosphere, C_{18}, 250 x 2 cm, 5 um, Alltech). Flow rate : 1 mL / min with 85:15 H_2O : CH_3CN (87:13 for DHAE II). The compounds were identified and their peak areas determined by their absorbances at 254 nm. A correction was made for the different extinction coefficients at 254 nm. Typical retention times: DHA (5.5 - 6.5 min, epoxyquinone (7.7 - 9.0 min), and quinone (9.0 - 10.0 min). The percent conversion was determined by dividing the area of the epoxyquinone peak by the sum of the area of substrate, epoxyquinone, and quinone peaks.

Synthesis Section

2, 5-dimethoxybenzanilide

To an oven dried 250 mL round bottom flask, the following items were added: 2,5-dimethoxyaniline (1.58 g, 10.3 mmol), benzoyl chloride (1.211 g, 8.6 mmol), and 100 mL freshly distilled CH_2Cl_2. The mixture was stirred and the temperature maintained below 40 °C. The solution was washed with two 40 mL portions of 5% NaOH solution, two 40 mL portions of 5% HCl solution, and two 40 mL portions of brine (sat'd NaCl). The organic layer was dried over Na_2SO_4 and rotavapped to give a dark gray solid. A flash column (80:20 Hexane:EtOAc) afforded an off white solid. Recrystallization in ethanol/water yielded a white solid (1.4 g, 62% yield). m.p. 84 - 85 °C ^{1}H NMR ($CDCl_3$, 300 MHz): δ 8.6 (1H, xc) δ 8.3 (1H, d, 3.5 Hz) δ 7.9 (2H, m) δ 7.5 (3H, m) δ 6.8 (1H, d, 9.6 Hz) δ 6.6 (1H, dd, 9.6, 3.5) δ 3.8 (3H, s) δ 3.75 (3H, s) ^{13}C NMR ($CDCl_3$, 75 MHz): δ 165.0, 155.1, 144.2, 138.5, 134.3, 129.8, 129.1, 127.6, 113.1, 109.0, 107.0, 57.6, 57.1 IR: 3329, 1654, 1619, 1600 HRMS: calculated 257.1048 found 257.1052

2',5'-dimethoxy-4-nitrobenzanilide

A solution consisting of dichloromethane and p-nitrobenzoyl chloride (3.12 g, 16.81 mmol) was added dropwise to a cooled (0 °C) solution of dichloromethane, 2,5-dimethoxyaniline (3.15 g, 20.6 mmol) and triethylamine (3.63 g, 35.9 mmol). The mixture was stirred for ten minutes and allowed to come to room temperature at which time an orange precipitate was formed. The solution was vacuum filtered to obtain an orange solid (4.17 g, 82%). m.p.: 184-185 °C ^{1}H NMR ($CDCl_3$, 300 MHz): δ 8.6 (1H, xc) δ 8.4 (2H, d, 8.7 Hz) δ 8.27 (1H, d, 2.9 Hz) δ 8.09 (2H, d, 8.7 Hz) δ 6.9 (1H, d, 8.7 Hz) δ 6.7 (1H, dd, 8.7 2.9) δ 3.9 (3H, s) δ 3.8 (3H, s) ^{13}C NMR ($CDCl_3$, 75 MHz): δ 163.5, 154.0, 149.0, 142.0, 140.0, 128.0, 127.8, 123.8, 110.5, 109.3, 106.0, 56.1, 55.7 IR: 3416, 3112, 1686, 1604, 1540, 1521 HRMS: calculated 302.0903 found 302.0900

2',5'-dimethoxy-4-cyanobenzanilide

In a 250 mL three-necked round bottom flask equipped with a water reflux condenser, an argon stream, and a rubber septum was added oxalyl chloride (1.69 g, 13.32 mmol) and p-cyano benzoic acid (1.00 g, 6.05 mmol). Several drops of DMF were added at the start of the reaction. This solution was heated until any excess oxalyl chloride had been removed. To the remaining solution was added ~75 mL freshly distilled dichloromethane to facilitate transfer. The acid chloride solution (a light peach color) was added dropwise to a dichloromethane solution containing 2,5-dimethoxyaniline (2.04 g, 13.32 mmol) and triethylamine (1.35 g, 13.32 mmol).

The mixture was allowed to stir for thirty minutes at which time it was quenched with water. The solution was then extracted with two 20 mL portions of 5% NaOH, two 20 mL portions of 5% HCl solution, and two 20 mL portions of brine. The organic layer was dried over Na_2SO_4 and rotavapped to afford a flaky yellow solid (1.10 g, 60% yield) m.p.: 149-151 °C ^{1}H NMR ($CDCl_3$, 300 MHz):

δ 8.6 (1H, xc) δ 8.25 (1H, d, 2.9) δ 8.0 (2H, d, 8.7) δ 7.8 (2H, d, 8.7) δ 6.9 (1H, d, 8.7) δ 6.7 (1H, dd, 8.7, 2.9) δ 3.9 (3H, s) δ 3.8 (3H, s) ^{13}C NMR ($CDCl_3$, 75 MHz): δ 197.0, 163.0, 154.0, 142.0, 139.2, 132.6, 127.6, 119.0, 115.5, 110.6, 109.4, 106.0, 56.2, 55.8 IR: 3418 2225 1677 1603 1539 HRMS: calculated 282.1005 found 282.1004

2',5'-dimethoxy-4-methylbenzanilide

A solution consisting of dichloromethane and p-toluoyl chloride (5.00 g, 32.3 mmol) was added dropwise to a cooled (0 °C) solution of dichloromethane, 2,5-dimethoxy aniline (5.10 g, 33.3 mmol) and triethylamine (7.3 g, 72.0 mmol). The mixture was stirred for thirty minutes and allowed to come to room temperature at which time the reaction was quenched with water. The solution was washed with three 25 mL portions of 5% HCl, three 25 mL portions of 5% NaOH, and three 25 mL portions of brine. The organic layer was rotavapped to afford a brown oil. Recrystallization from ethanol afforded an off white solid (7.76 g, 88%). m.p.: 66-67 °C ^{1}H NMR ($CDCl_3$, 300 MHz): δ 8.6 (1H, xc) δ 8.3 (1H, d, 2.9) δ 7.8 (2H, d, 8.7) δ 7.3 (2H, d, 8.7) δ 6.8 (1H, d, 8.7) δ 6.6 (1H, dd, 8.7, 2.9) δ 3.9 (3H, s) δ 3.8 (3H, s) δ 2.4 (3H, s) ^{13}C NMR ($CDCl_3$, 75 MHz): δ 165.4, 154.2, 142.5, 142.4, 132.6 129.6 128.8 127.2 110.9 109.0 106.0 56.6 56.0 21.7 IR: 3393 3137 1669 1601 1529 HRMS: calculated 272.1209 found 272.1207

2',5'-dimethoxy-4-aminobenzanilide

To an oven dried 250 mL round bottom flask was added 80 mL methanol followed by 2',5'-dimethoxy-4-nitrobenzanilide (3.86 g, 12.7 mmol), 5% Pd/C (1.00 g), and ammonium formate (3.77 g, 58.4 mmol). An argon stream was connected to the system. The solution was allowed to stir for one hour. At this time, the material was vacuum filtered to remove the Pd/C. An extraction with 5% HCl was done to separate the starting material from the product. The aqueous layer

was brought to pH 7 using 5% NaOH and extracted with dichloromethane. The organic layer was then dried over $MgSO_4$ and rotavapped to afford a flaky yellow solid (2.30 g, 67% yield). m.p.: 122.5-124 °C ^{1}H NMR ($CDCl_3$, 300 MHz): δ 8.5 (1H, xc) δ 8.3 (1H, d, 2.9 Hz) δ 7.7 (2H, d, 8.7) δ 6.85 (1H, d, 8.7) δ 6.7 (2H, d, 8.7) δ 6.6 (1H, dd, 8.7, 2.9) δ 4.1 (2H, br) δ 3.9 (3H, s) δ 3.8 (3H, s) ^{13}C NMR ($CDCl_3$, 300 MHz): δ 165.4, 154.0, 150.0, 142.0, 129.0, 124.0, 114.0, 111.0, 109.0, 106.0, 56.6, 56.0 IR: 3434 3337 3223 1645 1600 1517 HRMS: calculated 272.1161 found 272.1163

2',5'-dimethoxy-3-nitrobenzanilide

A solution consisting of dichloromethane and m-nitrobenzoyl chloride (3.20 g, 17.20 mmol) was added dropwise to a cooled (0 °C) solution of dichloromethane, 2,,5-dimethoxy aniline (2.79 g, 18.2 mmol) and triethylamine (7.3 g, 72.0 mmol). The mixture was stirred for thirty minutes and allowed to come to room temperature at which time the reaction was quenched with water. The solution was washed with three 25 mL portions of 5% HCl, three 25 mL portions of 5% NaOH, and three 25 mL portions of brine. The organic layer was rotavapped to afford a bright yellow solid (5.10 g, 98% yield). m.p.: 156 - 158 °C ^{1}H NMR ($CDCl_3$, 300 MHz): δ8.7 (1H, m), δ8.6 (1H, xc), δ8.4 (1H, m), δ8.25 (2H, m), δ7.7 (1H, t, 8.7 Hz), δ6.9 (1H, d, 8.7 Hz), δ6.7 (1H, dd, 8.7, 2.9 Hz), δ3.9 (3H, s), δ3.8 (3H, s) ^{13}C NMR ($CDCl_3$, 75 MHz): δ162.9, 154.1, 148.6, 142.6, 137.0, 133.1, 130.2, 127.9, 126.5, 122.2, 110.9, 109.6, 106.5, 56.5, 56.0 IR: 3394 3095 1673 1602 1541 HRMS: calculated 302.0903 found 302.0901

2',5'-dimethoxy-3-cyanobenzanilide

In a 250 mL 3-necked round bottom flask equipped with a water reflux condenser, an argon stream, and a rubber septum was added oxalyl chloride (4.37 g, 34.4 mmol) and m-cyano benzoic acid (2.00 g, 13.6 mmol). Several drops of

DMF were added at the start of the reaction. This solution was heated until any excess oxalyl chloride had been removed. To the remaining solution was added ~75 mL freshly distilled dichloromethane to facilitate transfer. The acid chloride solution was added dropwise to a dichloromethane solution containing 2,5-dimethoxyaniline (4.17 g, 27.2 mmol) and triethylamine (5.81 g, 54.4 mmol).

The mixture was allowed to stir for thirty minutes at which time it was quenched with water. The solution was then extracted with two 20 mL portions of 5% NaOH, two 20 mL portions of 5% HCl solution, and two 20 mL portions of brine. The organic layer was dried over Na_2SO_4 and rotavapped to afford a bright yellow solid (3.46 g, 90% yield). m.p. 115 - 117 °C ^{1}H NMR ($CDCl_3$, 300 MHz): δ8.55 (1H, xc), δ8.2 (2H, m), δ8.1 (1H, d, 8.7), δ7.8 (1H, d, 8.7), δ7.6 (1H, t, 8.7), δ6.8 (1H, d, 8.7) δ6.65 (1H, dd, 8.7, 2.9), δ3.9 (3H, s), δ3.8 (3H, s) ^{13}C NMR ($CDCl_3$, 75 MHz): δ162.9, 153.9, 142.5, 136.4, 135.0, 131.3, 130.9, 129.9 127.8, 118.1, 113.2, 110.8, 109.3, 106.4, 56.4, 55.9 IR: 3385 2231 1668 1600 1533 HRMS: calculated 282.1005 found 282.1004

2',5'-dimethoxy-3-methylbenzanilide

A solution consisting of dichloromethane and m-toluoyl chloride (5.00 g, 32.3 mmol) was added dropwise to a cooled (0 °C) solution of dichloromethane, 2,,5-dimethoxy aniline (5.00 g, 32.6 mmol) and triethylamine (7.3 g, 72.0 mmol). The mixture was stirred for thirty minutes and allowed to come to room temperature at which time the reaction was quenched with water. The solution was washed with three 25 mL portions of 5% HCl, three 25 mL portions of 5% NaOH, and three 25 mL portions of brine. The organic layer was rotavapped to afford a light brown solid. Recrystallization from ethanol afforded an off white solid (7.35 g, 84%) m.p.: 55-56 °C ^{1}H NMR ($CDCl_3$, 300 MHz): δ8.6 (1H, xc), δ8.3 (1H, d, 2.9), δ7.7 (2H, m), δ7.4 (2H, m), δ6.9 (1H, d, 8.7), δ6.6 (1H, dd, 8.7, 2.9) δ3.9 (3H, s), δ3.8 (3H, s), δ2.4 (3H, s) ^{13}C NMR ($CDCl_3$, 75 MHz): δ 165.0 155.0

142.0 138.5 134.0 132.0 129.0 128.9 128.0 124.6 111.0 109.0 106.0 56.5 56.0 22.0 HRMS: calculated 271.1209 found 271.1208

General procedure for removal of methyl ethers

To an oven dried round bottom flask was added the dimethoxy compound in CH_2Cl_2. The round bottom flask flask was fitted with a septum, flushed with argon, and cooled to –78 °C in a dry ice / acetone bath. BBr_3 (1.0 M in CH_2Cl_2) was added. A white smoke was emitted with each drop of boron tribromide added. After complete addition of boron tribromide, the solution was allowed to come to room temperature and was again flushed with argon. The solution was allowed to stir for 24 hours. At this time, the solution was poured over an ice bath (~100 mL) containing 2 g sodium dithionite that had been previously sparged with He for 1 hour. The solvent was removed in vacuo.

2',5'-dihydroxy-4-nitrobenzanilide (**8**)

Recrystallization in ethanol/water gave a dark orange/reddish solid (0.74 g, 93%). m.p.: 236-237 °C ^{1}H NMR ($CDCl_3$, 300 MHz): δ9.5 (1H, xc) δ8.5 (2H, d, 8.7), δ8.2 (2H, d, 8.7), δ7.5 (1H, d, 2.9), δ6.8 (1H, d, 8.7), δ6.6 (1H, dd, 8.7, 2.9) ^{13}C NMR ($CDCl_3$, 75 MHz): δ 165.0 152.1 151.5 142.7 141.7 129.1 127.3 125.0 118.6 113.4 110.7 IR: 3410 3128(br) 1663 1625 1602 1545 1518 HRMS: calculated 274.0590 found 274.0593

2',5'-dihydroxy-4-cyanobenzanilide (**20**)

A yellow precipitate formed immediately. Ethyl acetate was added to extract the desired compound. The organic layer was rotavapped to give a yellow solid (0.90 g, 96%) m.p.: 225-226 °C ^{1}H NMR ($CDCl_3$, 300 MHz): δ9.4 (1H, xc), δ8.2 (2H, d, 8.7), δ8.0 (2H, d, 8.7), δ7.5 (1H, d, 2.9), δ6.8 (1H, d, 8.7) δ6.65 (1H, dd, 8.7, 2.9) ^{13}C NMR ($CDCl_3$, 75 MHz): δ164.9 151.4 141.7 139.3 133.4 129.2

127.5 118.7 118.1 115.9 113.1 109.7 IR: 3415 3230 2232 1648 1551 HRMS: calculated 254.0691 found 254.0693

2',5'-dihydroxy-4-methylbenzanilide (**21**)

The organic layer was rotavapped to give an off white solid. Recrystallization in ethanol gave an off white solid (5.84 g, 98%). m.p.: 215-216 °C ^{1}H NMR ($CDCl_3$, 300 MHz): δ9.3 (1H, xc), δ8.5 (1H, xc), δ8.0 (3H, m), δ7.4 (3H, m), δ6.8 (1H, d, 8.7) δ6.65 (1H, dd, 8.7, 2.9), δ2.4 (3H, s) ^{13}C NMR ($CDCl_3$, 75 MHz): δ166.8 151.5 143.3 142.1 132.3 130.1 128.4 128.1 118.6 113.0 109.8 21.4 IR: 3418 3193(br) 1644 1554 HRMS: calculated 244.0974 found 244.0978

2',5'-dihydroxybenzanilide (**7**)

Recrystallization in ethanol under a blanket of argon gave a light yellow solid (0.50 g, 56%). m.p.: 198-199 °C ^{1}H NMR ($CDCl_3$, 300 MHz): δ9.3 (1H, xc), δ8.55 (1H, xc), δ8.0 (2H, m), δ7.6 (3H, m), δ7.4 (1H, d, 3.5 Hz), δ6.8 (1H, d, 9.6 Hz) δ6.55 (1H, dd, 9.6, 3.5) ^{13}C NMR ($CDCl_3$, 75 MHz): δ166.8 151.5 142.0 135.2 132.8 129.5 128.3 128.0 118.5 113.0 109.8 IR: 3416 3221 (br) 1648 1578 1549 HRMS: calculated 229.0739 found 229.0742

2',5'-dihydroxy-4-aminobenzanilide (**22**)

$NaHCO_3$ was added to bring the pH of the solution to neutral. A cloudy white precipitate formed immediately. Ethyl acetate was added to extract the desired compound. A solid was still present after addition of ethyl acetate. The solution was vacuum filtered quickly and immediately placed on high vacuum pump to remove any remaining solvent. A light brown solid was obtained (0.40 g, 67%). m.p.: 230-231 °C ^{1}H NMR ($CDCl_3$, 300 MHz): δ9.2 (1H, xc), δ8.7 (1H, xc), δ7.9 (1H, xc), δ7.8 (2H, d, 8.7), δ7.2 (1H, d, 2.9), δ6.8 (3H, m) δ6.5 (1H, dd, 8.7, 2.9) ^{13}C NMR ($CDCl_3$, 75 MHz): δ167.1 153.3 151.4 142.5 130.3 128.5 121.9

119.1 114.1 112.9 109.8 IR: 3415 3332(br) 1633 1540 1500 HRMS: calculated 244.0848 found 244.0851

2',5'-dihydroxy-3-nitrobenzanilide (**23**)

The organic layer was rotavapped to give an orange solid. The two solids were combined to give a light orange solid (1.30 g, 71% yield). m.p.: 222-223 °C ^{1}H NMR ($CDCl_3$, 300 MHz): δ9.6 (1H, br), δ8.8 (1H, m), δ8.4 (2H, m), δ7.9 (1H, t, 8.7), δ6.8 (1H, d, 8.7) δ6.6 (1H, dd, 8.7, 2.9), δ2.9 (2H, xc) ^{13}C NMR ($CDCl_3$, 75 MHz): δ164.5 151.5 149.3 142.1 137.0 134.4 131.1 127.5 127.1 123.3 118.4 113.4 110.2 IR: 3408 3256 (br) 1655 1555 1528 HRMS: calculated 274.0592 found 274.0590

2',5'-dihydroxy-3-cyanobenzanilide (**24**)

The organic layer was rotavapped to give a light tan solid (1.28 g, 67%). m.p.: 218-219 °C ^{1}H NMR ($CDCl_3$, 300 MHz): δ9.4 (1H, br), δ8.4 (1H, d, 2.9), δ8.3 (1H, m), δ8.0 (1H, m), δ7.6 (1H, m), δ7.5 (1H, d, 2.9 Hz) δ6.8 (1H, d, 8.7), δ6.6 (1H, dd, 8.7, 2.9) ^{13}C NMR ($CDCl_3$, 75 MHz): δ164.9 151.5 142.1 136.6 135.9 132.8 132.1 130.8 127.5 118.7 118.3 113.6 113.3 110.1 IR: 3440 3420 3150(br) 2244 HRMS: calculated 254.0691 found 254.0694

2',5'-dihydroxy-3-methylbenzanilide (**25**)

The organic layer was rotavapped to give a light pink solid (0.40 g, 73%). m.p.: 187-188 °C ^{1}H NMR ($CDCl_3$, 300 MHz): δ7.8 (2H, m), δ7.4 (3H, m), δ6.8 (1H, d, 8.7) δ6.5 (1H, dd, 8.7, 2.9), δ2.4 (3H, s) ^{13}C NMR ($CDCl_3$, 75 MHz): δ167.0 151.5 141.9 139.4 135.1 133.5 129.5 128.9 127.9 125.4 118.2 112.9 109.8 21.4 IR: 3426 3203 1652 1627 1616 1587 1552 HRMS: calculated 243.0895 found 243.0899

2',5'-dimethoxy-4-acetamidobenzanilide

In a 25 mL round bottom flask was added acetic anhydride (5 mL, 53.0 mmol) followed by 2',5'-dimethoxy-4-aminobenzanilide (0.263 g, 0.966 mmol). The reaction was stirred for seven hours at 35 °C. The workup of the reaction mixture consisted of extraction with dichloromethane followed two 5 mL portions of 5% NaOH. The organic layer was dried over anhydrous Na_2SO_4 and rotavapped to give a flaky yellow solid (0.21 g, 68%). m.p.: 172-173 °C ^{1}H NMR ($CDCl_3$, 300 MHz): δ8.6 (1H, xc), δ8.24 (1H, d, 3.5 Hz), δ7.88 (2H, d, 9.5 Hz), δ7.65 (2H, d, 9.5 Hz), δ6.81 (1H, d, 8.9 Hz), δ6.64 (1H, dd, 8.9, 3.2 Hz), δ5.8 (1H, xc), δ3.9(3H, s), δ3.8(3H, s), δ2.22 (3H, s) ^{13}C NMR ($CDCl_3$, 75 MHz): δ168.5 164.5 153.9 142.3 141.1 130.3 128.3 128.1 119.2 110.7 108.8 105.9 24.7 IR: 3423 1693 1641 1601 HRMS: calculated 314.1269 found 314.1267

2',5'-dihydroxy-4-acetamidobenzanilide

The organic layer was rotavapped to give a light yellow solid (0.040 g, 25% yield). m.p.: °C ^{1}H NMR ($CDCl_3$, 300 MHz): δ8.0 (2H, d, 9.5 Hz), δ7.8 (2H, d, 9.5 Hz), δ7.3 (1H, d, 3.5 Hz) δ6.8 (1H, d, 9.5 Hz), δ6.7 (1H, dd, 9.2, 3.5 Hz), δ2.18(3H, s) ^{13}C NMR ($CDCl_3$, 75 MHz): δ169.3 166.2 151.4 143.8 142.0 129.3 128.0 119.2 118.6 112.9 109.7 24.3 IR: 3351 1672 1632 1608 HRMS: calculated 286.0954 found 286.0954

The next five compounds were all prepared according to the following procedure. To an oven dried round bottom flask were added 2,5-dimethoxyaniline followed by triethylamine. A solution of the corresponding anhydride was then added dropwise over several minutes. After TLC analysis (CH_2Cl_2) indicated the reaction had completed, the reaction mixture was poured over cold water. The organic layer was subjected to a basic aqueous work-up. The organic layer was dried over anhydrous $MgSO_4$, gravity filtered, and the solvent removed in vacuo.

N-(2,5-dimethoxyphenyl)-propionamide

A tan solid was obtained (1.03 g, 84%), m.p. 60-61 °C. ^{1}H NMR ($CDCl_3$, 300 MHz): δ 8.13 (1H, d, J = 2.4 Hz), δ 7.80 (1H, bs), δ 6.76 (1H, d, J = 8.9 Hz), δ 6.53 (1H, dd, J = 8.9, 3.0 Hz), δ 3.76 (3H, s) δ 3.70 (3H, s) δ 2.41 (2H, q, J = 7.5 Hz) δ 1.23 (3H, t, J = 7.5 Hz) ^{13}C NMR ($CDCl_3$, 300 MHz): δ172.4 154.3 142.3 128.8 111.0 108.8 106.2 56.6 56.1 31.4 10.0 IR: 3258 1677 1595 HRMS: calculated 209.1052 found 209.1055

N-(2,5-dimethoxyphenyl)-2,2,2-trifluoroacetamide

Crude material was run through small plug of silica gel (EtOAc) to afford a pinkish white solid (0.93 g, 57%), m.p. 68-69 °C. ^{1}H NMR ($CDCl_3$, 300 MHz): δ 8.58 (1H, bs), δ 8.01 (1H, d, J = 3.0 Hz), δ 6.85 (1H, d, J = 9.0 Hz), δ 6.70 (1H, dd, J = 9.0, 3.0 Hz), δ 3.89 (3H, s) δ 3.80 (3H, s) ^{13}C NMR ($CDCl_3$, 300 MHz): δ154.2 142.9 125.9 118.0 114.1 111.4 111.1 106.9 56.7 56.2 IR: 3302 3096 3016 2962 2943 2839 1717 1599 HRMS: calculated 249.06128 found 249.06124

N-(2,5-dimethoxyphenyl)-2,2,2-trimethylacetamide

Material run through a short plug of silica gel (CH_2Cl_2) to afford a light tan solid (1.08 g, 78%), m.p. 51-53 °C. ^{1}H NMR ($CDCl_3$, 300 MHz): δ 8.18 (2H, d, J = 3.0 Hz), δ 6.79 (1H, d, J = 8.9 Hz), δ 6.56 (1H, dd, J = 8.9, 3.0 Hz), δ 3.85 (3H, s) δ 3.78 (3H, s) ^{13}C NMR ($CDCl_3$, 300 MHz): δ 177.0 154.4 142.5 129.0 111.1 109.1 105.7 56.7 56.2 40.5 28.0 IR: 3434 2966 1815 1671 1619 1602 HRMS: calculated 237.1365 found 237.1366

N-(2,5-dimethoxyphenyl)-butanamide

An off white crystalline solid was obtained (0.81 g, 62%), m.p. 36-38 °C. ^{1}H NMR ($CDCl_3$, 300 MHz): δ 8.14 (1H, d, J = 2.9 Hz), δ 7.79 (1H, bs), δ 6.76 (1H, d, J = 8.9 Hz) δ 6.54 (1H, dd, J = 8.9, 3.0 Hz), δ 3.82 (3H, s) δ 3.76 (3H, s) δ 2.36 (2H, t, J = 7.3 Hz), δ 1.75 (2H, septet, J = 7.3 Hz), δ 1.00 (3H, t, J = 7.4 Hz) ^{13}C NMR ($CDCl_3$, 300 MHz): δ 171.6 154.3 142.3 128.8 111.0 108.8 106.2 56.6 56.1 40.3 19.4 14.1 IR: 3247 2964 2839 1701 1660 1595 HRMS: calculated 223.12084 found 223.12063

N-(tert-butoxycarbonyl)-2,5-dimethoxyaniline (**32**)

Solvent removal gave a dark amber oil which was purified by short path distillation. A light amber oil was obtained (5.27 g, 65%). ^{1}H NMR ($CDCl_3$, 300 MHz): δ 7.79 (1H, bs), δ 7.10 (1H, bs), δ 6.75 (1H, d, J = 8.8 Hz) δ 6.49 (1H, dd, J = 8.9, 3.1 Hz), δ 3.82 (3H, s) δ 3.78 (3H, s) Hz), δ 1.52 (9H, s) ^{13}C NMR ($CDCl_3$, 300 MHz): δ 154.5 152.9 142.1 129.2 111.2 107.5 104.7 56.6 56.2 28.8 IR: 3438 2977 2937 2835 1729 1604 HRMS: calculated 253.13137 found 253.13141

1-(2,5-Dimethoxyphenyl)-propan-2-one (**30**)

Methyl iodide (2.0 mL, 4.56 g, 32.1 mmol) was added dropwise to a solution containing lithium metal (0.200 g, 28.8 mmol) and diethyl ether (50 mL). An argon bubbler was added to the system. After approximately two hours, this solution was added in one portion to a solution containing diethyl ether (50 mL) and 2,5-dimethoxyphenylacetic acid (0.283 g, 1.44 mmol). This combined mixture was allowed to stir for two hours before being poured into cold water. The organic layer was separated and washed with 5% NaOH (2 x 25 mL), dried over sodium sulfate, and the solvent removed in vacuo. An orange oil was obtained after

removal of solvent. Subsequent short path distillation yielded light yellow oil (.212 g, 75%). ^{1}H NMR ($CDCl_3$, 300 MHz): δ 7.11 (3H, m) δ 3.78 (3H, s) δ 3.75 (3H, s), δ 3.52 (2H, s), δ 2.16 (3H, s) ^{13}C NMR ($CDCl_3$, 300 MHz): δ 207.1 153.9 152.0 125.0 117.7 113.1 111.8 56.3 56.0 44.3 29.6 IR: 3400 2938 2835 1712 1502 HRMS: calculated 194.0943 found 194.0942

2,5-dimethoxyphenylacetate (**31**)

A deep red solid was obtained after removal of solvent. After recrystallization from ethyl acetate, a tan solid was obtained (0.80 g, 68%), m.p. 55-59 °C. ^{1}H NMR ($CDCl_3$, 300 MHz): δ 6.89 (1H, d, J = 8.9 Hz) δ 6.73 (1H, dd, J = 9.1, 3.0 Hz), δ 6.64 (1H, d, J = 3.0 Hz), δ 3.78 (3H, s) δ 3.75 (3H, s), δ 2.31 (3H, s) ^{13}C NMR ($CDCl_3$, 300 MHz): δ 169.4 154.1 145.7 140.7 113.8 111.8 109.9 56.9 56.2 21.0 IR: 3070 2971 2840 2062 1766 1642 1593 HRMS: calculated 196.07356 found 196.07369

5,8-Dimethoxy-3,4-dihydro-1H-quinolin-2-one

Recrystallization from ethyl acetate gave yellow crystals (0.100 g, 50%), m.p. 99-100.5 °C. ^{1}H NMR ($CDCl_3$, 300 MHz): δ 7.84 (1H, bs), δ 6.65 (1H, d, J = 8.8 Hz) δ 6.44 (1H, d, J = 9.0 Hz), δ 3.77 (3H, s) δ 3.75 (3H, s), δ 2.90 (2H, t, J = 8.3 Hz), δ 2.53 (2H, t, J = 7.4 Hz) ^{13}C NMR ($CDCl_3$, 300 MHz): δ 170.6 151.1 140.7 127.9 112.7 109.4 104.4 56.5 56.1 30.4 19.3 IR: 3240 3000 2841 1671 1605 HRMS: calculated 207.08954 found 207.08975

N-(2,5-dihydroxyphenyl)-propionamide (**26**)

Solvent removal gave a light brown solid (0.34 g, 65%), m.p. 143-145 °C (decomp.). ^{1}H NMR ($CDCl_3$, 300 MHz): δ 8.97 (1H, bs), δ 8.19 (1H, bs), δ 7.04

(1H, d, J = 3.0 Hz) δ 6.71 (1H, d, J = 8.7 Hz), δ 6.50 (1H, dd, J = 8.6, 2.9 Hz), δ 2.95 (1H, s), δ 2.47 (2H, q, J = 7.6 Hz), δ 1.16 (3H, t, J = 7.7 Hz) ^{13}C NMR ($CDCl_3$, 300 MHz): δ 173.9 150.9 141.5 127.6 118.5 112.4 108.8 29.7 9.6 IR: 3407 3293 1637 1549 HRMS: calculated 181.07389 found 181.07394

N-(2,5-dihydroxyphenyl)-2,2,2-trifluoroacetamide (**29**)

Removal of solvent gave an off white / pink solid (0.24 g, 68%), m.p. 217 °C (decomp.). ^1H NMR ($CDCl_3$, 300 MHz): δ 9.19 (1H, bs), δ 8.50 (1H, bs), δ 8.00 (1H, s), δ 7.53 (1H, d, J = 2.8 Hz) δ 6.82 (1H, d, J = 8.7 Hz), δ 6.59 (1H, dd, J = 8.7, 2.8 Hz) ^{13}C NMR ($CDCl_3$, 300 MHz): δ 151.2 141.1 124.9 117.8 116.2 113.8 110.9 109.3 ^{19}F (acetone-d^6, 282 MHz): δ -76.8 IR: 3383 1704 1566 HRMS: calculated 221.02998 found 221.03013

N-(2,5-dihydroxyphenyl)-butanamide (**27**)

Solvent removal gave an off white solid (0.33 g, 76%), m.p. 138-140 °C (decomp.). ^1H NMR ($CDCl_3$, 300 MHz): δ 9.03 (1H, bs), δ 8.44 (1H, bs), δ 7.94 (1H, s), δ 7.02 (1H, d, J = 2.7 Hz) δ 6.72 (1H, d, J = 8.8 Hz), δ 6.51 (1H, dd, J = 8.8, 2.7 Hz), d 2.44 (2H, t, J = 7.4 Hz), d 1.70 (2H, heptet, J = 7.4 Hz), δ 0.96 (3H, t, J = 7.3 Hz) ^{13}C NMR ($CDCl_3$, 300 MHz): δ 173.2 150.9 141.6 127.5 118.6 112.5 108.9 38.5 19.3 13.4 IR: 3406 2966 1656 HRMS: calculated 195.08954 found 195.08954

N-(2,5-dihydroxyphenyl)-2,2,2-trimethylacetamide (**28**)

Solvent removal generated a sticky brown solid (0.44 g, 83%) m.p. 152-155 °C. ^1H NMR ($CDCl_3$, 300 MHz): δ 8.54 (1H, bs), δ 8.35 (1H, bs), δ 7.80 (1H, s), δ 7.31 (1H, d, J = 2.9 Hz) δ 6.73 (1H, d, J = 8.7 Hz), δ 6.48 (1H, dd, J = 8.6, 2.9 Hz),

δ 1.30 (9H, s) ^{13}C NMR ($CDCl_3$, 300 MHz): δ 177.9 150.9 140.9 127.7 117.4 111.7 108.9 39.8 27.4 IR: 3348 2976 1650 1600 HRMS: calculated 209.1052 found 209.1051

5,8-Dihydroxy-3,4-dihydro-1H-isoquinolin-2-one (**33**)

Solvent removal gave a light yellow solid (0.30 g, 70%), m.p. 203-206 °C. ^1H NMR ($CDCl_3$, 300 MHz): δ 8.09 (1H, bs), δ 7.85 (1H, bs), δ 7.83 (1H, s), δ 6.59 (1H, d, J = 8.6 Hz) δ 6.36 (1H, d, J = 8.7 Hz), δ 2.89 (2H, m), δ 2.47 (2H, m) ^{13}C NMR ($CDCl_3$, 300 MHz): δ 172.2 147.3 137.3 126.9 113.6 111.6 109.6 30.0 19.0 IR: 3302 1667 1609 HRMS: calculated 179.05824 found 179.05851

References:

1. Ohkata, K.; Kojima, S.; Hiraga, Y.; Kanosue, Y. *Chem. Letters* **2001,** 418-9
2. Sierks, M. R.; Svensson, B. *Biochemistry* **2000**, 39, 8585-8592
3. Waldemar, A.; Hamdullah, K.; Chantu R., S-M. *Synlett* **2002,** 3, 510-512
4. Block, O.; Klein, G.; Altenbach, H.; Brauer, D. *J. Org. Chem.* **2000**, 65(3), 716-721
5. Wipf, P.; Coish, P. D. G. *J. Org. Chem.* **1999,** 64(14), 5053 – 5061
6. Alcaraz, L.; Macdonald, G.; Ragot, J.; Lewis, N. J.; Taylor, R. J. K. *Tetrahedron* **1999,** 55(12), 3707 – 3716
7. Conje Grove, J. J. ; Wei, X.; Taylor, R. J. K. *Chem. Comm.* **1999,** 5, 421 – 422
8. Kapfer, I.; Lewis, N. J.; Macdonald, G.; Taylor, R. J. K. *Tetrahedron Lett.* **1996**, 37 (12), 2101 – 2104
9. Johnson, C. R.; Miller, M. W. *J. Org. Chem.* **1995**, 60, 6674 – 6675

10. Sattler, I.; Thiericke, R.; Zeeck, A. *Nat. Prod. Rep.* **1998** 221-240

11. Keillor, J. W.; Roupioz, Y.; Rivard, C.; Lherbet, C.; Castonguay, R.; Menard, A. *Biochemistry* **2001**, 40, 12678-12685

12. Armstrong, R. N.; Bernat, B. A.; Svennson, R.; Morgenstern, R. *Biochemistry*, **2001**, 40, 3378 – 3384

13. Gokel, G. W.; Abel, E.; Suzuki, I.; Murillo, O. *J. Am. Chem. Soc.* **1996**, 118, 7628-7629

14. Whittaker, J. W.; Whittaker, M. M. *Biochemistry* **2001**, 40, 7140 – 7148

15. Personal conversation with Ana Barrios. Lack of p-hydroquinone inhibition was identified only for DHAE II, but based on similarities between the two enzymes, it most likely applies to DHAE I as well.

16. Kirchmeier, M. Purification of 2,5-dihydroxyacetanilide Epoxidase and Mechanism of Hydroquinone Epoxidases. *Ph. D. Thesis,* Oregon State Univ. 1997

17. R. H. C.; *J. Chem. Soc., Perkins I* **1981**, 2574 – 2576

18. Quinn, D. M.; Hui, D. Y.; Baker, N.; Lee, K.; Feaster, S. R. *Biochemistry*, **1996**, 35, 16723-16734

19. Nakagawa, K.; Manabe, Y.; Osaki, M.; Yo, E.; Tominaga, M. *Chem. Pharm. Bull.* **1981**, 29(8), 2161 – 2165

20. Segel, I. *Enzyme Kinetics* John Wiley and Sons, Inc. **1975** Chapters 1-4

21. Wong, C-Y.; Koeller, K. M. *Nature* **2001**, 409, 232 – 240

22. Dowd, P.; Ham, S-K.; Hershline, R. *J. Am. Chem. Soc.* **1992**, 114 (23), 7613 – 7617

23. Dowd, P.; Ham, S-K.; Geib, S. J. *J. Am. Chem. Soc.* **1991**, 113, 7734 – 7743

24. Boll, M.; Mobitz, H. *Biochemistry* **2002**, 41, 1752 – 1758

25. Ramaraj, R.; Rajagopal, S.; Ganesan, M. *J. Org. Chem.* **2002**, 67, 1506 – 1514

26. Richey Jr., H. G.; Maclin, K. M. *J. Org. Chem.* **2002**, 67, 4370 – 4371

27. Mohr, P.; Pommerening, K. *Affinity chromatography* M. Dekker **1985**

28. Dean, P. D. G.; Johnson, W. S.; Middle, F. A. *Affinity chromatography : a practical approach* IRL Press **1985**

29. Scouten, W. H.; *Affinity chromatography* New York : Wiley, **1981**.

30. Chapman, N. B.; *Advances in linear free energy relationships* London, New York, Plenum Press **1972**

31. Johnson, C. D. *The Hammett equation* Cambridge ; New York : Cambridge University Press, **1980**

32. Hammett, L. P. *Physical organic chemistry; reaction rates, equilibria, and mechanisms* New York, McGraw-Hill **1970**

33. Carpenter, B. K. *Determination of organic reaction mechanisms* New York: Wiley, **1984**.

34. Kohno, J.; Nishio, M.; Kawano, K.; Nakanishi, N.; Suzuki, S.-I.; Uchida, T.; Komatsubara, S. J. *J. Antibiot.*, **1996**, 49, 1212

35. Lee, M.D.; Fantini, A.A.; Morton, G.O.; James, J.C.; Borders, D.B.; Testa, R.J. *J. Antibiot.* **1984**, 37, 1149-1152

36. Box, S. J.; Gilpin, M.L.; Gwynn, M.; Hanscomb, G.; Spear, S.R.; Brown, A.G. *J. Antibiot.* **1983**, 36, 1631-1637.

37. Williams, K. M.; Marshall, T. *J. Biochem. Biophys. Meth.* **1993**, 26(2-3), 237

Chapter 3:

Rationale and Design of Ligands for Affinity Column Separation of DHAE I and DHAE II

Introduction to Protein Purification

Nowhere are the principles of molecular recognition more prevalent than in protein purification.[1-9,17] Every interaction between protein and support requires a combination of intermolecular interactions, although one interaction usually dominates. The different techniques available for the separation of a protein from a complex mixture can be classified into five main areas: separations based on charge, hydrophobicity, size, molecular weight, and separations based on affinity for a specific ligand. Of these five techniques, only separations based on affinity interactions are specific to the enzyme targeted for isolation.[1-9]

The focus of this chapter is to design rational ligands based on data obtained in the Hammett study and to attempt an affinity separation of DHAE I and DHAE II using the designed ligands. However, other purification techniques were used in conjunction with this affinity approach and therefore it will be helpful to discuss the other separation techniques. Affinity column purification not only represents a specific technique for purification of enzyme; it also allows a larger fraction of active enzyme to be recovered in a shorter period of time.

By understanding the non-specific chemical nature of the common purification techniques, an understanding can be gained of the importance of affinity purification to the isolation of DHAE I and DHAE II.

Separations Based on Charge

Separation based on ion-ion interactions represents one of the largest classes of protein purification techniques. Each protein in the mixture has a unique surface charge at the pH used in the isolation step that is dependent upon the identity and number of amino acid side chains present on the surface of the enzyme. Application of the sample mixture to a support bearing the opposite

charge results in binding of proteins that elute under varying ionic strength conditions. There are obvious advantages to using an ion exchange resin in protein purification. Mainly, these large-throughput columns have high-resolution power and can withstand elevated flow rates. Several proteins, however, may have similar charges under the chosen experimental conditions and will elute under the same ionic strength conditions. Another common elution method is variation of the pH. It is also possible that each protein, regardless of the surface charge, interacts differently with the support or the elution salt. This technique usually results only in a partial purification of the enzyme mixture.

Separations Based on Hydrophobicity

Hydrophobic interaction chromatography (HIC), based on van der Waals attractions, can complement ion exchange chromatography. By adding a high concentration of salt to a protein mixture and applying this new solution to a hydrophobic support, the proteins in the mixture will be repelled by the high ionic strength and attracted to the hydrophobic support. The strength of this interaction is dependent on the degree of surface area contact between the support and the protein. Again, it is possible that two or more proteins will have similar hydrophobic interactions and therefore elute in the same fraction. Numerous hydrophobic supports are available and in an isolation procedure it may be necessary to try several types of hydrophobic chromatography columns.

Separations Based on Size and Molecular Weight

The next two purification methods are related and are based on the size or molecular weight of the proteins. By using a solid support containing pores of

defined diameter, proteins small enough to enter the pore will be retarded by inclusion within the support and therefore elute at a longer retention time. The amount of time spent interacting with the support depends on the native conformation of the protein and any conformational effects resulting from the solution pH.

Separations Based on Affinity

Affinity purification represents the most powerful separation technique available in protein purification. By identifying a substrate or inhibitor known to bind to the enzyme of interest and attaching this molecule to a solid support should allow for *selective* binding. The enzyme binds to the attached substrate and allows the other proteins in the mixture to flow through the resin. After at least five column volumes of buffer are added to ensure removal of the contaminating proteins in the mixture, the enzyme of interest can be eluted.

Within the last ten years, a variant of affinity chromatography has surfaced which is based on an immune system interaction.[24] Protein antigens can bind to antibodies specific for that protein. The complex mixture of proteins is added to an immunoaffinity column, that has antibody covalently attached to a solid support; the protein of interest binds to its antibody allowing for its separation from this mixture. Numerous techniques are available to disrupt the antibody – protein interaction which allows for recovery of the desired protein. Several examples of the application of affinity chromatography in protein purification are given below.

Examples of Affinity Purification in Protein Work

Loog has shown the precise and excellent resolving power of affinity chromatography by developing bi-substrate analogue ligands in the purification of protein kinase A.[11] Protein kinases transfer the phosphoryl group from ATP to an acceptor amino acid residue within a protein. The number of protein kinases involved in regulatory pathways has risen to over 1000. Several attempts have been made to use peptides as affinity ligands for isolation of glycogen synthase kinase and casein kinase II. The peptides alone did not bind strongly enough to the adsorbent to allow for a clean separation.

By designing a bi-substrate analogue, Loog has shown that by proper selection of the peptide motif, it will be possible to separate different classes (basophilic, acidophilic, or proline oriented) of protein kinases. The bi-substrate consisted of a nucleotide resembling part (AdoC) and a peptide fragment connected to a Sepharose affinity resin via a linker (Figure 34).[11] Clean separation was obtained as indicated by SDS – PAGE.

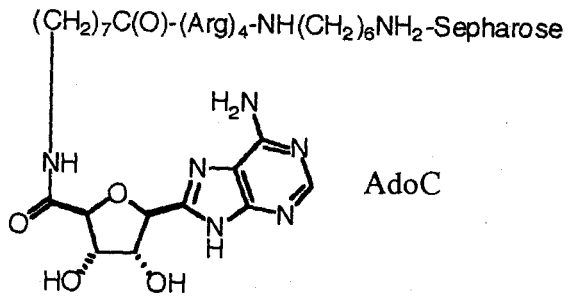

Figure 34: Bi-substrate analog applied to affinity separation of protein kinase A

Bostock et al. have been able to separate three different cutinases by using the affinity approach.[10] Cutinases, serine hydrolases, are extracellular fungal

enzymes that hydrolyze cutin, an insoluble lipid polyester. Trifluoromethyl ketones (TFK) are potent inhibitors of a variety of serine hydrolases. The inhibitory activities of TFK's are believed to arise from the formation of a hemiketal link that resembles the transition state for ester hydrolysis. By synthesizing the inhibitor, 3-(4-mercaptobutylthio)-1,1,1-trifluoro-2-propanone (MBTFP), and attaching this ligand to an epoxy-activated Sepharose via the sulfide group (Scheme 12), three different proteins with esterase activity were obtained.

Along the same lines Ibrahim and Anzellotti have recently used another common method, attachment of cofactor to affinity resin, to purify a 2-oxoglutarate-dependent dioxygenase.[12] By attaching the 2-oxoglutarate cofactor to an epoxy-activated Sepharose, they were able to cleanly separate (one band in SDS-PAGE) the dioxygenase from the cell free extract.

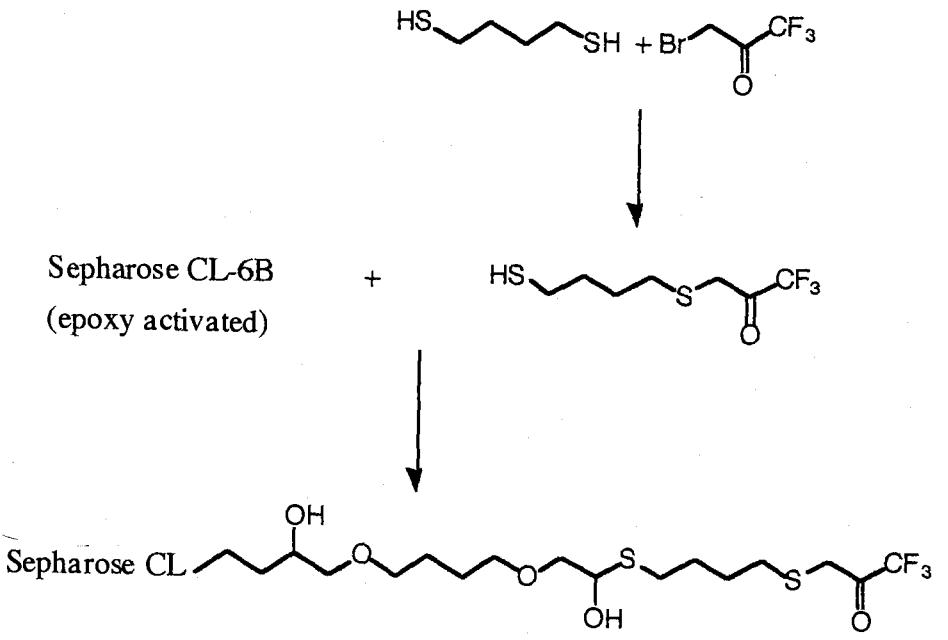

Scheme 12: Synthesis of MBTFP-Sepharose resin

Although these separations have resulted in isolation of the enzyme of interest, there are several variables that need to be addressed before performing an affinity separation.[13-16] Affinity purification consists of four steps: preparation of column, loading the column, elution of enzyme, and regeneration of the column. There are standard protocols for both preparation and regeneration of the column support. The middle two steps are unique to each separation.[7,8]

After loading the column, sufficient time should be allowed for equilibrium to be established between the enzyme and the support. Bostock et al.[10] and Loog et al.[11] allowed the affinity resin and enzyme to mix overnight by shaking before attempting to elute the enzyme. Ibrahim and Anzellotti added the enzyme, allowed a short equilibration time before adding elution buffer.

Elution conditions also varied among the three purifications discussed above. Ibrahim and Anzellotti and Bostock et al. used the same ligand connected to the affinity resin in the elution buffer to coax the enzyme off the support. Loog added Triton X-100 to the elution buffer. Although the conditions varied, all groups were successful in their purifications as a result of using the affinity approach in their isolation protocols.

Impetus for Using Affinity Approach

Shen first attempted the isolation of DHAE I in 1988.[18] Starting with 867 mg of protein, this mixture was first subjected to protamine sulfate, a DNA binding agent, followed by ammonium sulfate precipitation. Approximately one-third of the protein was lost during these two steps and resulted in only a 1.7 fold purification.

Six chromatographic steps were used after the sulfate precipitations. Starting with size exclusion followed by Acell QMA anion exchange chromatography resulted in an additional eight-fold purification. The 23.3 mg

isolated from the anion exchange column was applied to a phenyl 5-PW hydrophobic interaction chromatography and eluted with a potassium phosphate salt gradient. A 300 SW size exclusion column followed by a repeat of the phenyl 5-PW HIC column eluted with a Tris buffer gave a 640-fold overall purification. This isolation procedure resulted in 112 μg of protein that retained 7.9% of the original activity and gave eight bands according to SDS-PAGE. The band corresponding to DHAE I was never unambiguously identified.

This isolation protocol for DHAE I takes over five weeks to process and is very costly for the amount of enzyme obtained. For the isolation of larger quantities of enzyme, a different isolated scheme would have to be generated.

Kirchmeier continued further investigations into the isolation of DHAE I as well as DHAE II.[19] Starting with a large scale DE-52 anion exchange column, DHAE I and DHAE II consistently was eluted by 200 mM potassium chloride. Material isolated from the DE-52 column was concentrated using an Amicon CentriPrep 30s, before being applied to an immobilized metal ion affinity chromatography (IMAC) column. These two steps resulted in an 18-fold purification that retained 70% of the original activity. The protein mixture, 63 mg, was then subjected to C-5 HIC followed by phenyl HIC. At this point, 39% of the activity remained and 2160-fold purification was obtained. However, only 107 μg of enzyme mixture remained. One last anion exchange column was used (DEAE) that resulted in an overall 23000-fold purification, but resulted in only 6 μg of impure enzyme. There were still five bands present in a silver stained SDS-PAGE gel. A Bio-Rad 491 gel electrophoresis cell completed the purification scheme but resulted in a significant loss of activity (<5% activity remained). Homogeneous enzyme was isolated from the gel and subjected to N-terminal and internal sequencing. However, the amount of information was not sufficient to create genetic probes.

Every class of technique has been used in attempted purification of DHAE I and DHAE II except for affinity purification. Affinity purification is the most

specific technique than can be applied in protein purification. The substrate, a modification of the substrate, a good competitive inhibitor, or a co-factor can be attached to a polymer support and the enzyme mixture applied. The enzyme in question binds to the ligand and can be eluted when desired. This was our rationale for choosing affinity column purification to purify DHAE I and DHAE II.

Rationale for Design of Ligands

The necessity for an affinity column separation of DHAE I and DHAE II is evident from the above discussion. However, based on the proposed differences in substrate binding discussed in Chapter 2, two different ligands will be required for separation of these two enzymes.

In Chapter 2, we proposed that DHAE I binds so the amide substituent points toward the active site exterior. In addition to the Hammett study results, a group as large as an acetylamino substituent was accepted as a competitive inhibitor. For both of these reasons, the linker group required for attachment of inhibitor to affinity resin would remain on the same side as the amide functional group. DHAE II, however, is assumed to bind substrate on the side opposite the amide functional group. A linker would be necessary on carbons 3 or 4 (Figure 35). The amino group was chosen as the preferred linker group because of the greater stability of the resulting carbamate bond. The linker length represents the only unknown factor which could affect separation of DHAE I and DHAE II using this approach.

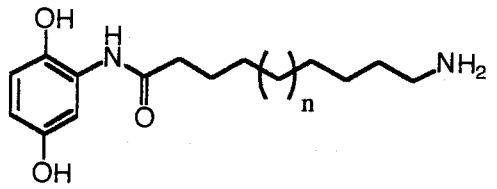

Ligand for DHAE I Affinity Column

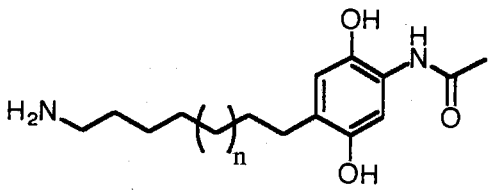

Ligand for DHAE II Affinity Column

Figure 35: Candidate ligands for affinity separation of DHAE I and DHAE II

Synthesis of Ligands for Affinity Columns

Addition of a linker to the side containing the amide bond can easily be accomplished. The synthesis of **35** starts from **22** and is complete in five steps (Scheme 13). Coupling of **22** with 6-bromohexanoyl chloride in the presence of triethylamine generated bromide in good yield. Conversion of bromide using sodium azide followed by hydrogenation of the corresponding azide using palladium on charcoal resulted in clean formation of the amine. The deprotection of the methyl groups using boron tribromide required protection of the amine. The trifluoroacetyl protected amine was generated by heating the amine in neat trifluoroacetic anhydride. Subsequent deprotection of the methylated hydroquinone gave the trifluoroacetyl protected amine in decent yield. Removal of the trifluoroacetyl group using acidic methanol and subsequent addition to the affinity resin gave the active resin (30% overall yield).

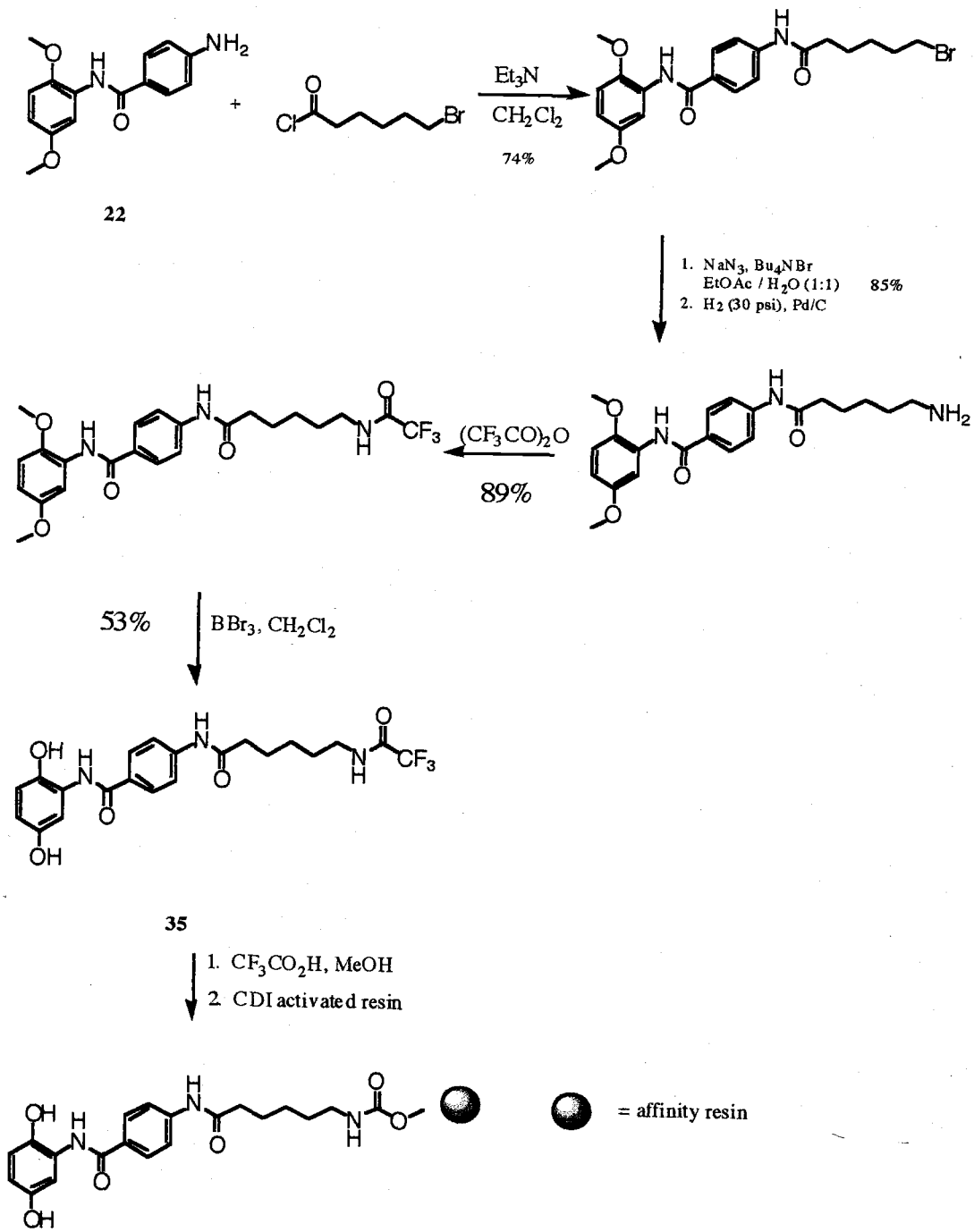

Scheme 13: Synthesis of ligand for DHAE I's affinity column

Retrosynthetic analysis allows for two possible synthetic routes of the ligand for DHAE II's affinity column (Scheme 14).

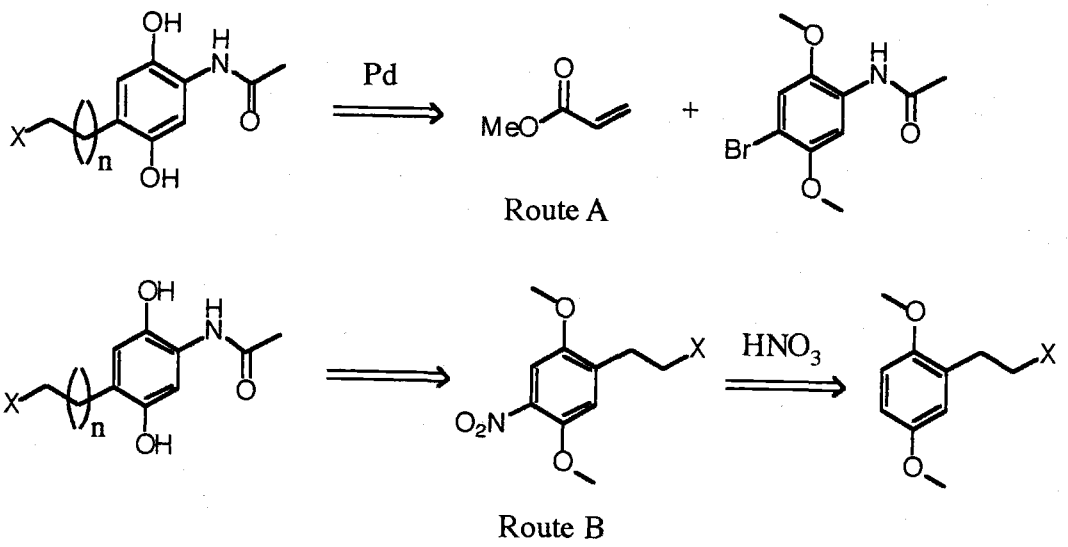

Scheme 14: Two possible synthetic routes to **37**

Initially, a carbon-carbon bond was envisioned at position C-4. 2,5-Dimethoxyacetanilide, a precursor to **1**, was believed to be the best starting material for the formation of this carbon – carbon bond. Because of the numerous examples in the literature using palladium catalysis to form these key bonds, it was believed that a Heck or Suzuki reaction could be used. The necessary halogen was added using NBS or NIS. Attempts using different forms of palladium catalysis failed to give the desired connection. Palladium catalysis is sensitive and a variety of factors can influence the outcome of the reaction. In this particular case, starting material was recovered in every case. This indicates the inability of the palladium to oxidatively add into the carbon – bromine bond. C-4 is a position of high electron density and this may prevent formation of the organopalladium intermediate.

Although the 4-bromo derivative failed to yield the desired connection using palladium catalysis, there had to be alternative methods that would utilize this intermediate. The 4-bromo derivative can be converted to the quinone, **38**, by removal of the methyl groups using boron tribromide followed by oxidation with silver (I) oxide. The position of the bromine may allow for Michael addition of a nucleophile at this position and with subsequent reduction of the quinone may generate the desired connection. However, there are potential pitfalls using this approach. Having an amine as the desired nucleophilic linking atom and the quinone functional group is a combination that could undergo numerous side reactions. The number of potential pitfalls outweighs the advantages of this approach (Scheme 15).

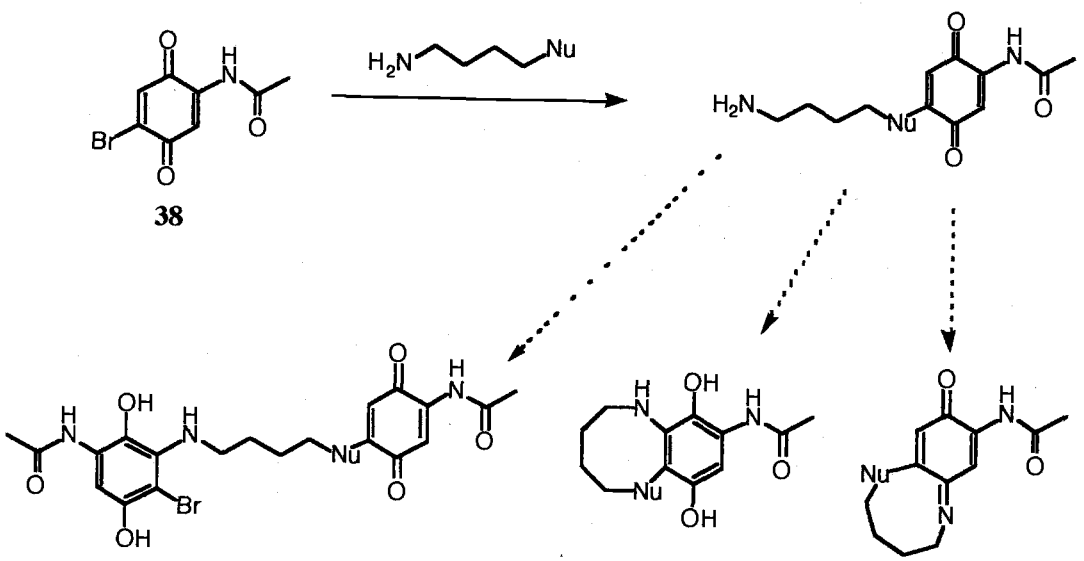

Scheme 15: Potential pitfalls to using quinone chemistry

The second possible synthetic route, route B, starts with the carbon – carbon bond already formed with the C-N bond of the amide added by aromatic nitration. There are a variety of 2,5-dimethoxy compounds commercially available with the carbon-carbon bond in the necessary position (Scheme 16).

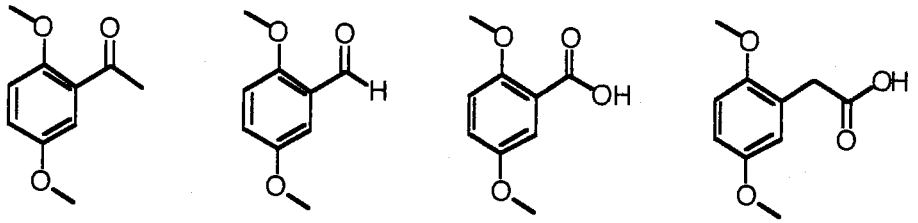

Scheme 16: Commercially available 2,5-dimethoxy compounds

2,5-Dimethoxybenzaldehyde, already available in the laboratory, was the starting material for this second route. A literature procedure, which proceeds through a diacetoxy acetal, was used. However, attempts at the generation of the 4-nitro benzaldehyde failed to give significant quantities of the desired compound.

For this reason, additional alternatives were attempted. A carbon-nitrogen bond can be created specifically at C-4 of 2,5-dimethoxyacetanilide using nitric acid in acetic acid at reduced temperatures. Reduction of the nitro group and subsequent coupling to 6-bromohexanoyl chloride generated the bromide in good yield. Conversion to the azide followed by hydrogenation generated the desired amine. Trifluoroacetyl protection gave the protected amine. However, in this synthesis, deprotection of the methyl ethers gave a mixture of quinone, hydroquinone, and several smaller impurities.

Finally, it was decided that the trifluoroacetyl protection was not necessary. Deprotection of the amine generating the amine-hydrobromide proceeded as desired. This material was added to the activated affinity resin without purification (Scheme 17).

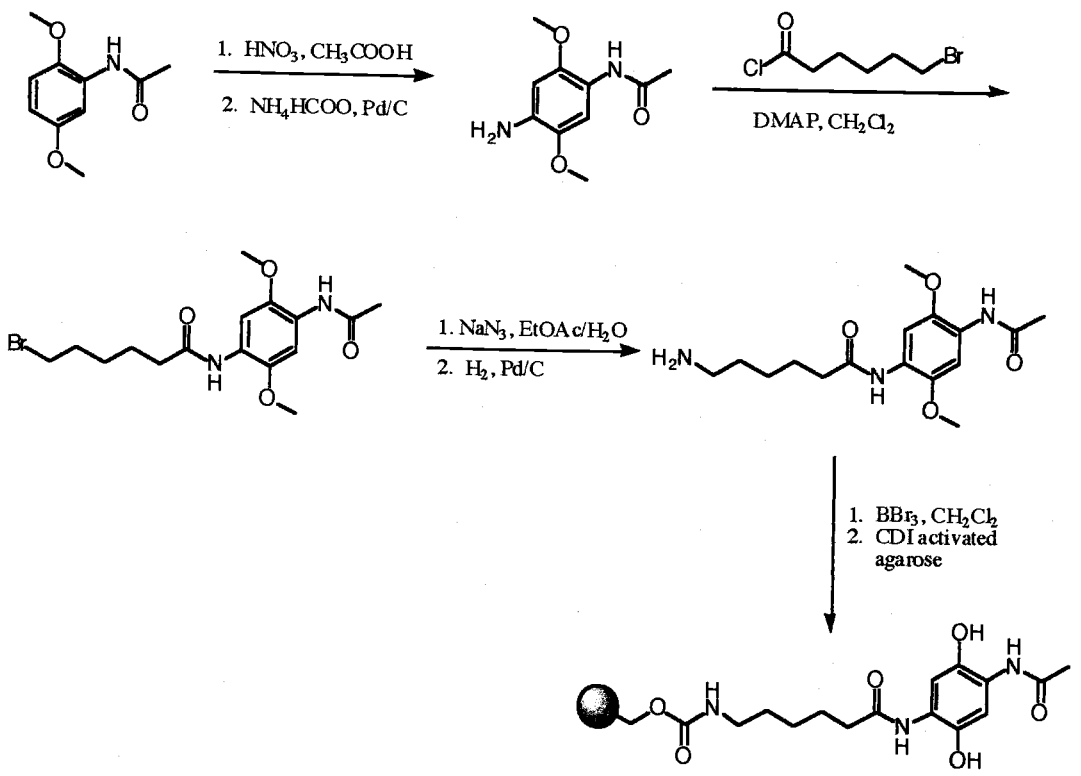

Scheme 17: Final synthesis of ligand for DHAE II synthesis

An unexpected outcome of this approach was the visual indication of the redox state of the attached ligand. When the bound ligand is oxidized and in the quinone form, the resin appears colored, pale yellow for DHAE I and pink for DHAE II. After passing a sodium dithionite solution through the resin, the resin turns white indicating the reduction of the quinone form to the hydroquinone form (Figure 36).[ref] Shen has shown that the quinone form of substrate does not bind to the enzyme.[18] Initially, this was the proposed method for elution of DHAE I and DHAE II from the affinity resin. By maintaining the resin in the reduced form, DHAE I and DHAE II will bind and simply by removing sodium dithionite from the elution solvent, the hydroquinone is oxidized to the quinone form and DHAE I or DHAE II is released. However, due to the possibility for reaction between the

quinone and any nucleophiles (amines and sulfides), it was best to maintain the ligand in the reduced form.

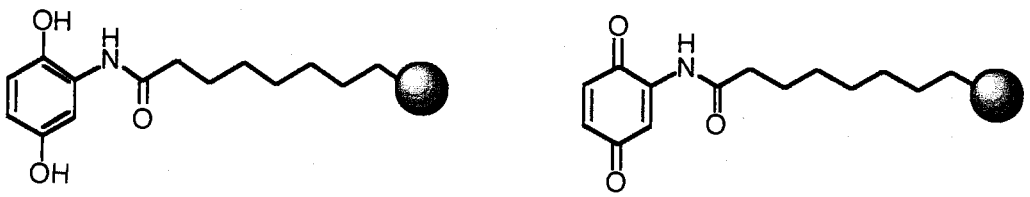

Reduced Form of Resin - White
DHAE I and DHAE II will bind

Oxidized Form of Resin - Colored
DHAE I and DHAE II will not bind

Figure 36: Redox activity of affinity resin

Results of Affinity Column Chromatography

Two different conditions were attempted for each column. In the first attempt for each column, the enzyme was eluted with **6**. Natural substrate, **1**, was used to elute the enzyme for each second attempt. Both of the first attempts did not result in active enzyme being eluted from the column. Thirty to thirty five fractions were taken and the buffer was allowed to flow by gravity through the columns.

The second attempt for DHAE I's affinity column resulted in protein being collected in fractions 2-4. Active enzyme was found in fractions 3 and 4. The third attempt for DHAE I resulted in protein being collected in fractions 3-23; however, the major fraction of protein eluted in fractions 3-6. Fractions 7 – 23 had a baseline protein concentration. Active fractions were obtained in fractions 4-23. The second attempt for DHAE II's affinity column gave protein in fractions 2-15. Active fractions were collected in fractions 4-15. The same pattern of protein elution was obtained here as in the third attempt of the DHAE I affinity column.

The specific activity of active fractions could not be calculated due to the presence of an overlapping peak in the HPLC spectrum.

Discussion of Results

There are several problems associated with the affinity columns generated for isolation of DHAE I and DHAE II. First, in order to keep the resin in the reduced state, sodium dithionite was added to all solutions applied to the column including the enzyme preparation. Sodium dithionite, at high concentrations, is an inhibitor of both enzymes and could potentially inhibit so well that no activity is seen in any fraction. For the first attempt at both columns, it is likely that the presence of sodium dithionite, compound **6**, and small amounts of ethanol caused rapid denaturation of each enzyme or inhibited each enzyme enough that no activity was detected.

For this reason, the affinity column for DHAE I (column 1) separation was attempted without sodium dithionite. All protein proceeds directly through the column and is collected in fractions 2-4. This suggests that the enzyme will not bind to the resin in the oxidized form and supports Shen's results. The last attempt at column 1 utilized the natural substrate in an attempt to elute DHAE I. Initially, it was believed that **1** would interfere with the detection of any activity or at least affect an accurate value for activity if detected. However, at this point, it is not necessary to get an accurate value for activity. We need only be able to detect which fractions have activity so that a gel can be run to determine purity.

Natural substrate was added to the column buffer after collecting twelve fractions. About three fractions later, the added substrate is detected as either the hydroquinone or the quinone in the enzymatic HPLC assay.

Small amounts of activity were observed in both the second and third attempts with the DHAE II affinity column (column 2) for isolation of DHAE II. It seems, however, that the column binds enzyme well. DHAE I trails off column 1

even in the presence of natural substrate (activity in fractions 5-17). The same phenomenon is observed in the second attempt of column 2; however, the activity is in fractions 4-15.

Electrophoresis (SDS-PAGE) was attempted to determine the purity of active fractions. Coomassie blue staining resulted in only several lanes showing bands, so the gel was de-stained and re-stained using a silver staining protocol. Most bands in the gel had several bands; indicating that this technique did not produce homogeneous enzyme.

Experimental:

For experimentals regarding cell growth, isolation, and enzyme purification using the DE-52 column see end of Chapter 2 – Experimental; pages 62-69.

Construction of the Standard Imidazole Concentration Curve

Aliquots of a 5 mM imidazole solution were created and the volume adjusted to 1 mL. 100 μL 1 M $NaHCO_3$ solution was added followed by 1 mL 0.02 M p-nitrobenzoyl chloride in acetone. The solutions turned yellow after addition of the acid chloride. This solution was allowed to stand for ten minutes before addition of 2 mL 1 M NaOH caused the color of the solution to turn to dark orange. These solutions were allowed to stand for thirty minutes before the absorbance was read at 465 nm. A calibration curve for imidazole concentration was created from this data.

Determination of Activation Level

A small sample of carbonyl di-imidazole activated agarose resin (Sigma) was vacuum filtered to give 106 mg of a white solid. This sample was added to a NaOH solution (0.15 M, 2 mL) and allowed to shake overnight. 2 mL additional NaOH solution was added and the mixture centrifuged. The supernatant was removed and the pH adjusted to 7 with 0.15 M HCl. Small samples of this solution were added to individual test tubes and diluted to 1 mL with dd H_2O. To this solution was added 100 μL 1 M $NaHCO_3$ solution followed by 1 mL 0.02 M p-nitrobenzoyl chloride solution in acetone. The solution turned yellow upon the addition of the last solution. This solution was allowed to stand for 10 minutes. 2 mL 1 M NaOH solution was added to this solution, the solution vortexed and

allowed to stand for thirty minutes before reading the absorbance at 465 nm. The imidazole concentration was determined by comparison to the standard curve.

Coupling of Ligand to Affinity Resin

A sample of the affinity resin was vacuum filtered to obtain approximately 4 g of a fluffy opaque white solid. This material was added to a helium-sparged phosphate buffer saline solution (pH 6.60, 0.02 M) followed by the desired ligand. The round bottom flask containing all three components was flushed with argon and a small pinch of sodium dithionite was added and the whole apparatus sealed with a septum. The solution was shaken at room temperature overnight before being poured into a column.

The affinity resin was washed with 25 mL portions of PBS, 1 M NaCl, and dd H_2O that contained 15 mg sodium dithionite. At this point, ~10 mL 0.3 M ethanolamine, pH 8.0, was added and the resin re-suspended by constantly inverting the column until all the resin was in solution. The column was again shaken, this time for four hours.

At this point, the resin was flushed with 70 mL 1 M NaCl containing 40 mg sodium dithionite. The resin was then stored in the cold room until needed.

Loading and Elution of Protein in Affinity Column

There were several conditions used for loading and elution of the enzyme from the column.

DHAE I

First attempt: (This procedure was also used for DHAE II's first attempt)

Enzyme solution (67 μg/mL, 6 mL) was added to the top of the resin along with sodium dithionite (20 mg) and the resin re-suspended in this solution. The column was capped and placed in a shaker and shaken in the cold room for 1 hour. At this point, the solution was allowed to flow by gravity. 30 fractions were collected of varying volumes. The first 20 fractions were eluted with a buffer solution (pH 7.0) containing 100 mM KP_i and 200 μM sodium dithionite. After collection of fraction 20, a solution of 400 μM of compound **7** (30% ethanol) was diluted with the buffer solution previously mentioned. 300 μL aliquots were taken for protein quantitation and to use in the enzymatic assay to determine activity.

Second attempt:

Enzyme solution (6 mL, 1310 μg/mL) was added directly to the top of the column and was allowed to flow under gravity until the protein solution entered the top of the resin. Buffer II was used to collect five fractions.

Third attempt:

Enzyme solution (6 mL, 1489 μg/mL) was added to the resin and the resin re-suspended and allowed to sit for 15 minutes. A pump was connected to the affinity column and set at 0.10 mL/min (not calibrated) and fractions were collected every eight minutes. At fraction 15, compound **1** was added to the buffer II solution. The sample did not dissolve completely. 300 μL aliquots were taken to test for activity and to determine protein concentration.

DHAE II Second Attempt:

Enzyme solution (8 mL, 1250 μg/mL) was added to the resin and the resin re-suspended and allowed to sit for 15 minutes. A pump was connected to the affinity column and set at 0.20 mL/min (not calibrated) and fractions were collected every five minutes. At fraction 15, a solution of compound **1** (10 mg) in 2 mL ethanol was added to 50 mL buffer II solution. 300 μL aliquots were taken to test for activity and to determine protein concentration.

Gel procedure

Standard SDS PAGE gels (15% acrylamide) were prepared and enzyme solutions were diluted to give approximately 500 ng protein mixture. 4X Loading dye was used. Gels were stained by microwave heating the gels with Coomassie blue reagent. Very few lines were observed so the gels were de-stained using standard procedures and a modified silver staining procedure was used.

Synthesis Section

4-bromo-2,5-dimethoxyphenyl-acetamide (**37**)

In an oven dried round bottom flask, 2,5-dimethoxyacetanilide (1.00 g, 5.10 mmol) was added to DMF (15 mL). To this stirred solution was added NBS (1.0 g, 5.60 mmol). The solution was stirred at room temperature open to the air for six hours. Water was added followed by CH_2Cl_2. The layers were separated and the organic layer evaporated to dryness in vacuo. The material was recrystallized from EtOH to afford light brown crystals (1.12 g, 80%). ^{1}H NMR ($CDCl_3$, 300 MHz): δ 8.22 (1H, s) δ 7.74 (1H, s xc), δ 7.03 (1H, s) δ 3.86 (3H, s), δ 3.83 (3H, s), δ 2.20 (3H, s) ^{13}C NMR ($CDCl_3$, 300 MHz): δ 168.7 150.5 142.3 128.1 115.3 105.1

104.3 57.2 56.8 25.4 IR: 3340 3132 2938 1669 HRMS: calculated: 273.00005 found: 237.00037

4-nitro-2,5-dimethoxyphenyl-acetamide

To an oven dried 100 mL round bottom flask was added: magnetic stir bar, 2,5-dimethoxyphenylacetamide (1.00 g, 5.12 mmol), followed by glacial acetic acid (50 mL). The reaction mixture was cooled to 5 °C with an ice bath. 70% Nitric acid (1.4 mL, 1.96 g, 31.1 mmol) was added dropwise over a ten minute period at which time the reaction mixture was allowed to come to room temperature. A bright yellow solid formed within five minutes. The precipitate was vacuum filtered and purified by running through a short plug of silica gel (0.96 g, 78%). ^{1}H NMR ($CDCl_3$, 300 MHz): δ 8.38 (1H, s) δ 8.04 (1H, s xc), δ 7.49 (1H, s) δ 3.91 (3H, s), δ 3.87 (3H, s), δ 2.22 (3H, s) ^{13}C NMR ($CDCl_3$, 300 MHz): δ 169.4 150.2 140.7 134.5 132.6 107.8 104.8 57.3 56.8 25.4 IR: 3364 2980 1702 1685 HRMS: calculated: 240.0746 found: 240.0746

4-acetylamino-2,5-dimethoxyaniline

A 100 mL oven dried round bottom flask containing 4-nitro-2,5-dimethoxyphenyl acetamide (0.500 g, mmol), 100% ethanol (40 mL), and 5% Pd/C (0.100 g) was placed inside a Parr hydrogenation bomb. Hydrogen was added to a final pressure of 50 atm. The reaction was allowed to stir overnight before releasing pressure and vacuum filtering solution. In vacuo removal of solvent afforded a dark brown solid (0.341 g, 78%). ^{1}H NMR ($CDCl_3$, 300 MHz): δ 7.94 (1H, s) δ 7.54 (1H, s xc), δ 6.32 (1H, s) δ 3.81 (3H, s), δ 3.77 (3H, s), δ 2.15 (3H, s) ^{13}C NMR ($CDCl_3$, 300MHz): δ 168.1 142.9 141.1 132.3 119.1 105.4 99.7 56.6 56.6 25.1 IR: 3421 3342 3227 2935 2832 1654 HRMS: calculated: 240.0746 found: 240.0746

6-bromo-N-(4-acetylamino-2,5-dimethoxyphenyl)-hexanamide

4-amino-2,5-dimethoxyphenyl acetamide (0.40 g, 1.9 mmol), CH_2Cl_2 (50 mL), and 4-dimethylaminopyridine (0.100 g, .21 mmol) were added to an oven dried 100 mL round bottom flask. A solution of 6-bromohexanoyl chloride (0.32 mL, 0.447 g, 2.09 mmol) and CH_2Cl_2 (10 mL) was added dropwise to the amine solution. The reaction was allowed to stir for two hours and was monitored for completion by TLC. Water was added to the reaction (50 mL) and the two layers were separated. The organic layer was washed with 5% $NaHCO_3$ (3 x 25 mL), 5% HCl (3 x 25 mL), brine (1 x 50 mL) and then dried over anhydrous $MgSO_4$. The drying agent was filtered and the solvent removed under vacuum to afford an off-white solid (0.54 g, 73%). ^1H NMR ($CDCl_3$, 300 MHz): δ 7.97 (1H, s), δ 7.95 (1H, s) δ 7.82 (1H, s), δ 7.80 (1H, bs), δ 3.73 (6H, s), δ 3.31 (2H, t, J = 7.5 Hz), δ 2.30 (2H, t, J = 7.4 Hz), δ 2.12 (3H, s), δ 1.79 (2H, m), δ 1.60 (2H, m), δ 1.41 (2H, m) ^{13}C NMR ($CDCl_3$, 300 MHz): δ 171.2 168.2 141.9 (2) 123.4 (2) 103.9 (2) 56.7 56.6 38.1 34.0 32.9 28.2 25.4 25.0 IR: 3244 3149 3047 2936 2864 1709 1654 HRMS: calculated: 563.0756 found: 563.0745

6-azido-N-(4-acetylamino-2,5-dimethoxyphenyl)-hexanamide

Bromide (2.50 g, 6.45 mmol), ethyl acetate (50 mL), water (50 mL), NaN_3 (2.10 g, 32.4 mmol), and tetrabutyl ammonium bromide (1.04 g, 3.23 mmol) were added to an oven dried 250 mL round bottom flask. The mixture was allowed to reflux overnight under a stream of Argon. The two layers were separated and the organic layer washed with water (2 x 50 mL). A grayish red solid was obtained upon removal of the organic solvent (1.34 g, 79%). ^1H NMR ($CDCl_3$, 300 MHz): δ 8.15 (1H, s), δ 8.12 (1H, s), δ 7.74 (2H, bs), δ 3.84 (6H, s), δ 3.26 (2H, t, J = 7.0 Hz), δ 2.38 (2H, t, J = 7.5 Hz), δ 2.17 (3H, s), δ 1.74 (2H, m), δ 1.63 (2H, m), δ 1.44 (2H, m) ^{13}C NMR ($CDCl_3$, 300 MHz): δ 171.2 168.6 141.7 (2) 123.4 (2)

103.6 103.5 56.7 56.6 51.6 38.0 29.1 26.7 25.3 (2) IR: 3246 2936 2094 1655 HRMS: calculated: 349.17499 found: 349.17500

6-amino-N-(4-acetylamino-2,5-dimethoxyphenyl)-hexanamide

To an oven dried 100 mL round bottom flask, the following items were added: azide (0.40 g, 1.15 mmol), 5% Pd/C (0.100 g), and ethanol (50 mL). The round bottom flask was added to a Parr hydrogenation bomb. The bomb was sealed and hydrogen gas was added to a final pressure of 50 atm. The reaction mixture was stirred for one hour before the pressure was released slowly. The reaction mixture was vacuum filtered and the solvent evaporated under vacuum. An off-white solid was obtained (0.27 g, 73%). ^{1}H NMR ($CDCl_3$, 300 MHz): δ 8.17 (1H, s) δ 8.13 (1H, s) δ 7.74 (2H, bs) δ 3.85 (6H, s) δ 2.71 (2H, t, J = 7.0 Hz) δ 2.39 (2H, t, J = 7.5 Hz) δ 2.18 (3H, s) δ 1.89 (2H, bs), δ 1.74 (2H, p, J = 7.4 Hz) δ 1.44 (4H, m) ^{13}C NMR ($CDCl_3$, 75 MHz): δ 171.5 168.5 141.7 (2) 123.4 123.3 103.5 (2) 56.7 56.6 42.3 38.2 33.6 26.8 25.7 25.3 IR: 3246 2936 1655 HRMS: calculated 323.18539 found 323.18451

6-trifluoroacetylamino-N-(4-acetylamino-2,5-dimethoxyphenyl)-hexanamide

To a solution of the amine (0.050 g, 0.16 mmol), ether (20 mL), and dichloromethane (10 mL) was added a solution containing ether (5 mL) and trifluoroacetic anhydride (1.0 mL, 1.48 g, 7.08 mmol). After allowing the reaction mixture to stir for thirty minutes at room temperature, solid NaHCO3 was added to the reaction. The reaction was heated for ten additional minutes. Water (10 mL) was added after allowing the reaction to cool. Separation of the layers and removal of the organic solvent gave a light pink solid (0.051 g, 79%) ^{1}H NMR ($CDCl_3$, 300 MHz): δ 8.16 (1H, s) δ 8.15 (1H, s) δ 7.74 (2H, bs) δ 3.86 (6H, s) δ 3.41 (2H, q, J = 6.6 Hz) δ 2.42 (2H, t, J = 7.0 Hz) δ 2.19 (3H, s) δ 1.68 (4H, m) δ 1.46 (2H, m)

^{13}C NMR ($CDCl_3$, 75 MHz): δ 171.2 168.5 141.7 123.5 123.3 103.6 103.5 56.7 56.6 39.7 37.5 28.6 26.2 25.3 24.4 ^{19}F NMR: δ –76.2 IR: 3246 2936 1655 HRMS: calculated 323.18539 found 323.18451

N-(2,5-dimethoxyphenyl)-4-[6-bromo-hexanoylamino]-benzamide

22 (8.00 g, 29.4 mmol), CH_2Cl_2 (100 mL), and triethylamine (4.3 mL, 3.12 g, 30.9 mmol) were added to an oven dried 500 mL round bottom flask. 6-bromohexanoyl chloride (4.6 mL, 6.21 g, 29.1 mmol) was added dropwise over a ten-minute period. The reaction was allowed to stir overnight. The organic layer was washed with 5% NaOH (3 x 25 mL), 5% HCl (3 x 25 mL), brine (1 x 50 mL) and then dried over anhydrous $MgSO_4$. The drying agent was filtered and the solvent removed under vacuum to afford a brown solid. Recrystallization from ethyl acetate gave a white solid (9.62 g, 74%), m.p. 146-147 °C. ^1H NMR ($CDCl_3$, 300 MHz): δ 8.56 (1H, bs) d 8.25 (1H, d, J = 3.0 Hz) d 7.85 (2H, d, J = 8.6 Hz) δ 7.72 (1H, bs), δ 7.67 (2H, d, J = 8.5 Hz) δ 6.84 (1H, d, J = 9.1 Hz) d 6.62 (1H, dd, J = 8.9, 3.2 Hz) δ 3.89 (3H, s), δ 3.81 (3H, s), δ 3.41 (2H, t, J = 6.7 Hz), δ 2.41 (2H, t, J = 7.6 Hz), δ 1.89 (2H, pentet, J = 7.5 Hz), δ 1.76 (2H, pentet, J = 7.7 Hz), δ 1.52 (2H, m) ^{13}C NMR ($CDCl_3$, 300 MHz): δ 171.7 165.0 154.3 142.8 141.7 130.7 128.8 128.5 119.7 111.1 109.2 106.4 56.7 56.2 37.8 34.0 32.8 28.1 24.9 IR: 3314 3002 2940 2842 1664 1645 1598 HRMS: calculated: 449.10749 found: 449.10759

N-(2,5-dimethoxyphenyl)-4-[6-azido-hexanoylamino]-benzamide

Bromide (5.00 g, 11.1 mmol), ethyl acetate (100 mL), water (50 mL), NaN_3 (1.67 g, 25.7 mmol), and tetrabutyl ammonium bromide (0.83 g, 2.57 mmol) were added to an oven dried 250 mL round bottom flask. The mixture was allowed to reflux overnight under a stream of Argon. The two layers were separated and the

organic layer washed with brine (2 x 50 mL) and dried over sodium sulfate. A white solid was obtained upon removal of the organic solvent (3.97 g, 86%), m.p. 99-101 °C. ^{1}H NMR ($CDCl_3$, 300 MHz): δ 8.57 (1H, bs), δ 8.56 (1H, bs), d 8.20 (1H, d, J = 3.2 Hz) d 7.81 (2H, d, J = 8.8 Hz) d 7.73 (2H, d, J = 8.8 Hz) d 6.82 (1H, d, J = 8.9 Hz), d 6.59 (1H, dd, J = 8.8, 3.0 Hz) δ 3.87 (3H, s) d 3.78 (3H, s) δ 3.24 (2H, t, J = 7.3 Hz), δ 2.42 (2H, t, J = 7.7 Hz) δ 1.73 (2H, m), δ 1.59 (2H, m), δ 1.41 (2H, m) ^{13}C NMR ($CDCl_3$, 300 MHz): δ 172.2 165.3 154.2 142.9 142.3 130.3 128.7 128.4 119.8 111.1 108.9 106.7 56.7 56.2 37.7 29.0 26.7 25.3 13.9 IR: 3432 3318 2184 2077 1800 1731 1704 1669 HRMS: calculated: 411.1907 found: 411.1900

N-(2,5-dimethoxyphenyl)-4-[6-amino-hexanoylamino]-benzamide

To an oven dried 100 mL round bottom flask, the following items were added: azide (3.49 g, 8.5 mmol), 5% Pd/C (0.550 g) and ethanol (50 mL). The round bottom flask was added to a Parr hydrogenation bomb. The bomb was sealed and hydrogen gas was added to a final pressure of 50 atm. The reaction mixture was stirred for one hour before the pressure was released slowly. The reaction mixture was vacuum filtered and the solvent evaporated under vacuum. A cream colored solid was obtained (3.22 g, 98%), m.p. 166-170 °C. ^{1}H NMR ($CDCl_3$, 300 MHz): δ 8.73 (1H, bs xc) δ 8.56 (1H, bs xc) δ 8.20 (d, 1H, J = 3.0 Hz) δ 7.81 (2H, m) δ 7.69 (2H, m) δ 6.80 (1H, d, J =8.9 Hz) δ 6.58 (1H, dd, J = 8.7, 3.0 Hz) δ 3.86 (3H, s) δ 3.77 (3H, s) δ 2.66 (2H, t, J=6.9 Hz) δ 2.36 (2H, t, J = 7.6 Hz), δ 1.70 (2H, p, J = 7.1 Hz) δ 1.40 (2H, m) ^{13}C NMR ($CDCl_3$, 75 MHz): δ 172.5 165.3 154.3 142.9 142.3 130.3 128.7 128.4 119.8 111.1 109.1 106.6 56.7 56.2 42.2 37.8 33.4 26.7 25.6 IR: 3545, 3421, 3349, 3307, 1701, 1690, 1598 HRMS: calculated 385.20016 found 385.19995

N-(2,5-dimethoxyphenyl)-4-[6-(2,2,2-trifluoro-acetylamino)-hexanoylamino]-benzamide

To a solution of the amine (0.500 g, 1.30 mmol) and triethylamine (0.5 mL) was added neat trifluoroacetic anhydride (3.0 mL, 4.46 g). The reaction was heated for thirty minutes at which time ether was added. A white precipitate forms and is collected by vacuum filtration. The product is isolated as a clean white solid (0.56 g, 89%), m.p. 172-173 °C. ^{1}H NMR ($CDCl_3$, 300 MHz): δ 9.40 (1H, bs xc) δ 8.77 (1H, bs xc) δ 8.46 (1H, bs xc), δ 8.17 (d, 1H, J = 3.0 Hz) δ 7.92 (2H, m) δ 7.81 (2H, m) δ 6.97 (1H, d, J =8.8 Hz) δ 6.63 (1H, dd, J = 8.7, 3.0 Hz) δ 3.90 (3H, s) δ 3.76 (3H, s) δ 3.34 (2H, q, J=6.6 Hz) δ 2.42 (2H, t, J = 7.6 Hz), δ 1.67 (4H, m) δ 1.42 (2H, m) ^{13}C NMR ($CDCl_3$, 75 MHz): δ 171.8 164.4 154.2 143.4 143.2 143.0 129.7 128.4 119.0 118.9 111.4 107.9 107.3 107.2 56.3 55.4 39.7 37.0 28.9 26.5 25.1 ^{19}F NMR: δ –75.0 IR: 3426 3337 3308 3089 2945 1724 1691 1653 1596 HRMS: calculated 481.1828 found 481.1825

N-(2,5-dihydroxyphenyl)-4-[6-(2,2,2-trifluoro-acetylamino)-hexanoylamino]-benzamide (**35**)

To an oven dried round bottom flask was added the dimethoxy compound (0.299 g, 0.62 mmol) in CH_2Cl_2. The round bottom flask flask was fitted with a septum, flushed with Argon, and cooled to –78 °C using a dry ice / acetone bath. BBr_3 (1.86 mL, 0.473 g, 1.86 mmol) was added. A white smoke was emitted with each drop of boron tribromide added. After complete addition of boron tribromide, the solution was allowed to come to room temperature and was again flushed with Argon. The solution was allowed to stir for 24 hours. At this time, the solution was poured over an ice bath (~20 mL). Compound could not be extracted into ethyl acetate, therefore vacuum filtration was performed and a fluffy white solid was obtained (0.150 g, 53%). ^{1}H NMR ($CDCl_3$, 300 MHz): d 9.46 (1H, s xc) d 9.38 (1H, s xc) δ 9.05 (1H, bs xc) δ 8.88 (1H, bs xc) δ 7.91 (d, 2H, J = 8.4 Hz) δ

7.74 (2H, d, J = 8.6 Hz) δ 7.27 (1H, d, J = 2.6 Hz) δ 6.72 (1H, d, J =8.8 Hz) δ 6.43 (1H, dd, J = 8.0, 3.0 Hz) δ 3.17 (2H, t, J = 6.3 Hz) d 3.86 (3H, s) δ 2.49 (1H, bs) δ 2.35 (2H, t, J=7.3 Hz) δ 1.55 (4H, m) δ 1.29 (2H, m) ^{13}C NMR ($CDCl_3$, 75 MHz): δ 172.6 165.4 157.3 156.8 150.8 143.3 141.8 129.2 129.1 127.4 119.2 117.5 112.5 110.8 39.9 37.1 28.9 26.7 25.4 HRMS: calculated 435.1391 found 435.1406

References:

1. Janson, J.-C.; Ryden, L. *Protein purification: principles, high-resolution methods, and applications* 2nd ed. New York : Wiley-Liss, **c1998.**

2. Bollag, D.M.; Rozycki, M.D.; Edelstein, S. J. *Protein methods* 2nd ed. New York : Wiley-Liss, **c1996**

3. Marshak, D. R. *Strategies for protein purification and characterization : a laboratory course manual* Plainview, N.Y. : Cold Spring Harbor Laboratory Press, **1996.**

4. Scopes, R. K. *Protein purification : principles and practice* 3rd ed. New York : Springer-Verlag, **c1994**
5. Ngo, T. T. *Molecular interactions in bioseparations* New York : Plenum Press, **c1993**

6. Wheelwright, S. M. *Protein purification : design and scale up of downstream processing* Munich ; New York : Hanser Publishers ; New York : **1991**

7. Ladisch, M. R. *Protein purification : from molecular mechanisms to large-scale processes* Washington, DC : American Chemical Society, **1990.**

8. Deutscher, M.P. *Guide to protein purification* San Diego : Academic Press, **c1990**

9. Harris, E. L. V.; Angal, S. *Protein purification applications: a practical approach* Oxford ; New York : IRL Press, **1990.**

10. Bostock, R.M.; Lee, Y-M.; Hammock, B.D.; Michailides, T.J.; Wang, G-Y. *Archives of Biochem. and Biophys.* **2000**, 382 (1), 31-38

11. Loog, M.; Uri, A.; Jarv, J.; Ek, P. *FEBS Letters* **2000**, 480, 244-248

12. Ibrahim, R.K.; Anzellotti, D. *Archives of Biochem. and Biophys.* **2000**, 382(2), 161-172

13. Margalet, V.; Alvarez, J. *Archives of Biochem. and Biophys.* **2000**, 378(1), 151-156

14. Gomicia, J. A.; Nuttall, S.D.; Deutschel, S. E.; Irving, R. A.; Dyall-Smith, M.L. *Biochem. J.* **2000**, 346, 251-254

15. Van Onckelen, H.; Slegers, H.; Witters, E.; Roef, L.; Laukens, K. *FEBS Letters* **2001**, 508, 75-79

16. De Michaelis, M. I.; Bonza, M. C.; Luoni, L. *FEBS Letters* **2000**, 482, 225-230

17. Wilson, K.; Walker, J. *Principles and Techniques of Practical Biochemistry*, Fifth Edition, Cambridge University Press, UK, **2000**

18. Shen, B. LL-C10037a and MM14201: *Structure, Biosynthesis, and Enzymology of two Epoxyquinone Antibiotics*. Thesis, Oregon State University, **1990**.

19. Kirchmeier, M.J. *Purification of 2,5-Dihydroxyacetanilide Epoxidase and Mechanism of Hydroquinone Epoxidases*. Thesis, Oregon State University, **1997**

20. Tietze, L.; Noebel, T.; Spescha, M. *J. Am. Chem. Soc.* **1998**, 120 (35), 8971-8977

21. Miyaura *J. Am. Chem. Soc.* **1989**, 111(1), 314-321

22. Ferrer, P.; Avendano, C.; Soolhuber, M. *Tetrahedron* **1997**, 53(9), 3231-3242

23. Jones, G. B.; Qabaja, G. *J. Org. Chem.* **2000**, 65(21), 7187-7194

24. Subramanian, A. *Molecular Biotechnology*, **2002**, 20, 41-47

Chapter 4

Conclusions
and
Ideas for Further Research

At the start of this research six years ago, much information had been obtained regarding both DHAE I and DHAE II.[1,2] Shen and Gould had outlined the biosynthetic pathway responsible for the production of the antibiotics produced by each strain of *Streptomyces* and identified DHAE I and DHAE II as enzymes requiring further study. The pH dependency, metal ion requirements, molecular weight, and basic kinetics for each enzyme were determined. A crude purification scheme was designed, but was costly and lengthy. Kirchmeier and Gould made some necessary modifications to the isolation scheme and were able to obtain N-terminal and partial internal amino acid sequences. However, the quantity of enzyme isolated prevented the application of this information to gene cloning for either enzyme. Kirchmeier also discovered a class of inhibitors for DHAE I and DHAE II that became critical to the desired research goals.

Despite the information gained, a purification procedure capable of generating larger quantities of enzyme was still needed. Pure enzyme is crucial to further exploration of the mechanism, metal ion requirements, cloning, and alternative substrate kinetics of DHAE I and DHAE II. So, this research began with these goals in mind: 1) identify inhibitors that bind at the micromolar level and in the process explore the function of the amide bond in substrate binding 2) attach inhibitors to affinity column to facilitate purification of each enzyme 3) design alternative substrates to support utility of DHAE I and DHAE II as reagents in organic synthesis.

What has this work accomplished?

The third element of molecular recognition as well as conformation of the amide bond required for catalytic activity has been determined. A strong linear relationship was obtained in the Hammett study with competitive inhibitors of DHAE I indicating the importance of electron density of the amide carbonyl on the

strength of inhibition and therefore on the strength of binding. The relationship of electron density on competitive inhibition in DHAE II was negated by the large amount of scatter in the Hammett plot indicating steric factors dominate the recognition interaction. It is possible that the same factors of molecular recognition are present in both enzymes; however, the substituted benzanilides were not the best probes for the DHAE II enzyme.

Having completed the identification of all three recognition elements for both enzymes, the utility of this information was tested by creating an affinity column. Due to the differences in substrate binding discovered by the Hammett study, it was necessary to synthesize two different ligands. The affinity columns generated for the isolation of each enzyme did not allow for clean separation. The conditions of the purification need to be optimized or an inhibitor needs to be designed without the hydroquinone moiety in order for this method to be effective.

The last aspect of research undertaken was to design and test alternative substrates with each enzyme. The last remaining question regarding the orientation of the substrate in the binding pocket was explored by creating a molecule with a restricted amide bond. Surprisingly, **33** was accepted as an alternative substrate suggesting that the conformation of the amide bond was similar to the conformation in **33**. This information will be useful in further alternative substrate studies.

Suggestions for Future Research

Purification represents the most significant challenge remaining in this research. No significant research will be accomplished without pure enzyme. Pure enzyme will allow for cloning[3-5] that in turn will allow for milligram quantities of enzyme. The mechanism of the reaction and metal ion requirements can be explored. Attempts at obtaining X-ray crystal data would be excellent support for

the conclusions drawn from this body of research. An X-ray crystal structure would also clarify the position of the active site amino acids and other key aspects of the recognition process. Mutants can then be created to further explore the mechanism of the reaction and flexibility of the active site.

Means of Exploring Epoxidation Mechanism

There are several questions still remaining about the mechanism of this enzymatic oxidation: 1) Is the metal ion involved in binding and activating dioxygen? 2) Does the enzyme operate under radical or two electron processes? 3) Which hydroxyl group of the substrate initiates the reaction?

To explore question one requires pure enzyme and an understanding of the three dimensional nature of the active site. Chan and Lin recently identified a photochemically labile protecting group for the hydroquinone system, although this structure would have to be modified before application to the mechanism of DHAE I or DHAE II (Figure 37).[7] The 2-thiol pyridine (PTOC) moiety would have to be tested at each hydroxyl group to determine if a one-electron process is occurring and at which hydroxyl group the radical center is preferred. However, to apply this system to the mechanism of DHAE I or DHAE II would require pure enzyme and the ability to accumulate fast, pre-steady state kinetics.

To explore the possibility of a two-electron process and to provide support for removal of a proton in the active site, the ability to determine which hydrogen is removed selectively needs to be addressed. By creating a structurally similar substrate that varies only in the functional group present in positions 2 and 5, we can begin to answer question 3. The simplest modification is replacement of the hydroxyl group with an amino group. The two possibilities are shown in Scheme 16.

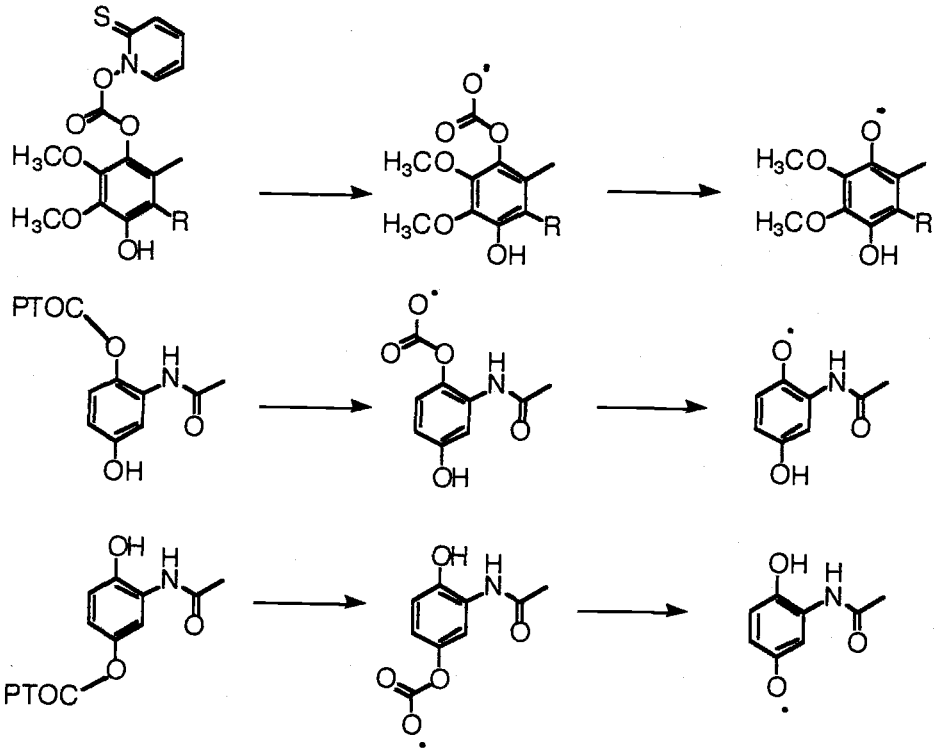

Figure 37: Formation of semiquinone to test one electron nature of mechanism and application to DHAE I / II

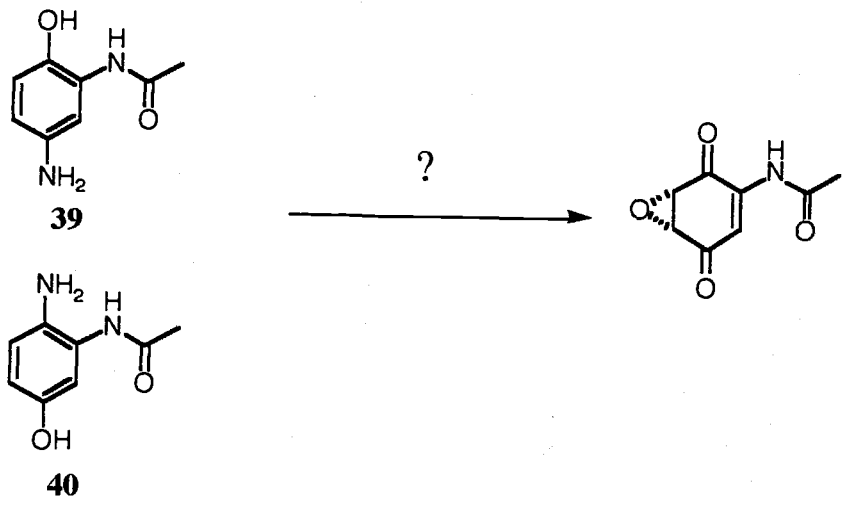

Scheme 18: Two variations on substrate structure useful in mechanistic studies

Two physical properties of the system change as a result of this modification. First, the pK_a of the amine N-H bond is approximately twelve orders of magnitude higher and therefore the N-H bond is not as easily broken as the phenol O-H bond. Second, p-aminophenols are more easily oxidized[6] than the hydroquinones. This may potentially result in product being formed more easily than in the hydroquinone system.

By testing **39** and **40** with both DHAE I and DHAE II, the position of the active site basic residue can be determined. Since the pK_a of the aniline hydrogen is significantly higher than the phenol hydrogen, it would be expected that the aniline hydrogen would not be removed when in the active site. Therefore, if the compound were to act as an inhibitor versus an alternative substrate, then we can conclude that the active site base is positioned near C-5 (or C-2). An example of the Dowd mechanism as it applies to the proposed inhibitor / alternative substrate shown above is again shown in Scheme 19. As you can see, the introduction of an amine in replacement of a hydroxyl group should not affect the enzymatic process.

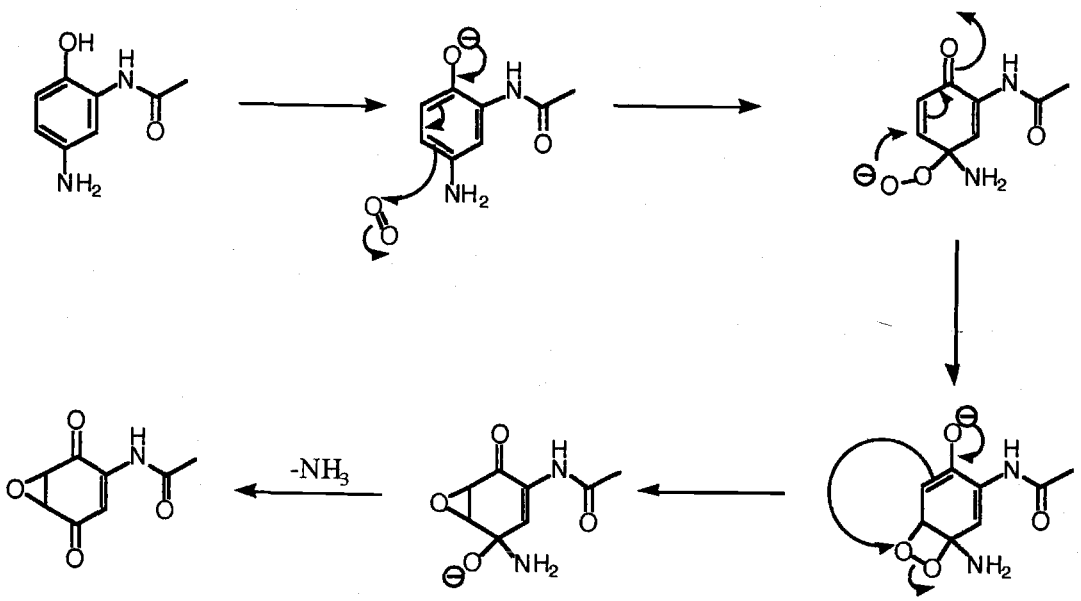

Scheme 19: Replacement of hydroxyl group on C-5 has no effect on mechanism

Synthesis of Mechanistic Substrates

The synthesis of **39** can be easily accomplished in three steps starting from commercially available 2-methoxy-5-nitro-aniline. Acetylation of the amine using acetyl chloride followed by reduction of the nitro group generates the methoxy protected aminophenol. The methyl ether can be removed using several different conditions (Scheme 20).[8-10]

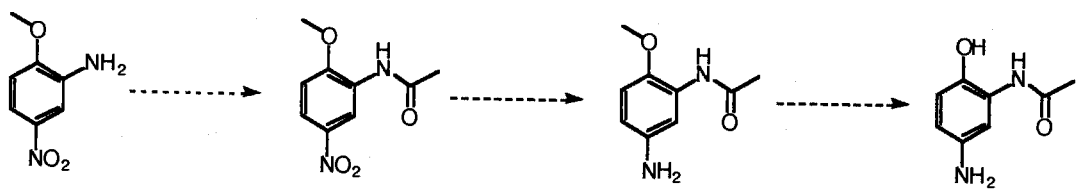

Scheme 20: Potential synthesis of 5-amino-2-hydroxyacetanilide (**39**)

The synthesis of **40** can be envisioned in four steps starting from 4-amino-2-nitroaniline. First, the amine and the alcohol would require protection. Numerous conditions exist for this transformation.[11,12] After reduction of the nitro and acetylation of the newly formed amino group, the aminophenol can be generated by removal of the protecting groups (Scheme 21).

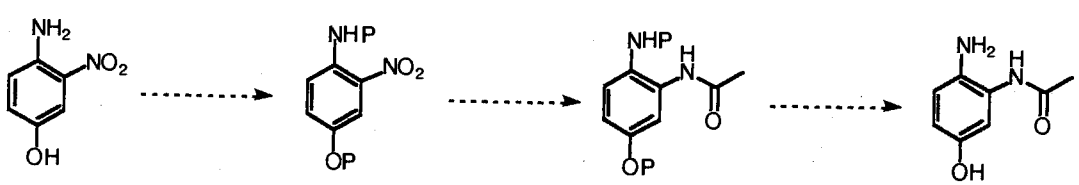

Scheme 21: Potential synthesis of 2-amino-5-hydroxyacetanilide (**40**)

Ideas for Affinity Column Ligands

Although the redox activity of the ligand has been used as a visual indicator of the oxidation state of the bound ligand, a simpler synthetic procedure needs to be developed. To facilitate this, additional inhibitors need to be discovered that do not contain the hydroquinone moeity. By replacing at least one hydroxyl group in **35** or **36**, a more stable, less easily oxidized ligand for the affinity column has been created.

The simplest possible modification would be to replace the hydroxyl group with a hydroxymethyl group. The advantage of this change is that it still retains the hydrogen bond donor recognition element. The disadvantage is the introduction of a sterically larger group that may potentially destroy the inhibitory activity. Other potential ideas and their possible synthesis are shown in Figures 38 and Schemes 22 and 23.

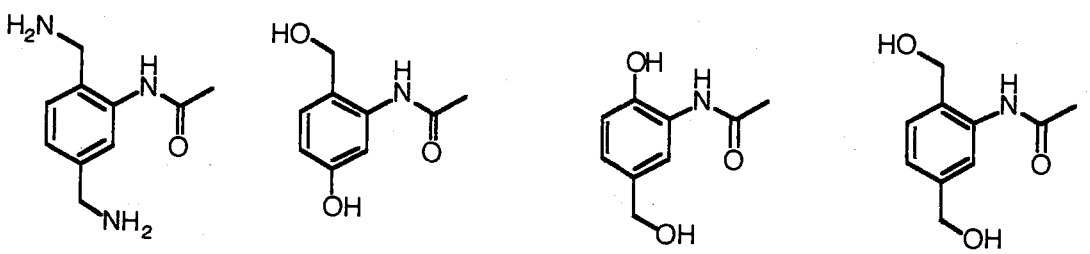

41 **42** **43** **44**

Figure 38: Potential models for second generation affinity ligands

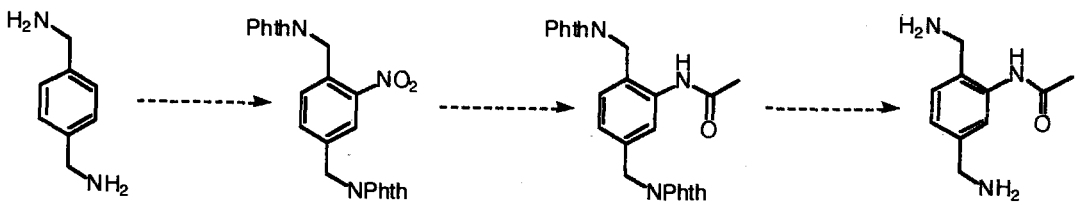

Scheme 22: Potential synthesis of 2,5-bis-aminomethyl-acetanilide (**41**)

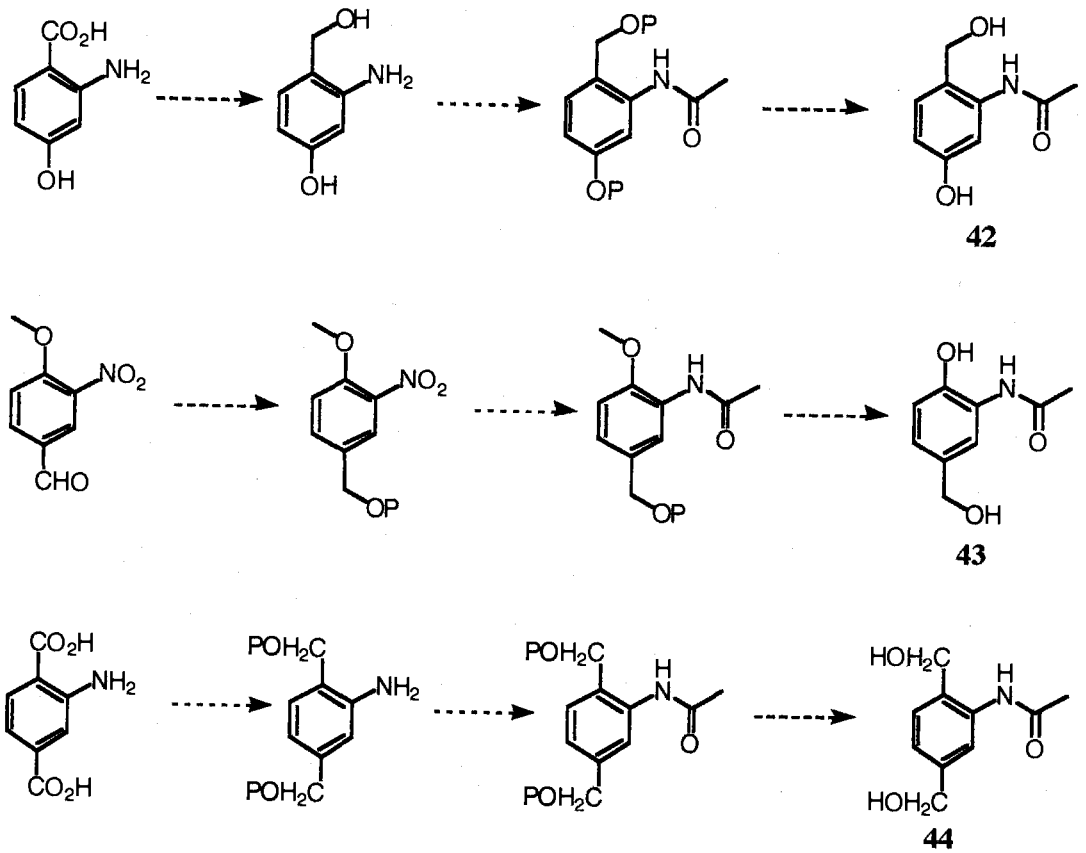

Scheme 23: Potential synthesis of compounds **42-44**

References

1. Shen, B. *LL-C10037a and MM14201: Structure, Biosynthesis, and Enzymology of two Epoxyquinone Antibiotics*. Thesis, Oregon State University, **1990**.

2. Kirchmeier, M. J. *Purification of 2,5-dihydroxyacetanilide Epoxidase and Mechanism of Hydroquinone Epoxidases* Ph.D. Thesis, Oregon State University **1997**

3. Brown, T. A. *Gene cloning and DNA analysis: an introduction* Oxford University Press, Malden, MA c2001

4. Drlica, K. *Understanding DNA and gene cloning: a guide for the curious* Wiley **c1997**

5. Hyone-Myong, E. *Enzymology primer for recombinant DNA technology* Academic Press, San Diego **c1996**

6. Tomilov, A. P. *Electrochemistry of organic compounds* Halsted Press, NY **c1972**

7. Chan, S. I.; Lin, C. C.; Hansen, K. C.; Schultz, B. E. *J. Org. Chem.* **2000**, 65, 3244-3247

8. Bhatt, M. V.; Kulkarni, S. U. *Synthesis* **1983**, 249

9. McOmie, J. F. W.; Watts, M. L.; West, D. E. *Tetrahedron* **1968**, 24, 2289

10. Jung, M. E.; Lyster, M. A. *J. Org. Chem.* **1977**, 42, 3761

11. Sundberg, R. J.; Carey, F. A. *Advanced Organic Chemistry, Part A* Fourth Edition, Kluwer Academic, New York, **c2000**

12. Bodansky, M. *The practice of peptide synthesis* Springer – Verlag, New York **c1994**

BIBLIOGRAPHY

Armstrong, R. N.; Bernat, B. A.; Svennson, R.; Morgenstern, R. *Biochemistry*, **2001**, 40, 3378 – 3384

Alcaraz, L.; Macdonald, G.; Ragot, J.; Lewis, N. J.; Taylor, R. J. K. *Tetrahedron* **1999,** 55(12), 3707 – 3716

Balzani, V.; Credi, A.; Raymo, F.M.; Stoddart, J.F. *Angew. Chem. Int. Ed.* **2000**, 39, 3348-3391

Beer, P.D.; Gale, P.A. *Angew. Chem. Int. Ed.* **2001**, 40, 486-516

Behr, J-P *The Lock and Key Principle Perspectives in Supramolecular Chemistry Vol. 1* Wiley and Sons **1994** 1-24

Bhatt, M. V.; Kulkarni, S. U. *Synthesis* **1983**, 249

Block, O.; Klein, G.; Altenbach, H.; Brauer, D. *J. Org. Chem.* **2000**, 65(3), 716-721

Blundell, T.; White, H. E.; Emsley, J.; Wood, S. P.; Dhanaraj, V.; Rufino, S.; Guruprasad, K.; Srinivasan, N.; Sowdhamini, R. *Pharm. Acta. Helv.* **1995**, 69, 185-192.

Bodansky, M. *The practice of peptide synthesis* Springer – Verlag, New York **c1994**

Boll, M.; Mobitz, H. *Biochemistry* **2002**, 41, 1752 – 1758

Bollag, D.M.; Rozycki, M.D.; Edelstein, S. J. *Protein methods* 2nd ed. New York : Wiley-Liss, **c1996**

Bostock, R.M.; Lee, Y-M.; Hammock, B.D.; Michailides, T.J.; Wang, G-Y. *Archives of Biochem. and Biophys.* **2000**, 382 (1), 31-38

Box, S. J.; Gilpin, M. L.; Gwynn, M.; Hanscomb, G.; Spear, S. R.; Brown, A. G. *J. Antibiot.* **1983** 36 1631

Brown, T. A. *Gene cloning and DNA analysis: an introduction* Oxford University Press, Malden, MA **c2001**

Carpenter, B. K. *Determination of organic reaction mechanisms* New York: Wiley, **1984**.

Chang, C-H.; Duke, J. L.; McCabe, D. D.; Weber, P. C.; Lewandowski, F. A.; Schadt, M. C.; Hodge, C. N.; Eyermann, C. J.; Lam, P. Y. S.; Jadhav, P. K.; Huston, E. E.; Deloskey, R. J.; Ala, P. J. *J. Biol. Chem.* **1998**, 273 (20), 12325 – 12331

Chan, S. I.; Lin, C. C.; Hansen, K. C.; Schultz, B. E. *J. Org. Chem.* **2000**, 65, 3244-3247

Chapman, N. B.; *Advances in linear free energy relationships* London, New York, Plenum Press **1972**

Conje Grove, J. J. ; Wei, X.; Taylor, R. J. K. *Chem. Comm.* **1999,** 5, 421 – 422

Cramer, F. *Angew. Chem.* **1952**, 64, 437

Dean, P. D. G.; Johnson, W. S.; Middle, F. A. *Affinity chromatography : a practical approach* IRL Press **1985**

Delaage, M. *Molecular Recognition Mechanisms* VCH Publishers **1991** 1-14

Delaage, M. *Molecular Recognition Mechanisms* VCH Publishers **1991** 219-238

De Michaelis, M. I.; Bonza, M. C.; Luoni, L. *FEBS Letters* **2000**, 482, 225-230

Deutscher, M.P. *Guide to protein purification* San Diego : Academic Press, **c1990**

Dodziuk, H. *Introduction to Supramolecular Chemistry* Kluwer Academic Publishers **2002** 1-58

Dowd, P.; Ham, S-K.; Hershline, R. *J. Am. Chem. Soc.* **1992**, 114 (23), 7613 – 7617

Dowd, P.; Ham, S-K.; Geib, S. J. *J. Am. Chem. Soc.* **1991**, 113, 7734 – 7743

Drlica, K. *Understanding DNA and gene cloning: a guide for the curious* Wiley **c1997**

Eliseev, A. V.; Rudra, S. *J. Am. Chem. Soc.* **1998**, 120 (45), 11543-11547

Feiters, M. C.; Rowan, A. E.; Nolte, R. J. M. *Chem. Soc. Rev.*, **2000**, 29, 375-384

Ferrer, P.; Avendano, C.; Soolhuber, M. *Tetrahedron* **1997**, 53(9), 3231-3242

Fischer, E. *Chem. Ber.* **1894** 27 2985

Gomicia, J. A.; Nuttall, S.D.; Deutschel, S. E.; Irving, R. A.; Dyall-Smith, M.L. *Biochem. J.* **2000**, 346, 251-254

Gokel, G. W.; Abel, E.; Suzuki, I.; Murillo, O. *J. Am. Chem. Soc.* **1996**, 118, 7628-7629

Gordon, J. I.; Sikorski, J. A.; Getman, D. P.; Devadas, B.; Brown, D. L.; Freeman, S. K.; Zupec, M. E.; Rocque, W. J.; McWherter, C. A. *J. Biol. Chem.* **1997**, 272 (1), 11874 – 11880

Hammett, L. P. *Physical organic chemistry; reaction rates, equilibria, and mechanisms* New York, McGraw-Hill **1970**

Han, M.; Hara, M. *Proc. Natl. Acad. Sci. USA* **1995**, 92, 3333-3337

Harris, E. L. V.; Angal, S. *Protein purification applications: a practical approach* Oxford ; New York : IRL Press, **1990**.

Harris, E. M. S.; Aleshin, A. E.; Firsov, L. M.; Honzatko, R. B. *J. Biol. Chem.* **1994**, 269, 15631-15639

Hyone-Myong, E. *Enzymology primer for recombinant DNA technology* Academic Press, San Diego **c1996**

Ibrahim, R.K.; Anzellotti, D. *Archives of Biochem. and Biophys.* **2000**, 382(2), 161-172

Jansen, J. F. G. A.; Meijer, E. W. *J. Am. Chem. Soc.* **1995**, 117, 4417

Janson, J.-C.; Ryden, L. *Protein purification: principles, high-resolution methods, and applications* 2nd ed. New York : Wiley-Liss, **c1998**.

Johnson, C. D. *The Hammett equation* Cambridge ; New York : Cambridge University Press, **1980**

Johnson, C. R.; Miller, M. W. *J. Org. Chem.* **1995**, 60, 6674 – 6675

Johnson, W. W.; Clement, R. P.; Casciano, C. N.; Barecki, M.; Lew, K.; Wang, E. *Chem. Res. Toxicol.* **2001**, 14, 1596-1603

Jones, G. B.; Qabaja, G. *J. Org. Chem.* **2000**, 65(21), 7187-7194

Jung, M. E.; Lyster, M. A. *J. Org. Chem.* **1977**, 42, 3761

Kaifer, A. E.; *Acc. Chem. Res.* **1999**, 32 (1), 62-71

Kapfer, I.; Lewis, N. J.; Macdonald, G.; Taylor, R. J. K. *Tetrahedron Lett.* **1996**, 37 (12), 2101 – 2104

Keillor, J. W.; Roupioz, Y.; Rivard, C.; Lherbet, C.; Castonguay, R.; Menard, A. *Biochemistry* **2001**, 40, 12678-12685

Khosla, C.; Cane, D. E.; Kudo, F.; Wu, N. *J. Am. Chem. Soc.* **2000**, 122 (20), 4847-4852

Kim, J-J. P.; Dahms, N. M.; Weix, D. J.; Roberts, D. L. *Cell* **1998**, 93, 639-648

Kimura, E. *Acc. Chem. Res.* **2001**, 34, 171-179

Kirchmeier, M.J. *Purification of 2,5-dihydroxyacetanilide Epoxidase and Mechanism of Hydroquinone Epoxidases.* Thesis, Oregon State University, **1997**

Kohno, J.; Nishio, M.; Kawano, K.; Nakanishi, N.; Suzuki, S.-I.; Uchida, T.; Komatsubara, S. J. *J. Antibiot.*, **1996**, 49, 1212

Konig, B.; Reichenbach-Klinke, R. *J. Chem. Soc., Dalton Trans.* **2002**, 121-130

Koshland, D. E. Jr.; *Proc. Natl. Acad. Sci.* USA **1958**, 44, 9

Koshland, D. E. Jr.; *Angew. Chem.* **1994**, 106, 2468

Kuramitsu, S.; Hirotsu, K.; Kawaguchi, S.; Nakai, T.; Ishijima, *J. Biol. Chem.* **2000**, 275 (25), 18939-18945

Ladisch, M. R. *Protein purification : from molecular mechanisms to large-scale processes* Washington, DC : American Chemical Society, **1990**.

Lee, M.D.; Fantini, A. A.; Morton, G. O.; James, J. C.; Borders, D. B.; Testa, R. T. *J. Antibiot.* **1984**, 37, 1149

Loog, M.; Uri, A.; Jarv, J.; Ek, P. *FEBS Letters* **2000**, 480, 244-248

Margalet, V.; Alvarez, J. *Archives of Biochem. and Biophys.* **2000**, 378(1), 151-156

Marshak, D. R. *Strategies for protein purification and characterization : a laboratory course manual* Plainview, N.Y. : Cold Spring Harbor Laboratory Press, **1996**

Massey, V.; Ballou, D. P.; Entsch, B.; Moran, G. R.; Palfey, B. A. *Biochemistry* **1999**, 38 (4), 1153-1158.

Matile, S., *Chem. Soc. Rev.* **2001**, 30, 158-167

Mattei, P.; Diedrich, F. *Helv. Chim. Acta* **1997**, 80, 1555

McOmie, J. F. W.; Watts, M. L.; West, D. E. *Tetrahedron* **1968**, 24, 2289

Meijer, E.W.; Baars, M. W. P. L. *Topics in Current Chemistry*, **2000**, 210, 131-182

Mohr, P.; Pommerening, K. *Affinity chromatography* M. Dekker **1985**

Miyaura *J. Am. Chem. Soc.* **1989**, 111(1), 314-321

Nakagawa, K.; Manabe, Y.; Osaki, M.; Yo, E.; Tominaga, M. *Chem. Pharm. Bull.* **1981**, 29(8), 2161 – 2165

Ngo, T. T. *Molecular interactions in bioseparations* New York : Plenum Press, **c1993**

Nolan, K.; Diamond, D. *Anal. Chem.* **2001**, 23A – 29A

Ogoshi, H.; Hayashi, T.; Asai, T.; Borgmeier, F. M.; Hokazono, H. *Chem. Eur. J.* **1998**, 4(7), 1266-1274

Ohkata, K.; Kojima, S.; Hiraga, Y.; Kanosue, Y. *Chem. Letters* **2001**, 418-9

Pedersen, C. J. *J. Am. Chem. Soc.* **1967**, 89, 7017

Penning, T. M. *J. Ster. Biochem. and Molec. Biol.* **1999**, 69, 211-225
Peters, T.; Biet, T. *Angew. Chem. Int. Ed.* **2001**, 40 (22), 4189-4192

Quinn, D. M.; Hui, D. Y.; Baker, N.; Lee, K.; Feaster, S. R. *Biochemistry*, **1996**, 35, 16723-16734

Ramaraj, R.; Rajagopal, S.; Ganesan, M. *J. Org. Chem.* **2002**, 67, 1506 – 1514

Rebek, J.; Renslo, A.R. *Angew. Chem. Int. Ed.* **2000**, 39 (18), 3281-3283

Reinhoudt, D. N.; Verboom, W.; Heida, J. F.; van Loon, J.-D. *Rec. Trav. Chim. Pays-Bas* **1992**, 111, 353

Richey Jr., H. G.; Maclin, K. M. *J. Org. Chem.* **2002**, 67, 4370 – 4371

R. H. C.; *J. Chem. Soc., Perkins I* **1981**, 2574 – 2576

Roberts, S.M.; Legon, A.C.; Buckingham, A. D. *Principles of Molecular Recognition* Blackie Academic and Professional **1993** 1-17

Roberts, S.M. *Molecular Recognition: Chemical and Biochemical Problems II* Royal Society of Chemistry **1992** 1-20

Rudkevich, D.M. *Chem. Eur. J.* **2000**, 6(15), 2679-2685

Sattler, I.; Thiericke, R.; Zeeck, A. *Nat. Prod. Rep.* **1998** 221-240

Scopes, R. K. *Protein purification : principles and practice* 3rd ed. New York : Springer-Verlag, **c1994**

Scouten, W. H.; *Affinity chromatography* New York : Wiley, **1981**.

Segel, I. *Enzyme Kinetics* John Wiley and Sons, Inc. **1975** Chapters 1-4

Shen, B. *LL-C10037a and MM14201: Structure, Biosynthesis, and Enzymology of two Epoxyquinone Antibiotics.* Ph.D. Thesis, Oregon State University, **1990**.

Sierks, M. R.; Svensson, B. *Biochemistry* **2000**, 39, 8585-8592

Subramanian, A. *Molecular Biotechnology*, **2002**, 20, 41-47

Sundberg, R. J.; Carey, F. A. *Advanced Organic Chemistry, Part A* Fourth Edition, Kluwer Academic, New York, **c2000**

Teague, S. J.; Davis, A. M. *Angew. Chem. Int. Ed.* **1999**, 38, 736-749

Tietze, L.; Noebel, T.; Spescha, M. *J. Am. Chem. Soc.* **1998**, 120 (35), 8971-8977

Tomilov, A. P. *Electrochemistry of organic compounds* Halsted Press, NY **c1972**

Tsou, C-L *Annals of N.Y. Acad. Sci.* **1998**, 864, 1-8

Van Onckelen, H.; Slegers, H.; Witters, E.; Roef, L.; Laukens, K. *FEBS Letters* **2001**, 508, 75-79

Waldemar, A.; Hamdullah, K.; Chantu R., S-M. *Synlett* **2002,** 3, 510-512

Wheelwright, S. M. *Protein purification : design and scale up of downstream processing* Munich ; New York : Hanser Publishers ; New York : **1991**

Whittaker, J. W.; Whittaker, M. M. *Biochemistry* **2001**, 40, 7140 – 7148

Williams, K. M.; Marshall, T. *J. Biochem. Biophys. Meth.* **1993**, 26(2-3), 237

Wilson, K.; Walker, J. *Principles and Techniques of Practical Biochemistry*, Fifth Edition, Cambridge University Press, UK, **2000**

Wipf, P.; Coish, P. D. G. *J. Org. Chem.* **1999,** 64(14), 5053 – 5061

Wong, C-Y.; Koeller, K. M. *Nature* **2001**, 409, 232 – 240

Wong, C-H. *Pure Appl. Chem.* **1997**, 69 (3), 419-422

APPENDICES

Appendix I

Kinetic Graphs for Competitive Inhibitors of DHAE I and DHAE II

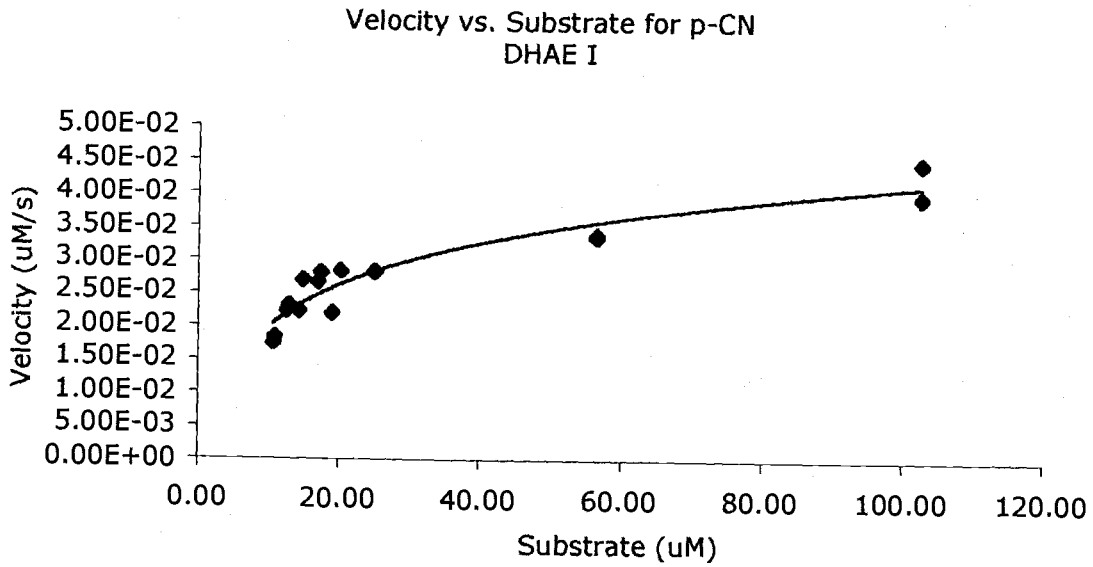
Velocity vs. Substrate for p-CN
DHAE I
Velocity (uM/s)
5.00E-02
4.50E-02
4.00E-02
3.50E-02
3.00E-02
2.50E-02
2.00E-02
1.50E-02
1.00E-02
5.00E-03
0.00E+00
0.00
20.00
40.00
60.00
80.00
100.00
120.00
Substrate (uM)

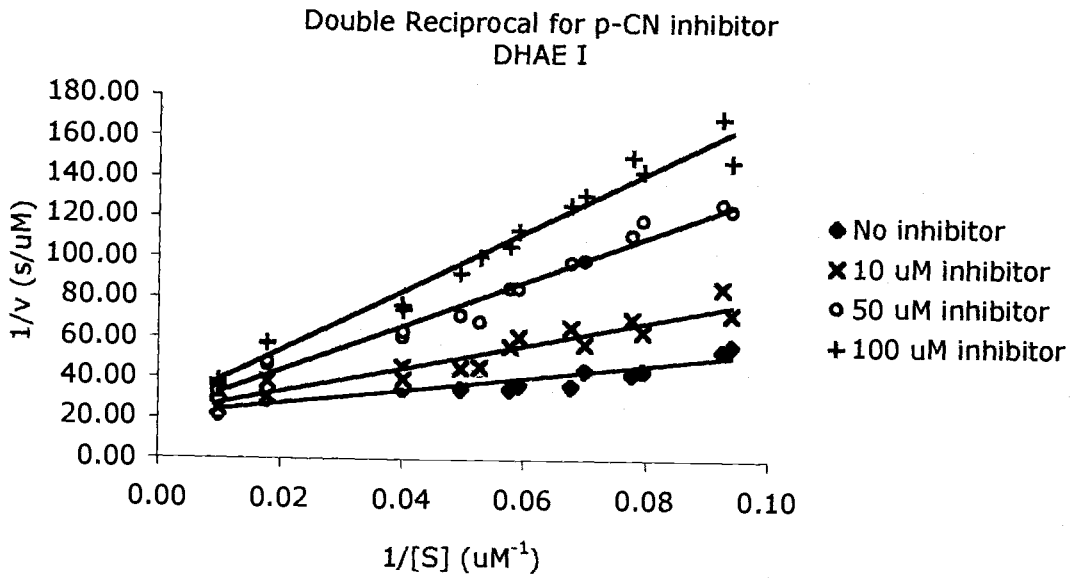
Double Reciprocal for p-CN inhibitor
DHAE I
1/v (s/uM)
180.00
160.00
140.00
120.00
100.00
80.00
60.00
40.00
20.00
0.00
0.00
0.02
0.04
0.06
0.08
0.10
1/[S] (uM-1)
No inhibitor
10 uM inhibitor
50 uM inhibitor
100 uM inhibitor

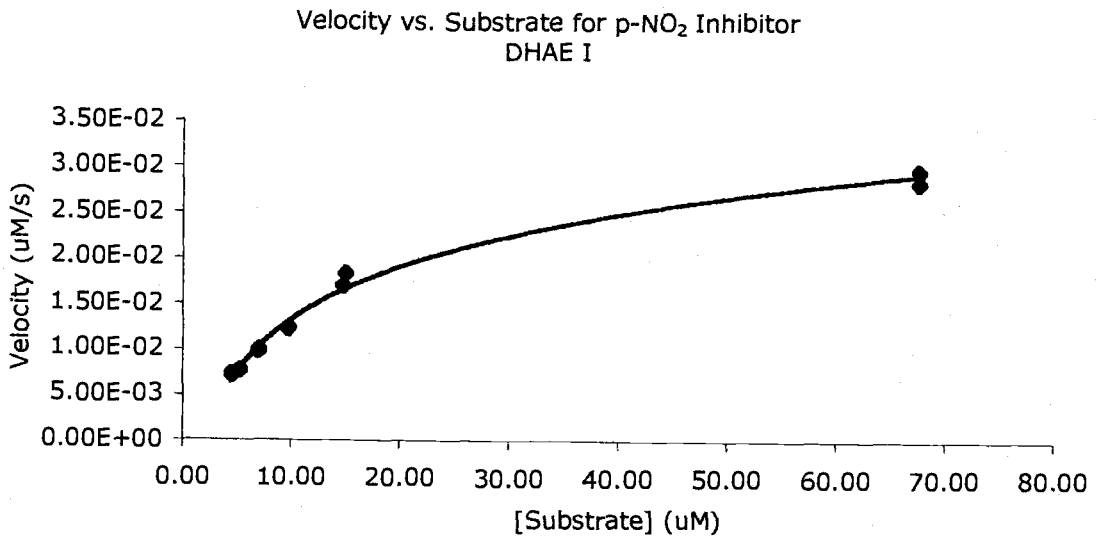
Velocity vs. Substrate for p-NO2 Inhibitor
DHAE I
Velocity (uM/s)
3.50E-02
3.00E-02
2.50E-02
2.00E-02
1.50E-02
1.00E-02
5.00E-03
0.00E+00
0.00
10.00
20.00
30.00
40.00
50.00
60.00
70.00
80.00
[Substrate] (uM)

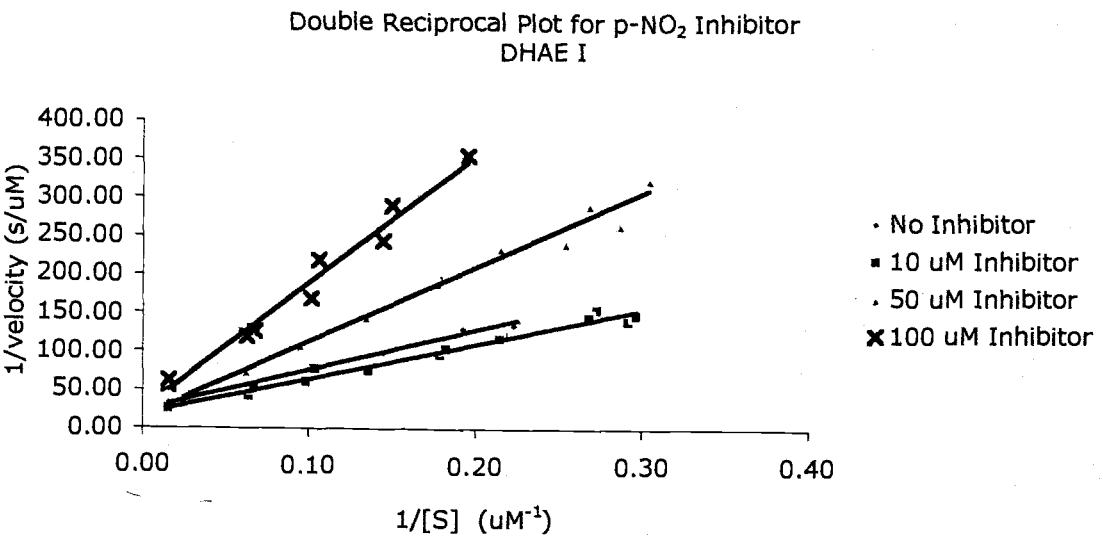
Double Reciprocal Plot for p-NO2 Inhibitor
DHAE I
1/velocity (s/uM)
400.00
350.00
300.00
250.00
200.00
150.00
100.00
50.00
0.00
0.00
0.10
0.20
0.30
0.40
1/[S] (uM-1)
No Inhibitor
10 uM Inhibitor
50 uM Inhibitor
100 uM Inhibitor

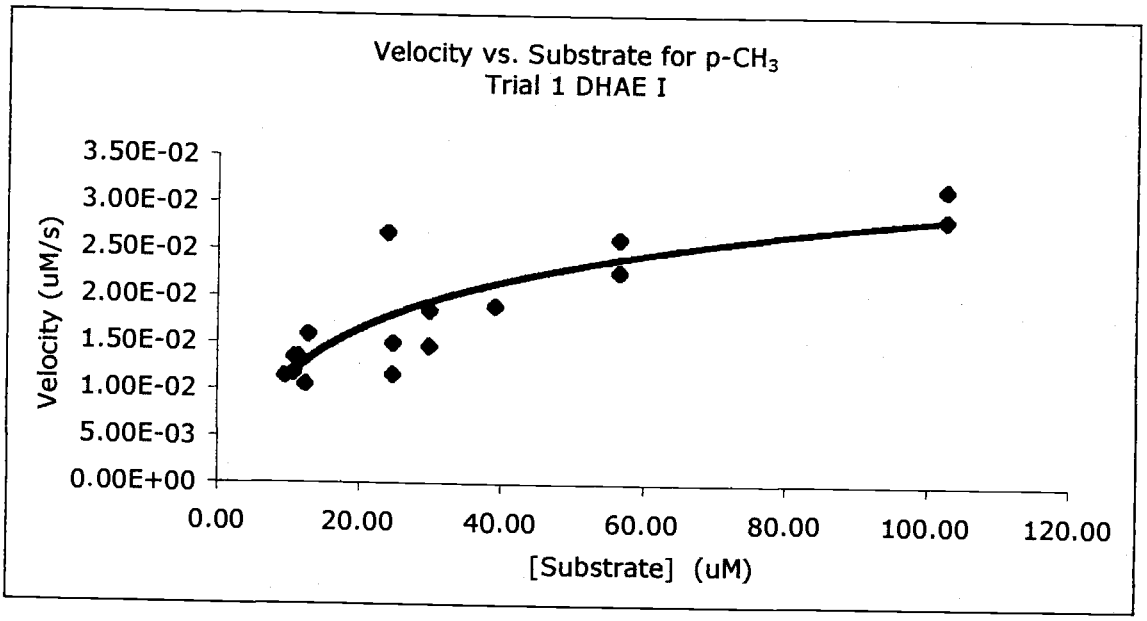
Velocity vs. Substrate for p-CH3
Trial 1 DHAE I
Velocity (uM/s)
3.50E-02
3.00E-02
2.50E-02
2.00E-02
1.50E-02
1.00E-02
5.00E-03
0.00E+00
0.00
20.00
40.00
60.00
80.00
100.00
120.00
[Substrate] (uM)

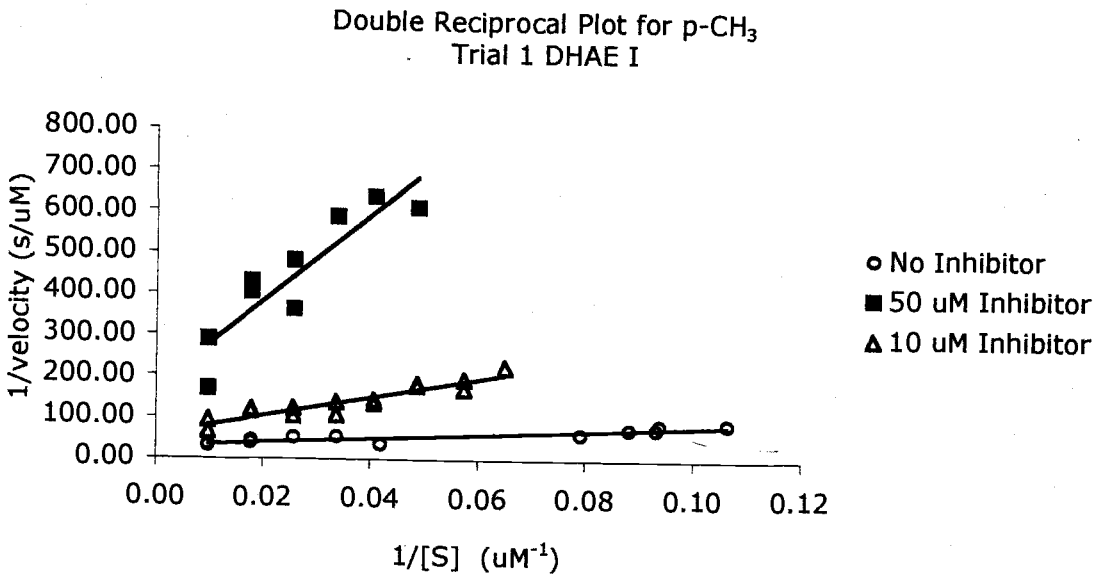
Double Reciprocal Plot for p-CH3
Trial 1 DHAE I
1/velocity (s/uM)
800.00
700.00
600.00
500.00
400.00
300.00
200.00
100.00
0.00
0.00
0.02
0.04
0.06
0.08
0.10
0.12
1/[S] (uM-1)
No Inhibitor
50 uM Inhibitor
10 uM Inhibitor

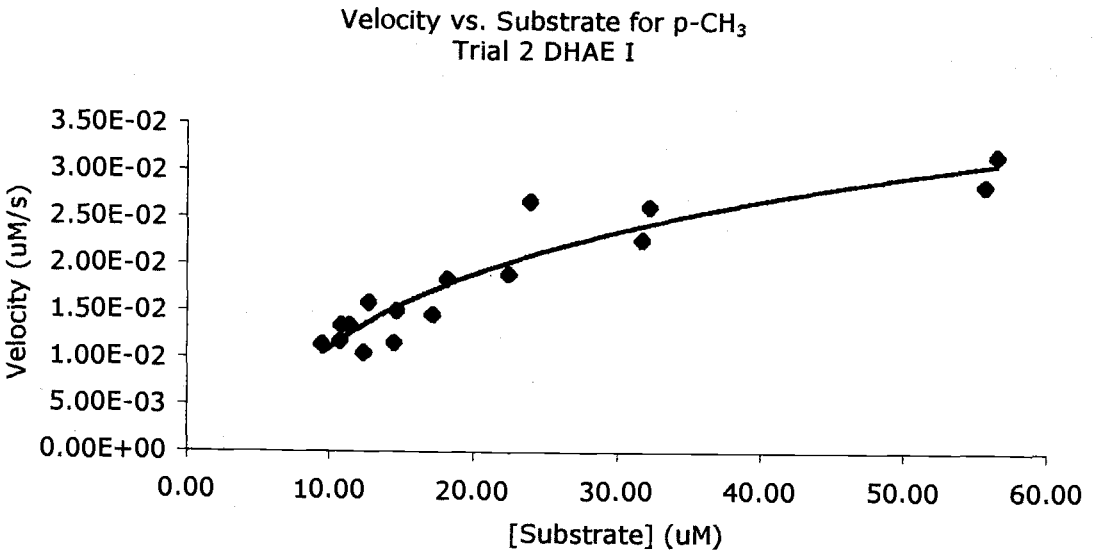
Velocity vs. Substrate for p-CH3
Trial 2 DHAE I
Velocity (uM/s)
3.50E-02
3.00E-02
2.50E-02
2.00E-02
1.50E-02
1.00E-02
5.00E-03
0.00E+00
0.00
10.00
20.00
30.00
40.00
50.00
60.00
[Substrate] (uM)

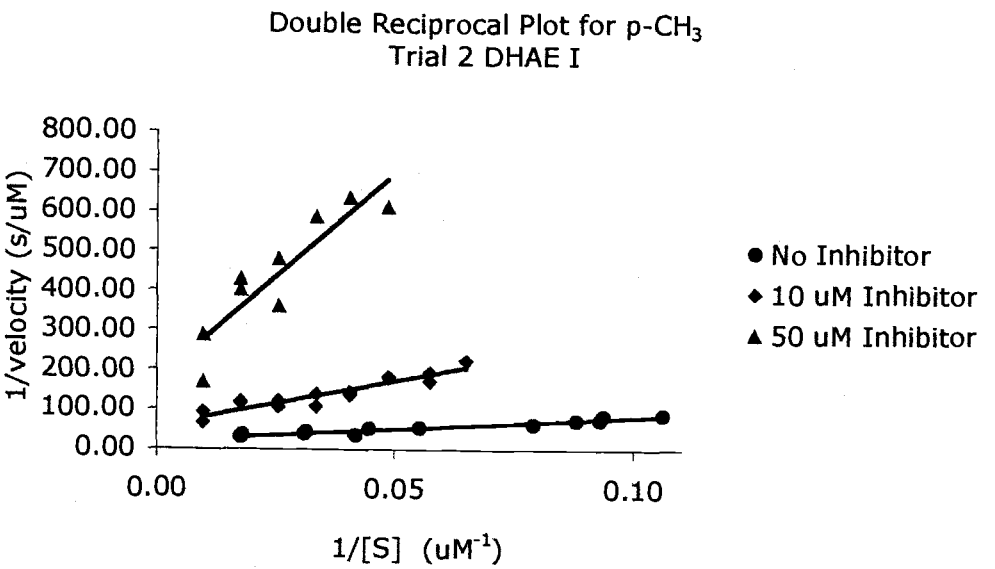
Double Reciprocal Plot for p-CH3
Trial 2 DHAE I
1/velocity (s/uM)
800.00
700.00
600.00
500.00
400.00
300.00
200.00
100.00
0.00
0.00
0.05
0.10
1/[S] (uM-1)
No Inhibitor
10 uM Inhibitor
50 uM Inhibitor

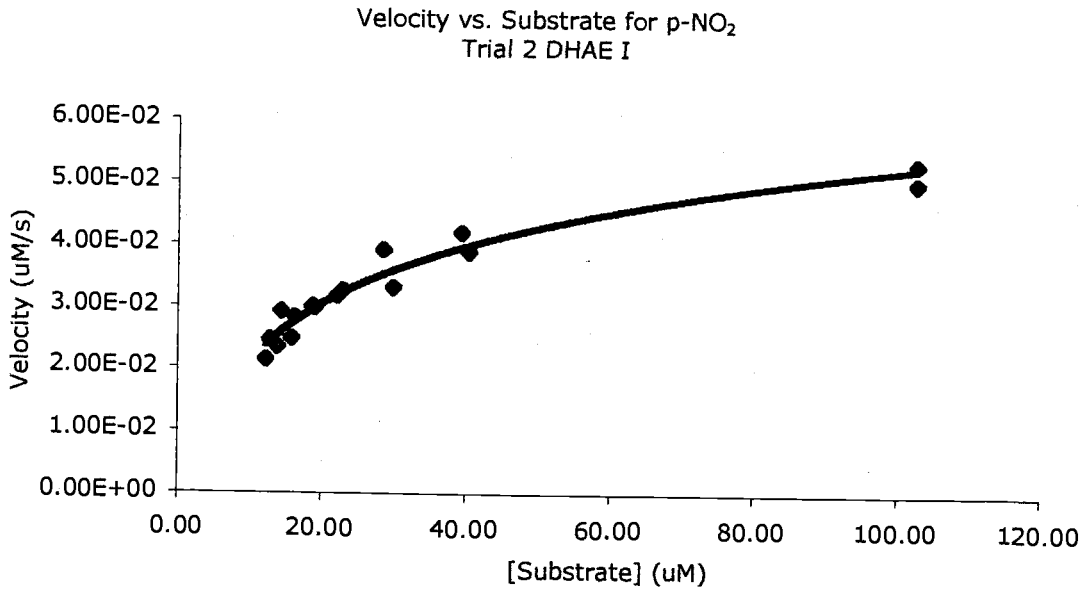
Velocity vs. Substrate for p-NO2
Trial 2 DHAE I
6.00E-02
5.00E-02
4.00E-02
3.00E-02
2.00E-02
1.00E-02
0.00E+00
Velocity (uM/s)
0.00
20.00
40.00
60.00
80.00
100.00
120.00
[Substrate] (uM)

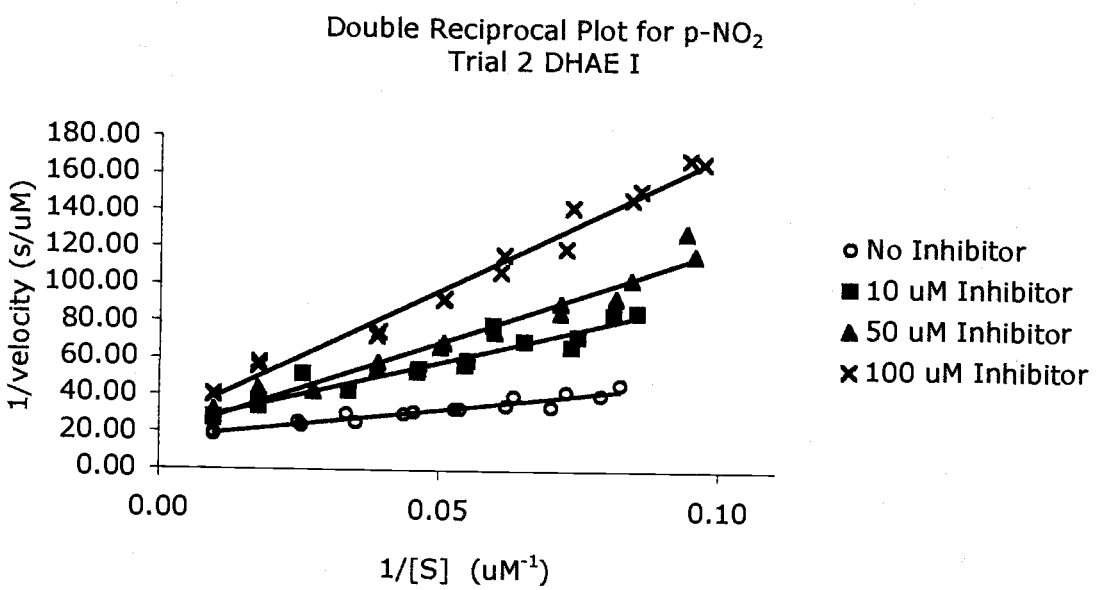
Double Reciprocal Plot for p-NO2
Trial 2 DHAE I
180.00
160.00
140.00
120.00
100.00
80.00
60.00
40.00
20.00
0.00
1/velocity (s/uM)
0.00
0.05
0.10
1/[S] (uM-1)
No Inhibitor
10 uM Inhibitor
50 uM Inhibitor
100 uM Inhibitor

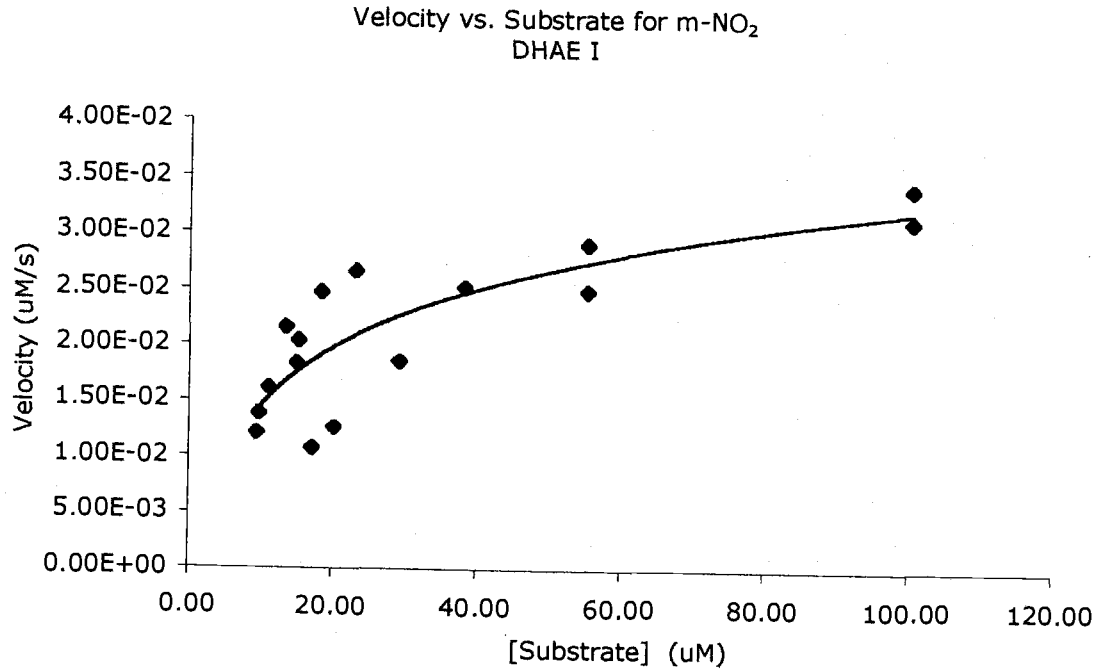
Velocity vs. Substrate for m-NO2
DHAE I
4.00E-02
3.50E-02
3.00E-02
2.50E-02
2.00E-02
1.50E-02
1.00E-02
5.00E-03
0.00E+00
Velocity (uM/s)
0.00
20.00
40.00
60.00
80.00
100.00
120.00
[Substrate] (uM)

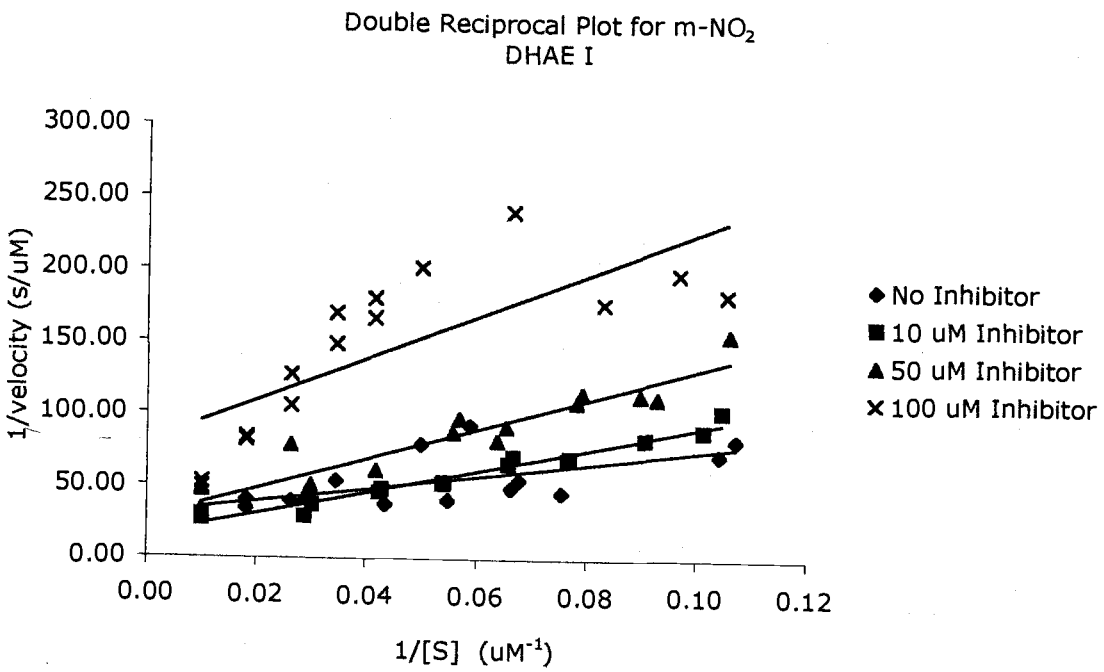
Double Reciprocal Plot for m-NO2
DHAE I
300.00
250.00
200.00
150.00
100.00
50.00
0.00
1/velocity (s/uM)
0.00
0.02
0.04
0.06
0.08
0.10
0.12
1/[S] (uM-1)
No Inhibitor
10 uM Inhibitor
50 uM Inhibitor
100 uM Inhibitor

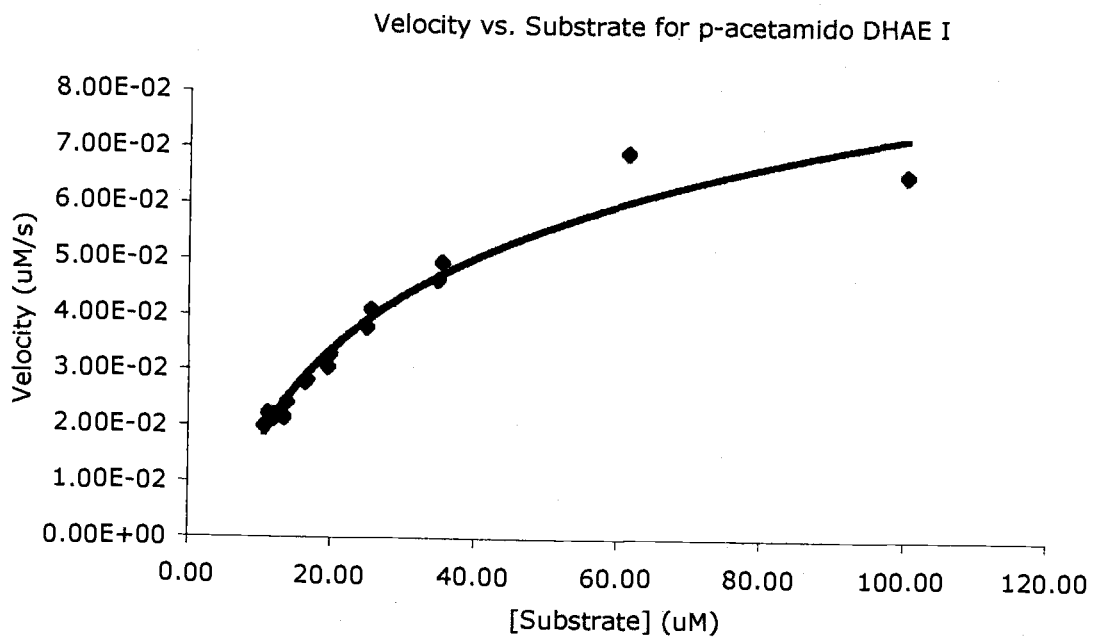
Velocity vs. Substrate for p-acetamido DHAE I
Velocity (uM/s)
8.00E-02
7.00E-02
6.00E-02
5.00E-02
4.00E-02
3.00E-02
2.00E-02
1.00E-02
0.00E+00
0.00
20.00
40.00
60.00
80.00
100.00
120.00
[Substrate] (uM)

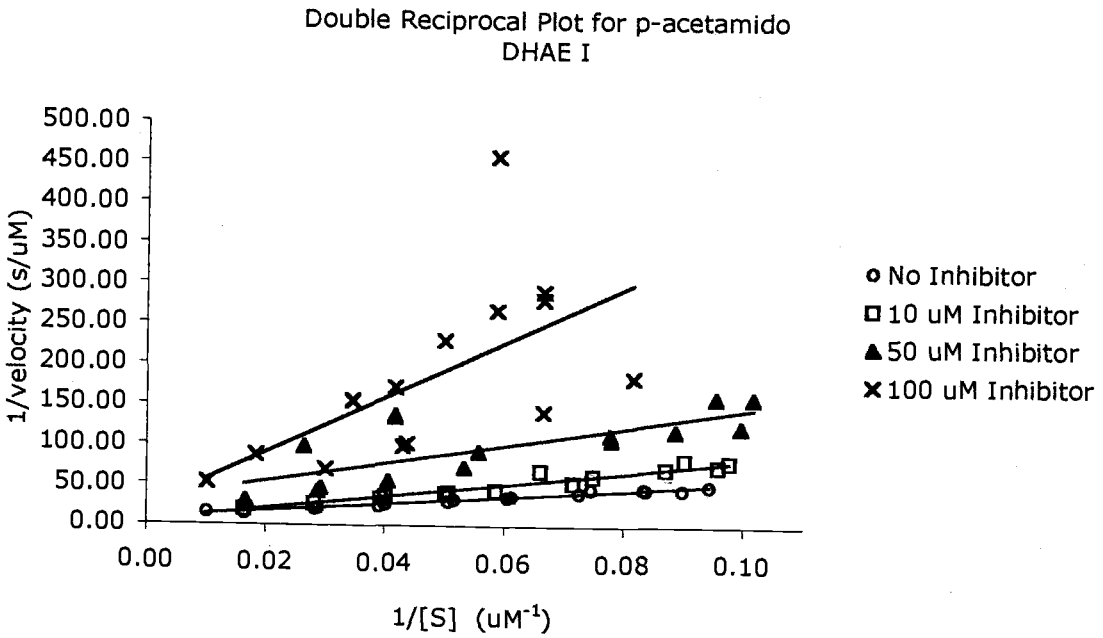
Double Reciprocal Plot for p-acetamido DHAE I
1/velocity (s/uM)
500.00
450.00
400.00
350.00
300.00
250.00
200.00
150.00
100.00
50.00
0.00
0.00
0.02
0.04
0.06
0.08
0.10
1/[S] (uM-1)
No Inhibitor
10 uM Inhibitor
50 uM Inhibitor
100 uM Inhibitor

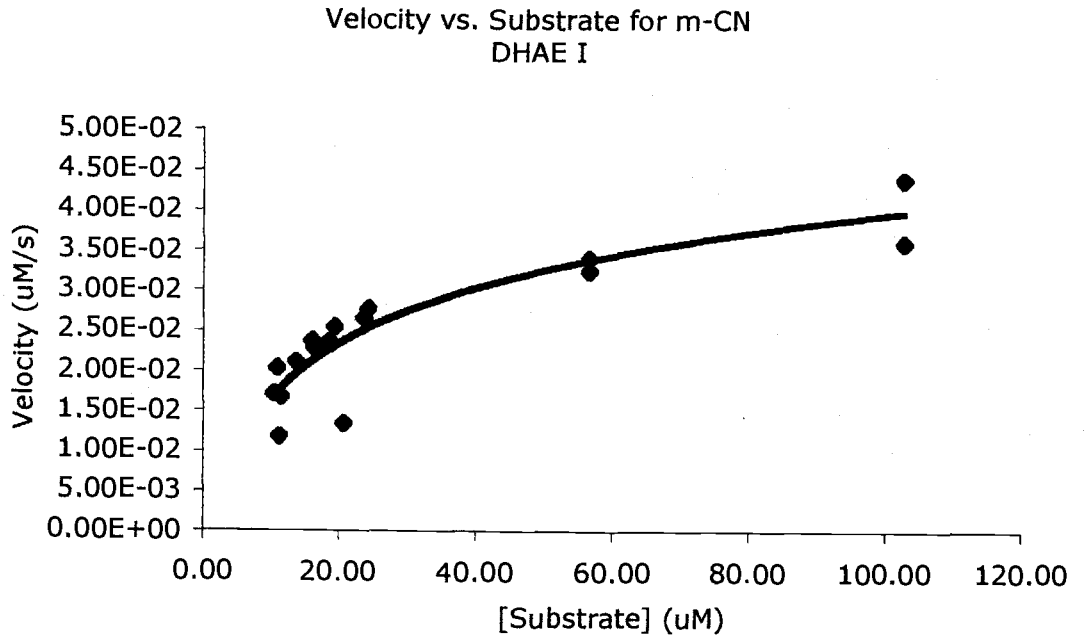
Velocity vs. Substrate for m-CN
DHAE I
5.00E-02
4.50E-02
4.00E-02
3.50E-02
3.00E-02
2.50E-02
2.00E-02
1.50E-02
1.00E-02
5.00E-03
0.00E+00
Velocity (uM/s)
0.00
20.00
40.00
60.00
80.00
100.00
120.00
[Substrate] (uM)

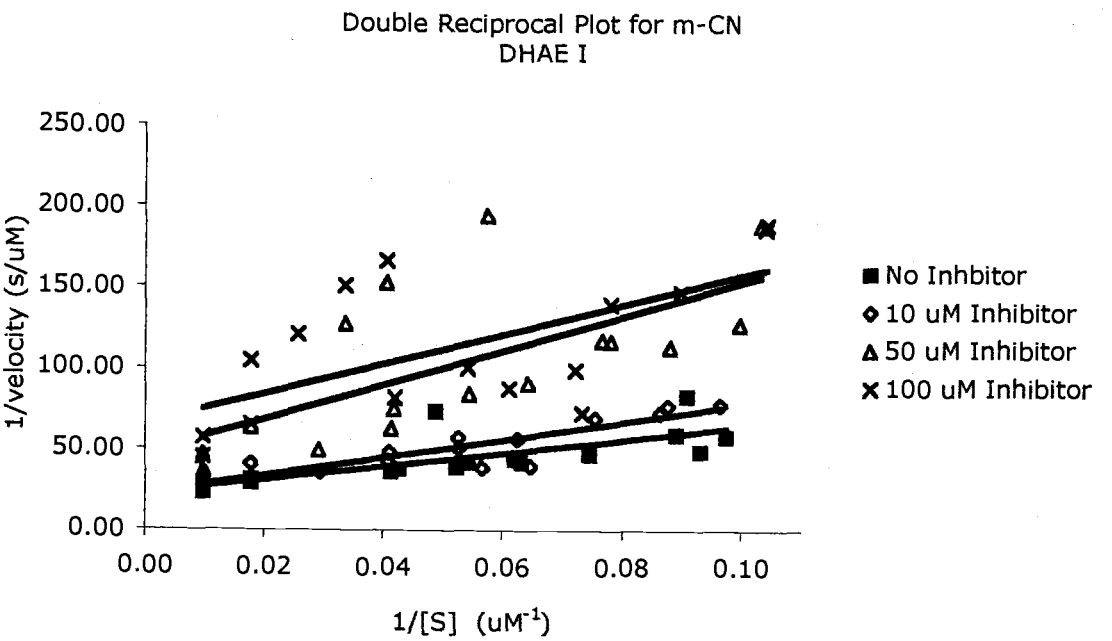
Double Reciprocal Plot for m-CN
DHAE I
250.00
200.00
150.00
100.00
50.00
0.00
1/velocity (s/uM)
0.00
0.02
0.04
0.06
0.08
0.10
1/[S] (uM-1)
No Inhbitor
10 uM Inhibitor
50 uM Inhibitor
100 uM Inhibitor

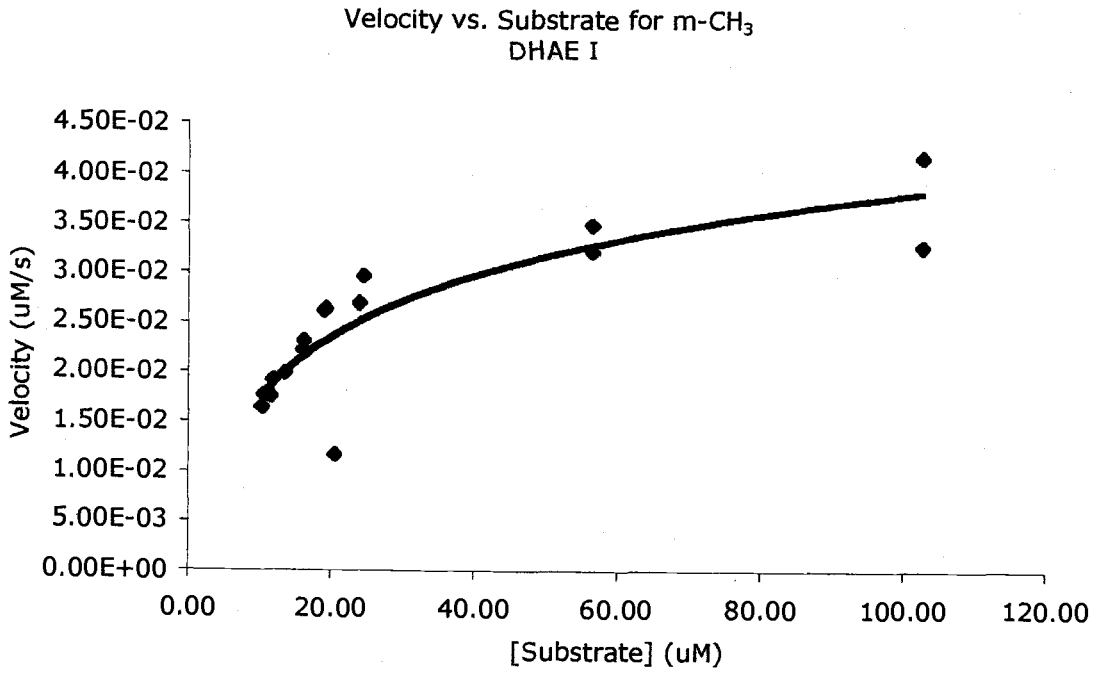
Velocity vs. Substrate for m-CH3
DHAE I
Velocity (uM/s)
4.50E-02
4.00E-02
3.50E-02
3.00E-02
2.50E-02
2.00E-02
1.50E-02
1.00E-02
5.00E-03
0.00E+00
0.00
20.00
40.00
60.00
80.00
100.00
120.00
[Substrate] (uM)

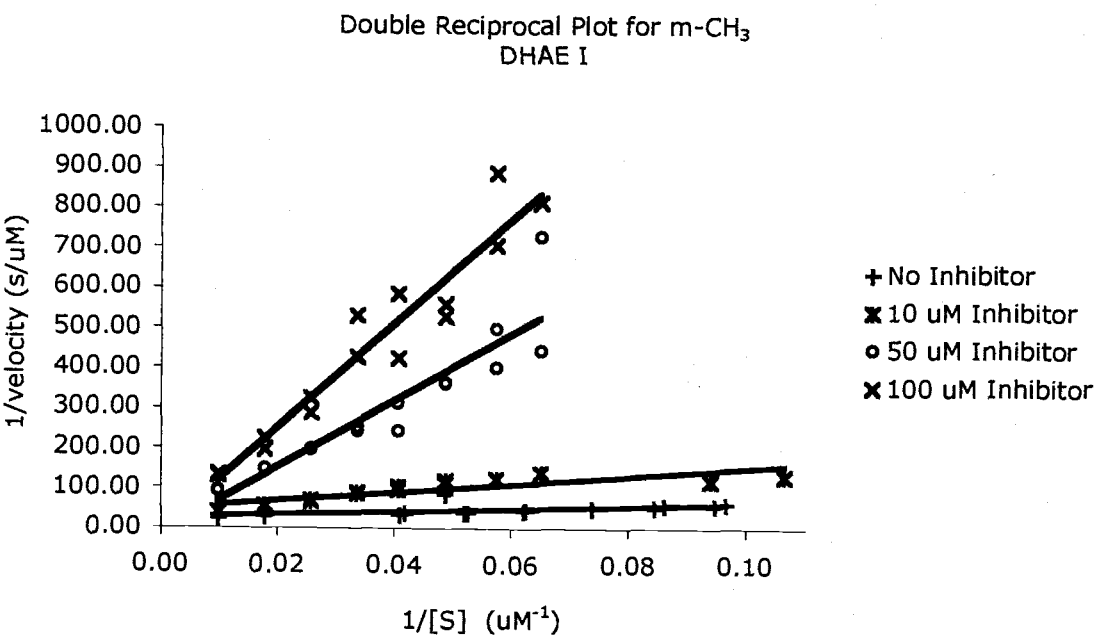
Double Reciprocal Plot for m-CH3
DHAE I
1/velocity (s/uM)
1000.00
900.00
800.00
700.00
600.00
500.00
400.00
300.00
200.00
100.00
0.00
0.00
0.02
0.04
0.06
0.08
0.10
1/[S] (uM-1)
No Inhibitor
10 uM Inhibitor
50 uM Inhibitor
100 uM Inhibitor

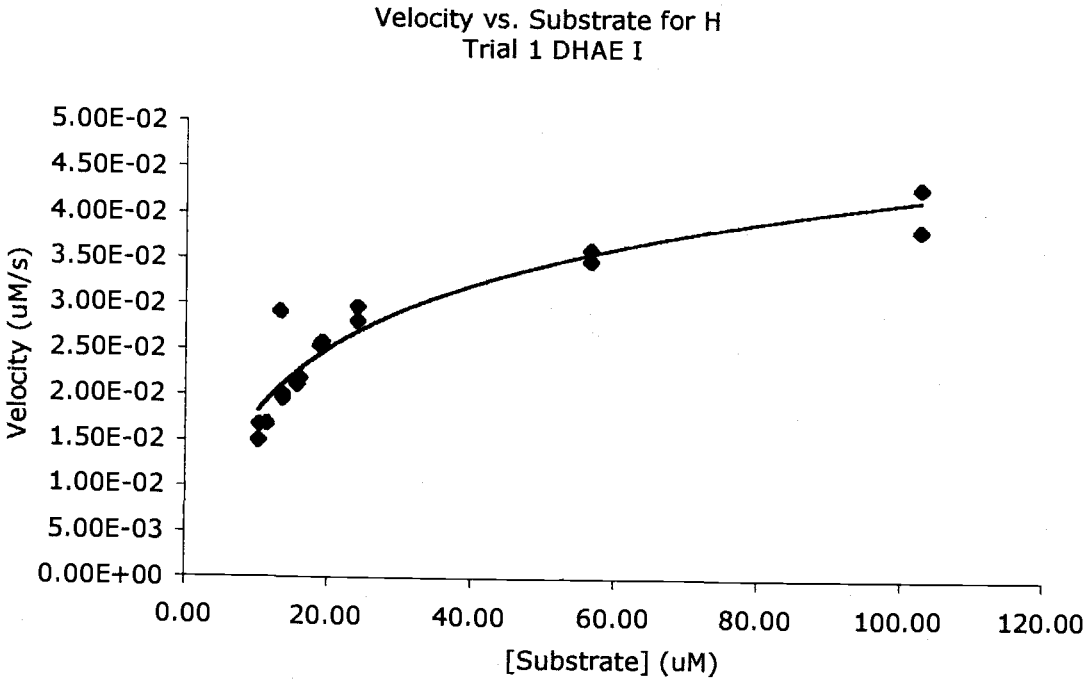
Velocity vs. Substrate for H
Trial 1 DHAE I
5.00E-02
4.50E-02
4.00E-02
3.50E-02
3.00E-02
2.50E-02
2.00E-02
1.50E-02
1.00E-02
5.00E-03
0.00E+00
Velocity (uM/s)
0.00
20.00
40.00
60.00
80.00
100.00
120.00
[Substrate] (uM)

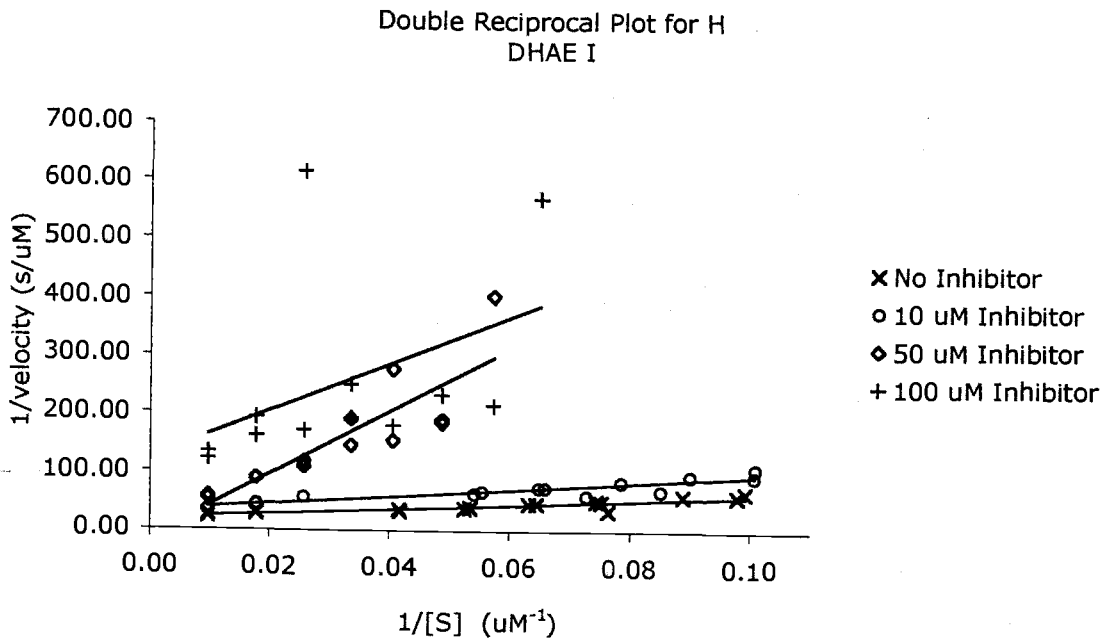
Double Reciprocal Plot for H
DHAE I
700.00
600.00
500.00
400.00
300.00
200.00
100.00
0.00
1/velocity (s/uM)
0.00
0.02
0.04
0.06
0.08
0.10
1/[S] (uM-1)
No Inhibitor
10 uM Inhibitor
50 uM Inhibitor
100 uM Inhibitor

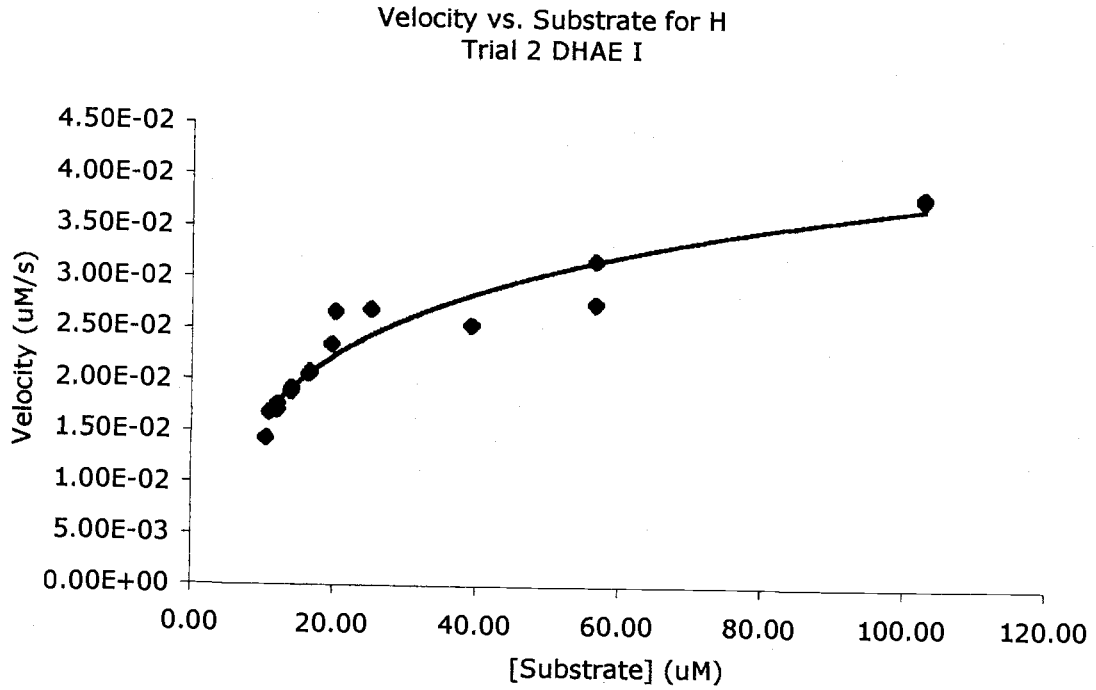
Velocity vs. Substrate for H
Trial 2 DHAE I
Velocity (uM/s)
4.50E-02
4.00E-02
3.50E-02
3.00E-02
2.50E-02
2.00E-02
1.50E-02
1.00E-02
5.00E-03
0.00E+00
0.00
20.00
40.00
60.00
80.00
100.00
120.00
[Substrate] (uM)

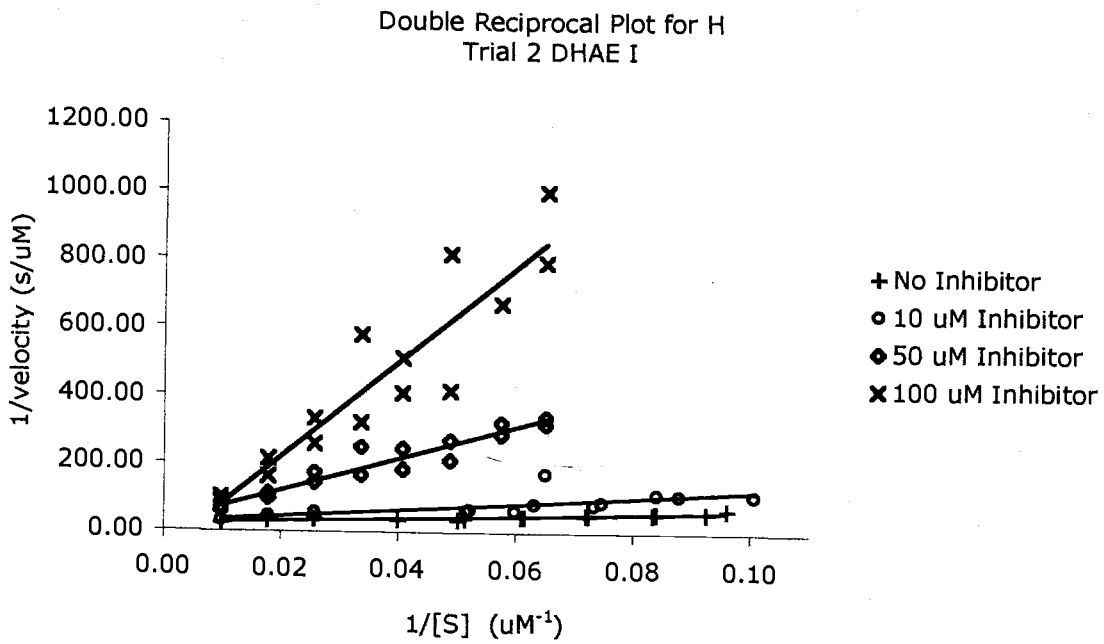
Double Reciprocal Plot for H
Trial 2 DHAE I
1/velocity (s/uM)
1200.00
1000.00
800.00
600.00
400.00
200.00
0.00
0.00
0.02
0.04
0.06
0.08
0.10
1/[S] (uM-1)
No Inhibitor
10 uM Inhibitor
50 uM Inhibitor
100 uM Inhibitor

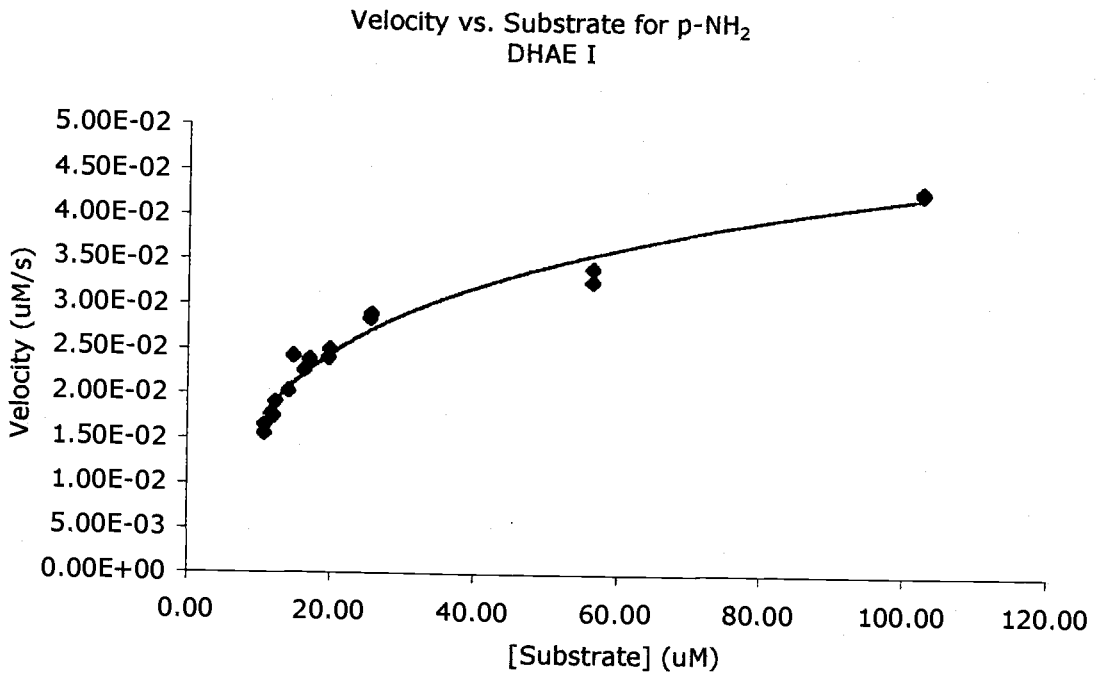
Velocity vs. Substrate for p-NH2
DHAE I
Velocity (uM/s)
5.00E-02
4.50E-02
4.00E-02
3.50E-02
3.00E-02
2.50E-02
2.00E-02
1.50E-02
1.00E-02
5.00E-03
0.00E+00
0.00
20.00
40.00
60.00
80.00
100.00
120.00
[Substrate] (uM)

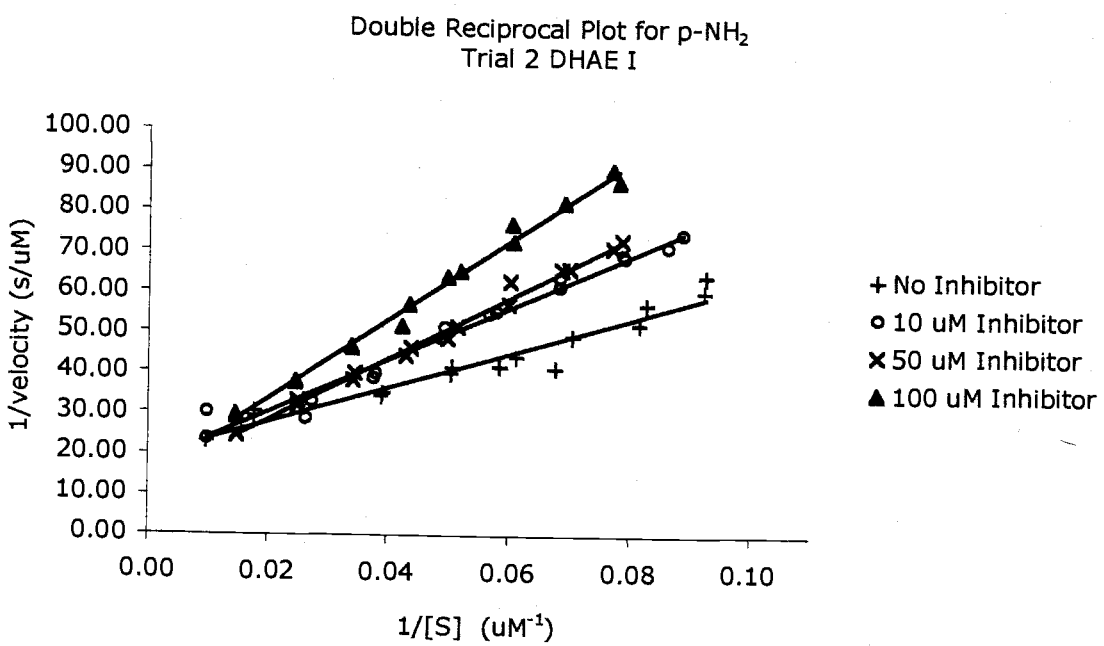
Double Reciprocal Plot for p-NH2
Trial 2 DHAE I
1/velocity (s/uM)
100.00
90.00
80.00
70.00
60.00
50.00
40.00
30.00
20.00
10.00
0.00
0.00
0.02
0.04
0.06
0.08
0.10
1/[S] (uM-1)
+ No Inhibitor
o 10 uM Inhibitor
× 50 uM Inhibitor
▲ 100 uM Inhibitor

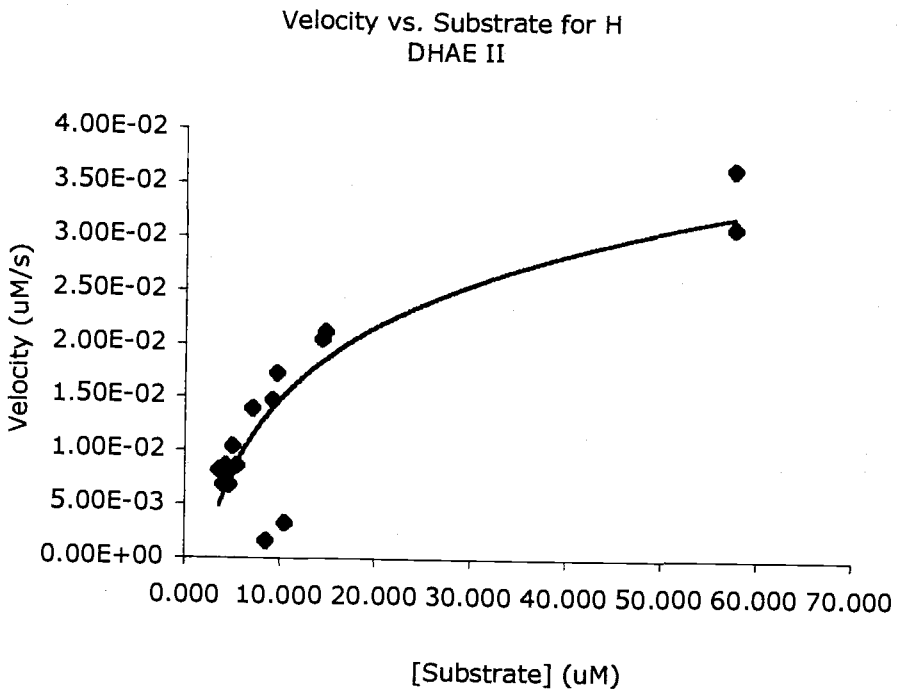
Velocity vs. Substrate for H
DHAE II
4.00E-02
3.50E-02
3.00E-02
2.50E-02
2.00E-02
1.50E-02
1.00E-02
5.00E-03
0.00E+00
Velocity (uM/s)
0.000 10.000 20.000 30.000 40.000 50.000 60.000 70.000
[Substrate] (uM)

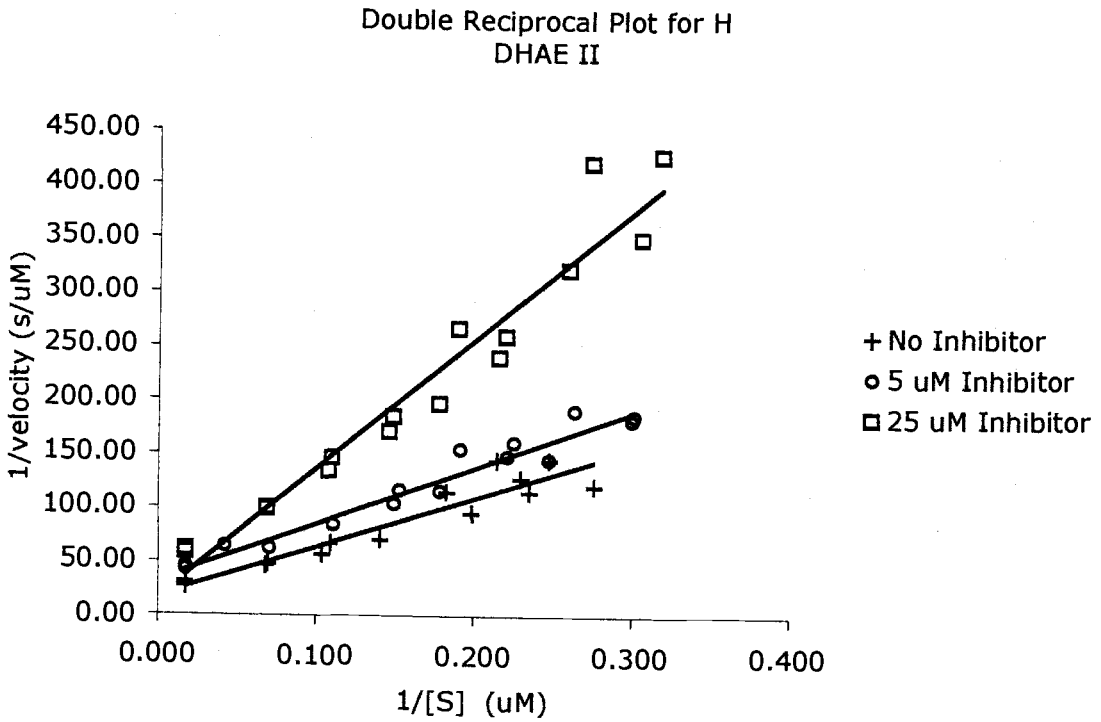
Double Reciprocal Plot for H
DHAE II
450.00
400.00
350.00
300.00
250.00
200.00
150.00
100.00
50.00
0.00
1/velocity (s/uM)
0.000 0.100 0.200 0.300 0.400
1/[S] (uM)
+ No Inhibitor
o 5 uM Inhibitor
□ 25 uM Inhibitor

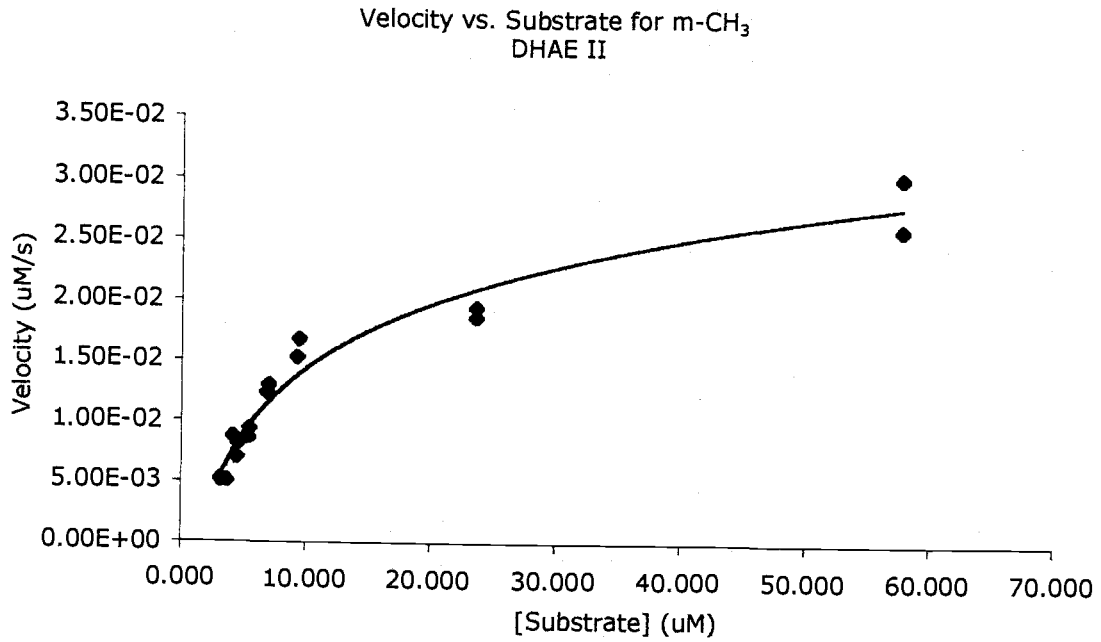
Velocity vs. Substrate for m-CH3
DHAE II
Velocity (uM/s)
3.50E-02
3.00E-02
2.50E-02
2.00E-02
1.50E-02
1.00E-02
5.00E-03
0.00E+00
0.000
10.000
20.000
30.000
40.000
50.000
60.000
70.000
[Substrate] (uM)

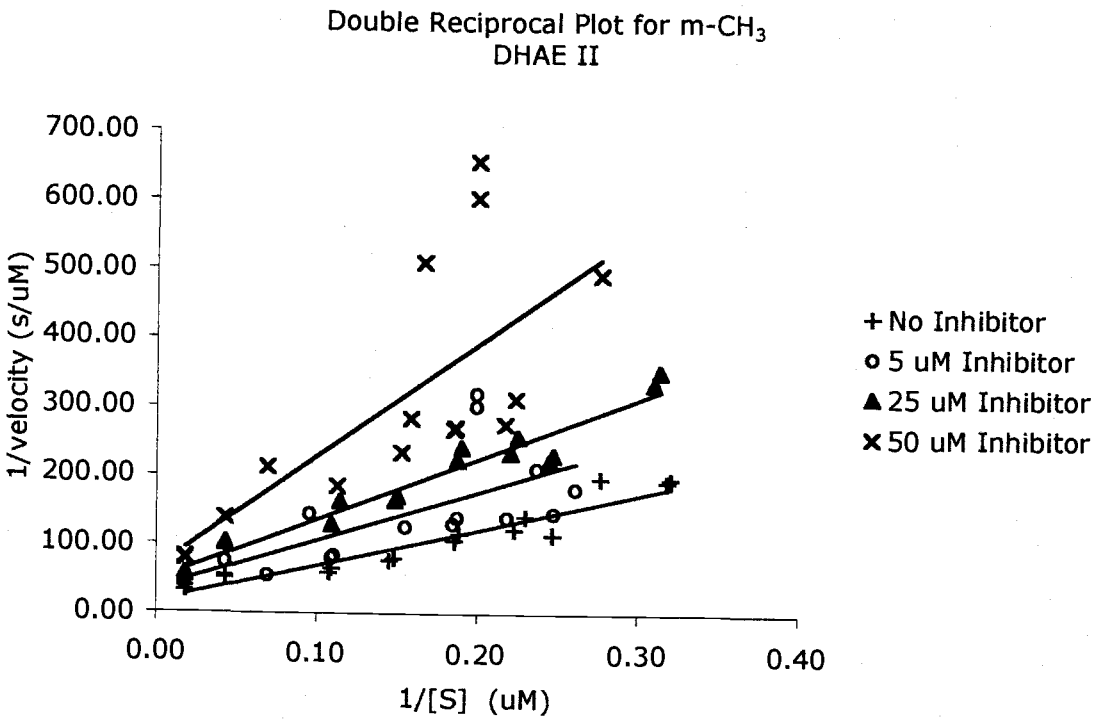
Double Reciprocal Plot for m-CH3
DHAE II
1/velocity (s/uM)
700.00
600.00
500.00
400.00
300.00
200.00
100.00
0.00
0.00
0.10
0.20
0.30
0.40
1/[S] (uM)
+ No Inhibitor
o 5 uM Inhibitor
▲ 25 uM Inhibitor
× 50 uM Inhibitor

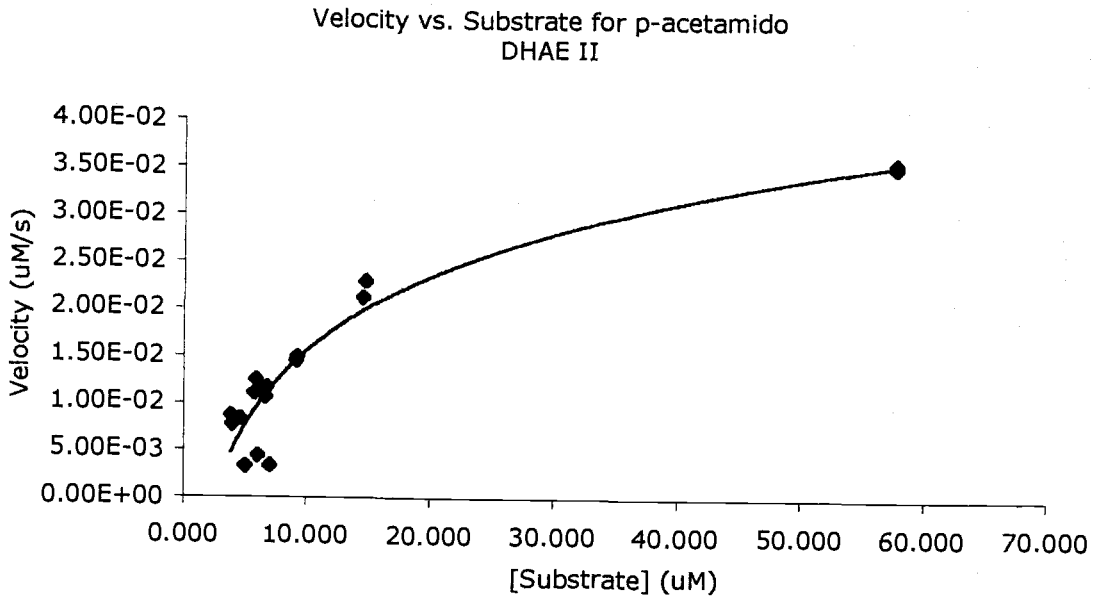
Velocity vs. Substrate for p-acetamido DHAE II
Velocity (uM/s)
4.00E-02
3.50E-02
3.00E-02
2.50E-02
2.00E-02
1.50E-02
1.00E-02
5.00E-03
0.00E+00
0.000
10.000
20.000
30.000
40.000
50.000
60.000
70.000
[Substrate] (uM)

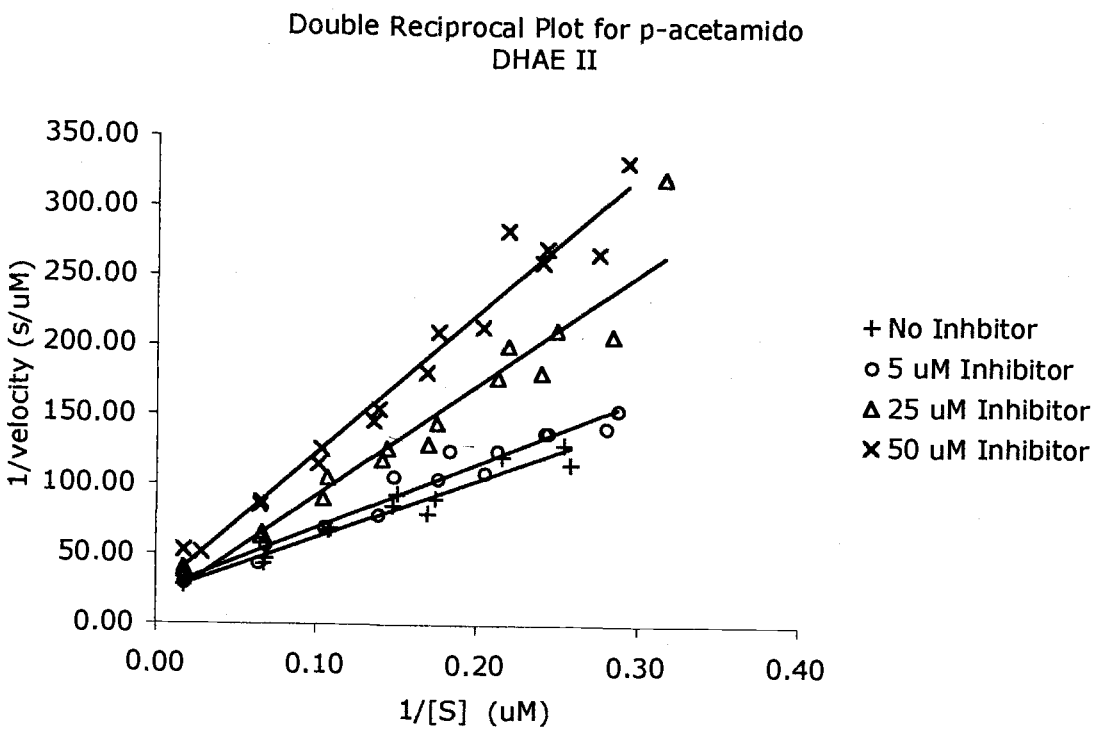
Double Reciprocal Plot for p-acetamido DHAE II
1/velocity (s/uM)
350.00
300.00
250.00
200.00
150.00
100.00
50.00
0.00
0.00
0.10
0.20
0.30
0.40
1/[S] (uM)
+ No Inhbitor
o 5 uM Inhibitor
Δ 25 uM Inhibitor
× 50 uM Inhibitor

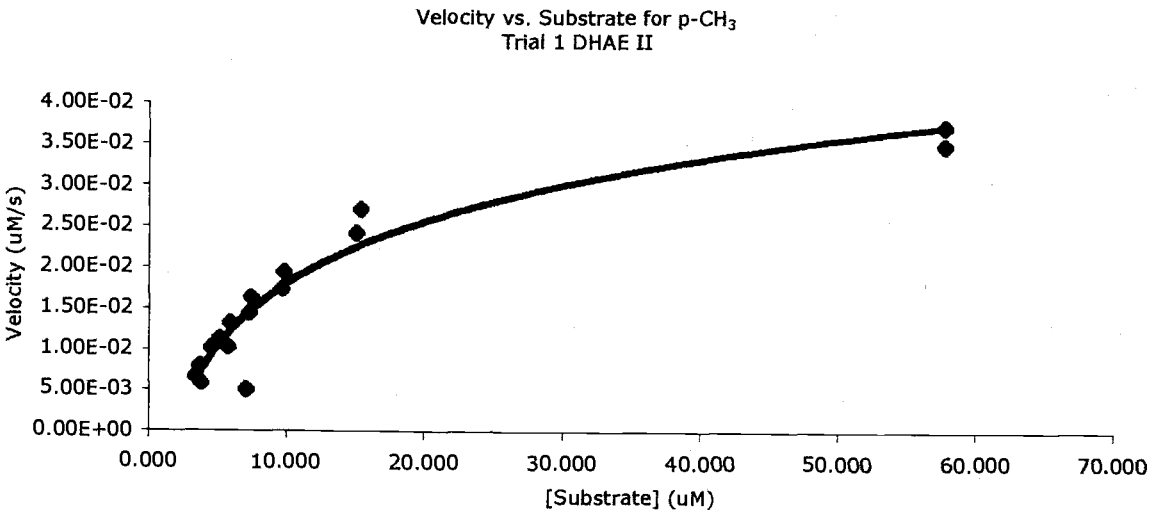
Velocity vs. Substrate for p-CH3
Trial 1 DHAE II
Velocity (uM/s)
4.00E-02
3.50E-02
3.00E-02
2.50E-02
2.00E-02
1.50E-02
1.00E-02
5.00E-03
0.00E+00
0.000
10.000
20.000
30.000
40.000
50.000
60.000
70.000
[Substrate] (uM)

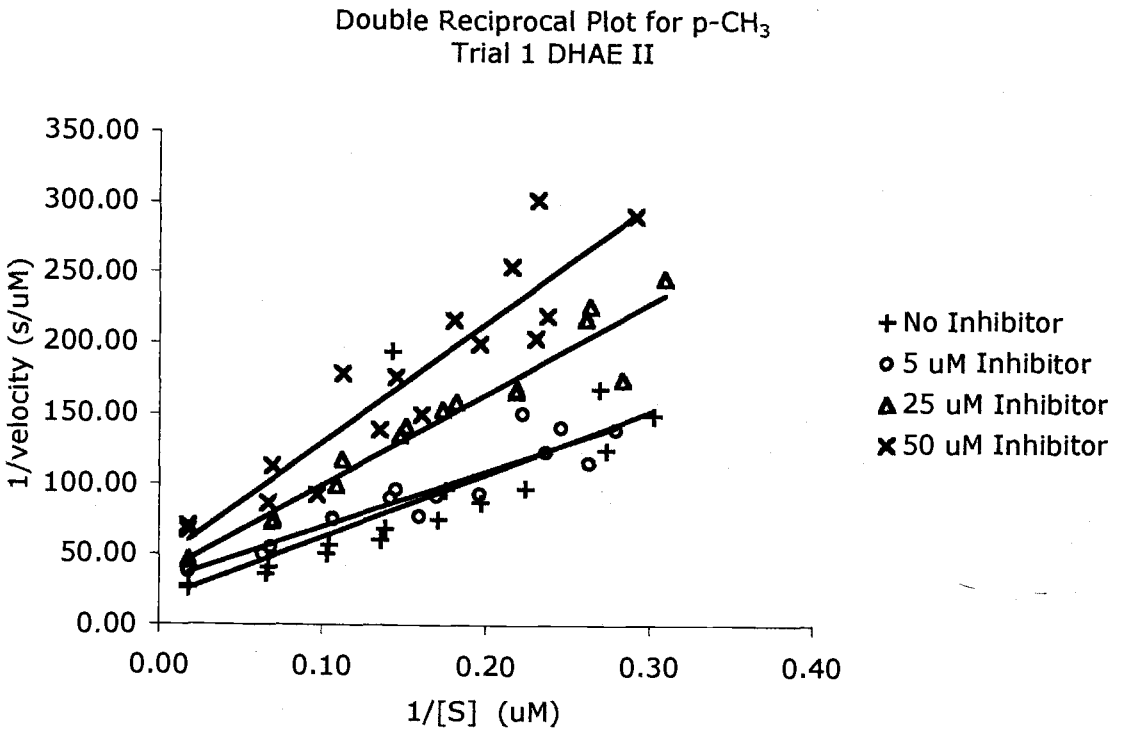
Double Reciprocal Plot for p-CH3
Trial 1 DHAE II
1/velocity (s/uM)
350.00
300.00
250.00
200.00
150.00
100.00
50.00
0.00
0.00
0.10
0.20
0.30
0.40
1/[S] (uM)
+ No Inhibitor
o 5 uM Inhibitor
Δ 25 uM Inhibitor
× 50 uM Inhibitor

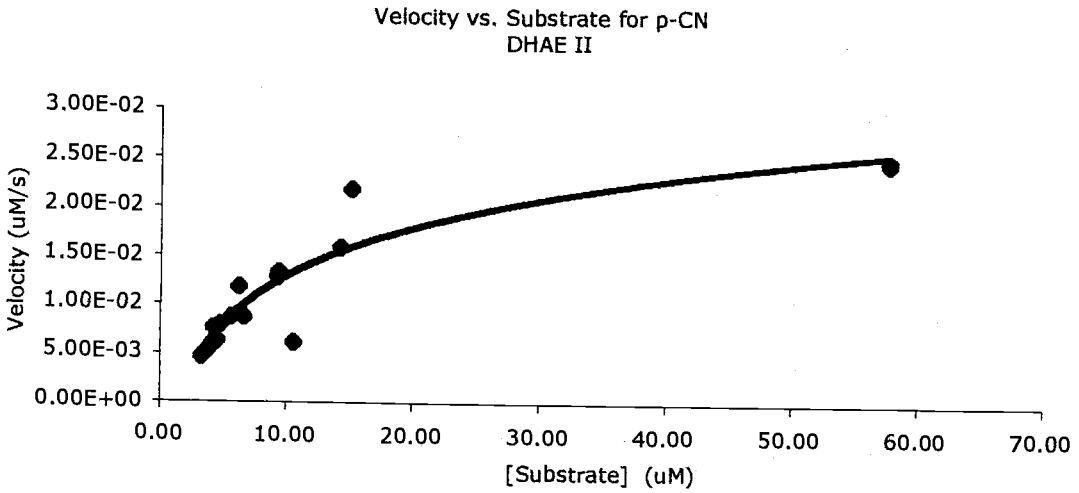
Velocity vs. Substrate for p-CN
DHAE II
3.00E-02
2.50E-02
2.00E-02
1.50E-02
1.00E-02
5.00E-03
0.00E+00
Velocity (uM/s)
0.00
10.00
20.00
30.00
40.00
50.00
60.00
70.00
[Substrate] (uM)

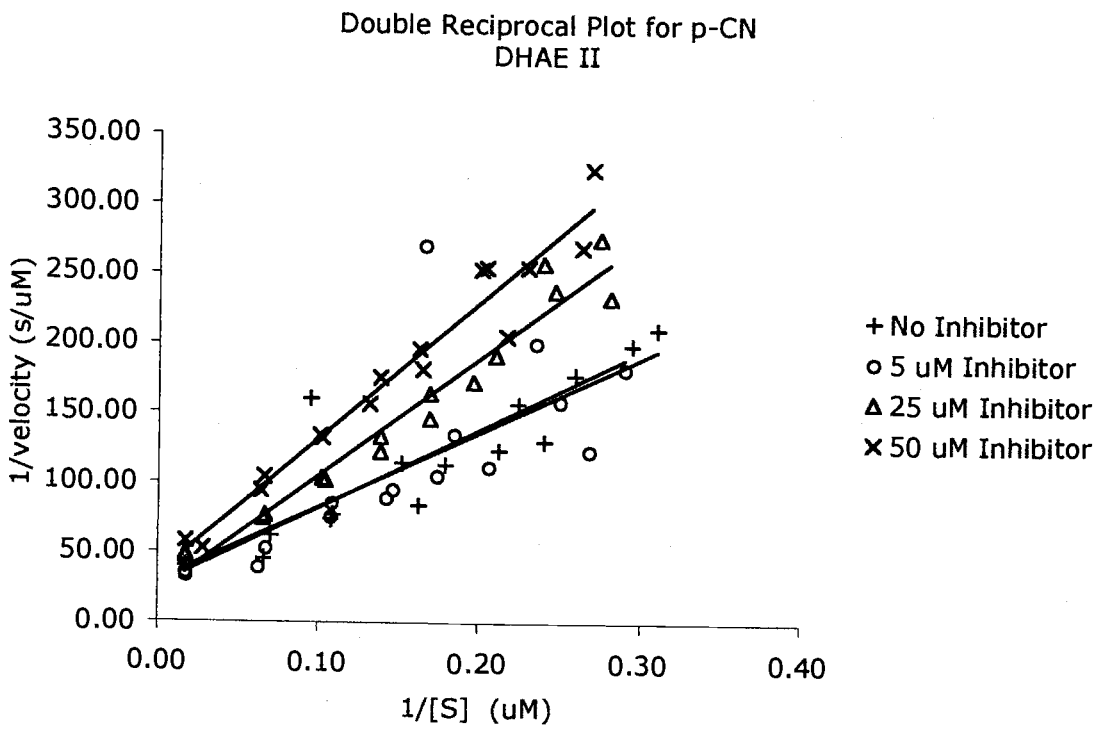
Double Reciprocal Plot for p-CN
DHAE II
350.00
300.00
250.00
200.00
150.00
100.00
50.00
0.00
1/velocity (s/uM)
0.00
0.10
0.20
0.30
0.40
1/[S] (uM)
+ No Inhibitor
o 5 uM Inhibitor
Δ 25 uM Inhibitor
× 50 uM Inhibitor

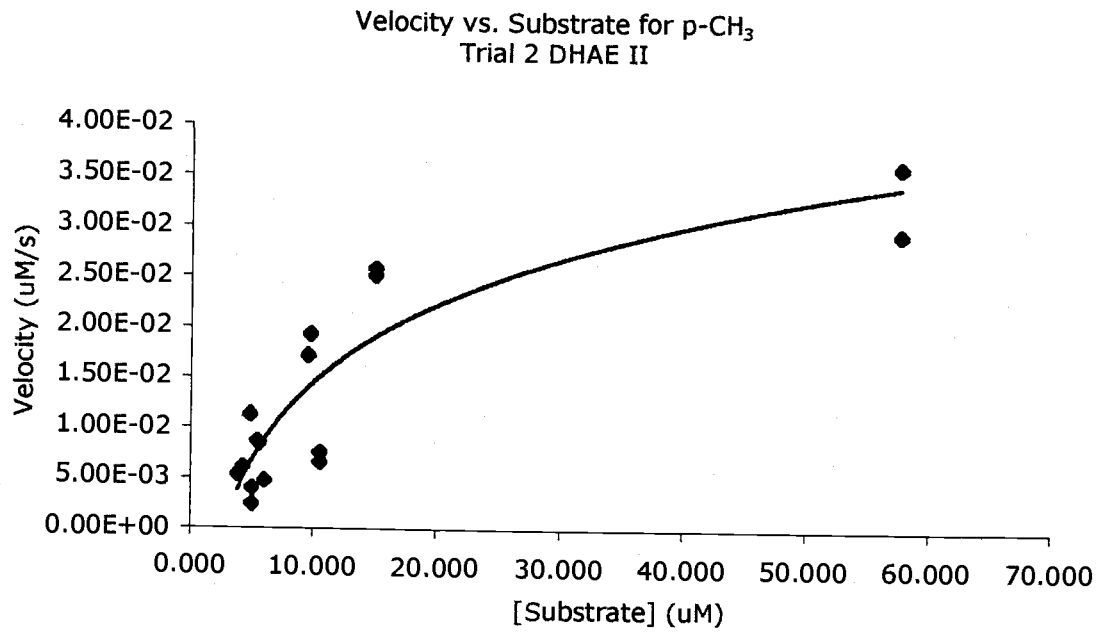
Velocity vs. Substrate for p-CH3
Trial 2 DHAE II
4.00E-02
3.50E-02
3.00E-02
2.50E-02
2.00E-02
1.50E-02
1.00E-02
5.00E-03
0.00E+00
Velocity (uM/s)
0.000
10.000
20.000
30.000
40.000
50.000
60.000
70.000
[Substrate] (uM)

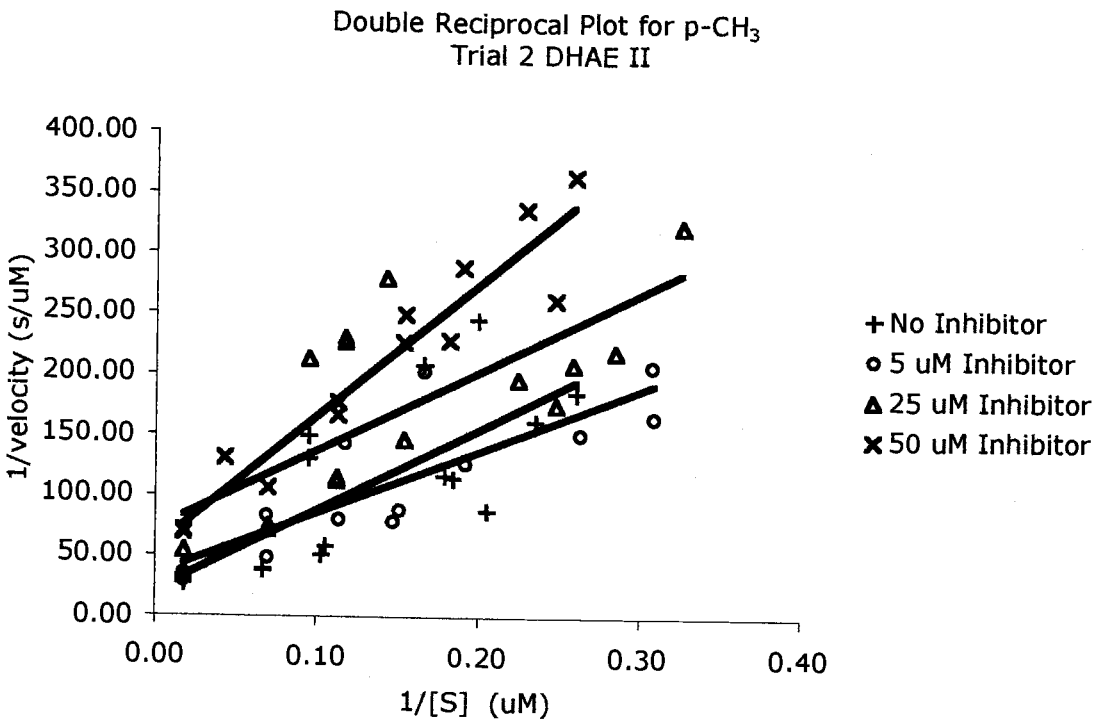
Double Reciprocal Plot for p-CH3
Trial 2 DHAE II
400.00
350.00
300.00
250.00
200.00
150.00
100.00
50.00
0.00
1/velocity (s/uM)
0.00
0.10
0.20
0.30
0.40
1/[S] (uM)
No Inhibitor
5 uM Inhibitor
25 uM Inhibitor
50 uM Inhibitor

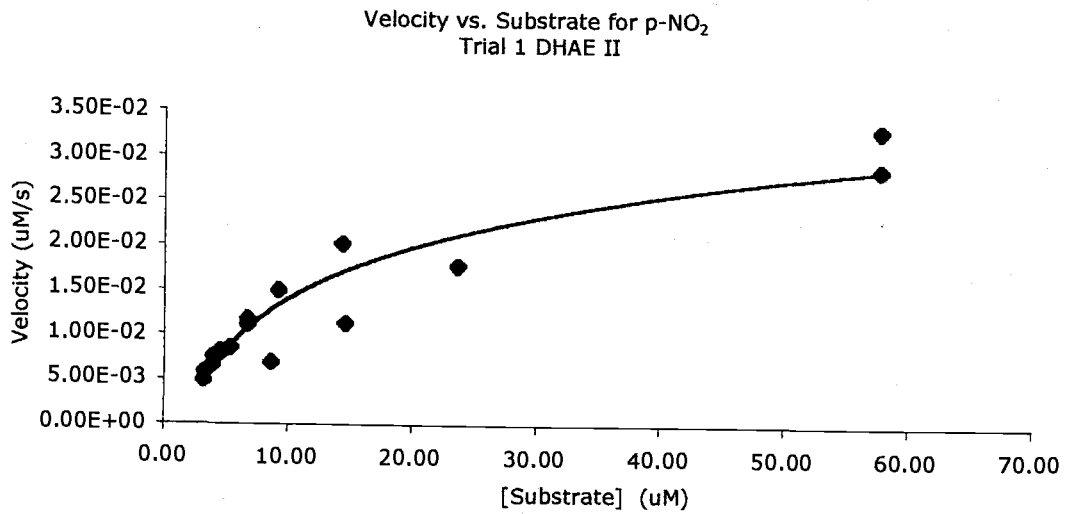
Velocity vs. Substrate for p-NO2
Trial 1 DHAE II
Velocity (uM/s)
3.50E-02
3.00E-02
2.50E-02
2.00E-02
1.50E-02
1.00E-02
5.00E-03
0.00E+00
0.00
10.00
20.00
30.00
40.00
50.00
60.00
70.00
[Substrate] (uM)

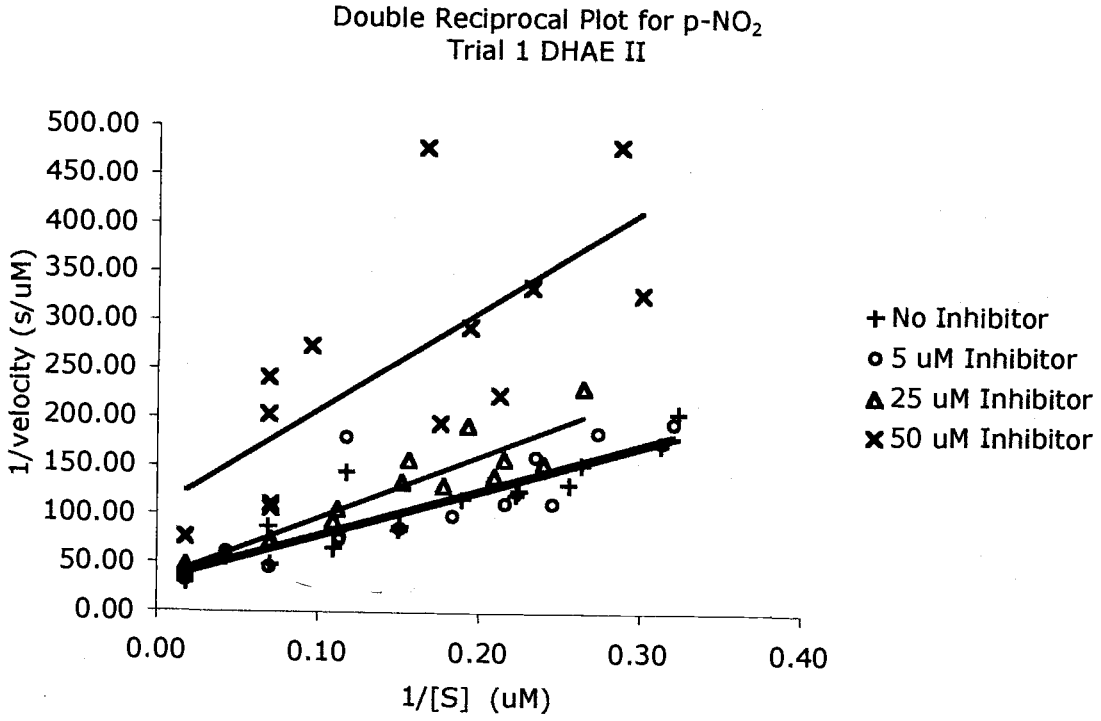
Double Reciprocal Plot for p-NO2
Trial 1 DHAE II
1/velocity (s/uM)
500.00
450.00
400.00
350.00
300.00
250.00
200.00
150.00
100.00
50.00
0.00
0.00
0.10
0.20
0.30
0.40
1/[S] (uM)
+ No Inhibitor
o 5 uM Inhibitor
▲ 25 uM Inhibitor
× 50 uM Inhibitor

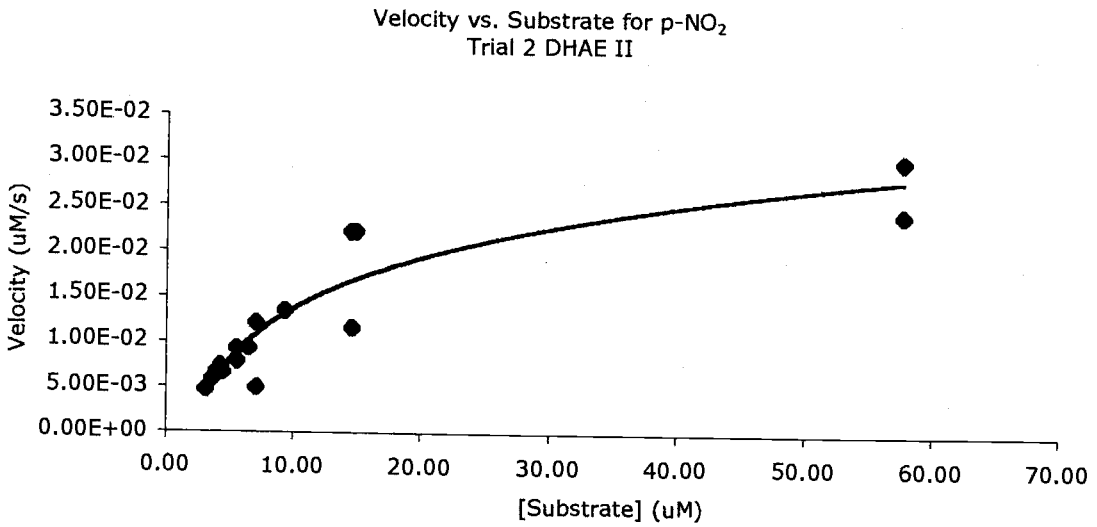
Velocity vs. Substrate for p-NO2
Trial 2 DHAE II
Velocity (uM/s)
3.50E-02
3.00E-02
2.50E-02
2.00E-02
1.50E-02
1.00E-02
5.00E-03
0.00E+00
0.00
10.00
20.00
30.00
40.00
50.00
60.00
70.00
[Substrate] (uM)

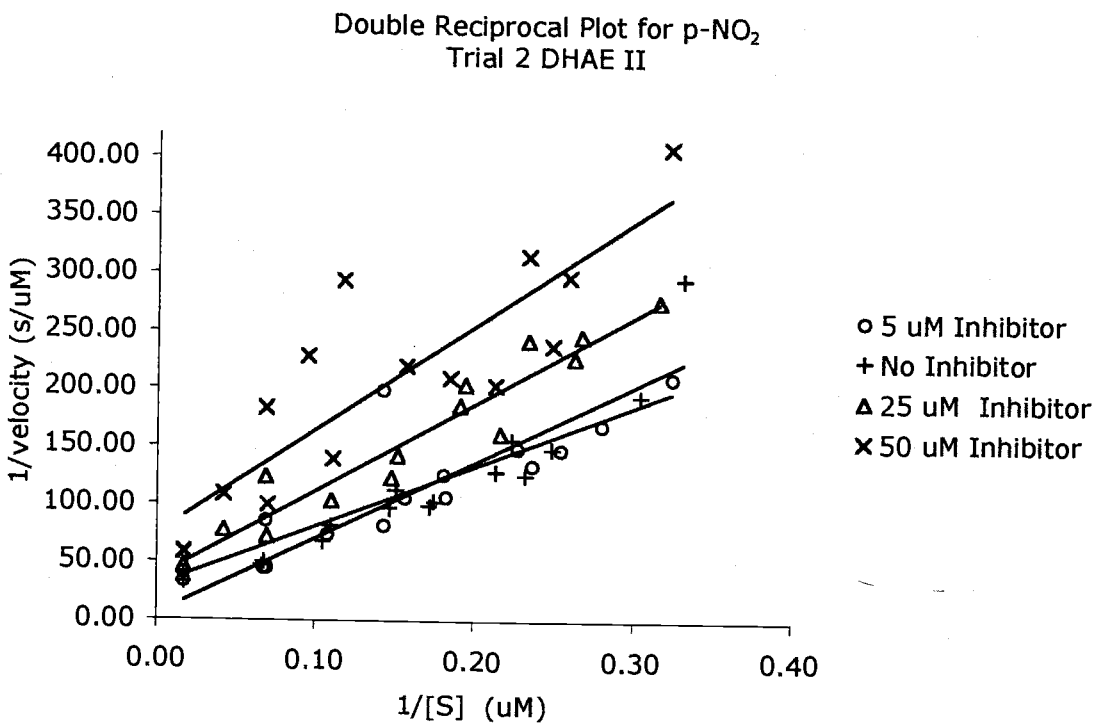
Double Reciprocal Plot for p-NO2
Trial 2 DHAE II
1/velocity (s/uM)
400.00
350.00
300.00
250.00
200.00
150.00
100.00
50.00
0.00
0.00
0.10
0.20
0.30
0.40
1/[S] (uM)
o 5 uM Inhibitor
+ No Inhibitor
Δ 25 uM Inhibitor
× 50 uM Inhibitor

Appendix II

Spectroscopic Data for New Compounds

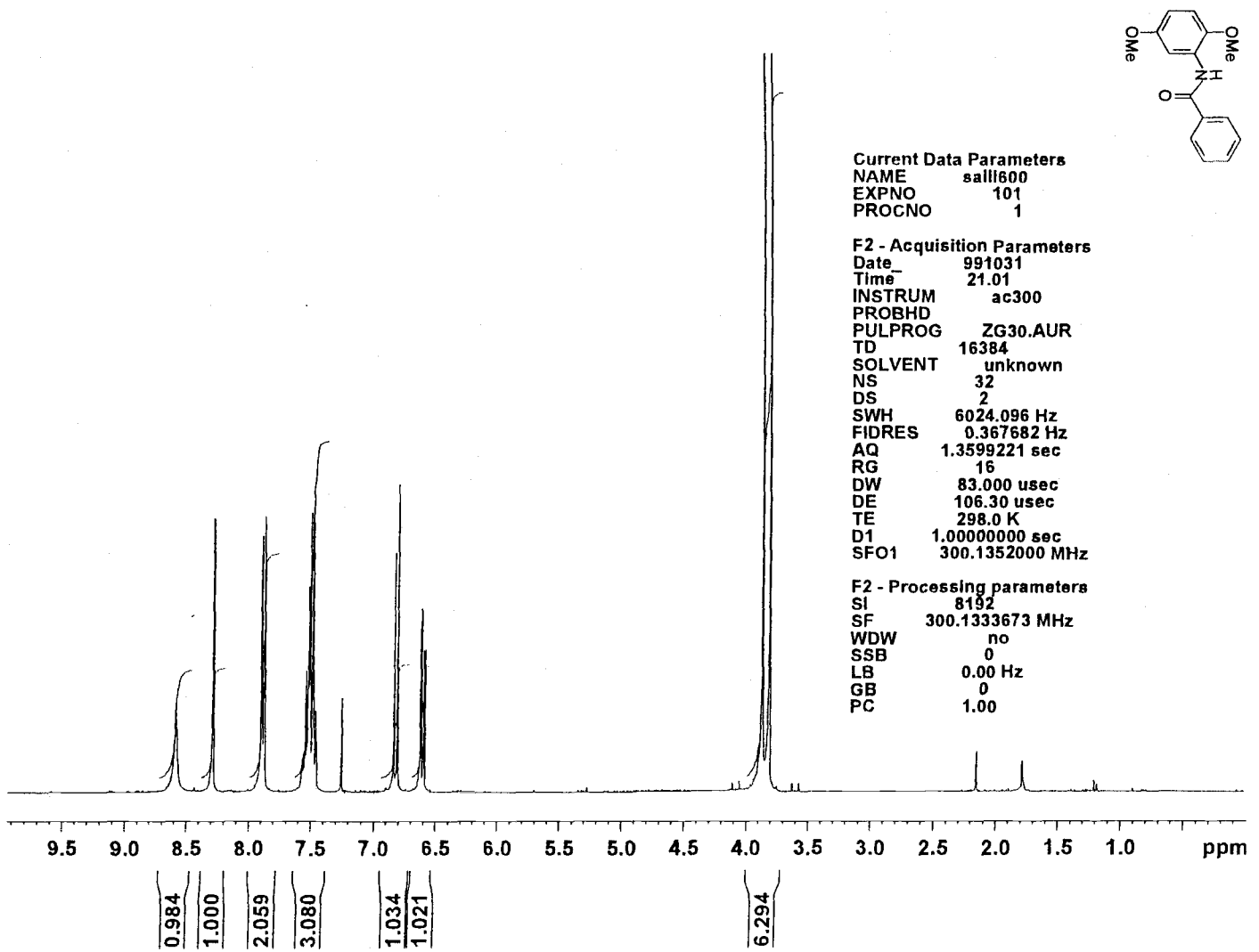
OMe
OMe
H
N
O
Current Data Parameters
NAME salli600
EXPNO 101
PROCNO 1
F2 - Acquisition Parameters
Date_ 991031
Time 21.01
INSTRUM ac300
PROBHD
PULPROG ZG30.AUR
TD 16384
SOLVENT unknown
NS 32
DS 2
SWH 6024.096 Hz
FIDRES 0.367682 Hz
AQ 1.3599221 sec
RG 16
DW 83.000 usec
DE 106.30 usec
TE 298.0 K
D1 1.00000000 sec
SFO1 300.1352000 MHz
F2 - Processing parameters
SI 8192
SF 300.1333673 MHz
WDW no
SSB 0
LB 0.00 Hz
GB 0
PC 1.00
9.5 9.0 8.5 8.0 7.5 7.0 6.5 6.0 5.5 5.0 4.5 4.0 3.5 3.0 2.5 2.0 1.5 1.0 ppm
0.984
1.000
2.059
3.080
1.034
1.021
6.294

156

165.202
153.935
142.355
135.161
131.770
128.773
128.426
127.005
110.705
108.843
105.887
77.484
77.060
76.636
56.303
55.804
OMe
OMe
N
H
O
Current Data Parameters
NAME salll600
EXPNO 201
PROCNO 1
F2 - Acquisition Parameters
Date_ 991031
Time 21.17
INSTRUM ac300
PROBHD
PULPROG ZG30.AUR
TD 65536
SOLVENT unknown
NS 464
DS 2
SWH 18518.518 Hz
FIDRES 0.282570 Hz
AQ 1.7695220 sec
RG 400
DW 27.000 usec
DE 36.30 usec
TE 298.0 K
D1 1.00000000 sec
SFO1 75.4766000 MHz
F2 - Processing parameters
SI 32768
SF 75.4685962 MHz
WDW EM
SSB 0
LB 3.00 Hz
GB 0
PC 1.00
190 180 170 160 150 140 130 120 110 100 90 80 70 60 50 40 30 20 10 ppm

S-5

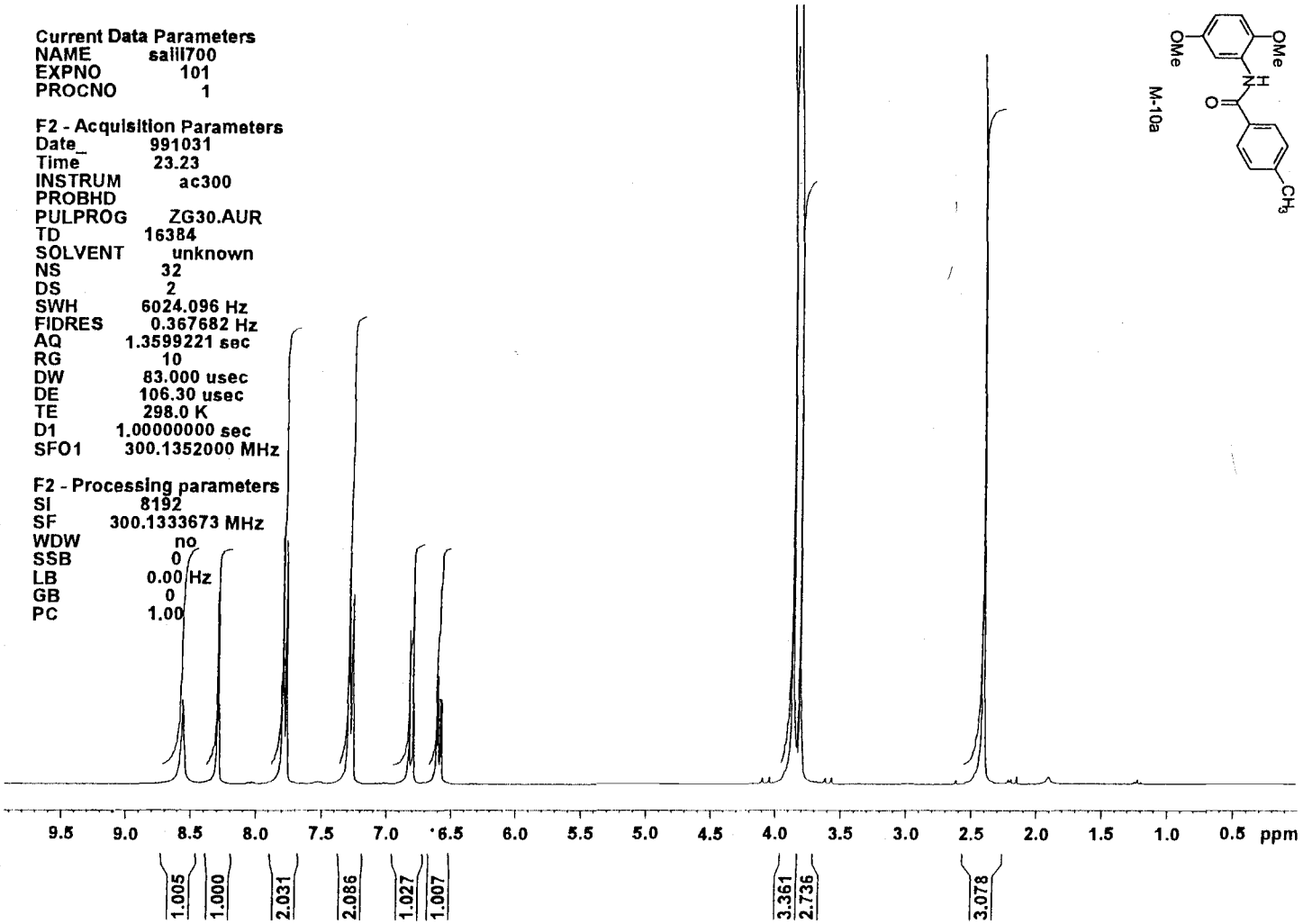
Current Data Parameters
NAME saiil700
EXPNO 101
PROCNO 1
F2 - Acquisition Parameters
Date_ 991031
Time 23.23
INSTRUM ac300
PROBHD
PULPROG ZG30.AUR
TD 16384
SOLVENT unknown
NS 32
DS 2
SWH 6024.096 Hz
FIDRES 0.367682 Hz
AQ 1.3599221 sec
RG 10
DW 83.000 usec
DE 106.30 usec
TE 298.0 K
D1 1.00000000 sec
SFO1 300.1352000 MHz
F2 - Processing parameters
SI 8192
SF 300.1333673 MHz
WDW no
SSB 0
LB 0.00 Hz
GB 0
PC 1.00
OMe
OMe
N
H
O
CH3
M-10a
9.5 9.0 8.5 8.0 7.5 7.0 6.5 6.0 5.5 5.0 4.5 4.0 3.5 3.0 2.5 2.0 1.5 1.0 0.5 ppm
1.005
1.000
2.031
2.086
1.027
1.007
3.361
2.736
3.078

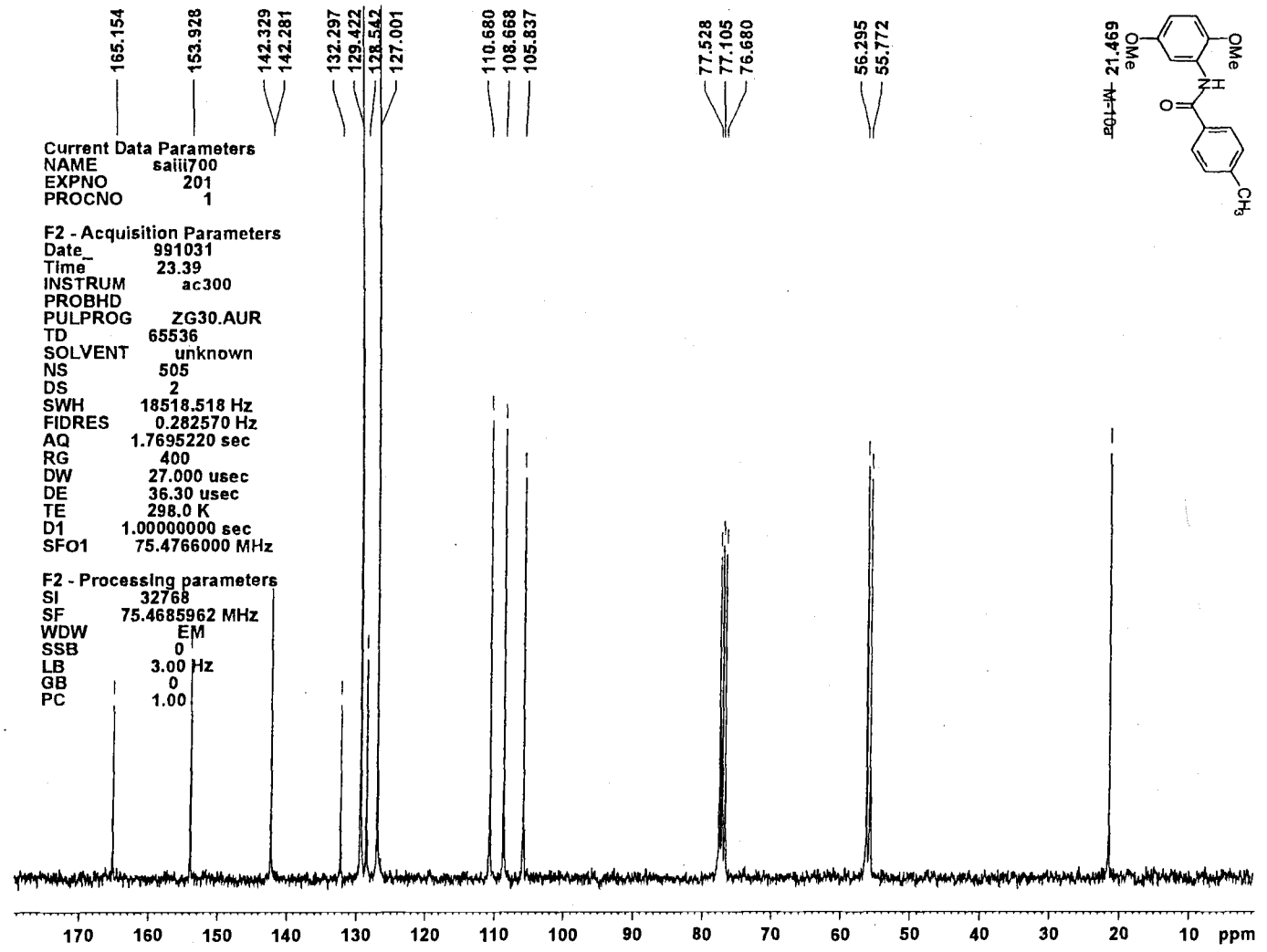
165.154
153.928
142.329
142.281
132.297
129.422
128.542
127.001
110.680
108.668
105.837
77.528
77.105
76.680
56.295
55.772
21.469
OMe
OMe
H
N
O
CH3
Current Data Parameters
NAME saiii700
EXPNO 201
PROCNO 1
F2 - Acquisition Parameters
Date_ 991031
Time 23.39
INSTRUM ac300
PROBHD
PULPROG ZG30.AUR
TD 65536
SOLVENT unknown
NS 505
DS 2
SWH 18518.518 Hz
FIDRES 0.282570 Hz
AQ 1.7695220 sec
RG 400
DW 27.000 usec
DE 36.30 usec
TE 298.0 K
D1 1.00000000 sec
SFO1 75.4766000 MHz
F2 - Processing parameters
SI 32768
SF 75.4685962 MHz
WDW EM
SSB 0
LB 3.00 Hz
GB 0
PC 1.00
170 160 150 140 130 120 110 100 90 80 70 60 50 40 30 20 10 ppm

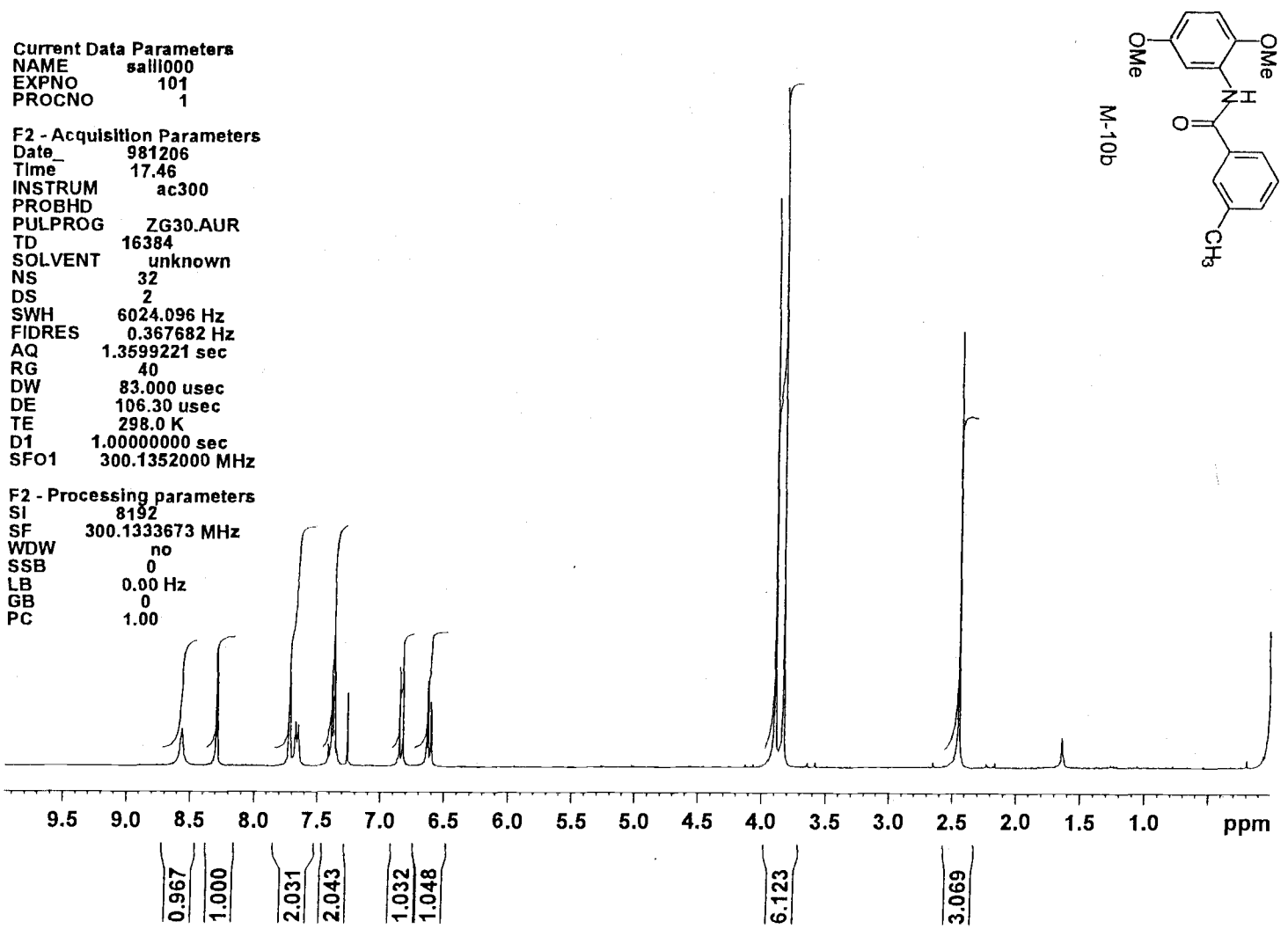
Current Data Parameters
NAME salll000
EXPNO 101
PROCNO 1
F2 - Acquisition Parameters
Date_ 981206
Time 17.46
INSTRUM ac300
PROBHD
PULPROG ZG30.AUR
TD 16384
SOLVENT unknown
NS 32
DS 2
SWH 6024.096 Hz
FIDRES 0.367682 Hz
AQ 1.3599221 sec
RG 40
DW 83.000 usec
DE 106.30 usec
TE 298.0 K
D1 1.00000000 sec
SFO1 300.1352000 MHz
F2 - Processing parameters
SI 8192
SF 300.1333673 MHz
WDW no
SSB 0
LB 0.00 Hz
GB 0
PC 1.00
OMe
OMe
H
N
O
CH3
M-10b
9.5 9.0 8.5 8.0 7.5 7.0 6.5 6.0 5.5 5.0 4.5 4.0 3.5 3.0 2.5 2.0 1.5 1.0 ppm
0.967
1.000
2.031
2.043
1.032
1.048
6.123
3.069

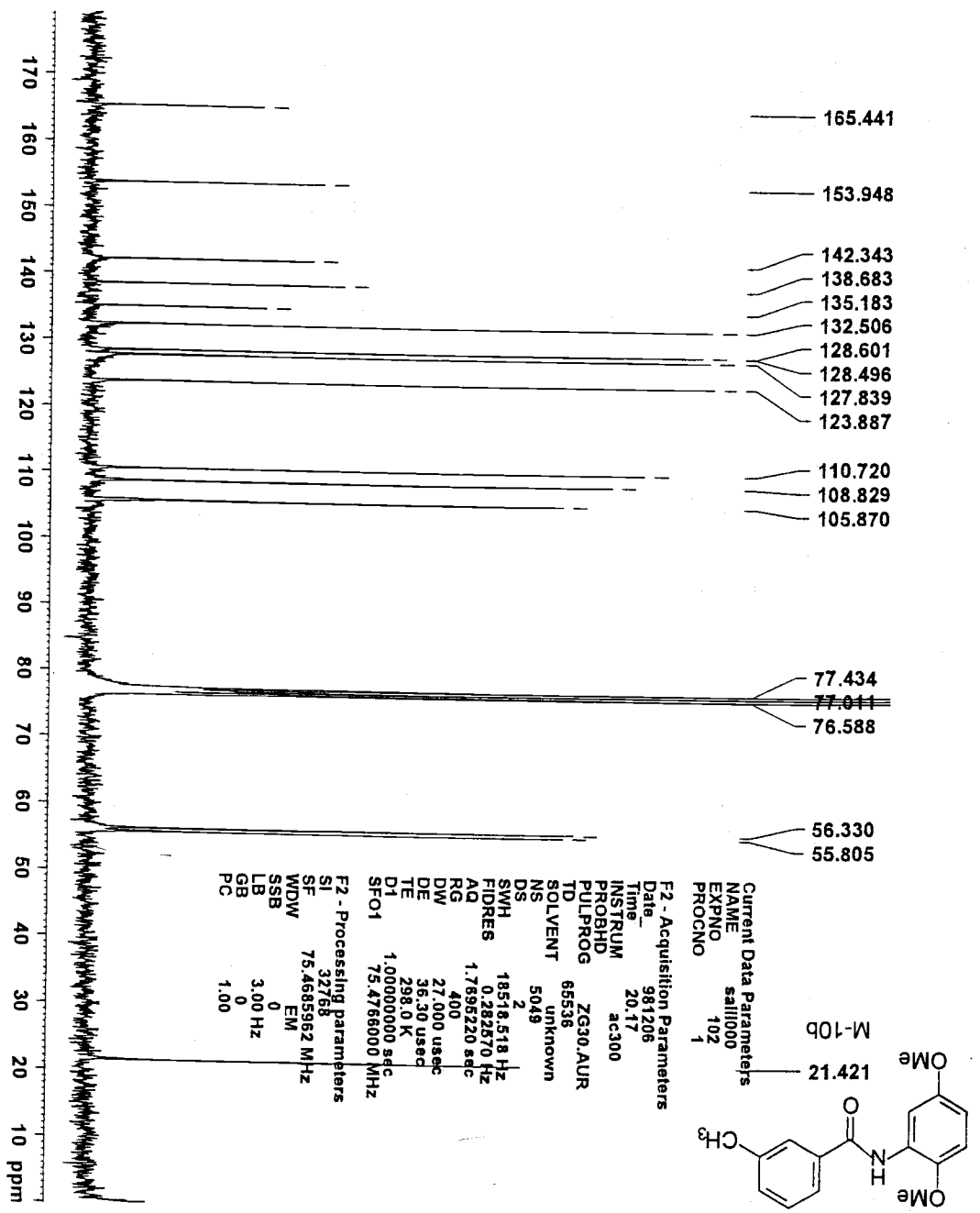
165.441
153.948
142.343
138.683
135.183
132.506
128.601
128.496
127.839
123.887
110.720
108.829
105.870
77.434
77.011
76.588
56.330
55.805
21.421
Current Data Parameters
NAME salli000
EXPNO 102
PROCNO 1
F2 - Acquisition Parameters
Date_ 981206
Time_ 20.17
INSTRUM ac300
PROBHD
PULPROG ZG30.AUR
TD 65536
SOLVENT unknown
NS 5049
DS 2
SWH 18518.518 Hz
FIDRES 0.282570 Hz
AQ 1.7696220 sec
RG 400
DW 27.000 usec
DE 36.30 usec
TE 298.0 K
D1 1.00000000 sec
SFO1 75.4766000 MHz
F2 - Processing parameters
SI 32768
SF 75.4685962 MHz
WDW EM
SSB 0
LB 3.00 Hz
GB 0
PC 1.00
M-10b
OMe
OMe
CH3
O
N
H
170 160 150 140 130 120 110 100 90 80 70 60 50 40 30 20 10 ppm

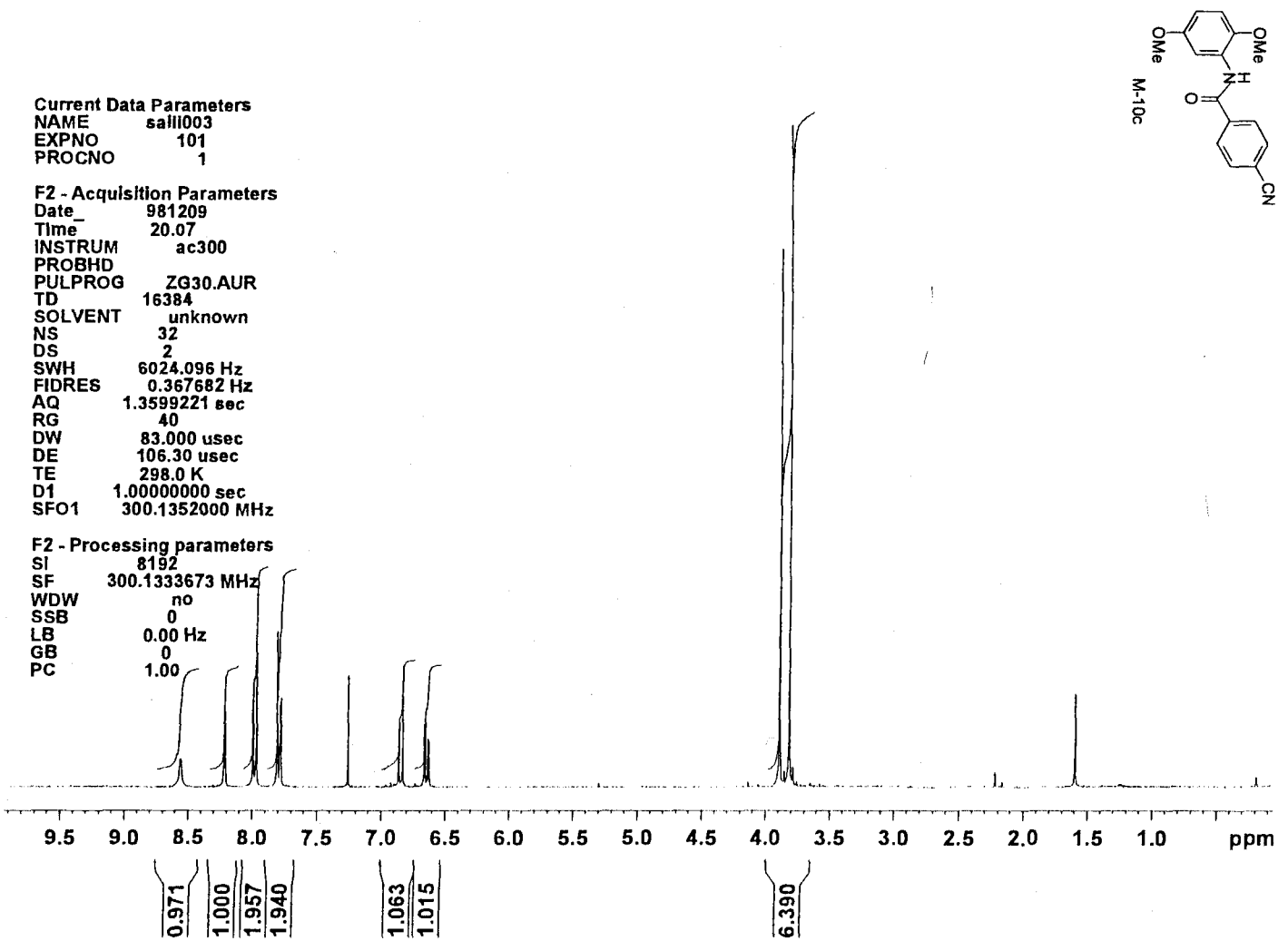
Current Data Parameters
NAME salli003
EXPNO 101
PROCNO 1
F2 - Acquisition Parameters
Date_ 981209
Time 20.07
INSTRUM ac300
PROBHD
PULPROG ZG30.AUR
TD 16384
SOLVENT unknown
NS 32
DS 2
SWH 6024.096 Hz
FIDRES 0.367682 Hz
AQ 1.3599221 sec
RG 40
DW 83.000 usec
DE 106.30 usec
TE 298.0 K
D1 1.00000000 sec
SFO1 300.1352000 MHz
F2 - Processing parameters
SI 8192
SF 300.1333673 MHz
WDW no
SSB 0
LB 0.00 Hz
GB 0
PC 1.00
OMe
OMe
H
N
O
CN
M-10c
9.5 9.0 8.5 8.0 7.5 7.0 6.5 6.0 5.5 5.0 4.5 4.0 3.5 3.0 2.5 2.0 1.5 1.0 ppm
0.971
1.000
1.957
1.940
1.063
1.015
6.390

S-11

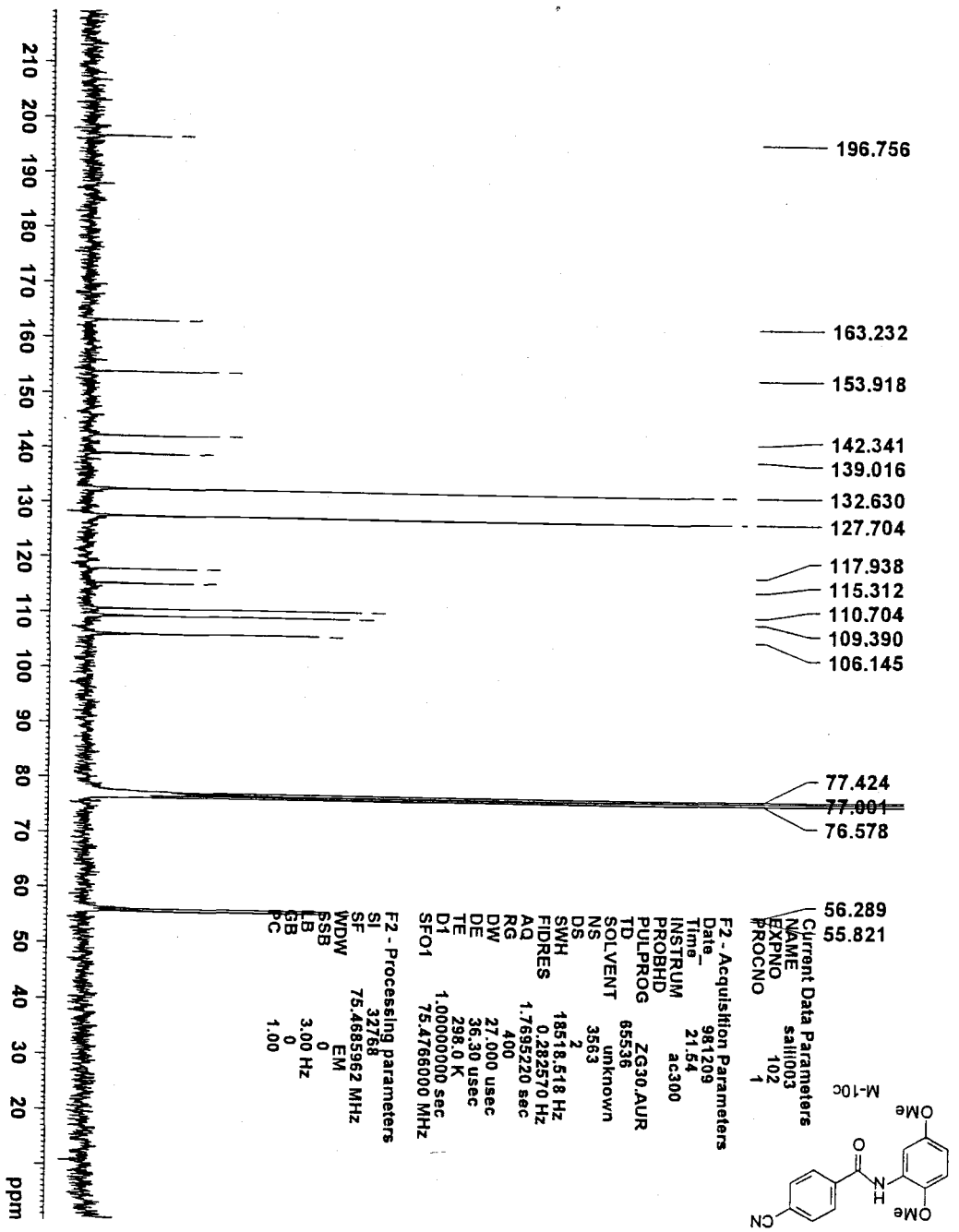
196.756
163.232
153.918
142.341
139.016
132.630
127.704
117.938
115.312
110.704
109.390
106.145
77.424
77.001
76.578
56.289
55.821
Current Data Parameters
NAME salli003
EXPNO 102
PROCNO 1
F2 - Acquisition Parameters
Date_ 981209
Time 21.54
INSTRUM ac300
PROBHD
PULPROG ZG30.AUR
TD 65536
SOLVENT unknown
NS 3563
DS 2
SWH 18518.518 Hz
FIDRES 0.282570 Hz
AQ 1.7695220 sec
RG 400
DW 27.000 usec
DE 36.30 usec
TE 298.0 K
D1 1.00000000 sec
SFO1 75.4766000 MHz
F2 - Processing parameters
SI 32768
SF 75.4685962 MHz
WDW EM
SSB 0
LB 3.00 Hz
GB 0
PC 1.00
M-10c
OMe
OMe
CN
210 200 190 180 170 160 150 140 130 120 110 100 90 80 70 60 50 40 30 20 ppm

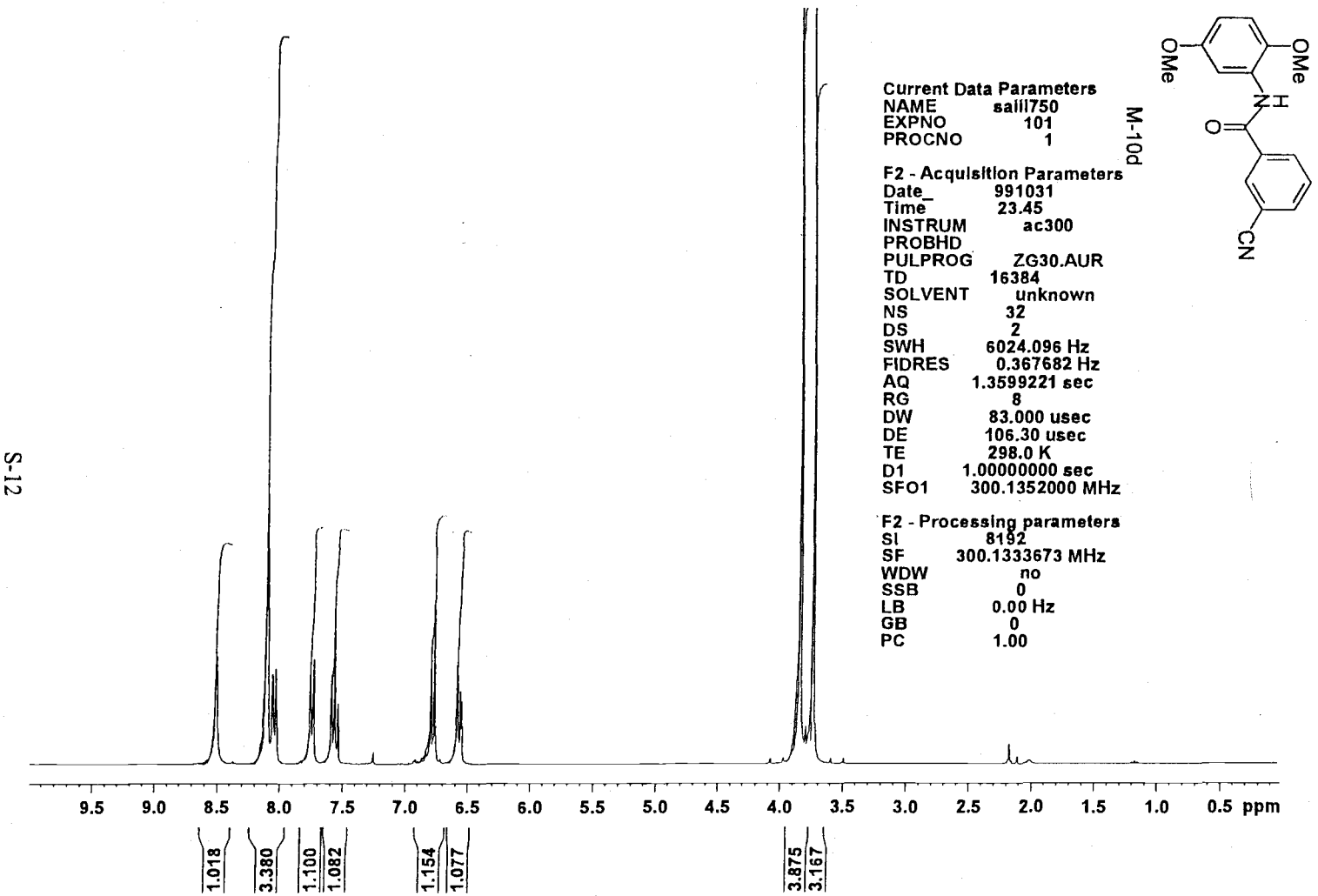
Current Data Parameters
NAME saiil750
EXPNO 101
PROCNO 1
M-10d
F2 - Acquisition Parameters
Date_ 991031
Time 23.45
INSTRUM ac300
PROBHD
PULPROG ZG30.AUR
TD 16384
SOLVENT unknown
NS 32
DS 2
SWH 6024.096 Hz
FIDRES 0.367682 Hz
AQ 1.3599221 sec
RG 8
DW 83.000 usec
DE 106.30 usec
TE 298.0 K
D1 1.00000000 sec
SFO1 300.1352000 MHz
F2 - Processing parameters
SI 8192
SF 300.1333673 MHz
WDW no
SSB 0
LB 0.00 Hz
GB 0
PC 1.00
OMe
OMe
N
H
O
CN
9.5 9.0 8.5 8.0 7.5 7.0 6.5 6.0 5.5 5.0 4.5 4.0 3.5 3.0 2.5 2.0 1.5 1.0 0.5 ppm
1.018
3.380
1.100
1.082
1.154
1.077
3.875
3.167

162.779
153.734
142.464
136.174
134.823
131.099
130.796
129.730
127.658
117.990
113.049
110.653
109.011
106.408
106.061
77.644
77.219
76.794
56.238
55.703
OMe
OMe
H
N
O
CN
M-10d
Current Data Parameters
NAME salli750
EXPNO 201
PROCNO 1
F2 - Acquisition Parameters
Date_ 991031
Time 23.59
INSTRUM ac300
PROBHD
PULPROG ZG30.AUR
TD 65536
SOLVENT unknown
NS 423
DS 2
SWH 18518.518 Hz
FIDRES 0.282570 Hz
AQ 1.7695220 sec
RG 400
DW 27.000 usec
DE 36.30 usec
TE 298.0 K
D1 1.00000000 sec
SFO1 75.4766000 MHz
F2 - Processing parameters
SI 32768
SF 75.4685962 MHz
WDW EM
SSB 0
LB 3.00 Hz
GB 0
PC 1.00
170 160 150 140 130 120 110 100 90 80 70 60 50 40 30 20 10 ppm

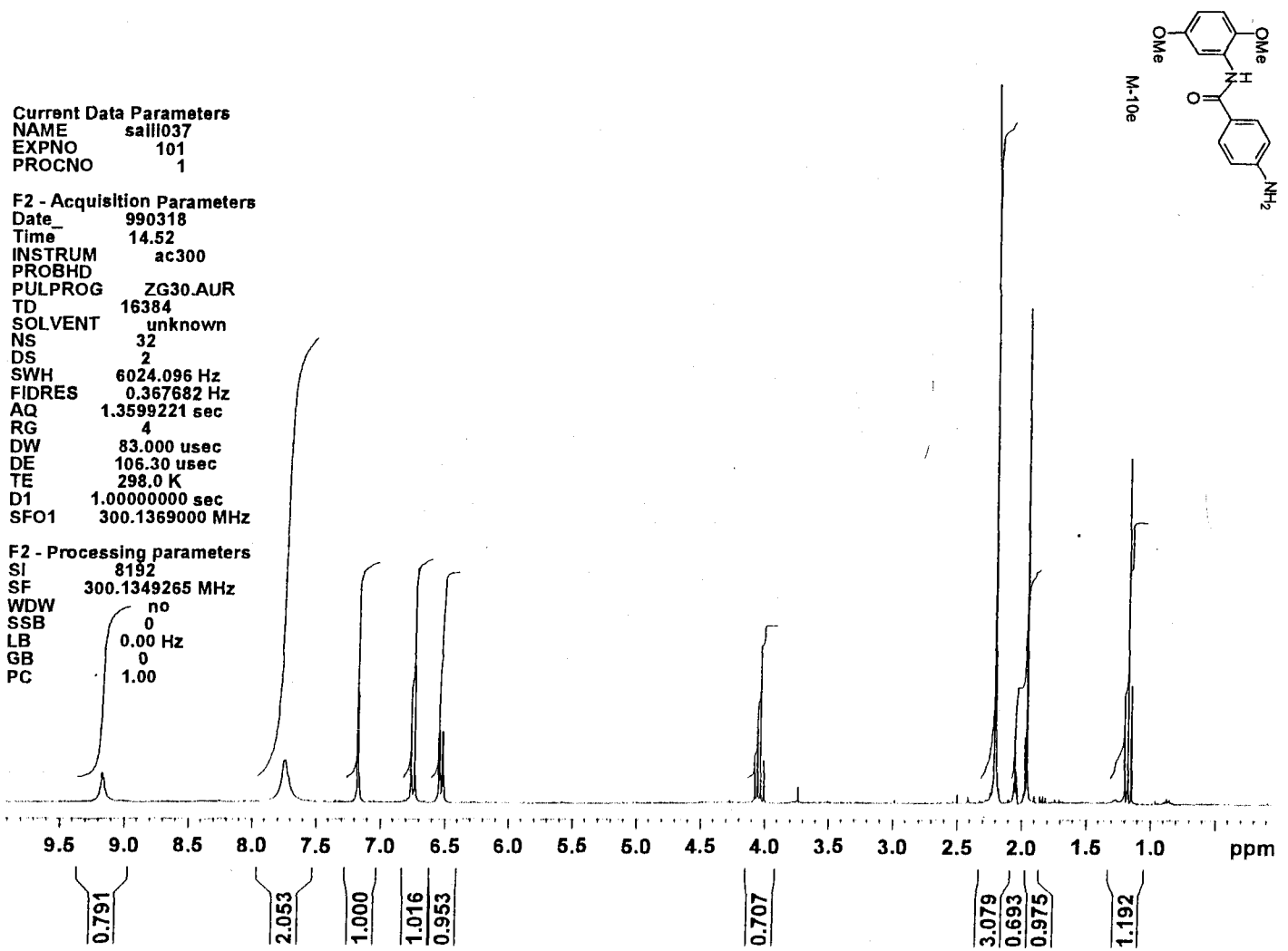
Current Data Parameters
NAME saiii037
EXPNO 101
PROCNO 1
F2 - Acquisition Parameters
Date_ 990318
Time 14.52
INSTRUM ac300
PROBHD
PULPROG ZG30.AUR
TD 16384
SOLVENT unknown
NS 32
DS 2
SWH 6024.096 Hz
FIDRES 0.367682 Hz
AQ 1.3599221 sec
RG 4
DW 83.000 usec
DE 106.30 usec
TE 298.0 K
D1 1.00000000 sec
SFO1 300.1369000 MHz
F2 - Processing parameters
SI 8192
SF 300.1349265 MHz
WDW no
SSB 0
LB 0.00 Hz
GB 0
PC 1.00
OMe
OMe
H
N
O
NH2
M-10e
9.5
9.0
8.5
8.0
7.5
7.0
6.5
6.0
5.5
5.0
4.5
4.0
3.5
3.0
2.5
2.0
1.5
1.0
ppm
0.791
2.053
1.000
1.016
0.953
0.707
3.079
0.693
0.975
1.192

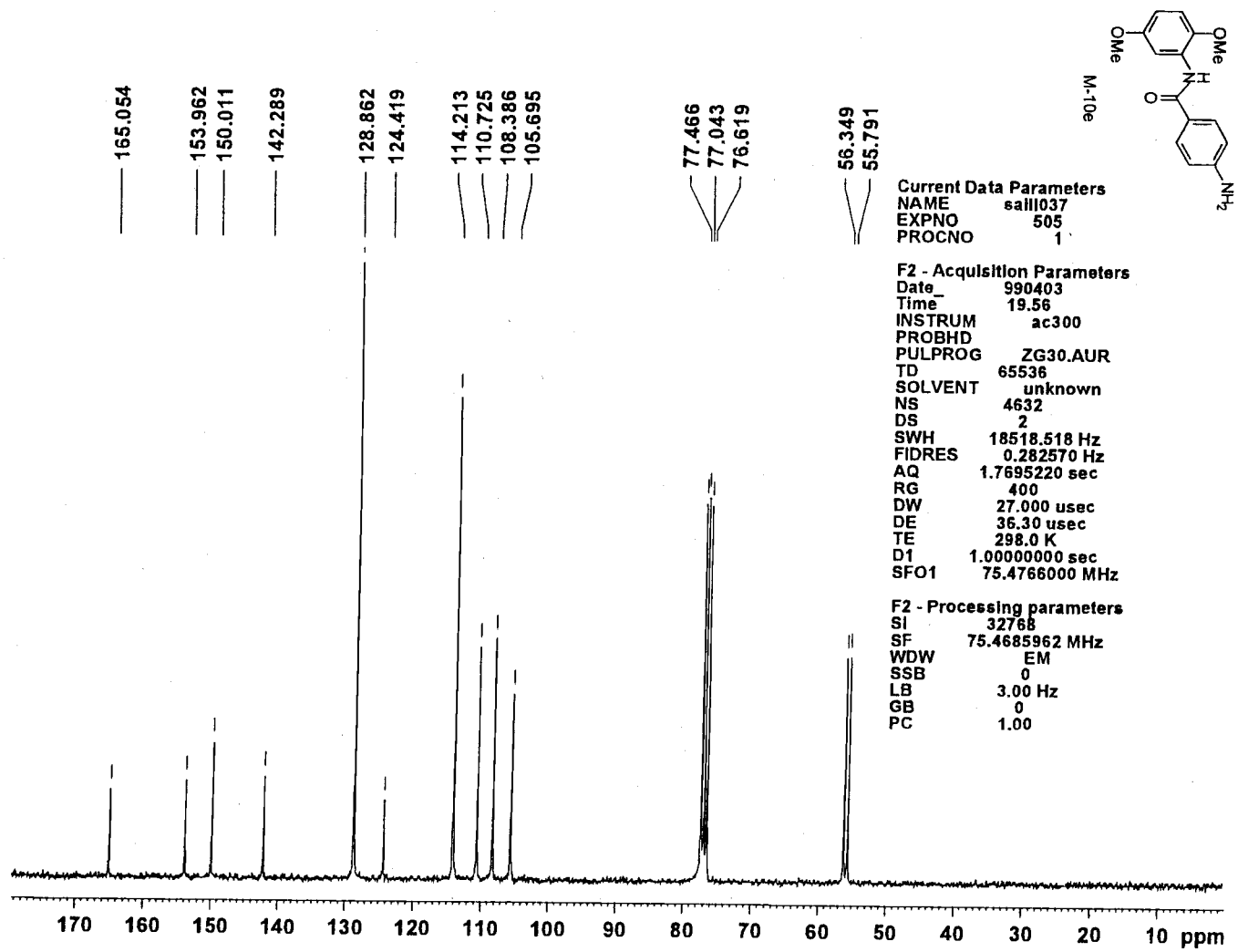
165.054
153.962
150.011
142.289
128.862
124.419
114.213
110.725
108.386
105.695
77.466
77.043
76.619
56.349
55.791
OMe
OMe
NH
O
NH2
M-10e
Current Data Parameters
NAME saiii037
EXPNO 505
PROCNO 1
F2 - Acquisition Parameters
Date_ 990403
Time 19.56
INSTRUM ac300
PROBHD
PULPROG ZG30.AUR
TD 65536
SOLVENT unknown
NS 4632
DS 2
SWH 18518.518 Hz
FIDRES 0.282570 Hz
AQ 1.7695220 sec
RG 400
DW 27.000 usec
DE 36.30 usec
TE 298.0 K
D1 1.00000000 sec
SFO1 75.4766000 MHz
F2 - Processing parameters
SI 32768
SF 75.4685962 MHz
WDW EM
SSB 0
LB 3.00 Hz
GB 0
PC 1.00
170 160 150 140 130 120 110 100 90 80 70 60 50 40 30 20 10 ppm

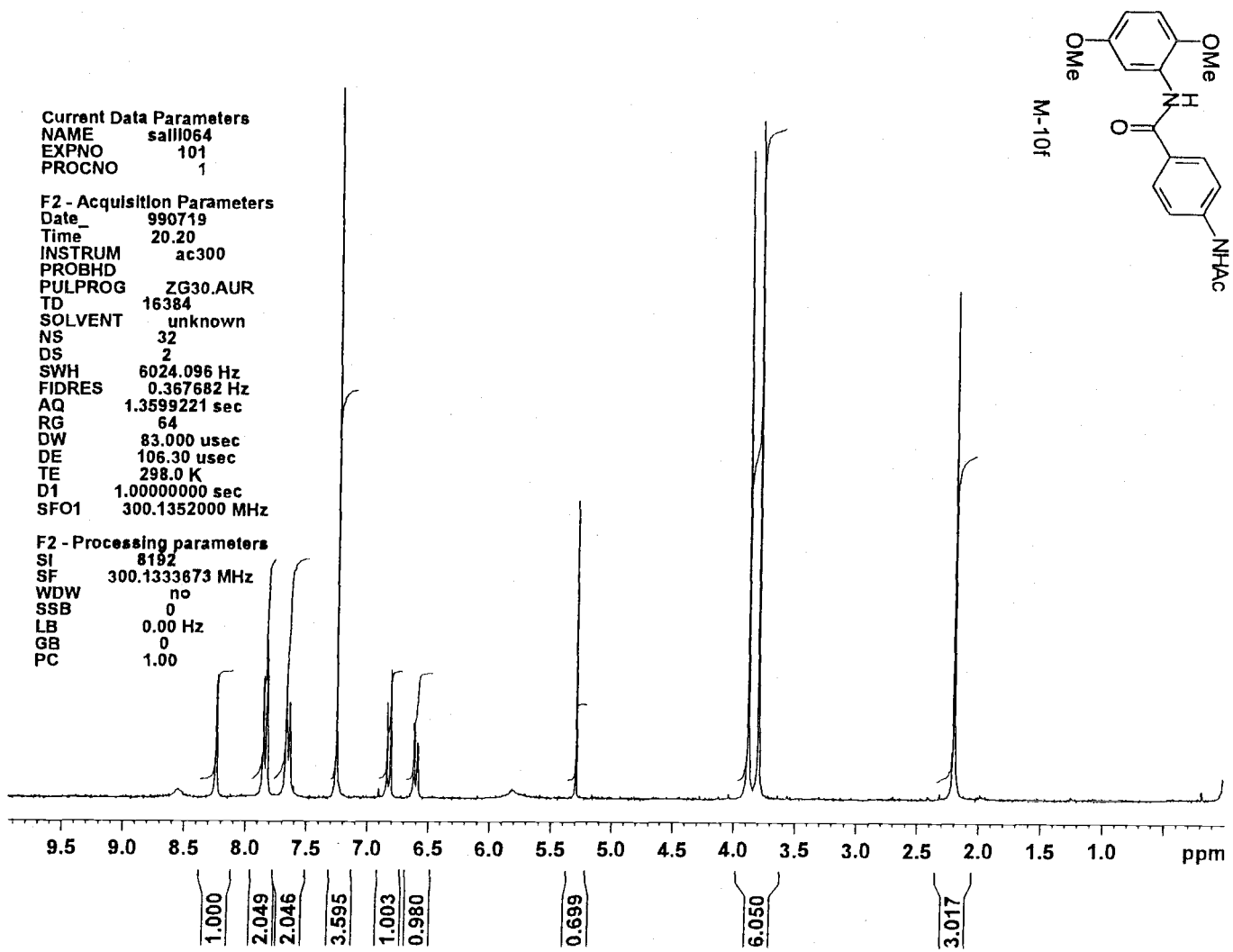
Current Data Parameters
NAME salll064
EXPNO 101
PROCNO 1
F2 - Acquisition Parameters
Date_ 990719
Time 20.20
INSTRUM ac300
PROBHD
PULPROG ZG30.AUR
TD 16384
SOLVENT unknown
NS 32
DS 2
SWH 6024.096 Hz
FIDRES 0.367682 Hz
AQ 1.3599221 sec
RG 64
DW 83.000 usec
DE 106.30 usec
TE 298.0 K
D1 1.00000000 sec
SFO1 300.1352000 MHz
F2 - Processing parameters
SI 8192
SF 300.1333673 MHz
WDW no
SSB 0
LB 0.00 Hz
GB 0
PC 1.00
OMe
OMe
NH
O
NHAc
M-10f
9.5 9.0 8.5 8.0 7.5 7.0 6.5 6.0 5.5 5.0 4.5 4.0 3.5 3.0 2.5 2.0 1.5 1.0 ppm
1.000
2.049
2.046
3.595
1.003
0.980
0.699
6.050
3.017

OMe
OMe
H
N
O
NHAc
M-10f
168.512
164.545
153.898
142.327
141.140
130.335
128.280
128.104
119.222
110.687
108.764
105.871
77.425
77.203
77.001
76.578
56.309
55.794
53.410
24.666
Current Data Parameters
NAME saiii064
EXPNO 201
PROCNO 1
F2 - Acquisition Parameters
Date_ 990719
Time 21.53
INSTRUM ac300
PROBHD
PULPROG ZG30.AUR
TD 65536
SOLVENT unknown
NS 3003
DS 2
SWH 18518.518 Hz
FIDRES 0.282570 Hz
AQ 1.7695220 sec
RG 400
DW 27.000 usec
DE 36.30 usec
TE 298.0 K
D1 1.00000000 sec
SFO1 75.4766000 MHz
F2 - Processing parameters
SI 32768
SF 75.4685962 MHz
WDW EM
SSB 0
LB 3.00 Hz
GB 0
PC 1.00
170 160 150 140 130 120 110 100 90 80 70 60 50 40 30 20 10 ppm

OMe
OMe
N
H
O
NO2
M-10g

Current Data Parameters
NAME salil001
EXPNO 101
PROCNO 1
F2 - Acquisition Parameters
Date_ 981207
Time 18.00
INSTRUM ac300
PROBHD
PULPROG ZG30.AUR
TD 16384
SOLVENT unknown
NS 32
DS 2
SWH 6024.096 Hz
FIDRES 0.367682 Hz
AQ 1.3599221 sec
RG 40
DW 83.000 usec
DE 106.30 usec
TE 298.0 K
D1 1.00000000 sec
SFO1 300.1352000 MHz
F2 - Processing parameters
SI 8192
SF 300.1333673 MHz
WDW no
SSB 0
LB 0.00 Hz
GB 0
PC 1.00
9.5 9.0 8.5 8.0 7.5 7.0 6.5 6.0 5.5 5.0 4.5 4.0 3.5 3.0 2.5 2.0 1.5 1.0 ppm
0.997
2.058
1.015
2.071
1.040
1.000
3.198
3.252

162.995
153.925
149.696
142.352
140.666
128.195
127.687
124.025
110.711
109.481
106.168
77.413
76.566
56.295
55.827
OMe
OMe
NH
O
NO2
M-109
Current Data Parameters
NAME salil001
EXPNO 102
PROCNO 1
F2 - Acquisition Parameters
Date_ 981207
Time 18.50
INSTRUM ac300
PROBHD
PULPROG ZG30.AUR
TD 65536
SOLVENT unknown
NS 1633
DS 2
SWH 18518.518 Hz
FIDRES 0.282570 Hz
AQ 1.7695220 sec
RG 400
DW 27.000 usec
DE 36.30 usec
TE 298.0 K
D1 1.00000000 sec
SFO1 75.4766000 MHz
F2 - Processing parameters
SI 32768
SF 75.4685962 MHz
WDW EM
SSB 0
LB 3.00 Hz
GB 0
PC 1.00
170 160 150 140 130 120 110 100 90 80 70 60 50 40 30 20 10 ppm

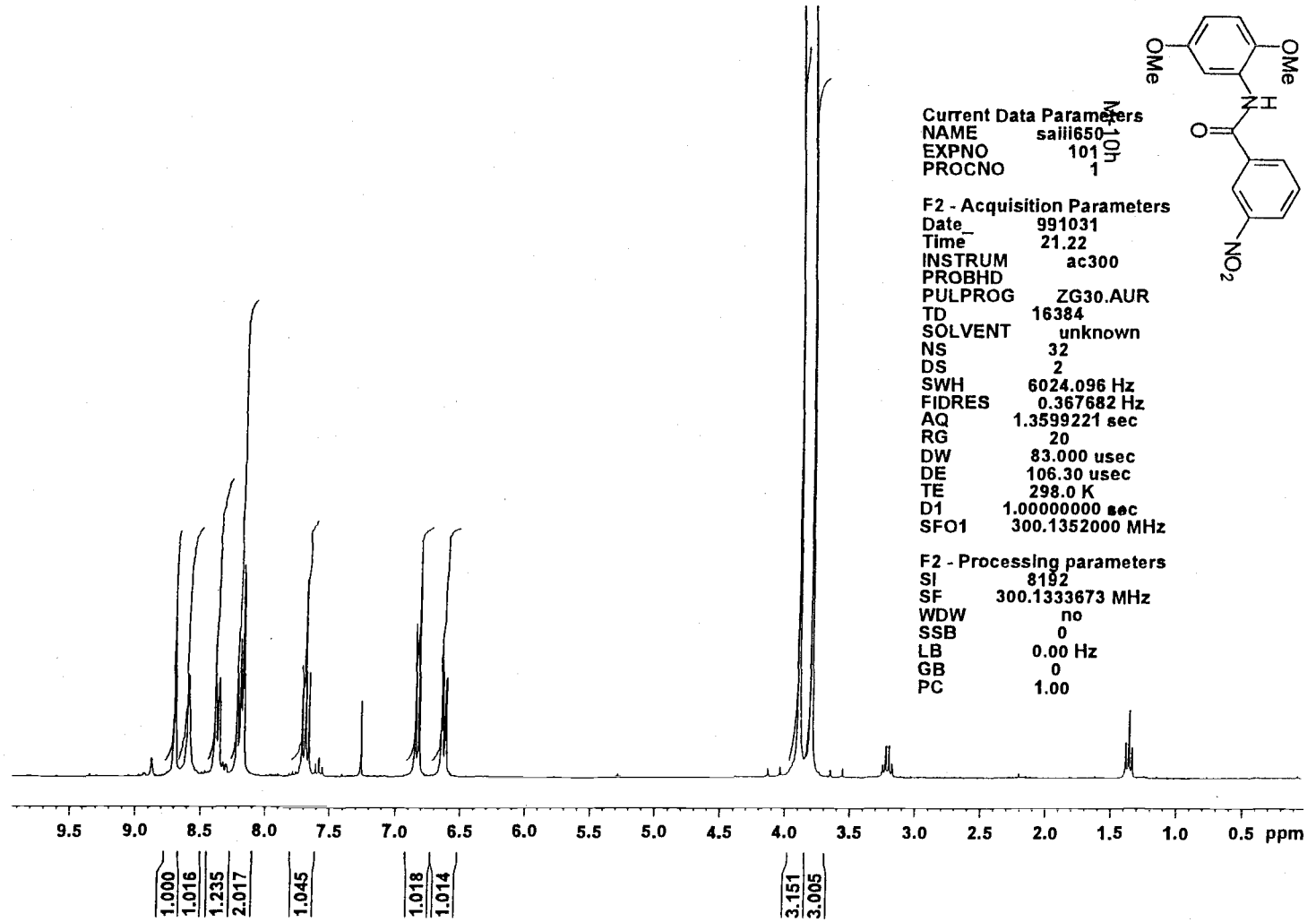
Current Data Parameters
NAME saiii650_10h
EXPNO 101
PROCNO 1
F2 - Acquisition Parameters
Date_ 991031
Time 21.22
INSTRUM ac300
PROBHD
PULPROG ZG30.AUR
TD 16384
SOLVENT unknown
NS 32
DS 2
SWH 6024.096 Hz
FIDRES 0.367682 Hz
AQ 1.3599221 sec
RG 20
DW 83.000 usec
DE 106.30 usec
TE 298.0 K
D1 1.00000000 sec
SFO1 300.1352000 MHz
F2 - Processing parameters
SI 8192
SF 300.1333673 MHz
WDW no
SSB 0
LB 0.00 Hz
GB 0
PC 1.00
OMe
OMe
H
N
O
NO2
9.5 9.0 8.5 8.0 7.5 7.0 6.5 6.0 5.5 5.0 4.5 4.0 3.5 3.0 2.5 2.0 1.5 1.0 0.5 ppm
1.000
1.016
1.235
2.017
1.045
1.018
1.014
3.151
3.005

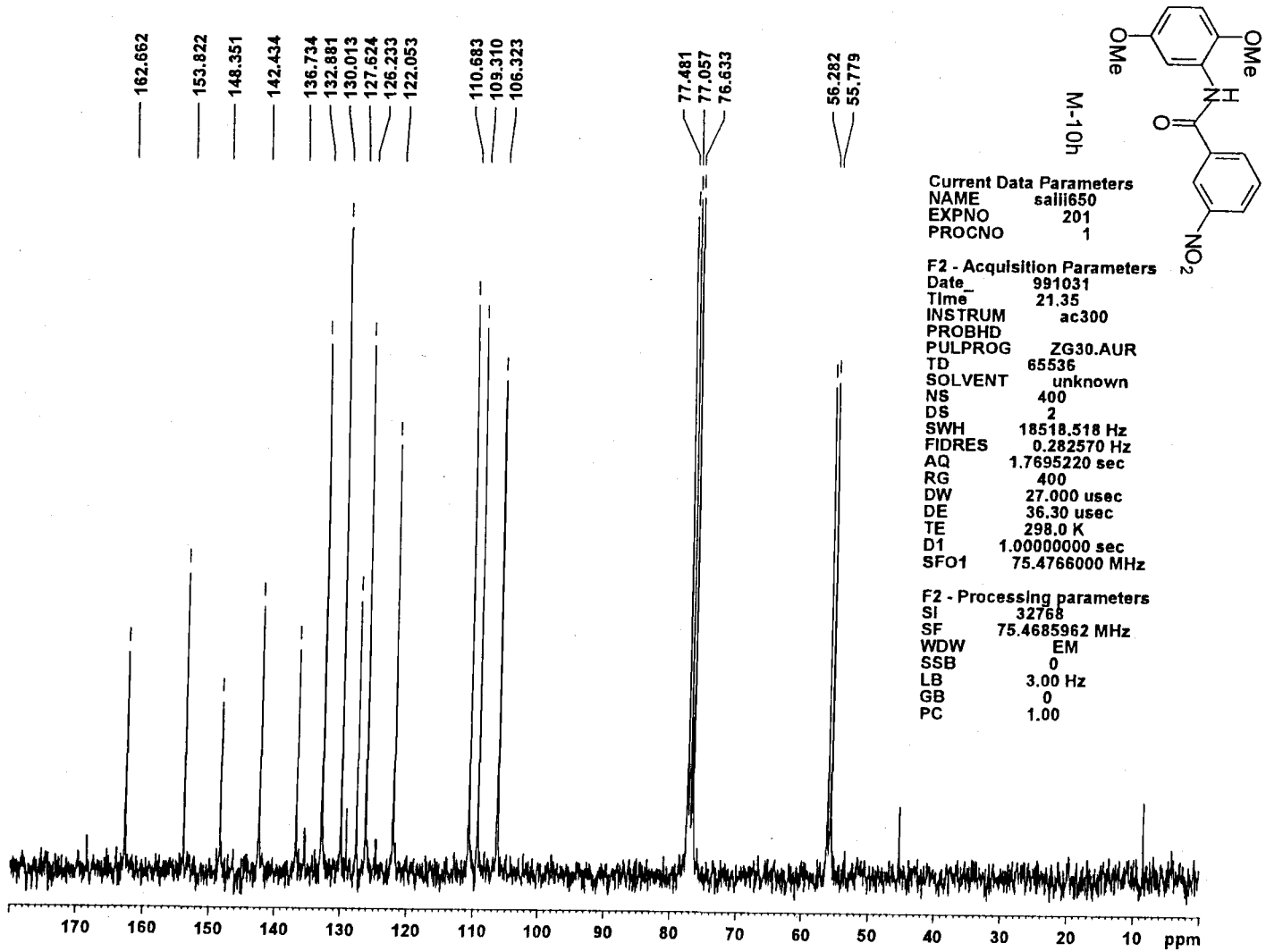
162.662
153.822
148.351
142.434
136.734
132.881
130.013
127.624
126.233
122.053
110.683
109.310
106.323
77.481
77.057
76.633
56.282
55.779
OMe
OMe
N
H
O
NO2
M-10h
Current Data Parameters
NAME salii650
EXPNO 201
PROCNO 1
F2 - Acquisition Parameters
Date_ 991031
Time 21.35
INSTRUM ac300
PROBHD
PULPROG ZG30.AUR
TD 65536
SOLVENT unknown
NS 400
DS 2
SWH 18518.518 Hz
FIDRES 0.282570 Hz
AQ 1.7695220 sec
RG 400
DW 27.000 usec
DE 36.30 usec
TE 298.0 K
D1 1.00000000 sec
SFO1 75.4766000 MHz
F2 - Processing parameters
SI 32768
SF 75.4685962 MHz
WDW EM
SSB 0
LB 3.00 Hz
GB 0
PC 1.00
170 160 150 140 130 120 110 100 90 80 70 60 50 40 30 20 10 ppm

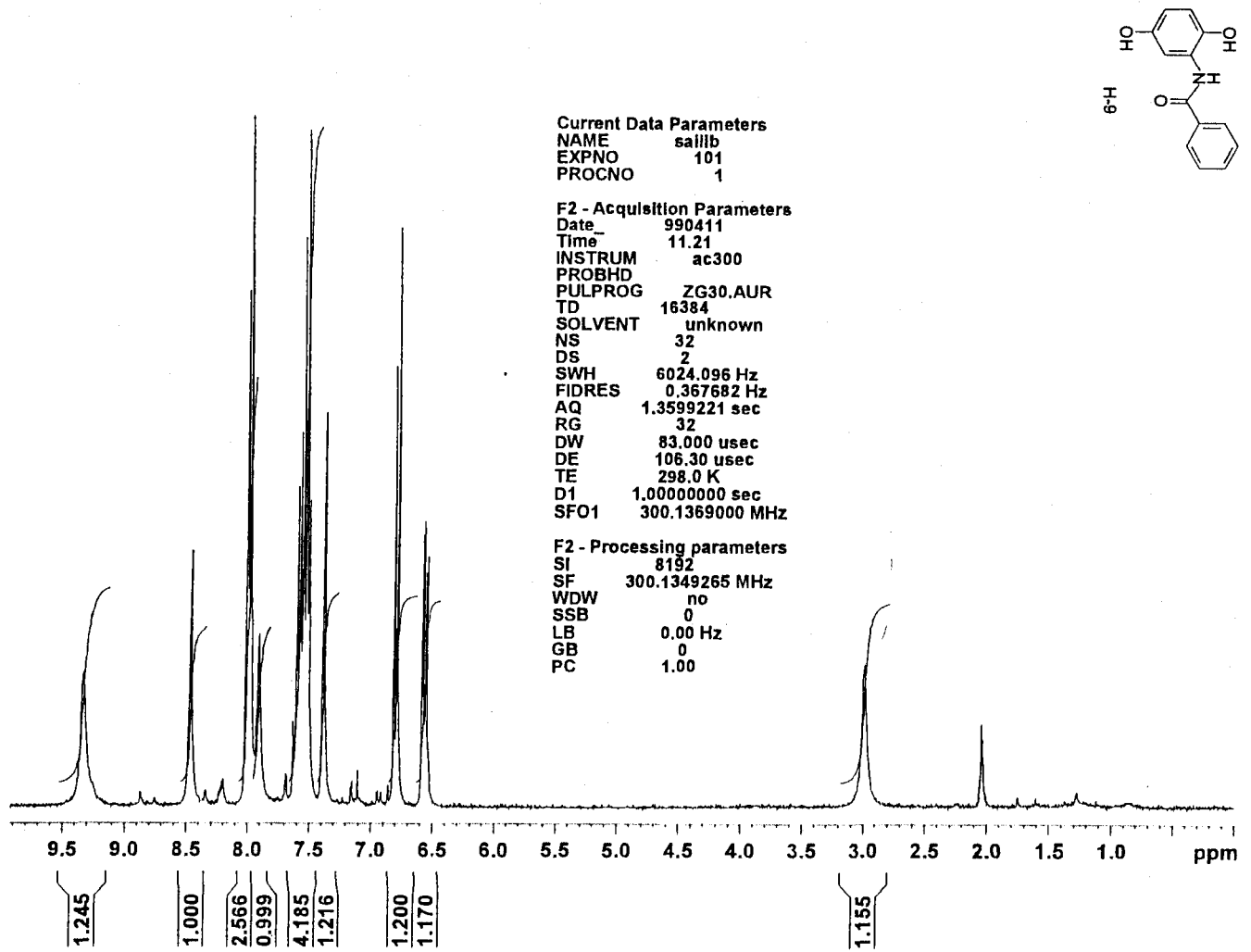
Current Data Parameters
NAME salilb
EXPNO 101
PROCNO 1
F2 - Acquisition Parameters
Date_ 990411
Time 11.21
INSTRUM ac300
PROBHD
PULPROG ZG30.AUR
TD 16384
SOLVENT unknown
NS 32
DS 2
SWH 6024.096 Hz
FIDRES 0.367682 Hz
AQ 1.3599221 sec
RG 32
DW 83.000 usec
DE 106.30 usec
TE 298.0 K
D1 1.00000000 sec
SFO1 300.1369000 MHz
F2 - Processing parameters
SI 8192
SF 300.1349265 MHz
WDW no
SSB 0
LB 0.00 Hz
GB 0
PC 1.00
9.5 9.0 8.5 8.0 7.5 7.0 6.5 6.0 5.5 5.0 4.5 4.0 3.5 3.0 2.5 2.0 1.5 1.0 ppm
1.245
1.000
2.566
0.999
4.185
1.216
1.200
1.170
1.155
HO
OH
NH
O
H-9

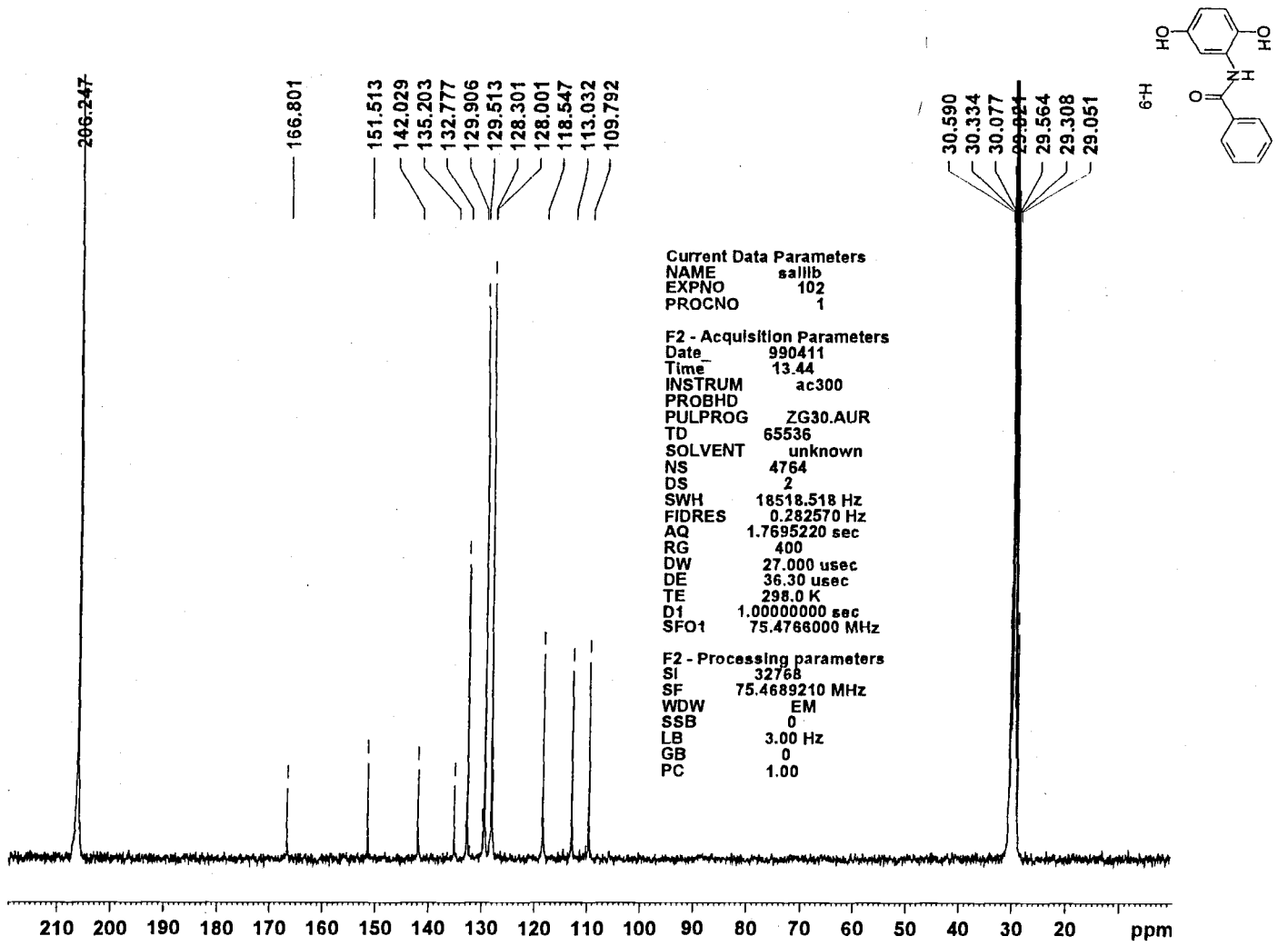
206.247
166.801
151.513
142.029
135.203
132.777
129.906
129.513
128.301
128.001
118.547
113.032
109.792
30.590
30.334
30.077
29.821
29.564
29.308
29.051
OH
OH
N
H
O
H-9
Current Data Parameters
NAME sallib
EXPNO 102
PROCNO 1
F2 - Acquisition Parameters
Date_ 990411
Time 13.44
INSTRUM ac300
PROBHD
PULPROG ZG30.AUR
TD 65536
SOLVENT unknown
NS 4764
DS 2
SWH 18518.518 Hz
FIDRES 0.282570 Hz
AQ 1.7695220 sec
RG 400
DW 27.000 usec
DE 36.30 usec
TE 298.0 K
D1 1.00000000 sec
SFO1 75.4766000 MHz
F2 - Processing parameters
SI 32768
SF 75.4689210 MHz
WDW EM
SSB 0
LB 3.00 Hz
GB 0
PC 1.00
210 200 190 180 170 160 150 140 130 120 110 100 90 80 70 60 50 40 30 20 ppm

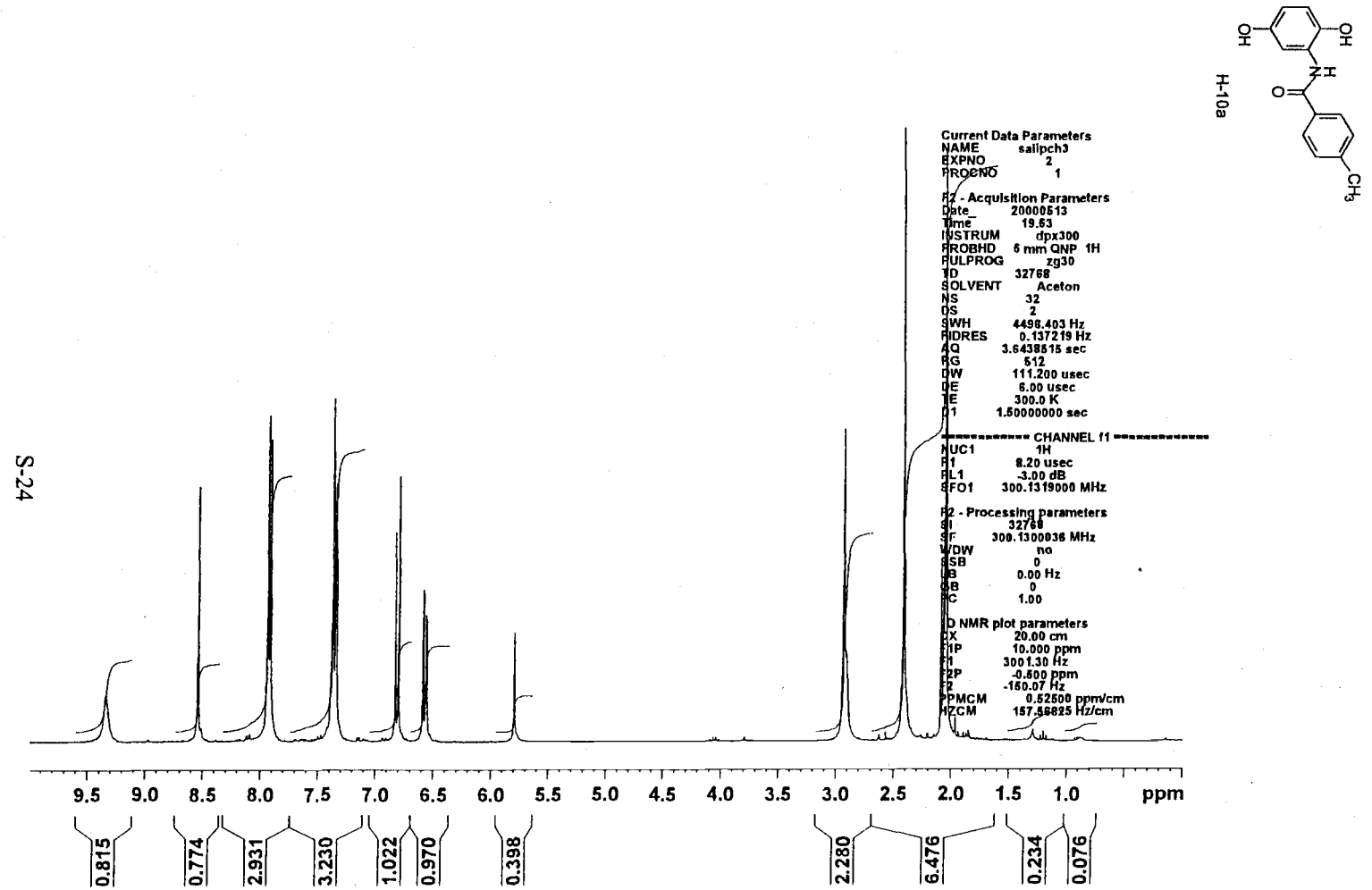
H-10a
HO
HO
N
H
O
CH3
Current Data Parameters
NAME sallpch3
EXPNO 2
PROCNO 1
F2 - Acquisition Parameters
Date_ 20000513
Time 19.63
INSTRUM dpx300
PROBHD 5 mm QNP 1H
PULPROG zg30
TD 32768
SOLVENT Aceton
NS 32
DS 2
SWH 4498.403 Hz
FIDRES 0.137219 Hz
AQ 3.6438515 sec
RG 512
DW 111.200 usec
DE 6.00 usec
TE 300.0 K
D1 1.50000000 sec
CHANNEL f1
NUC1 1H
P1 8.20 usec
PL1 -3.00 dB
SFO1 300.1319000 MHz
F2 - Processing parameters
SI 32768
SF 300.1300036 MHz
WDW no
SSB 0
LB 0.00 Hz
GB 0
PC 1.00
1D NMR plot parameters
CX 20.00 cm
F1P 10.000 ppm
F1 3001.30 Hz
F2P -0.500 ppm
F2 -150.07 Hz
PPMCM 0.52500 ppm/cm
HZCM 157.56825 Hz/cm
9.5 9.0 8.5 8.0 7.5 7.0 6.5 6.0 5.5 5.0 4.5 4.0 3.5 3.0 2.5 2.0 1.5 1.0 ppm
0.815
0.774
2.931
3.230
1.022
0.970
0.398
2.280
6.476
0.234
0.076

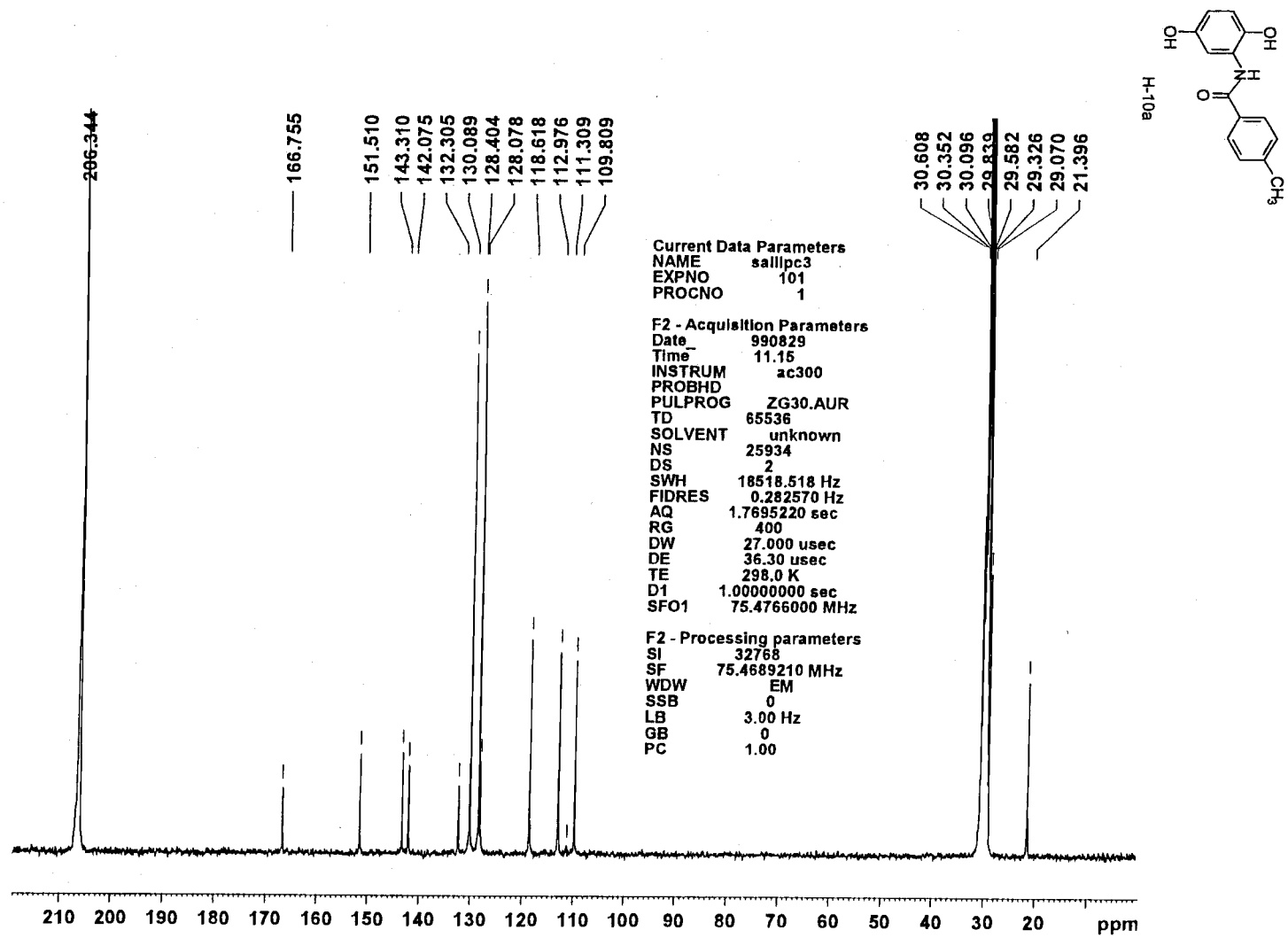
206.344
166.755
151.510
143.310
142.075
132.305
130.089
128.404
128.078
118.618
112.976
111.309
109.809
30.608
30.352
30.096
29.839
29.582
29.326
29.070
21.396
Current Data Parameters
NAME saillpc3
EXPNO 101
PROCNO 1
F2 - Acquisition Parameters
Date_ 990829
Time 11.15
INSTRUM ac300
PROBHD
PULPROG ZG30.AUR
TD 65536
SOLVENT unknown
NS 25934
DS 2
SWH 18518.518 Hz
FIDRES 0.282570 Hz
AQ 1.7695220 sec
RG 400
DW 27.000 usec
DE 36.30 usec
TE 298.0 K
D1 1.00000000 sec
SFO1 75.4766000 MHz
F2 - Processing parameters
SI 32768
SF 75.4689210 MHz
WDW EM
SSB 0
LB 3.00 Hz
GB 0
PC 1.00
210 200 190 180 170 160 150 140 130 120 110 100 90 80 70 60 50 40 30 20 ppm
H-10a
OH
OH
N
H
O
CH3

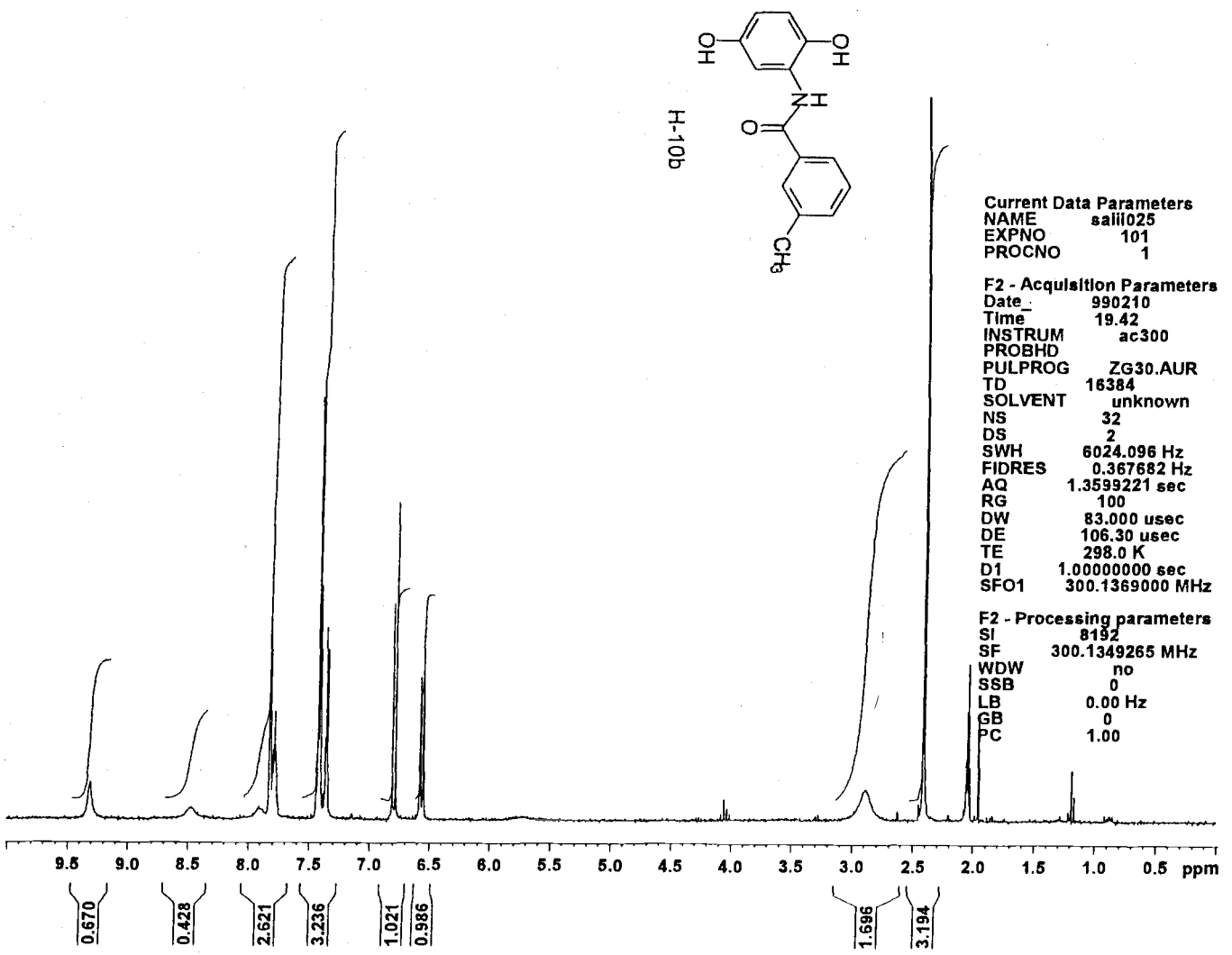
H-10b
OH
OH
N
H
O
CH3
Current Data Parameters
NAME salii025
EXPNO 101
PROCNO 1
F2 - Acquisition Parameters
Date_ 990210
Time 19.42
INSTRUM ac300
PROBHD
PULPROG ZG30.AUR
TD 16384
SOLVENT unknown
NS 32
DS 2
SWH 6024.096 Hz
FIDRES 0.367682 Hz
AQ 1.3599221 sec
RG 100
DW 83.000 usec
DE 106.30 usec
TE 298.0 K
D1 1.00000000 sec
SFO1 300.1369000 MHz
F2 - Processing parameters
SI 8192
SF 300.1349265 MHz
WDW no
SSB 0
LB 0.00 Hz
GB 0
PC 1.00
9.5 9.0 8.5 8.0 7.5 7.0 6.5 6.0 5.5 5.0 4.5 4.0 3.5 3.0 2.5 2.0 1.5 1.0 0.5 ppm
0.670
0.428
2.621
3.236
1.021
0.986
1.696
3.194

S-27

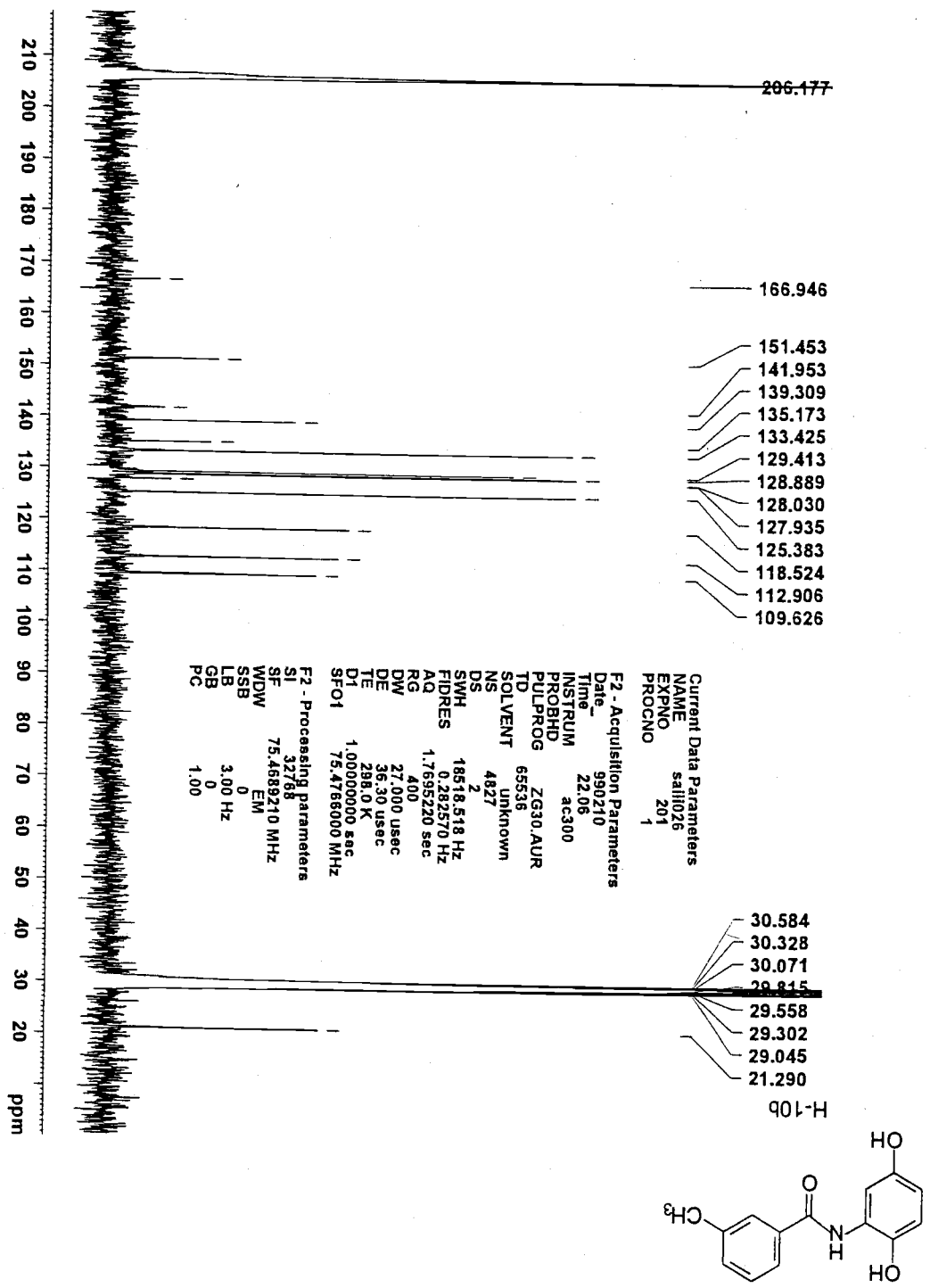
206.177
166.946
151.453
141.953
139.309
135.173
133.425
129.413
128.889
128.030
127.935
125.383
118.524
112.906
109.626
30.584
30.328
30.071
29.815
29.558
29.302
29.045
21.290
Current Data Parameters
NAME salli026
EXPNO 201
PROCNO 1
F2 - Acquisition Parameters
Date_ 990210
Time 22.06
INSTRUM ac300
PROBHD
PULPROG ZG30.AUR
TD 65536
SOLVENT unknown
NS 4827
DS 2
SWH 18518.518 Hz
FIDRES 0.282570 Hz
AQ 1.7695220 sec
RG 400
DW 27.000 usec
DE 36.30 usec
TE 298.0 K
D1 1.00000000 sec
SFO1 75.4766000 MHz
F2 - Processing parameters
SI 32768
SF 75.4689210 MHz
WDW EM
SSB 0
LB 3.00 Hz
GB 0
PC 1.00
210 200 190 180 170 160 150 140 130 120 110 100 90 80 70 60 50 40 30 20
ppm
H-10b
HO
O
N
H
HO
CH3

H-10c
OH
OH
N
H
O
CN
Current Data Parameters
NAME salli028
EXPNO 101
PROCNO 1
F2 - Acquisition Parameters
Date_ 990206
Time 17.02
INSTRUM ac300
PROBHD
PULPROG ZG30.AUR
TD 16384
SOLVENT unknown
NS 32
DS 2
SWH 6024.096 Hz
FIDRES 0.367682 Hz
AQ 1.3599221 sec
RG 100
DW 83.000 usec
DE 106.30 usec
TE 298.0 K
D1 1.00000000 sec
SFO1 300.1369000 MHz
F2 - Processing parameters
SI 8192
SF 300.1349265 MHz
WDW no
SSB 0
LB 0.00 Hz
GB 0
PC 1.00
9.5 9.0 8.5 8.0 7.5 7.0 6.5 6.0 5.5 5.0 4.5 4.0 3.5 3.0 2.5 2.0 1.5 1.0 ppm
0.727
2.214
2.596
1.080
1.000
2.847
10.874

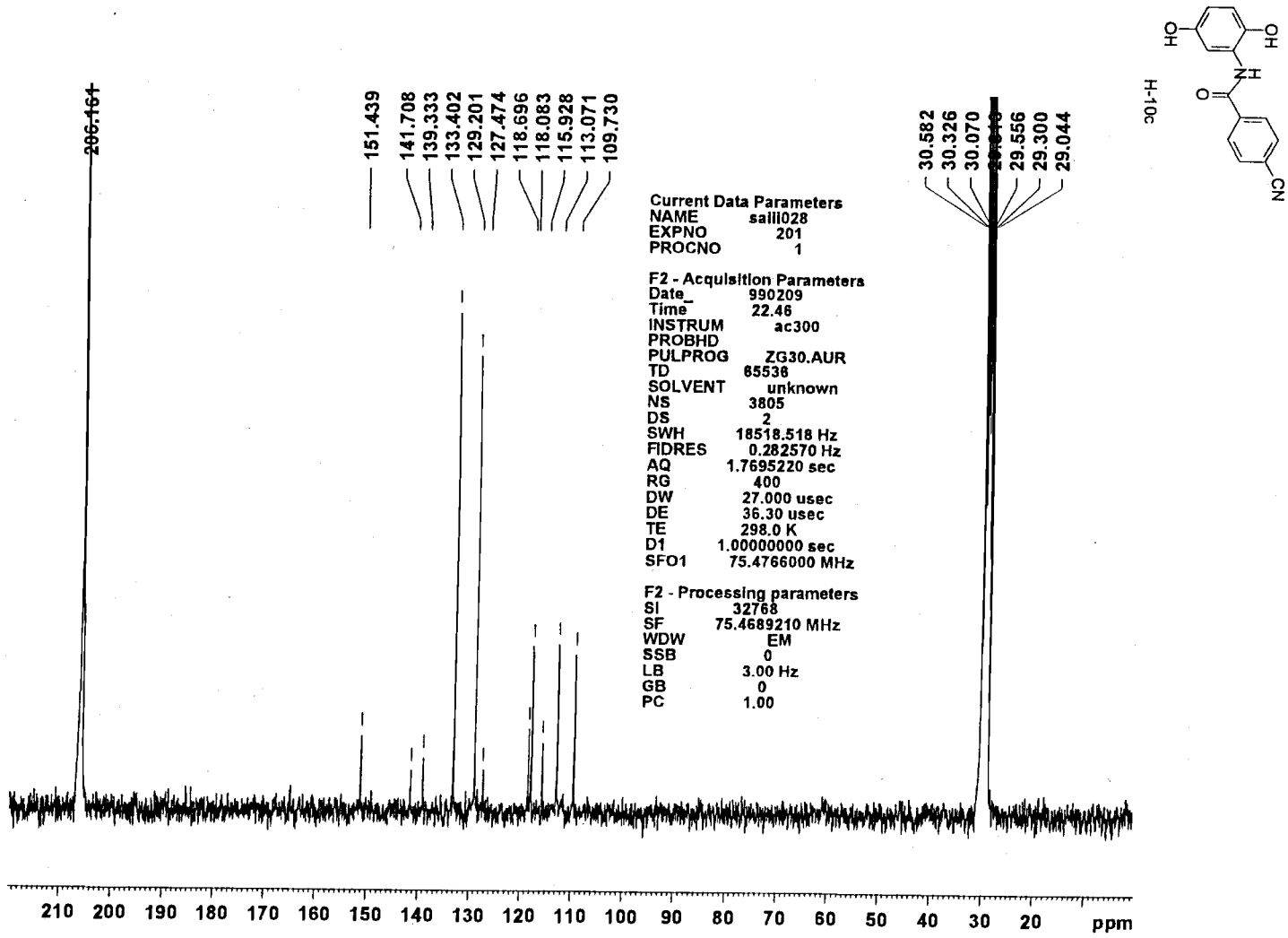
206.161
151.439
141.708
139.333
133.402
129.201
127.474
118.696
118.083
115.928
113.071
109.730
30.582
30.326
30.070
29.556
29.300
29.044
Current Data Parameters
NAME saiii028
EXPNO 201
PROCNO 1
F2 - Acquisition Parameters
Date_ 990209
Time 22.46
INSTRUM ac300
PROBHD
PULPROG ZG30.AUR
TD 65536
SOLVENT unknown
NS 3805
DS 2
SWH 18518.518 Hz
FIDRES 0.282570 Hz
AQ 1.7695220 sec
RG 400
DW 27.000 usec
DE 36.30 usec
TE 298.0 K
D1 1.00000000 sec
SFO1 75.4766000 MHz
F2 - Processing parameters
SI 32768
SF 75.4689210 MHz
WDW EM
SSB 0
LB 3.00 Hz
GB 0
PC 1.00
HO
HO
NH
O
CN
H-10c
210 200 190 180 170 160 150 140 130 120 110 100 90 80 70 60 50 40 30 20 ppm

M-10d
OMe
OMe
N
H
O
CN
Current Data Parameters
NAME saili800
EXPNO 101
PROCNO 1
F2 - Acquisition Parameters
Date_ 991031
Time 21.45
INSTRUM ac300
PROBHD
PULPROG ZG30.AUR
TD 16384
SOLVENT unknown
NS 32
DS 2
SWH 6024.096 Hz
FIDRES 0.367682 Hz
AQ 1.3599221 sec
RG 32
DW 83.000 usec
DE 106.30 usec
TE 298.0 K
D1 1.00000000 sec
SFO1 300.1369000 MHz
F2 - Processing parameters
SI 8192
SF 300.1349265 MHz
WDW no
SSB 0
LB 0.00 Hz
GB 0
PC 1.00
9.5 9.0 8.5 8.0 7.5 7.0 6.5 6.0 5.5 5.0 4.5 4.0 3.5 3.0 2.5 2.0 1.5 1.0 0.5 ppm
0.826
2.568
1.497
0.991
0.941
1.000
2.982

M-10d
OMe
OMe
N
H
O
CN
164.849
151.464
142.039
136.580
135.912
132.773
132.102
130.811
127.511
118.721
118.222
113.571
113.277
110.098
30.648
30.391
30.134
29.620
29.363
29.106
Current Data Parameters
NAME saili800
EXPNO 201
PROCNO 1
F2 - Acquisition Parameters
Date_ 991031
Time 23.17
INSTRUM ac300
PROBHD
PULPROG ZG30.AUR
TD 65536
SOLVENT unknown
NS 3078
DS 2
SWH 18518.518 Hz
FIDRES 0.282570 Hz
AQ 1.7695220 sec
RG 400
DW 27.000 usec
DE 36.30 usec
TE 298.0 K
D1 1.00000000 sec
SFO1 75.4766000 MHz
F2 - Processing parameters
SI 32768
SF 75.4689210 MHz
WDW EM
SSB 0
LB 3.00 Hz
GB 0
PC 1.00
170 160 150 140 130 120 110 100 90 80 70 60 50 40 30 20 10 ppm

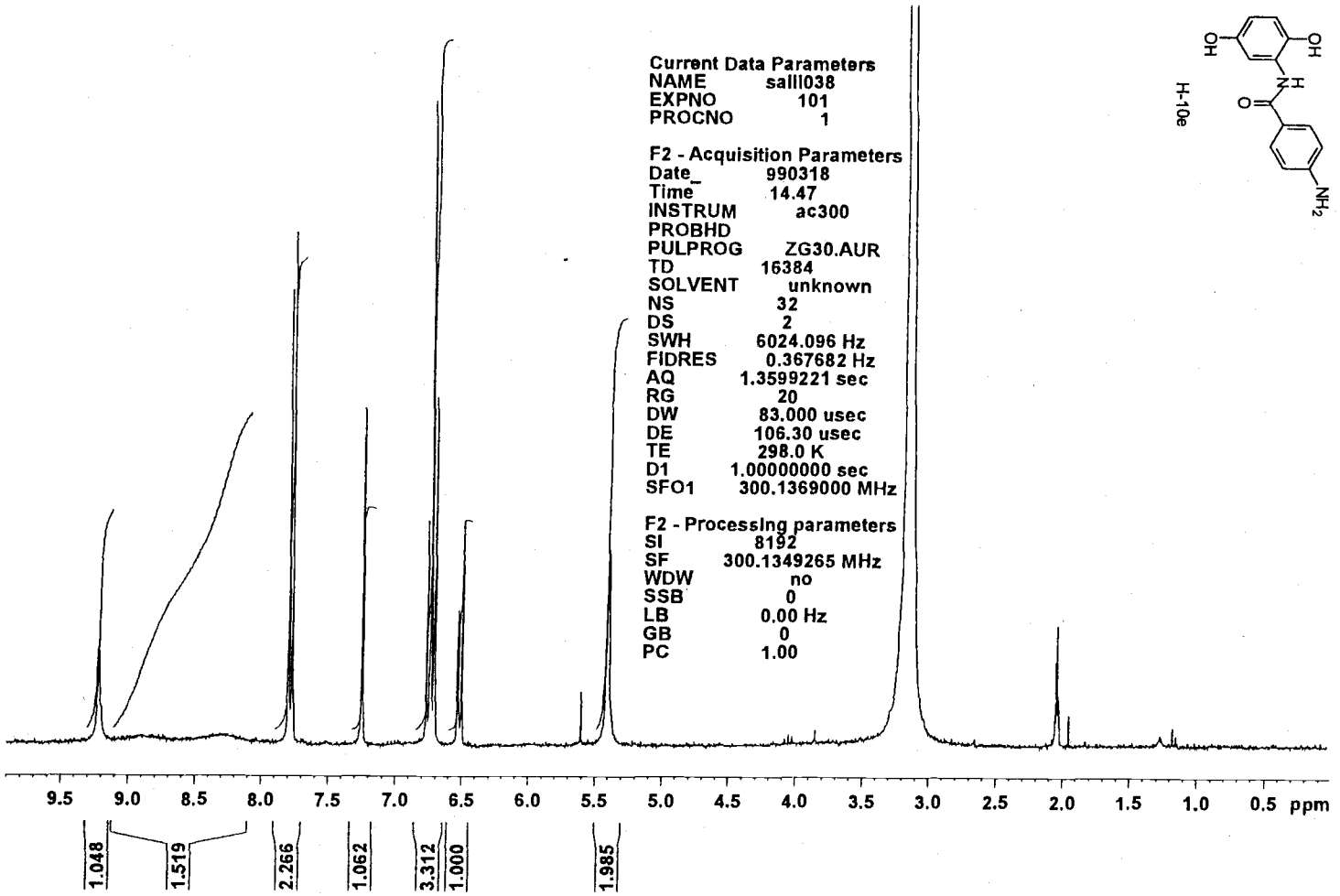
Current Data Parameters
NAME salll038
EXPNO 101
PROCNO 1
F2 - Acquisition Parameters
Date_ 990318
Time 14.47
INSTRUM ac300
PROBHD
PULPROG ZG30.AUR
TD 16384
SOLVENT unknown
NS 32
DS 2
SWH 6024.096 Hz
FIDRES 0.367682 Hz
AQ 1.3599221 sec
RG 20
DW 83.000 usec
DE 106.30 usec
TE 298.0 K
D1 1.00000000 sec
SFO1 300.1369000 MHz
F2 - Processing parameters
SI 8192
SF 300.1349265 MHz
WDW no
SSB 0
LB 0.00 Hz
GB 0
PC 1.00
H-10e
OH
OH
H
N
O
NH2
9.5 9.0 8.5 8.0 7.5 7.0 6.5 6.0 5.5 5.0 4.5 4.0 3.5 3.0 2.5 2.0 1.5 1.0 0.5 ppm
1.048
1.519
2.266
1.062
3.312
1.000
1.985

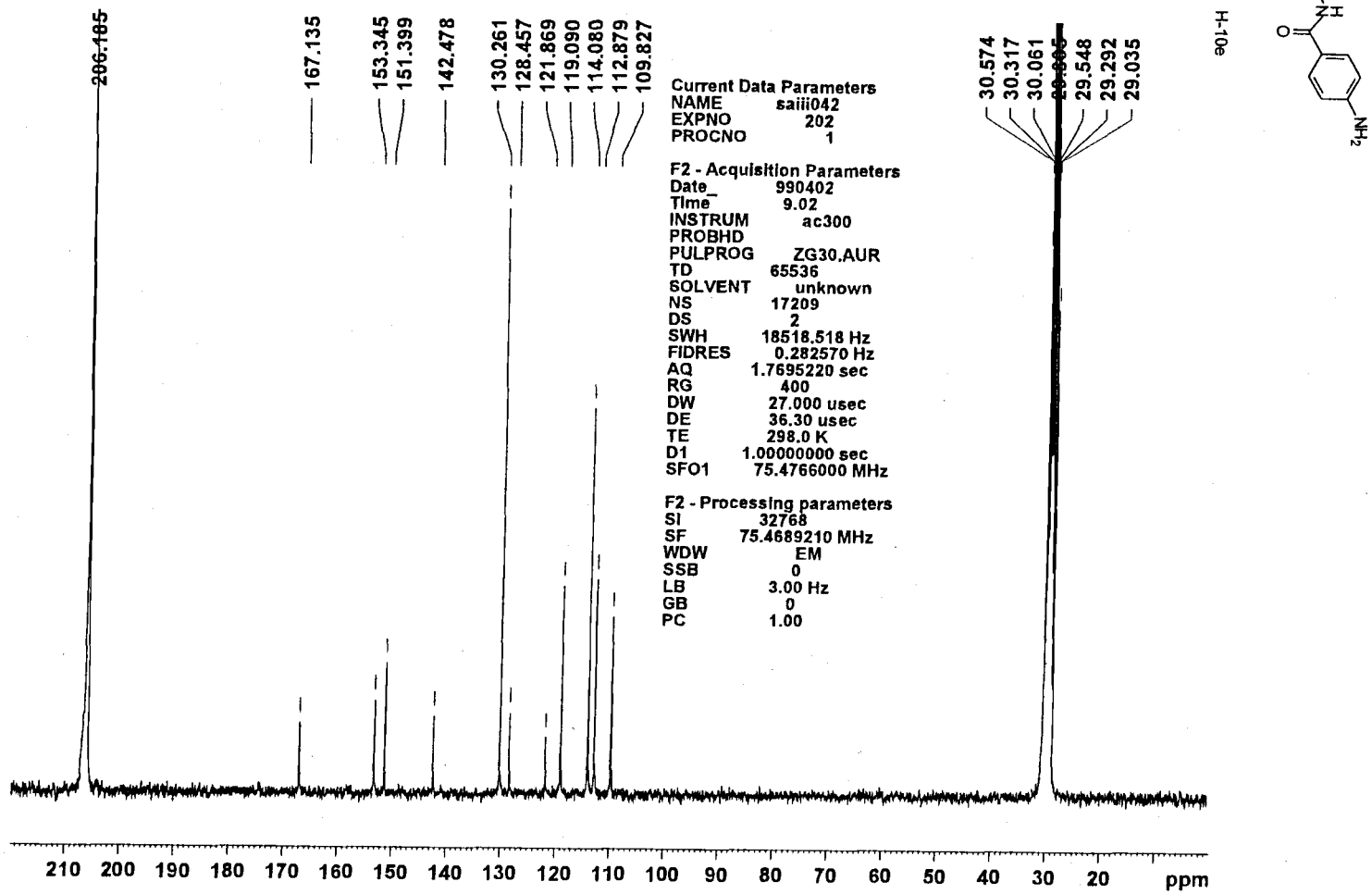
206.105
167.135
153.345
151.399
142.478
130.261
128.457
121.869
119.090
114.080
112.879
109.827
30.574
30.317
30.061
29.548
29.292
29.035
Current Data Parameters
NAME saiii042
EXPNO 202
PROCNO 1
F2 - Acquisition Parameters
Date_ 990402
Time 9.02
INSTRUM ac300
PROBHD
PULPROG ZG30.AUR
TD 65536
SOLVENT unknown
NS 17209
DS 2
SWH 18518.518 Hz
FIDRES 0.282570 Hz
AQ 1.7695220 sec
RG 400
DW 27.000 usec
DE 36.30 usec
TE 298.0 K
D1 1.00000000 sec
SFO1 75.4766000 MHz
F2 - Processing parameters
SI 32768
SF 75.4689210 MHz
WDW EM
SSB 0
LB 3.00 Hz
GB 0
PC 1.00
210 200 190 180 170 160 150 140 130 120 110 100 90 80 70 60 50 40 30 20 ppm
H-10e
HO
OH
NH
O
NH2

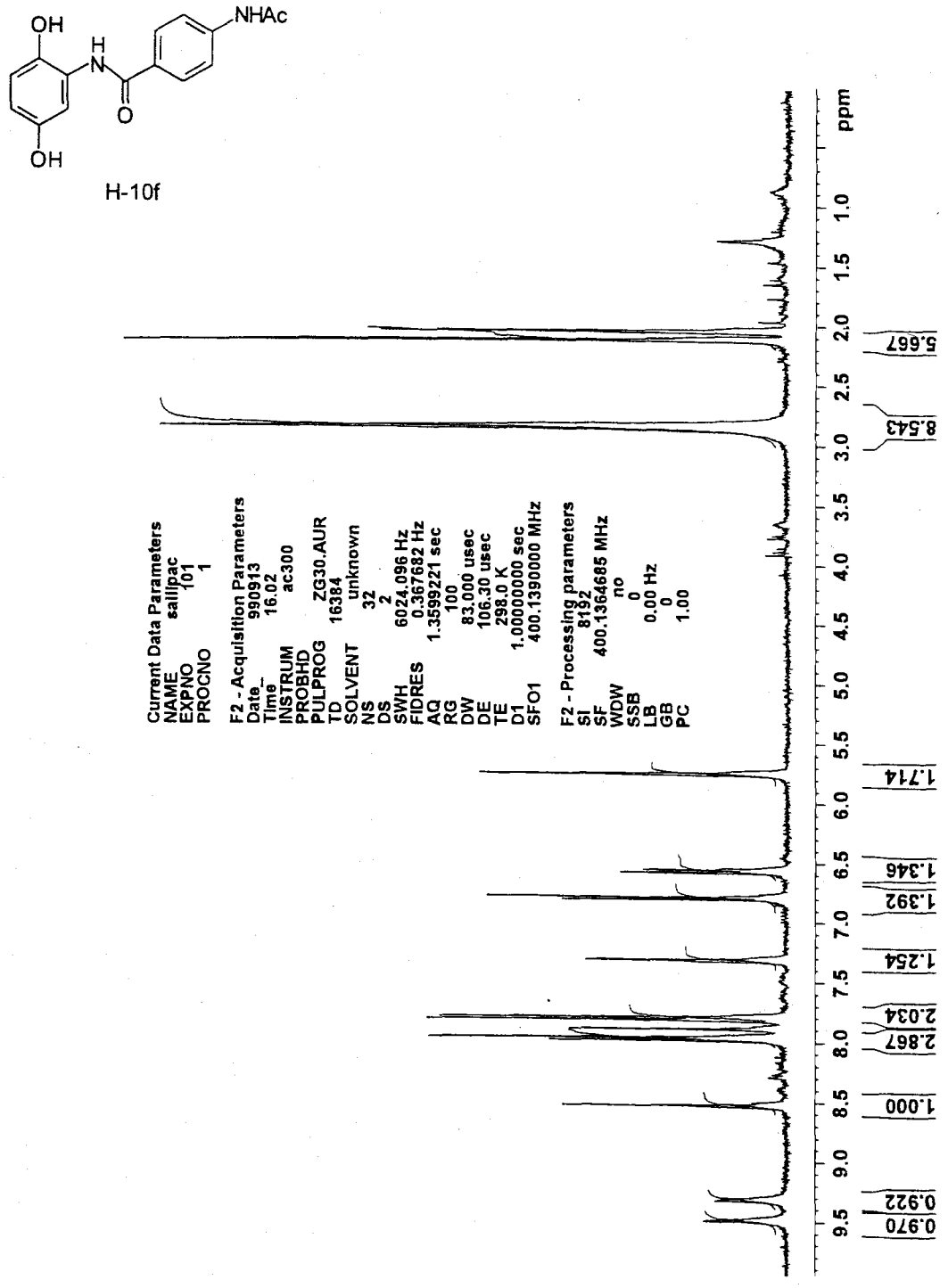
OH
H
N
O
NHAc
OH
H-10f
Current Data Parameters
NAME salilpac
EXPNO 101
PROCNO 1
F2 - Acquisition Parameters
Date_ 990913
Time 16.02
INSTRUM ac300
PROBHD
PULPROG ZG30.AUR
TD 16384
SOLVENT unknown
NS 32
DS 2
SWH 6024.096 Hz
FIDRES 0.367682 Hz
AQ 1.3599221 sec
RG 100
DW 83.000 usec
DE 106.30 usec
TE 298.0 K
D1 1.00000000 sec
SFO1 400.1390000 MHz
F2 - Processing parameters
SI 8192
SF 400.1364685 MHz
WDW no
SSB 0
LB 0.00 Hz
GB 0
PC 1.00
5.667
8.543
1.714
1.346
1.392
1.254
2.034
2.867
1.000
0.922
0.970
ppm

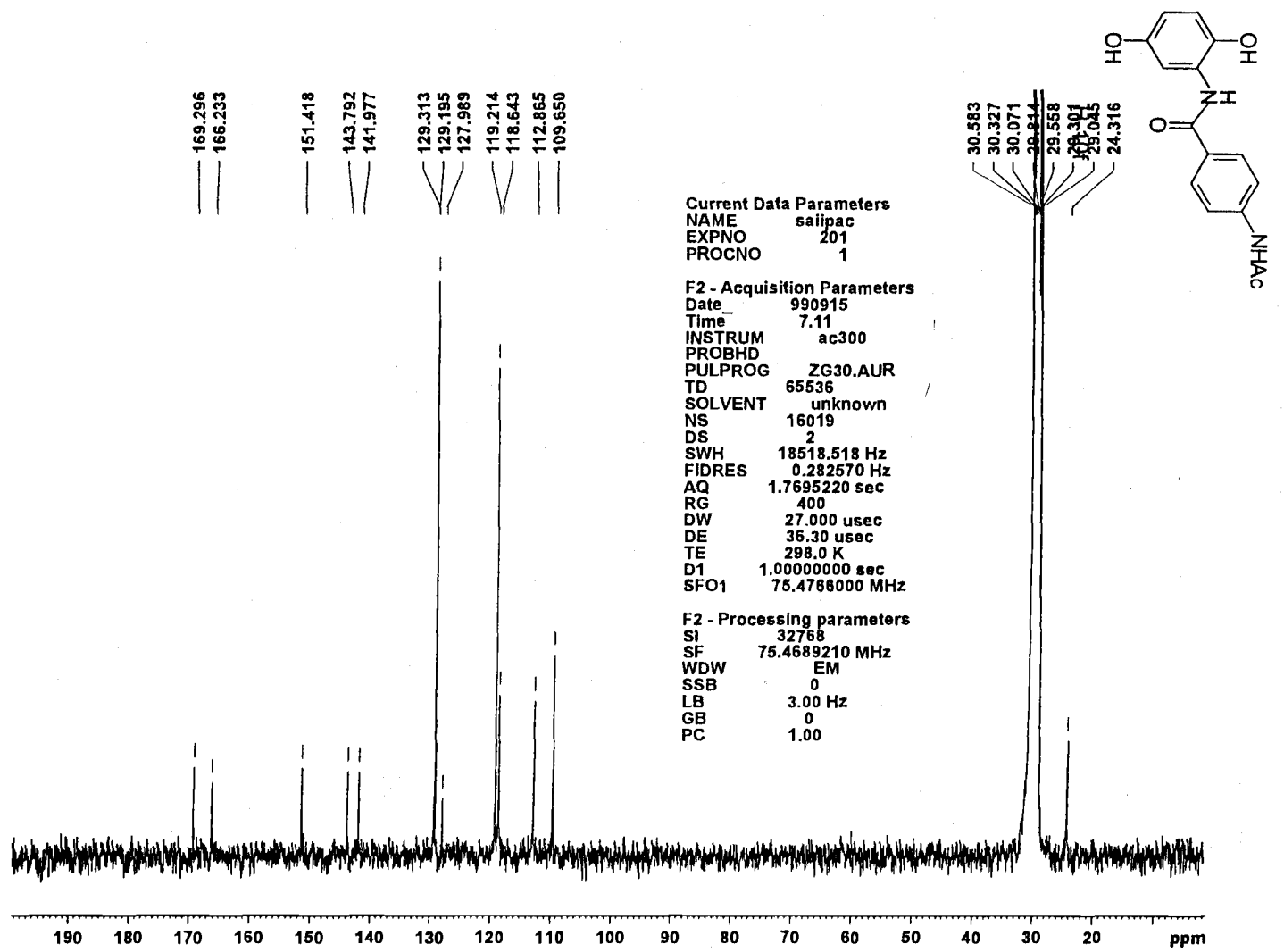
169.296
166.233
151.418
143.792
141.977
129.313
129.195
127.989
119.214
118.643
112.865
109.650
30.583
30.327
30.071
29.558
24.316
HO
HO
N
H
O
NHAc
Current Data Parameters
NAME saiipac
EXPNO 201
PROCNO 1
F2 - Acquisition Parameters
Date_ 990915
Time 7.11
INSTRUM ac300
PROBHD
PULPROG ZG30.AUR
TD 65536
SOLVENT unknown
NS 16019
DS 2
SWH 18518.518 Hz
FIDRES 0.282570 Hz
AQ 1.7695220 sec
RG 400
DW 27.000 usec
DE 36.30 usec
TE 298.0 K
D1 1.00000000 sec
SFO1 75.4766000 MHz
F2 - Processing parameters
SI 32768
SF 75.4689210 MHz
WDW EM
SSB 0
LB 3.00 Hz
GB 0
PC 1.00
190 180 170 160 150 140 130 120 110 100 90 80 70 60 50 40 30 20 ppm

Current Data Parameters
NAME saili002
EXPNO 101
PROCNO 1
F2 - Acquisition Parameters
Date_ 981208
Time 18.02
INSTRUM ac300
PROBHD
PULPROG ZG30.AUR
TD 16384
SOLVENT unknown
NS 32
DS 2
SWH 6024.096 Hz
FIDRES 0.367682 Hz
AQ 1.3599221 sec
RG 64
DW 83.000 usec
DE 106.30 usec
TE 298.0 K
D1 1.00000000 sec
SFO1 300.1369000 MHz
F2 - Processing parameters
SI 8192
SF 300.1349265 MHz
WDW no
SSB 0
LB 0.00 Hz
GB 0
PC 1.00
9.5 9.0 8.5 8.0 7.5 7.0 6.5 6.0 5.5 5.0 4.5 4.0 3.5 3.0 2.5 2.0 1.5 1.0 ppm
0.725
2.787
2.005
0.802
0.959
1.000
2.557
HO
HO
N
H
O
NO2
H-10g

206.261
164.834
151.504
150.711
141.867
141.046
129.788
127.558
124.553
118.090
113.212
109.908
30.593
30.337
30.080
29.567
29.310
29.054
Current Data Parameters
NAME saiii002
EXPNO 102
PROCNO 1
F2 - Acquisition Parameters
Date_ 981208
Time 19.20
INSTRUM ac300
PROBHD
PULPROG ZG30.AUR
TD 65536
SOLVENT unknown
NS 2557
DS 2
SWH 18518.518 Hz
FIDRES 0.282570 Hz
AQ 1.7695220 sec
RG 400
DW 27.000 usec
DE 36.30 usec
TE 298.0 K
D1 1.00000000 sec
SFO1 75.4766000 MHz
F2 - Processing parameters
SI 32768
SF 75.4689210 MHz
WDW EM
SSB 0
LB 3.00 Hz
GB 0
PC 1.00
OH
OH
H
N
O
NO2
H-109
210 200 190 180 170 160 150 140 130 120 110 100 90 80 70 60 50 40 30 20 ppm

Current Data Parameters
NAME salil049
EXPNO 101
PROCNO 1
F2 - Acquisition Parameters
Date_ 990527
Time 11.42
INSTRUM ac300
PROBHD
PULPROG ZG30.AUR
TD 16384
SOLVENT unknown
NS 32
DS 2
SWH 6024.096 Hz
FIDRES 0.367682 Hz
AQ 1.3599221 sec
RG 32
DW 83.000 usec
DE 106.30 usec
TE 298.0 K
D1 1.00000000 sec
SFO1 300.1369000 MHz
F2 - Processing parameters
SI 8192
SF 300.1349265 MHz
WDW no
SSB 0
LB 0.00 Hz
GB 0
PC 1.00
H-10h
OH
OH
H
N
O
NO2
9.5
9.0
8.5
8.0
7.5
7.0
6.5
6.0
5.5
5.0
4.5
4.0
3.5
3.0
2.5
2.0
1.5
1.0
ppm
0.738
1.000
2.043
1.026
0.985
0.993
1.004

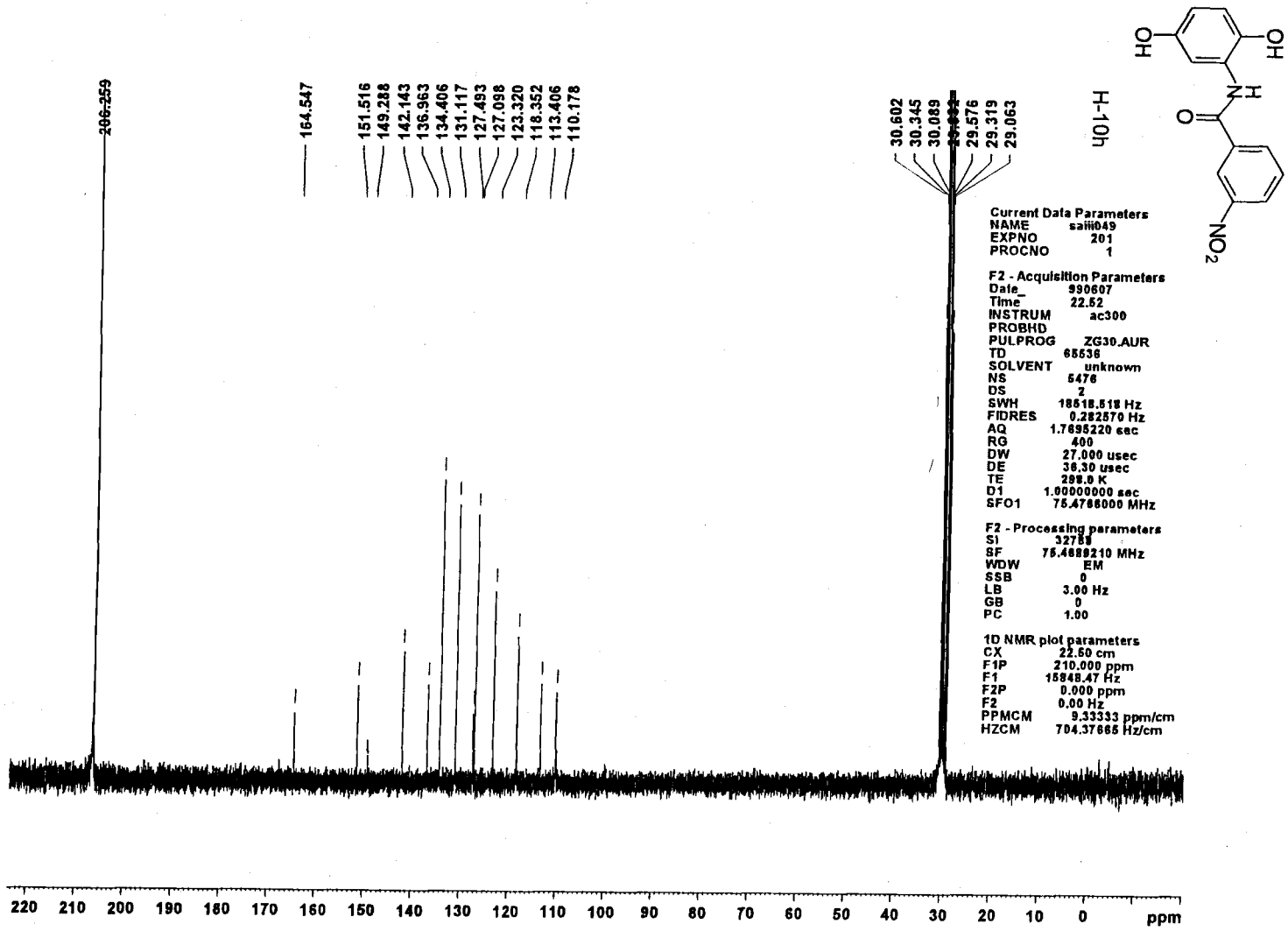
206.259
164.547
151.516
149.288
142.143
136.963
134.406
131.117
127.493
127.098
123.320
118.352
113.406
110.178
30.602
30.345
30.089
29.576
29.319
29.063
H-10h
OH
OH
N
H
O
NO2
Current Data Parameters
NAME saiii049
EXPNO 201
PROCNO 1
F2 - Acquisition Parameters
Date_ 990607
Time 22.52
INSTRUM ac300
PROBHD
PULPROG ZG30.AUR
TD 65536
SOLVENT unknown
NS 5476
DS 2
SWH 18518.518 Hz
FIDRES 0.282570 Hz
AQ 1.7695220 sec
RG 400
DW 27.000 usec
DE 36.30 usec
TE 298.0 K
D1 1.00000000 sec
SFO1 75.4766000 MHz
F2 - Processing parameters
SI 32768
SF 75.4688210 MHz
WDW EM
SSB 0
LB 3.00 Hz
GB 0
PC 1.00
1D NMR plot parameters
CX 22.50 cm
F1P 210.000 ppm
F1 15848.47 Hz
F2P 0.000 ppm
F2 0.00 Hz
PPMCM 9.33333 ppm/cm
HZCM 704.37665 Hz/cm
220 210 200 190 180 170 160 150 140 130 120 110 100 90 80 70 60 50 40 30 20 10 0 ppm

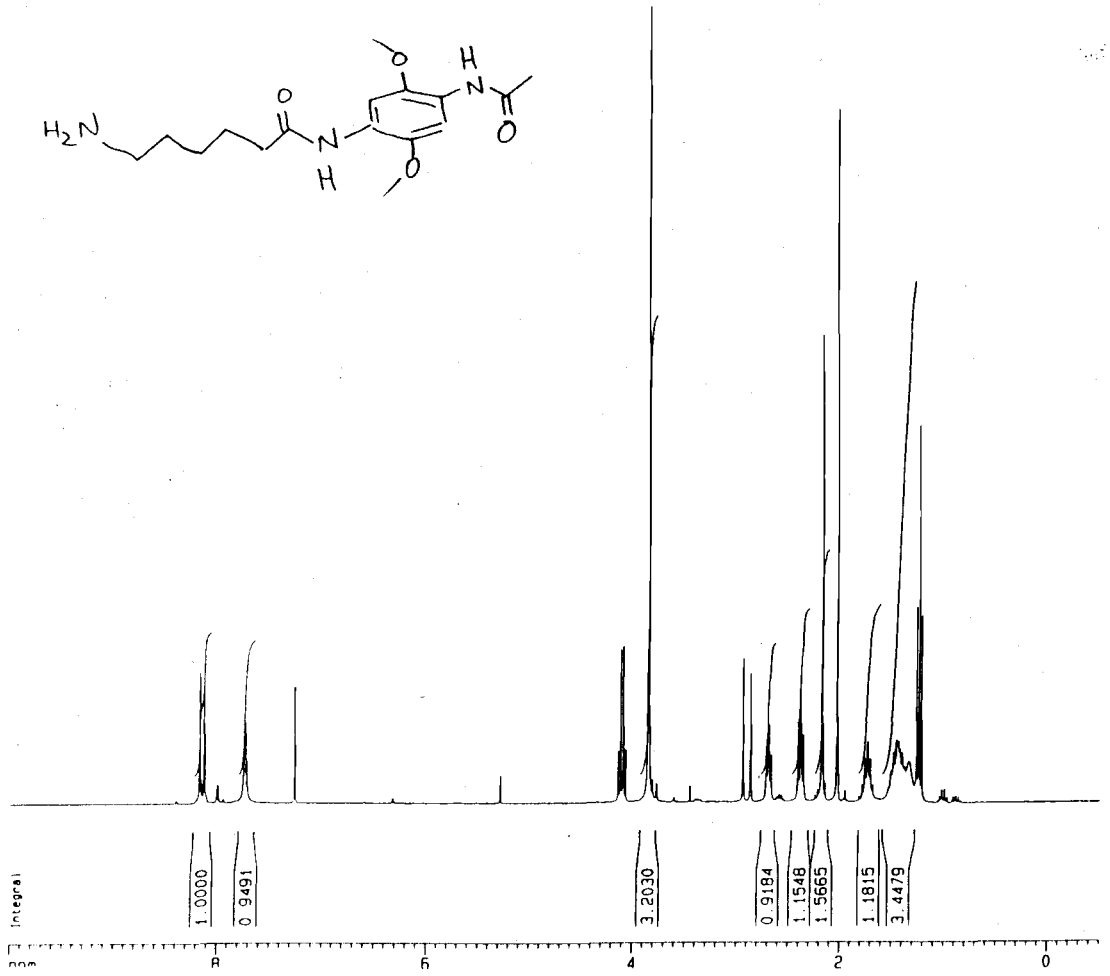

Current Data Parameters

NAME	sav085
EXPNO	1
PROCNO	1
DU	/n
USER	scotta

F2 - Acquisition Parameters

Date_	20020715
Time	9.06
INSTRUM	dpx300
PROBHD	5 mm QNP 1H
PULPROG	zg30
TD	32768
SOLVENT	CDCl3
NS	32
DS	2
SWH	4496.403 Hz
FIDRES	0.137219 Hz
AQ	3.6438515 sec
RG	256
DW	111.200 usec
DE	6.00 usec
TE	300.0 K
D1	1.50000000 sec

========== CHANNEL f1 ==========

NUC1	1H
P1	8.20 usec
PL1	-3.00 dB
SFO1	300.1319000 MHz

F2 - Processing parameters

SI	32768
SF	300.1300063 MHz
WDW	no
SSB	0
LB	0.00 Hz
GB	0
PC	1.00

1D NMR plot parameters

CX	20.00 cm
F1P	10.000 ppm
F1	3001.30 Hz
F2P	-0.500 ppm
F2	-150.07 Hz
PPMCM	0.52500 ppm/cm
HZCM	157.56825 Hz/cm

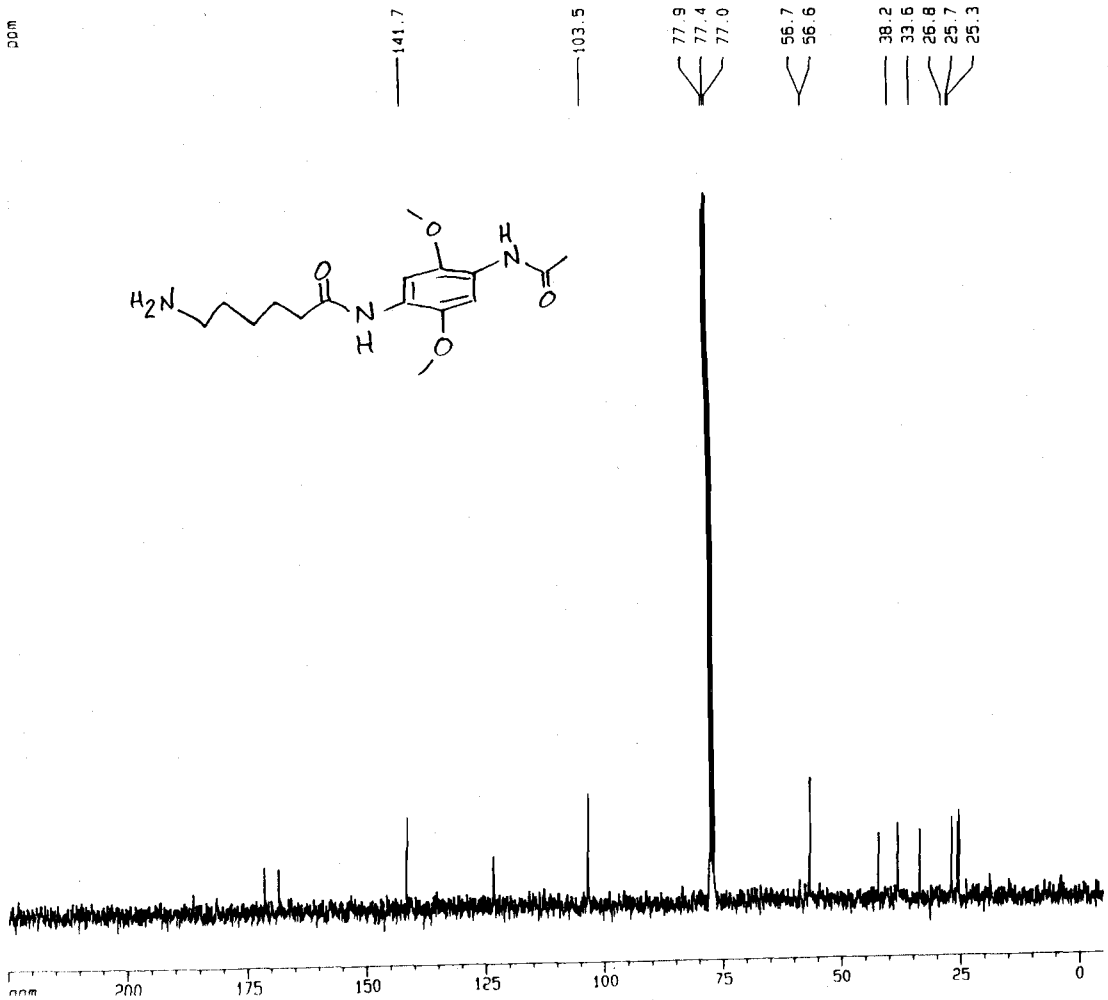

Current Data Parameters
NAME sav066
EXPNO 7
PROCNO 1

F2 - Acquisition Parameters
Date_ 20020530
Time 13.07
INSTRUM dpx300
PROBHD 5 mm DNP 1H
PULPROG zgpg30
TD 65536
SOLVENT
NS 620
DS 2
SWH 18832.393 Hz
FIDRES 0.287360 Hz
AQ 1.7400308 sec
RG 8192
DW 26.550 usec
DE 6.00 usec
TE 300.0 K
D1 0.00300000 sec
D11 0.03000000 sec
D12 0.00002000 sec

********** CHANNEL f1 **********
NUC1 13C
P1 7.60 usec
PL1 -3.00 dB
SFO1 75.4756431 MHz

********** CHANNEL f2 **********
CPDPRG2 waltz16
NUC2 1H
PCPD2 80.00 usec
PL2 2.00 dB
PL12 17.55 dB
PL13 19.00 dB
SFO2 300.1312007 MHz

F2 - Processing parameters
SI 131072
SF 75.4677190 MHz
WDW EM
SSB 0
LB 3.00 Hz
GB 0
PC 1.40

1D NMR plot parameters
CX 20.00 cm
F1P 225.000 ppm
F1 16980.24 Hz
F2P -5.000 ppm
F2 -377.34 Hz
PPMCM 11.50000 ppm/cm
HZCM 867.87878 Hz/cm

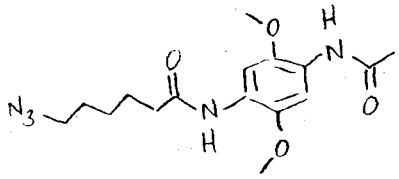

Current Data Parameters

NAME	sav084
EXPNO	1
PROCNO	1
DU	/z
USER	scotta

F2 - Acquisition Parameters

Date_	20020714
Time	11.38
INSTRUM	dpx400
PROBHD	5 mm BBO Z-G
PULPROG	zg30
TD	32768
SOLVENT	CDCl3
NS	32
DS	2
SWH	5995.204 Hz
FIDRES	0.182959 Hz
AQ	2.7329011 sec
RG	256
DW	83.400 usec
DE	6.00 usec
TE	300.0 K
D1	2.00000000 sec

---------- CHANNEL f1 -----

NUC1	1H
P1	11.30 usec
PL1	0.00 dB
SFO1	400.0126001 MHz

F2 - Processing parameters

SI	65536
SF	400.0100000 MHz
WDW	no
SSB	0
LB	0.00 Hz
GB	0
PC	1.00

1D NMR plot parameters

CX	21.00 cm
F1P	10.000 ppm
F1	4000.10 Hz
F2P	-0.200 ppm
F2	-80.00 Hz
PPMCM	0.48571 ppm/c
HZCM	194.29057 Hz/cm

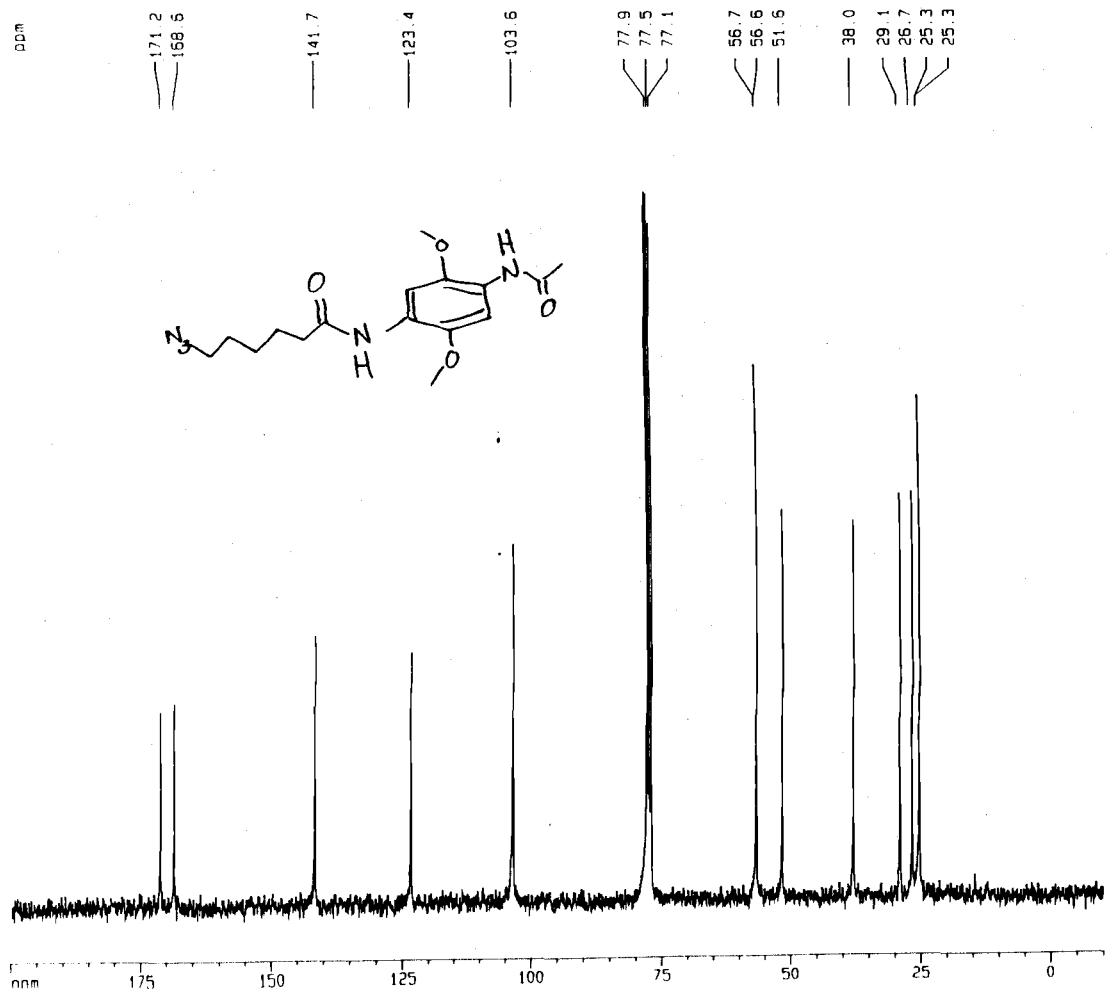

Current Data Parameters

NAME	sav065
EXPNO	4
PROCNO	1
DU	/n
USER	scotta

F2 - Acquisition Parameters

Date_	20020522
Time	18.16
INSTRUM	dpx300
PROBHD	5 mm QNP 1H
PULPROG	zgpg30
TD	65536
SOLVENT	
NS	2048
DS	2
SWH	18832.393 Hz
FIDRES	0.287360 Hz
AQ	1.7400308 sec
RG	8192
DW	26.550 usec
DE	6.00 usec
TE	300.0 K
D1	0.00300000 sec
D11	0.03000000 sec
D12	0.00002000 sec

---------- CHANNEL f1 ----------

NUC1	13C
P1	7.60 usec
PL1	-3.00 dB
SFO1	75.4756431 MHz

---------- CHANNEL f2 ----------

CPDPRG2	waltz16
NUC2	1H
PCPD2	80.00 usec
PL2	2.00 dB
PL12	17.55 dB
PL13	19.00 dB
SFO2	300.1315007 MHz

F2 - Processing parameters

SI	131072
SF	75.4677190 MHz
WDW	EM
SSB	0
LB	3.00 Hz
GB	0
PC	1.40

1D NMR plot parameters

CX	20.00 cm
F1P	200.000 ppm
F1	15093.54 Hz
F2P	-10.000 ppm
F2	-754.68 Hz
PPMCM	10.50000 ppm/cm

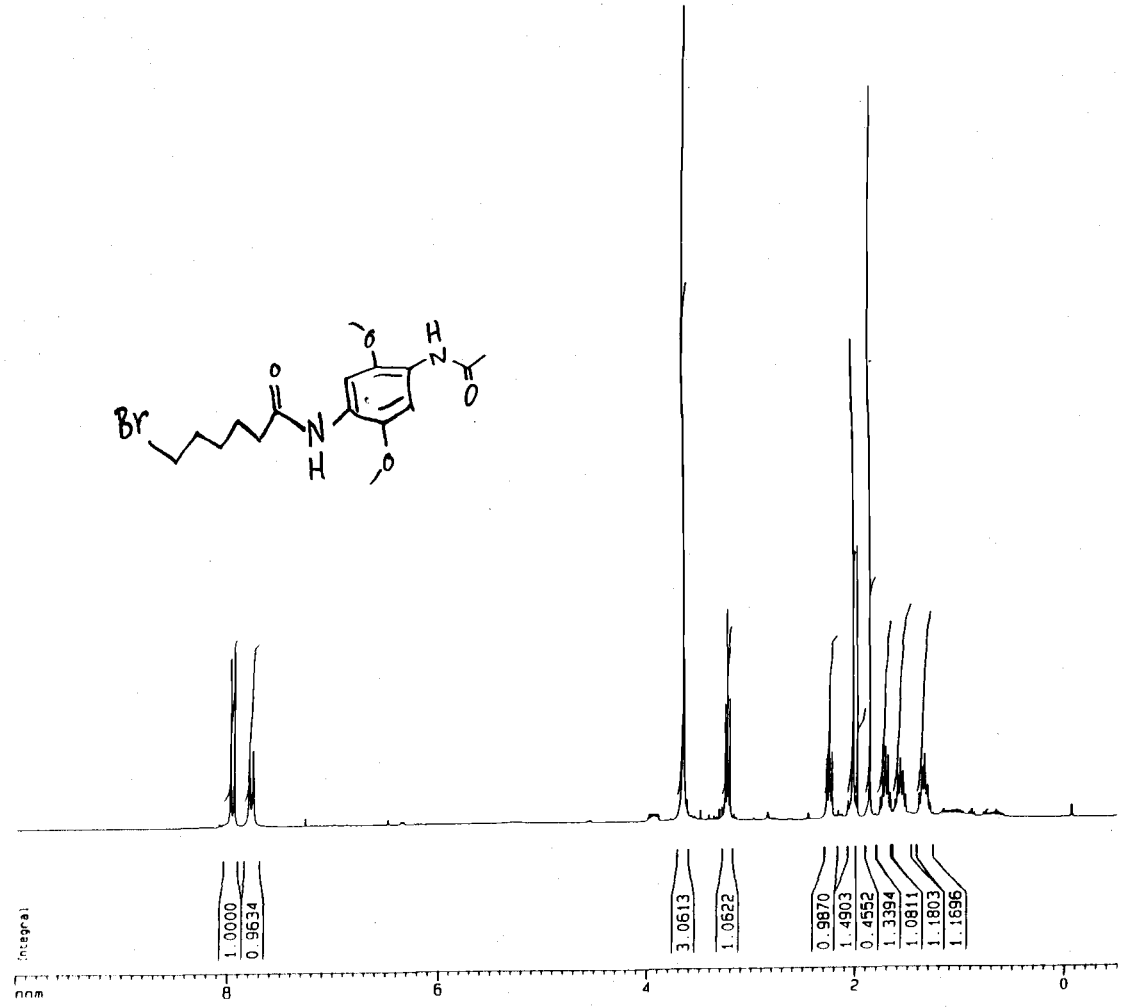

Current Data Parameters

NAME	sav082
EXPNO	1
PROCNO	1

F2 - Acquisition Parameters

Date_	20020712
Time	15.07
INSTRUM	dpx300
PROBHD	5 mm QNP 1H
PULPROG	zg30
TD	32768
SOLVENT	CDCl3
NS	32
DS	2
SWH	4496.403 Hz
FIDRES	0.137219 Hz
AQ	3.6438515 sec
RG	20.2
DW	111.200 usec
DE	6.00 usec
TE	300.0 K
D1	1.50000000 sec

---------- CHANNEL f1 ----------

NUC1	1H
P1	8.20 usec
PL1	-3.00 dB
SFO1	300.1319000 MHz

F2 - Processing parameters

SI	32768
SF	300.1300063 MHz
WDW	no
SSB	0
LB	0.00 Hz
GB	0
PC	1.00

1D NMR plot parameters

CX	20.00 cm
F1P	10.000 ppm
F1	3001.30 Hz
F2P	-0.500 ppm
F2	-150.07 Hz
PPMCM	0.52500 ppm/cm
HZCM	157.56825 Hz/cm

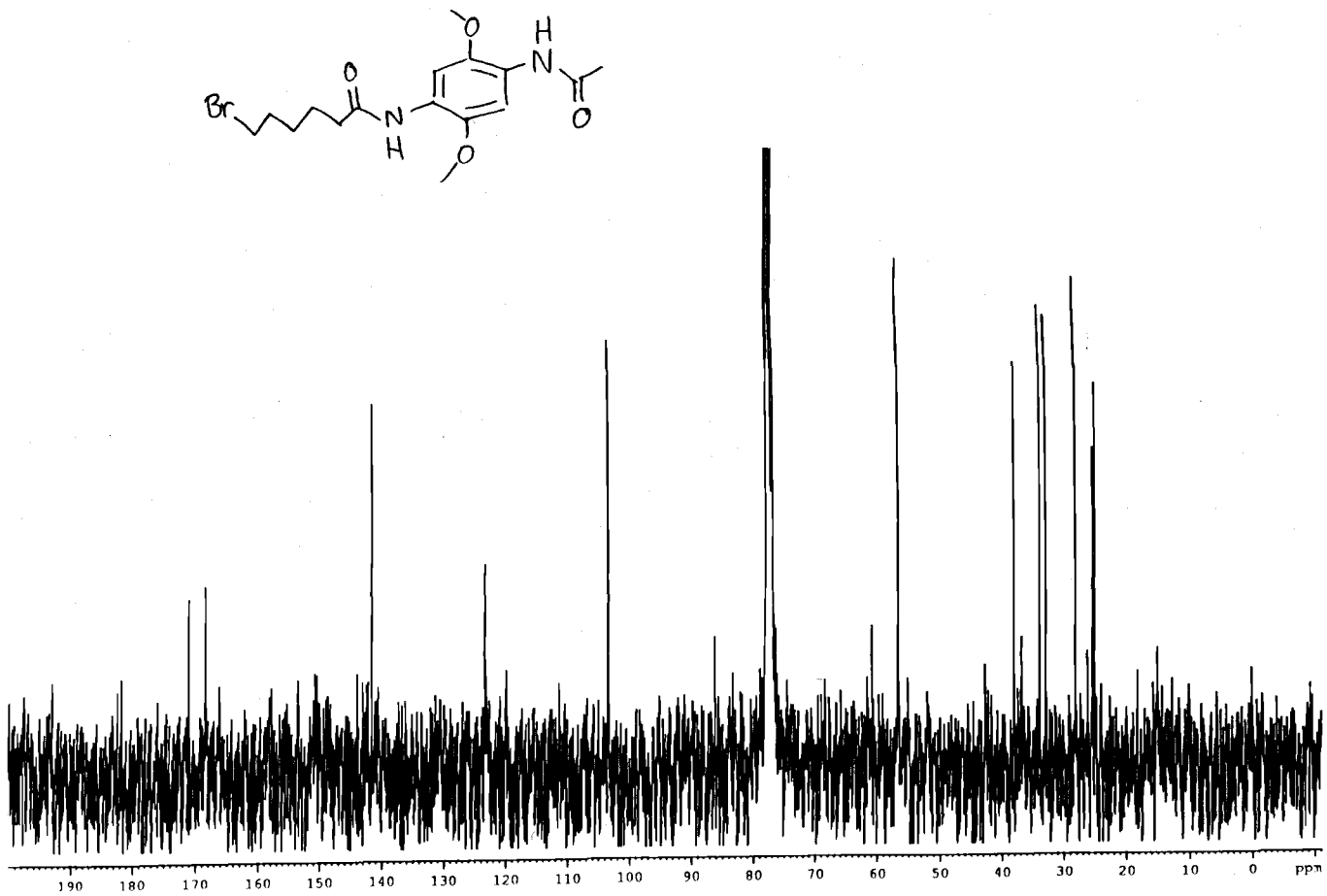
Br
O
N
H
O
O
H
N
O
190
180
170
160
150
140
130
120
110
100
90
80
70
60
50
40
30
20
10
0
ppm

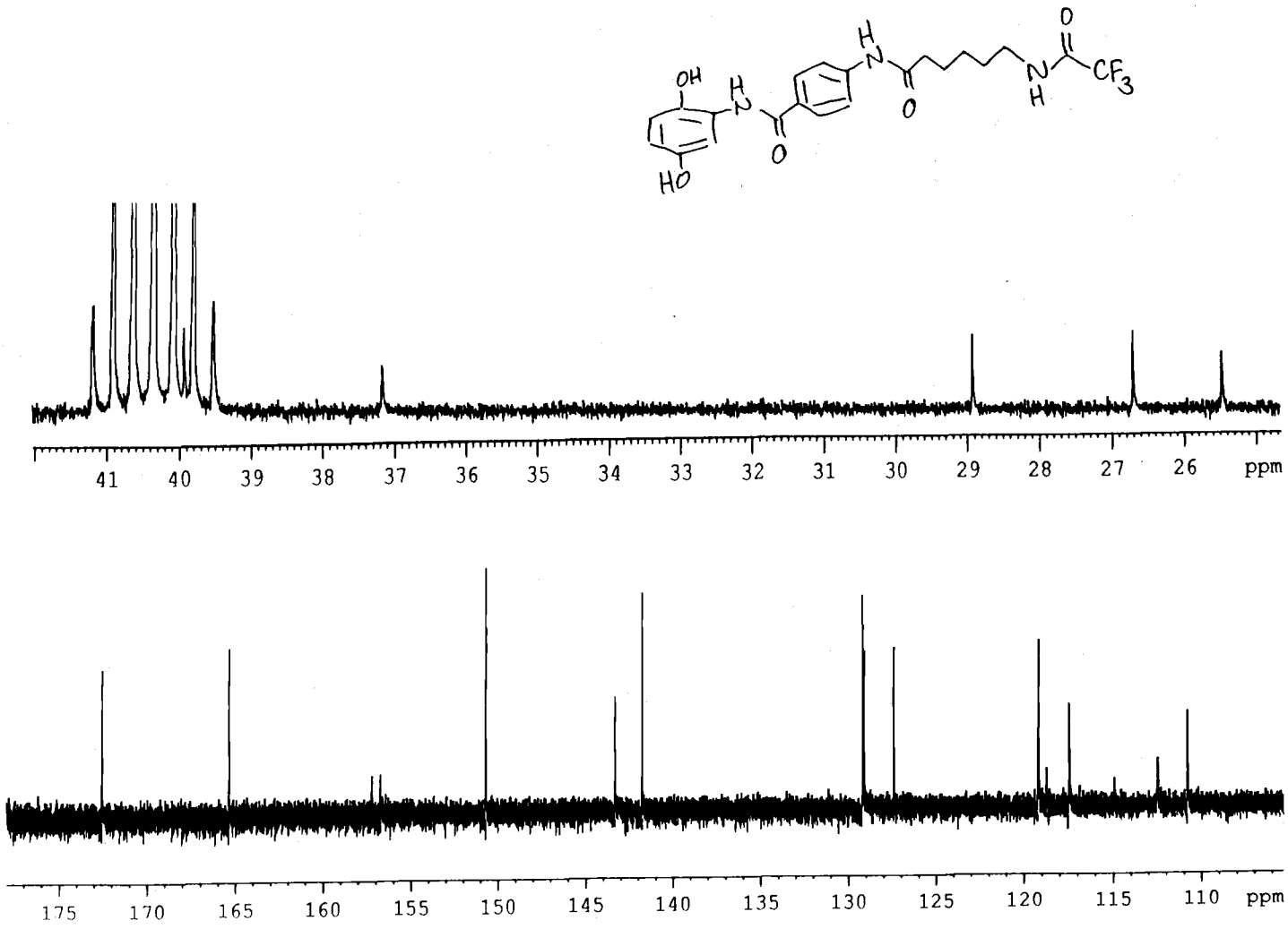
OH
HO
H
N
O
H
N
O
N
H
O
CF3
41 40 39 38 37 36 35 34 33 32 31 30 29 28 27 26 ppm
175 170 165 160 155 150 145 140 135 130 125 120 115 110 ppm

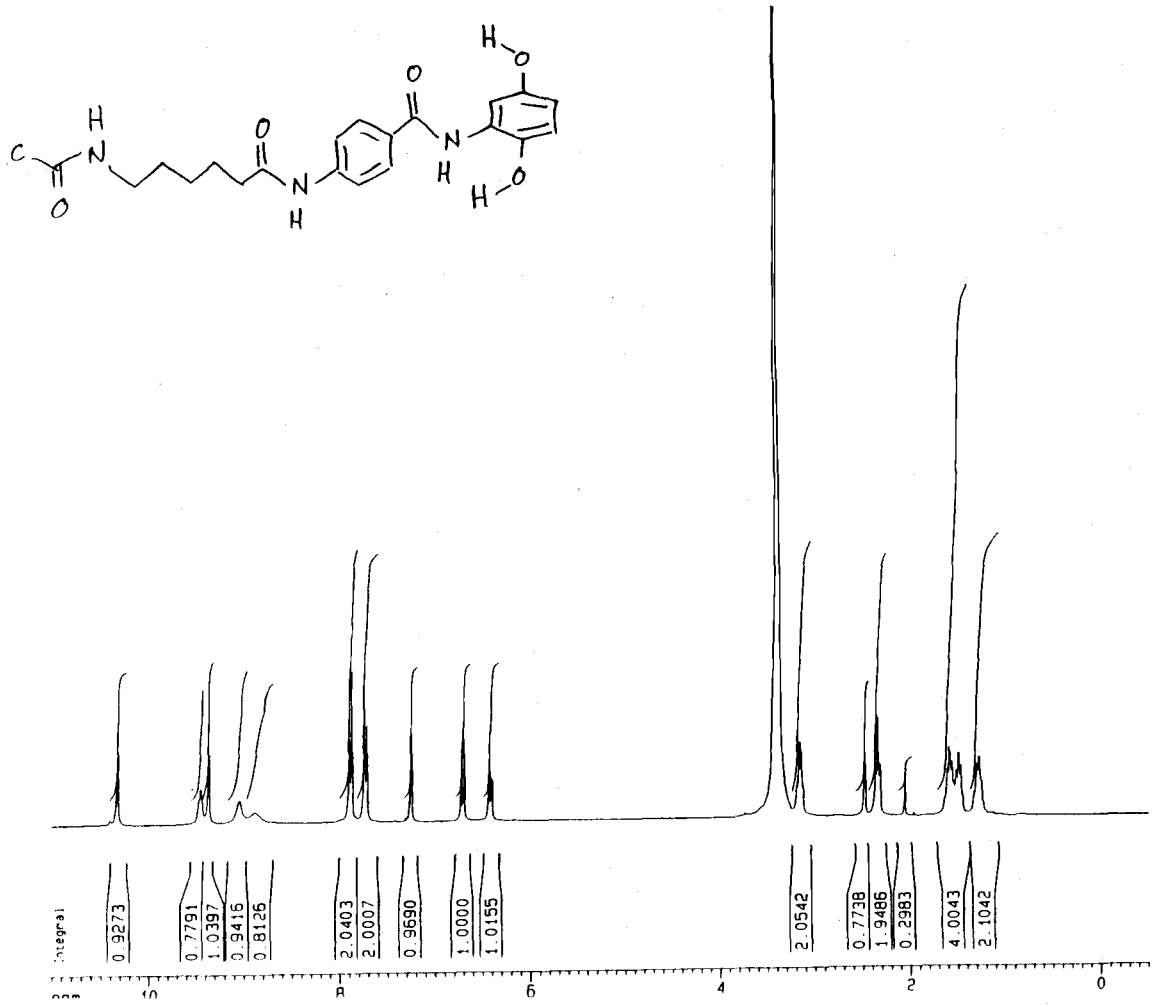

Current Data Parameters
NAME sav068
EXPNO 5
PROCNO 1

F2 - Acquisition Parameters
Date_ 20020529
Time 20.38
INSTRUM dpx300
PROBHD 5 mm QNP 1H
PULPROG zg30
TD 32768
SOLVENT DMSO
NS 32
DS 2
SWH 5411.255 Hz
FIDRES 0.165138 Hz
AQ 3.0278132 sec
RG 256
DW 92.400 usec
DE 6.00 usec
TE 300.0 K
D1 1.50000000 sec

========== CHANNEL f1 ========
NUC1 1H
P1 8.20 usec
PL1 -3.00 dB
SFO1 300.1322000 MHz

F2 - Processing parameters
SI 32768
SF 300.1300036 MHz
WDW no
SSB 0
LB 0.00 Hz
GB 0
PC 1.00

1D NMR plot parameters
CX 20.00 cm
F1P 11.000 ppm
F1 3301.43 Hz
F2P -0.500 ppm
F2 -150.07 Hz
PPMCM 0.57500 ppm/cm
HZCM 172.57477 Hz/cm

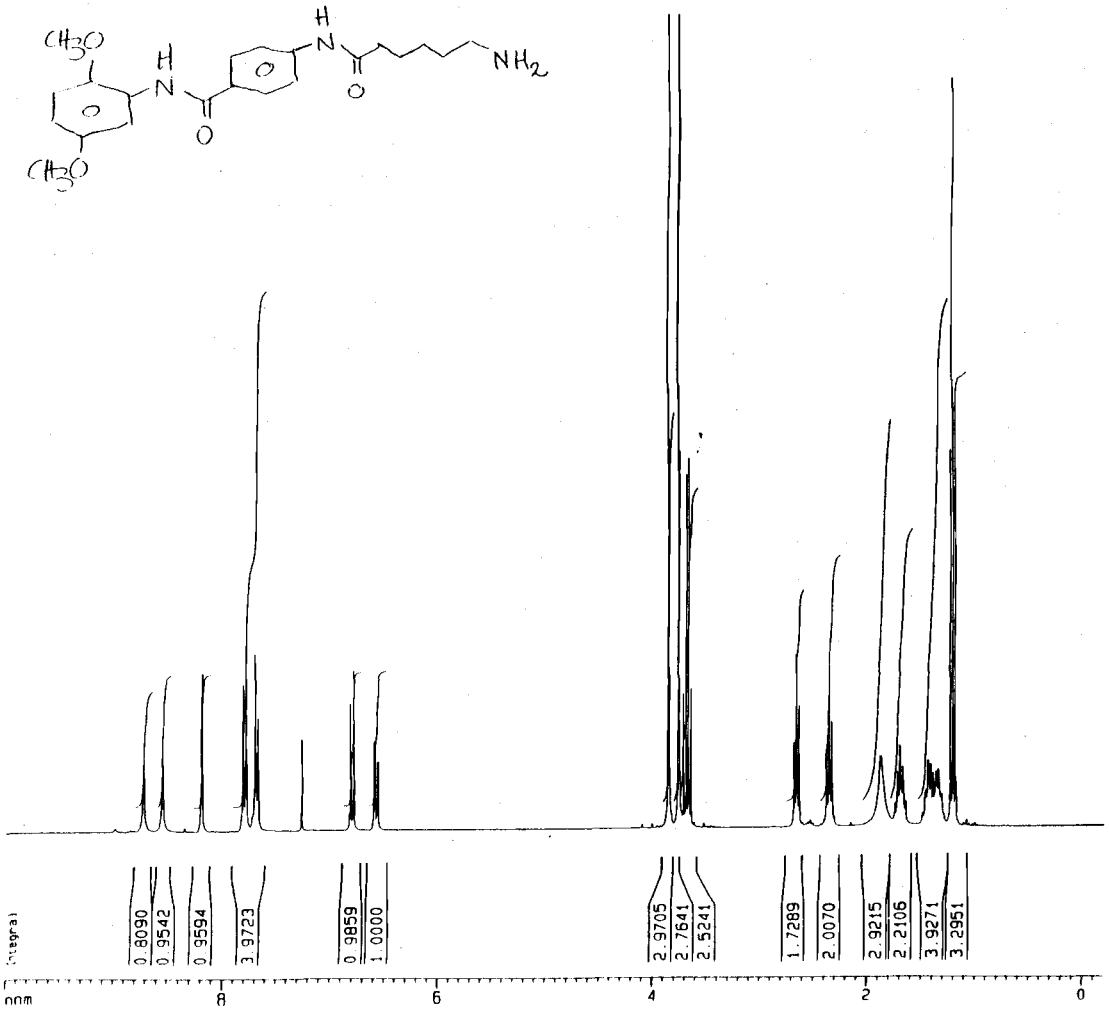

Current Data Parameters

NAME	saiv041
EXPNO	1
PROCNO	1

F2 - Acquisition Parameters

Date_	20000913
Time	11.54
INSTRUM	dpx300
PROBHD	5 mm QNP 1H
PULPROG	zg30
TD	32768
SOLVENT	CDCl3
NS	32
DS	2
SWH	4496.403 Hz
FIDRES	0.137219 Hz
AQ	3.6438515 sec
RG	128
DW	111.200 usec
DE	6.00 usec
TE	300.0 K
D1	1.50000000 sec

---------- CHANNEL f1 ----------

NUC1	1H
P1	8.20 usec
PL1	-3.00 dB
SFO1	300.1319000 MHz

F2 - Processing parameters

SI	32768
SF	300.1300036 MHz
WDW	no
SSB	0
LB	0.00 Hz
GB	0
PC	1.00

1D NMR plot parameters

CX	20.00 cm
F1P	10.000 ppm
F1	3001.30 Hz
F2P	-0.200 ppm
F2	-60.03 Hz
PPMCM	0.51000 ppm/cm
HZCM	153.06630 Hz/cm

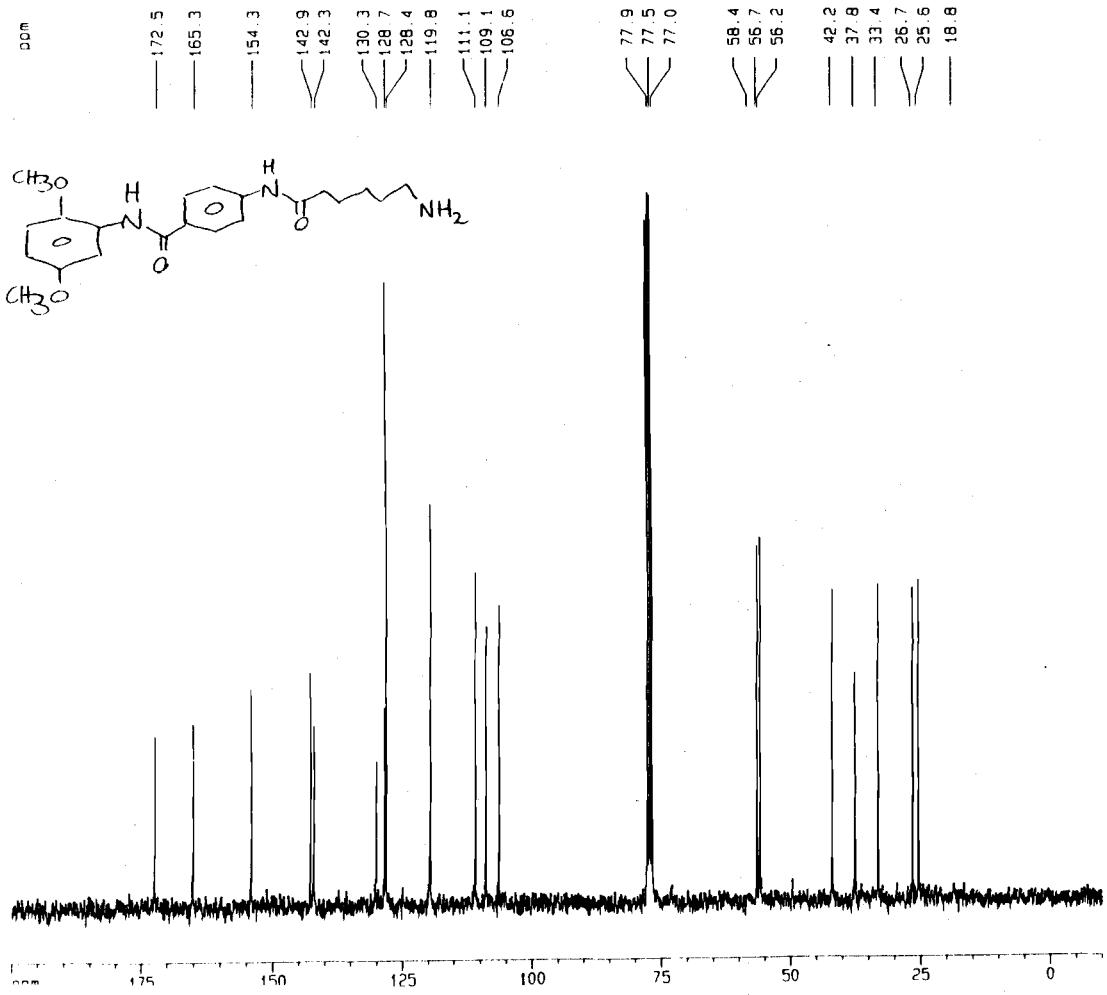

Current Data Parameters

NAME	sairv041
EXPNO	3
PROCNO	1

F2 - Acquisition Parameters

Date_	20000913
Time	18.20
INSTRUM	dpx300
PROBHD	5 mm GNP 1H
PULPROG	zgpg30
TD	65536
SOLVENT	CDCl3
NS	600
DS	2
SWH	18832.393 Hz
FIDRES	0.287360 Hz
AQ	1.7400308 sec
RG	8192
DW	26.550 usec
DE	6.00 usec
TE	300.0 K
D1	0.00300000 sec
d11	0.03000000 sec
d12	0.00002000 sec

********** CHANNEL f1 **********

NUC1	13C
P1	7.60 usec
PL1	-3.00 dB
SF01	75.4756431 MHz

********** CHANNEL f2 **********

CPDPRG2	waltz16
NUC2	1H
PCPD2	80.00 usec
PL2	2.00 dB
PL12	17.55 dB
PL13	19.00 dB
SF02	300.1315007 MHz

F2 - Processing parameters

SI	131072
SF	75.4677190 MHz
WDW	EM
SSB	0
LB	3.00 Hz
GB	0
PC	1.40

1D NMR plot parameters

CX	20.00 cm
F1P	200.000 ppm
F1	15093.54 Hz
F2P	-10.000 ppm
F2	-754.68 Hz
PPMCM	10.50000 ppm/cm
HZCM	792.41107 Hz/cm

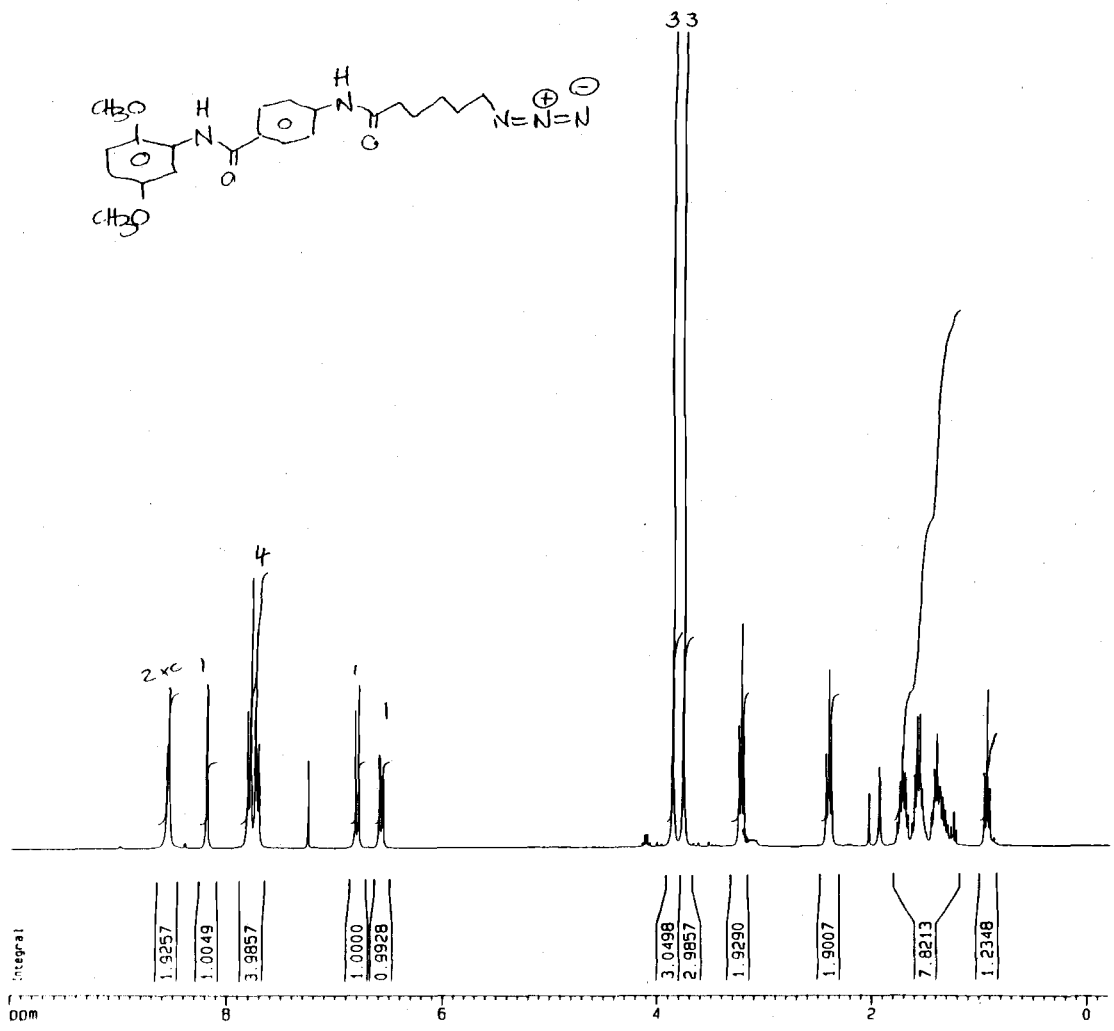

Current Data Parameters

NAME	saiv039
EXPNO	1
PROCNO	1

F2 - Acquisition Parameters

Date_	20000911
Time	14.33
INSTRUM	dpx300
PROBHD	5 mm QNP 1H
PULPROG	zg30
TD	32768
SOLVENT	CDCl3
NS	32
DS	2
SWH	4496.403 Hz
FIDRES	0.137219 Hz
AQ	3.6438515 sec
RG	128
DW	111.200 usec
DE	6.00 usec
TE	300.0 K
D1	1.50000000 sec

---------- CHANNEL f1 ---------

NUC1	1H
P1	8.20 usec
PL1	-3.00 dB
SFO1	300.1319000 MHz

F2 - Processing parameters

SI	32768
SF	300.1300036 MHz
WDW	no
SSB	0
LB	0.00 Hz
GB	0
PC	1.00

1D NMR plot parameters

CX	20.00 cm
F1P	10.000 ppm
F1	3001.30 Hz
F2P	-0.200 ppm
F2	-60.03 Hz
PPMCM	0.51000 ppm/cm
HZCM	153.06630 Hz/cm

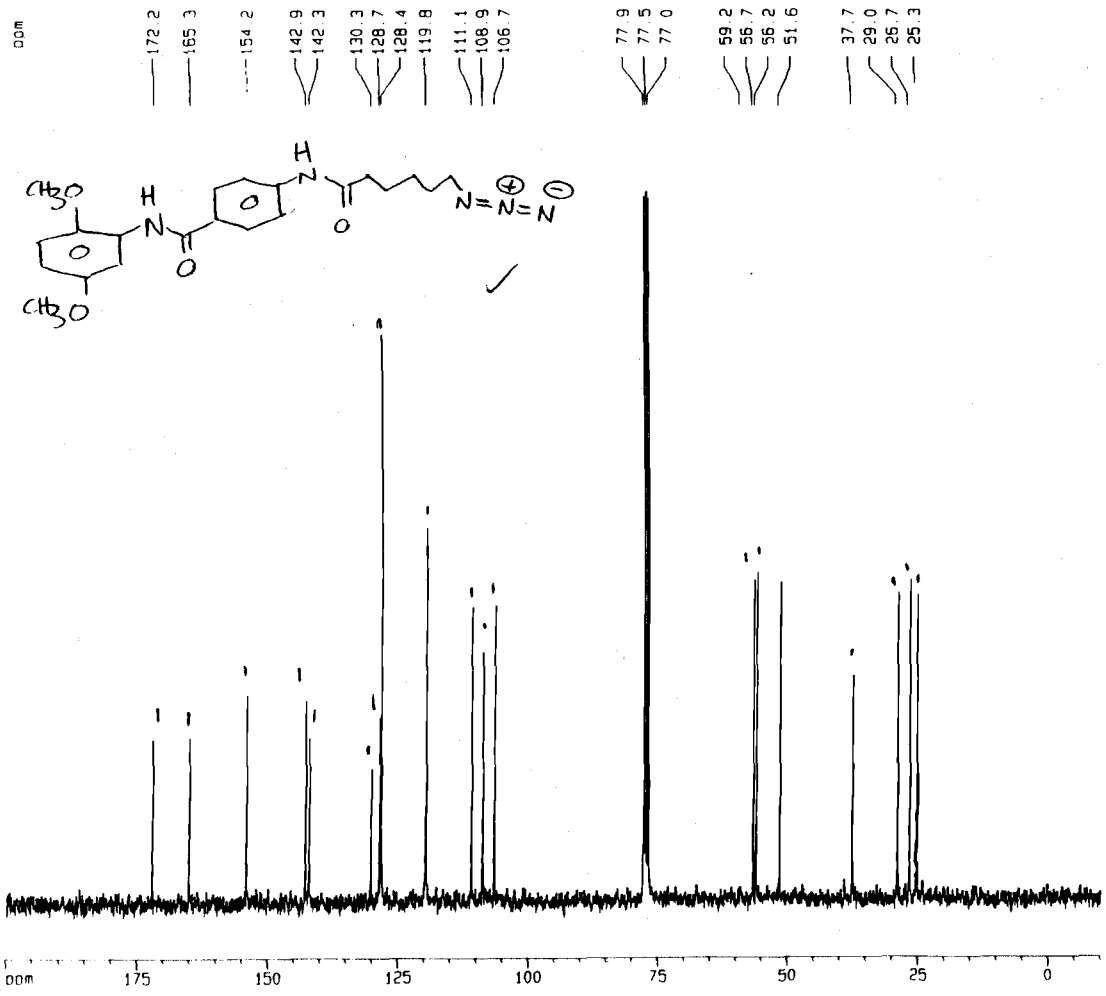

Current Data Parameters
NAME sslv039
EXPNO 3
PROCNO 1

F2 - Acquisition Parameters
Date_ 20000911
Time 17.23
INSTRUM dpx300
PROBHD 5 mm DMP 1H
PULPROG zgpg30
TD 65536
SOLVENT CDCl3
NS 701
DS 2
SWH 18832.393 Hz
FIDRES 0.287360 Hz
AQ 1.7400308 sec
RG 8192
DW 26.550 usec
DE 6.00 usec
TE 300.0 K
D1 0.00300000 sec
d11 0.03000000 sec
d12 0.00002000 sec

********** CHANNEL f1 **********
NUC1 13C
P1 7.60 usec
PL1 -3.00 dB
SFO1 75.4756431 MHz

********** CHANNEL f2 **********
CPDPRG2 waltz16
NUC2 1H
PCPD2 80.00 usec
PL2 2.00 dB
PL12 17.55 dB
PL13 19.00 dB
SFO2 300.1315007 MHz

F2 - Processing parameters
SI 131072
SF 75.4677190 MHz
WDW EM
SSB 0
LB 3.00 Hz
GB 0
PC 1.40

1D NMR plot parameters
CX 20.00 cm
F1P 200.000 ppm
F1 15093.54 Hz
F2P -10.000 ppm
F2 -754.68 Hz
PPMCM 10.50000 ppm/cm

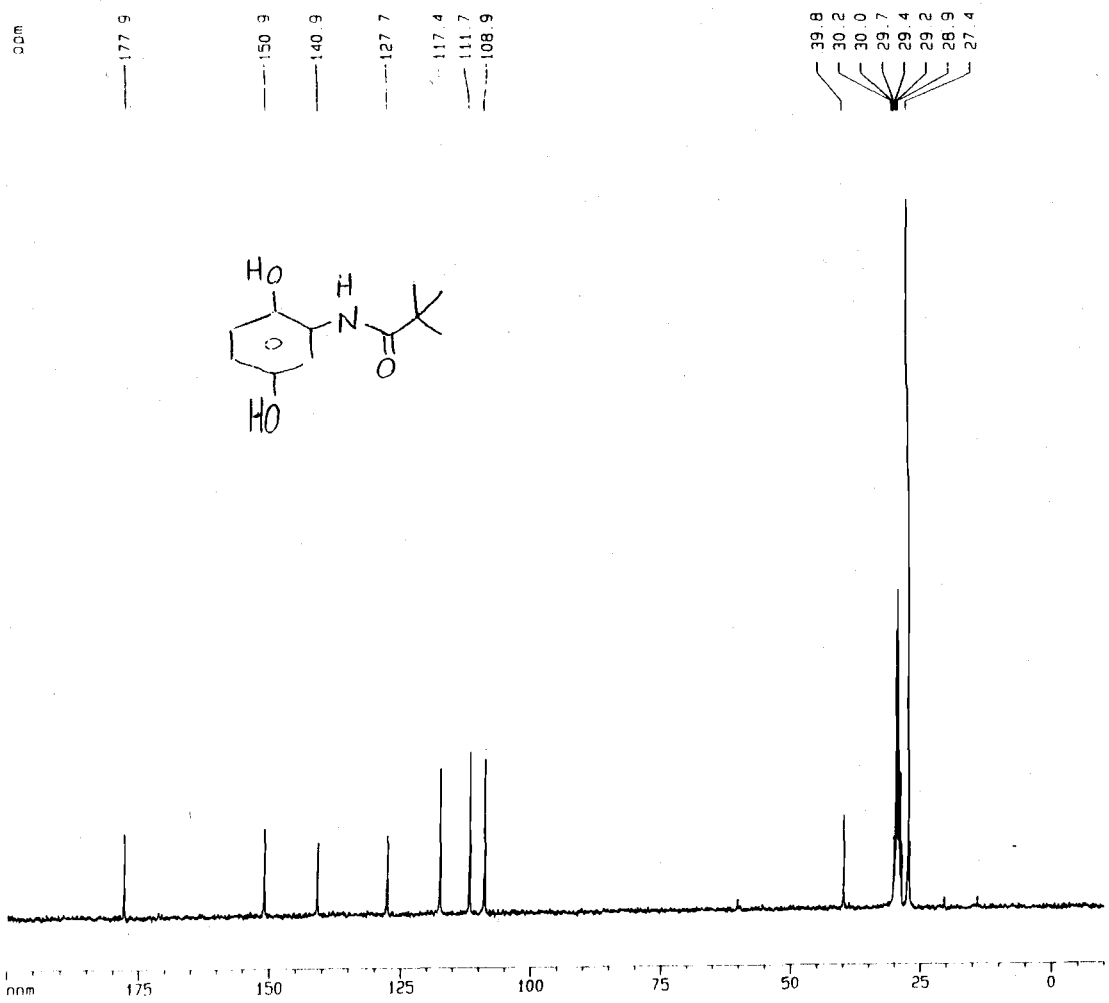

Current Data Parameters
NAME saiv051
EXPNO 2
PROCNO 1

F2 - Acquisition Parameters
Date_ 20000927
Time 14.14
INSTRUM dpx300
PROBHD 5 mm QNP 1H
PULPROG zgpg30
TD 65536
SOLVENT CDCl3
NS 402
DS 2
SWH 18832.393 Hz
FIDRES 0.287360 Hz
AQ 1.7400308 sec
RG 8192
DW 26.550 usec
DE 6.00 usec
TE 300.0 K
D1 0.00300000 sec
d11 0.03000000 sec
d12 0.00002000 sec

********** CHANNEL f1 **********
NUC1 13C
P1 7.60 usec
PL1 -3.00 dB
SF01 75.4756431 MHz

********** CHANNEL f2 **********
CPDPRG2 waltz16
NUC2 1H
PCPD2 80.00 usec
PL2 2.00 dB
PL12 17.55 dB
PL13 19.00 dB
SF02 300.1315007 MHz

F2 - Processing parameters
SI 131072
SF 75.4677190 MHz
WDW EM
SSB 0
LB 3.00 Hz
GB 0
PC 1.40

1D NMR plot parameters
CX 20.00 cm
F1P 200.000 ppm
F1 15093.54 Hz
F2P -10.000 ppm
F2 -754.68 Hz
PPMCM 10.50000 ppm/cm
HZCM 793.41103 Hz/cm

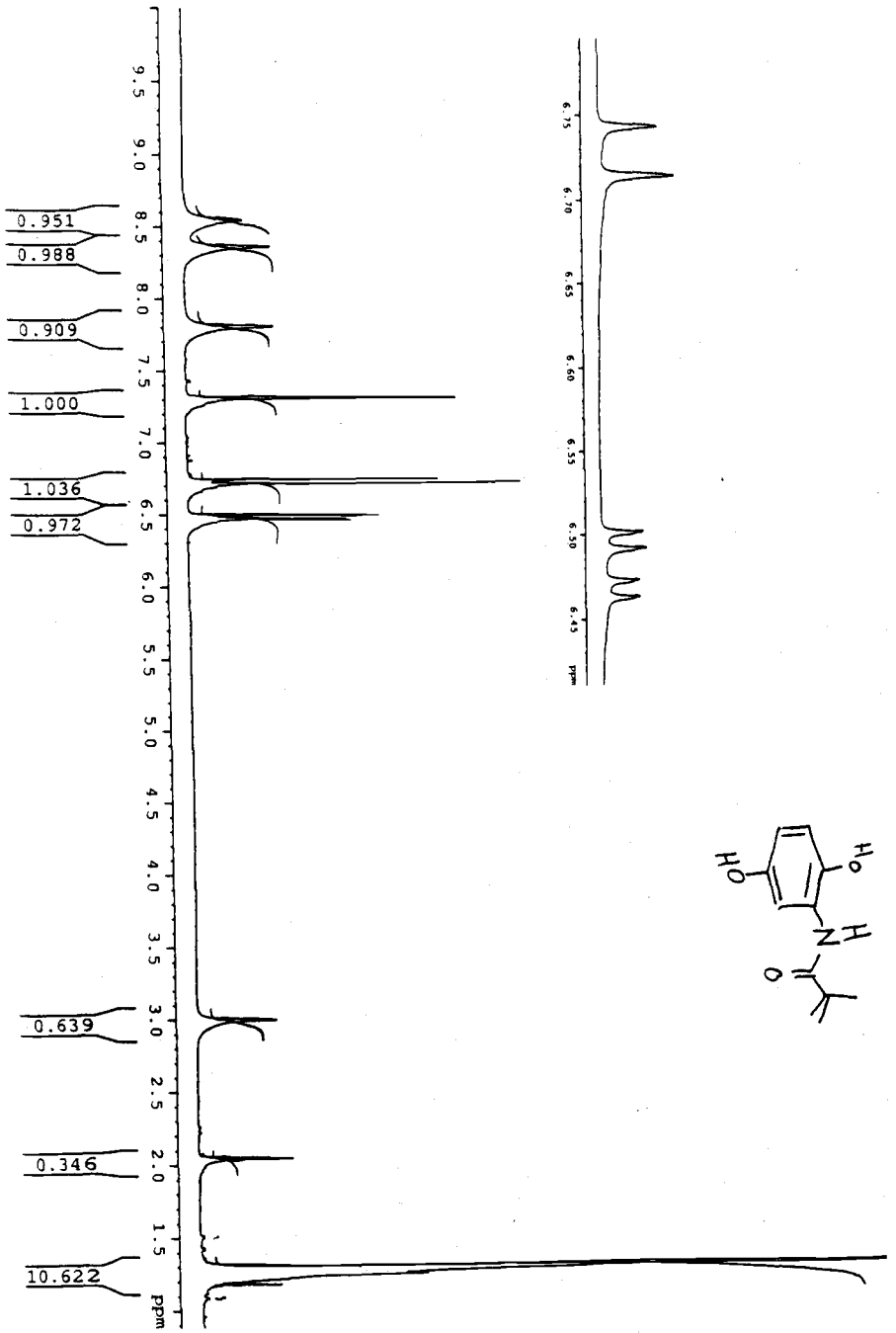
0.951
0.988
0.909
1.000
1.036
0.972
0.639
0.346
10.622
ppm
HO
HO
N
H
O

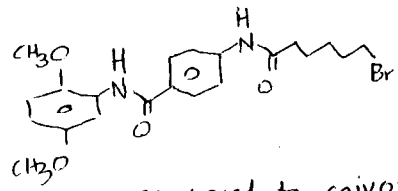

compared to saiv037 (4)

1. xc for second NH has shifted
2. H_2O peak around 1.7 is smaller

Current Data Parameters
NAME saiv037
EXPNO 6
PROCNO 1

F2 - Acquisition Parameters
Date_ 20000910
Time 18.30
INSTRUM dpx300
PROBHD 5 mm QNP 1H
PULPROG zg30
TD 32768
SOLVENT CDCl3
NS 32
DS 2
SWH 4496.403 Hz
FIDRES 0.137219 Hz
AQ 3.6438515 sec
RG 406.4
DW 111.200 usec
DE 6.00 usec
TE 300.0 K
D1 1.50000000 sec

------------ CHANNEL f1 ----------
NUC1 1H
P1 8.20 usec
PL1 -3.00 dB
SFO1 300.1319000 MHz

F2 - Processing parameters
SI 32768
SF 300.1300036 MHz
WDW no
SSB 0
LB 0.00 Hz
GB 0
PC 1.00

1D NMR plot parameters
CX 20.00 cm
F1P 10.000 ppm
F1 3001.30 Hz
F2P -0.500 ppm
F2 -150.07 Hz
PPMCM 0.52500 ppm/cm
HZCM 157.56825 Hz/cm

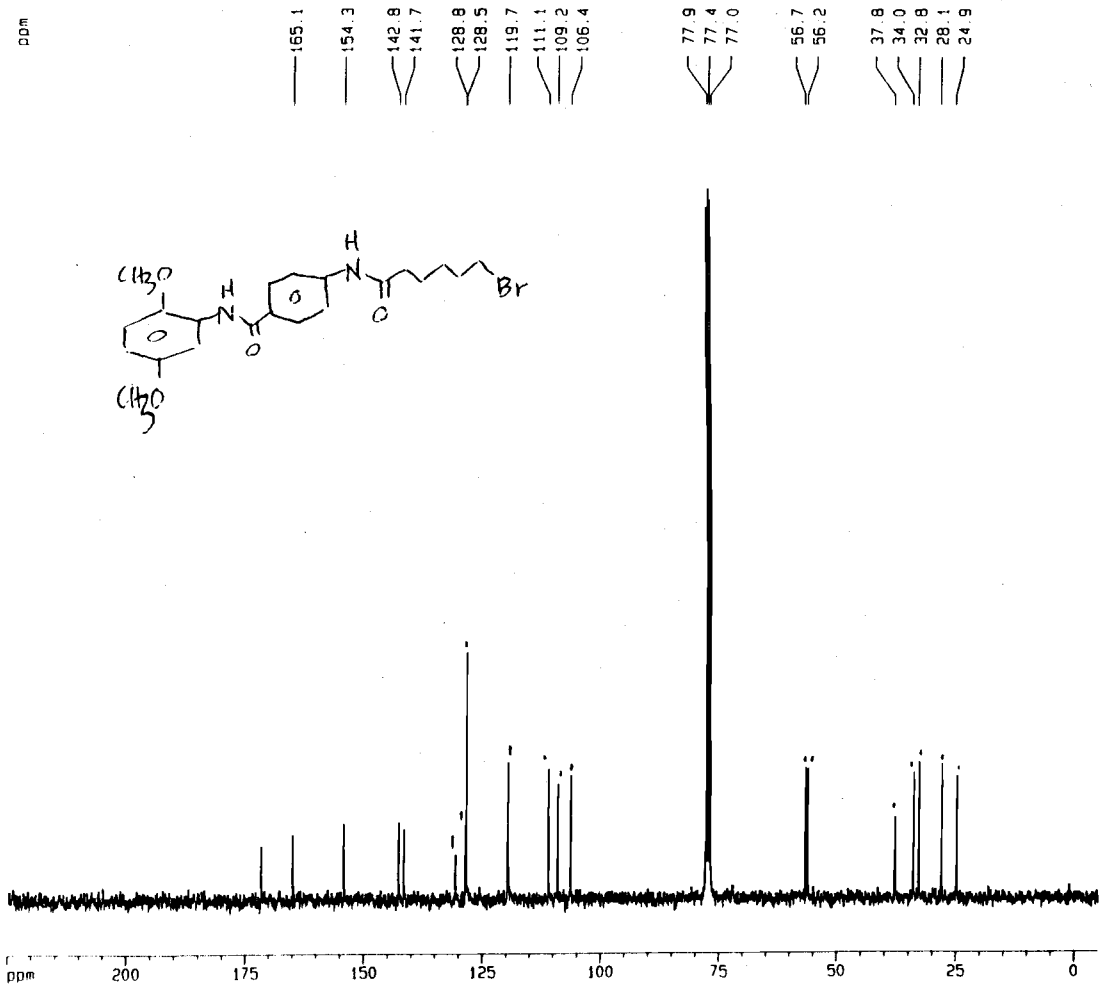

Current Data Parameters

NAME	saiv037
EXPNO	7
PROCNO	1

F2 - Acquisition Parameters

Date_	20000910
Time	19.01
INSTRUM	dpx300
PROBHD	5 mm QNP 1H
PULPROG	zgpg30
TD	65536
SOLVENT	CDCl3
NS	1025
DS	2
SWH	18832.393 Hz
FIDRES	0.287360 Hz
AQ	1.7400308 sec
RG	8192
DW	26.550 usec
DE	6.00 usec
TE	300.0 K
D1	0.00300000 sec
d11	0.03000000 sec
d12	0.00002000 sec

---------- CHANNEL f1 ----------

NUC1	13C
P1	7.60 usec
PL1	-3.00 dB
SFO1	75.4756431 MHz

---------- CHANNEL f2 ----------

CPDPRG2	waltz16
NUC2	1H
PCPD2	80.00 usec
PL2	2.00 dB
PL12	17.55 dB
PL13	19.00 dB
SFO2	300.1315007 MHz

F2 - Processing parameters

SI	131072
SF	75.4677190 MHz
WDW	EM
SSB	0
LB	3.00 Hz
GB	0
PC	1.40

1D NMR plot parameters

CX	20.00 cm
F1P	225.000 ppm
F1	16980.24 Hz
F2P	-5.000 ppm
F2	-377.34 Hz
PPMCM	11.50000 ppm/cm
HZCM	867.87878 Hz/cm

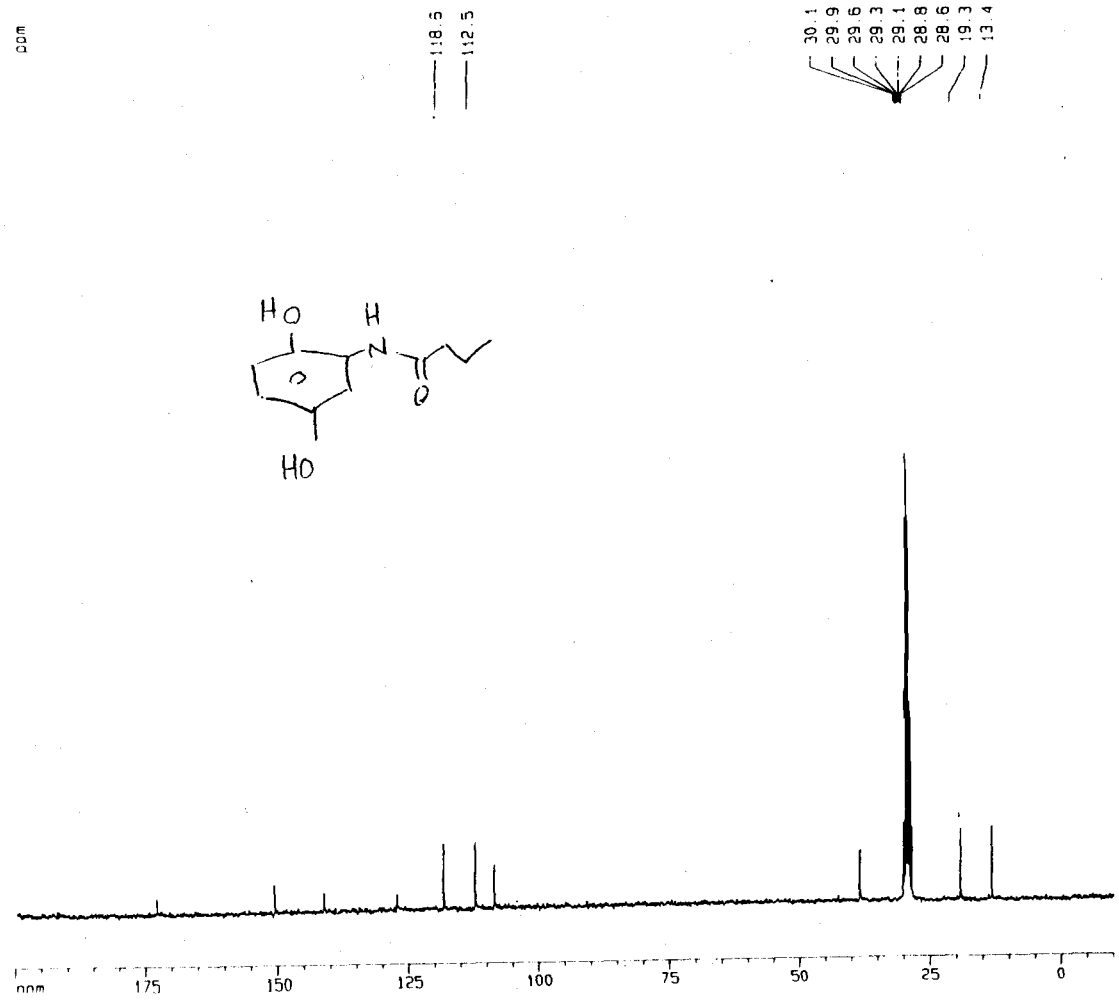

Current Data Parameters
NAME salv050
EXPNO 2
PROCNO 1

F2 - Acquisition Parameters
Date_ 20000927
Time 15.25
INSTRUM dpx300
PROBHD 5 mm QNP 1H
PULPROG zgpg30
TD 65536
SOLVENT CDCl3
NS 400
DS 2
SWH 10832.393 Hz
FIDRES 0.287360 Hz
AQ 1.7400308 sec
RG 8192
DW 26.550 usec
DE 6.00 usec
TE 300.0 K
D1 0.00300000 sec
d11 0.03000000 sec
d12 0.00002000 sec

********** CHANNEL f1 **********
NUC1 13C
P1 7.60 usec
PL1 -3.00 dB
SF01 75.4756431 MHz

********** CHANNEL f2 **********
CPDPRG2 waltz16
NUC2 1H
PCPD2 80.00 usec
PL2 2.00 dB
PL12 17.55 dB
PL13 19.00 dB
SF02 300.1315007 MHz

F2 - Processing parameters
SI 131072
SF 75.4677190 MHz
WDW EM
SSB 0
LB 3.00 Hz
GB 0
PC 1.40

1D NMR plot parameters
CX 20.00 cm
F1P 200.000 ppm
F1 15093.54 Hz
F2P -10.000 ppm
F2 -754.68 Hz
PPMCM 10.50000 ppm/cm
HZCM 792.41107 Hz/cm

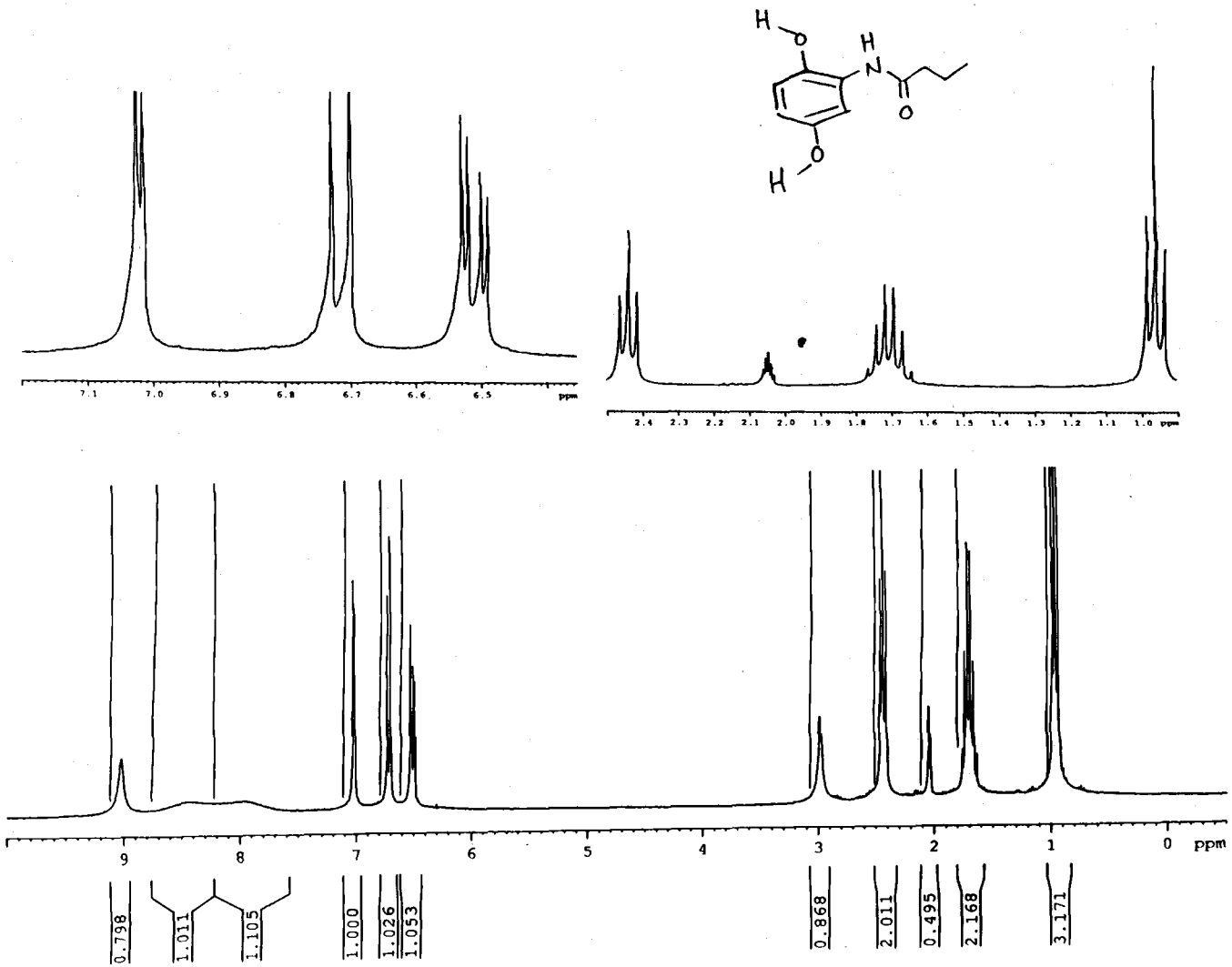
H
O
H
N
O
O
H
7.1
7.0
6.9
6.8
6.7
6.6
6.5
ppm
2.4
2.3
2.2
2.1
2.0
1.9
1.8
1.7
1.6
1.5
1.4
1.3
1.2
1.1
1.0 ppm
9
8
7
6
5
4
3
2
1
0
ppm
0.798
1.011
1.105
1.000
1.026
1.053
0.868
2.011
0.495
2.168
3.171